Order Number 8914754

Molecular interaction and synergism in binary mixtures of surfactants at the solid/liquid interface

Gu, Ben, Ph.D.

City University of New York, 1988

U·M·I
300 N. Zeeb Rd.
Ann Arbor, MI 48106

MOLECULAR INTERACTION AND SYNERGISM IN BINARY MIXTURES OF SURFACTANTS AT THE SOLID/LIQUID INTERFACE

BY

BEN GU

A dissertation
submitted to the Graduate Faculty in Chemistry
in partial fulfillment of the
requirements for the degree of
Doctor of Philosophy,
The City University of New York

1988

This manuscript has been read and accepted for the Graduate Faculty in Chemistry in satisfaction of the dissertation requirement for the degree of Doctor of Philosophy.

9/14/88
Date

Chair of Examining Committee

9/14/88
Date

Executive Officer

P. Somasundaran

Supervisory Committee

The City University of New York

Abstract

Molecular Interaction and Synergism
in Binary Mixtures of Surfactants
at the Solid/Liquid Interface

by

Ben Gu

Advisor: Professor Milton J. Rosen

A nonideal solution treatment has been developed and used to calculate the mole fractions, X, and interaction parameters, β, between two surfactants in the monolayer at various interfaces. Treatment "R", based upon the assumption of the same ratio of interfacial areas in the mixed and individual surfactant monolayers, gives X values in close agreement with these obtained by using the Gibbs equation and a β value that is essentially constant with change in X and surface pressure, π. Treatment "E", based upon the assumption of insignificant change in surfactant molar area in the mixture, gives X and β values that deviate more.

Equations have been derived for the conditions under which synergism in interfacial tension reduction efficiency in binary mixtures of surfactants at the liquid/hydrophobic solid interface and for various properties of the mixture at the point of maximum

synergism. The dependence of attractive interaction between two surfactants in the monolayer on the nature of the solid surface, the ionic strength of solution, the chain length and the structure of the surfactants has been studied.

New equations, based upon the Butler equation and combining the 2-D gas and 2-D solution approaches, are used to calculate the adsorption free energies of mixed surfactants at the L/V and S/L interfaces. Both standard free energies of adsorption, calculated from Rosen-Aronson equation, and those obtained by the new equations become more negative with increasing surfactant chain length at all interfaces investigated and a linear relationship was found at the L/V interface. But the increment decreases with increase in chain length at the S/L interfaces.

The relative adsorption of the surfactants at the solid/liquid and liquid/vapor interfaces, determined by using adhesion tension vs. surface tension plots, decreases in the order: Parafilm > Teflon > polyethylene and this is consistent with the results obtained by using Gibbs adsorption equation. The critical surface tensions of Teflon and Parafilm obtained by extrapolating the plots of $\gamma_{lv}\text{Cos}\theta$ vs. γ_{lv} from cationic-anionic surfactant mixtures and pure liquids are identical.

Dedication

To My Mother

Acknowledgements

I will be forever grateful to Professor Milton J. Rosen. His excellent scientific guidance, understanding, friendship and invaluable helpness have made this thesis a reality. The thanks here cannot fully show my deep appreciation but all of these will be long remembered.

Professors Seymour Aronson, Gary P. Mennitt of Brooklyn College of CUNY and P. Somasundaran of Columbia University, the members of my supervisory committee, contributed their time and advice throughout the course of this work. I am deeply grateful for their kindness and helpness.

To all member of my big family, thanks are due for their support, encouragement and unselfish sacrifices through the years of this study.

Finally my thanks and good wishes to all the friendly people who provided friendship and valuable conversation in the Surfactant Research Institute.

CONTENTS

TABLES

FIGURES

CHAPTER I

INTRODUCTION

I.A. General Aspects

The subject of the solid/liquid interface and related phenomena, such as wetting and floatation, has attracted surface chemists and has been the focus of a wide range of investigations because it is so important in our everyday life, in food processing and soil chemistry, and in the dye, paper, paint, pharmaceutical, rubber, mineral processing and petroleum industries.

Although solid/liquid interfacial phenomena have been observed and made use of for long time, detailed quantitative studies have been limited because of 1) the complex nature of the phenomena involving three interfaces: solid/liquid, solid/vapor and liquid/vapor, and 2) the imperfect nature of the solid surface in

actual practice.

The objectives of this work are 1) to examine the properties of mixtures of surfactants, such as molecular interactions and synergism in mixed monolayers at the solid/liquid interface, and 2) the free energies of adsorption of surfactants at the solid/liquid interface.

I.A.1 Molecular Interactions and Synergism

Mixtures of dissimilar and homologous surfactants are more extensively used than the individual surfactants because they are often more surface active and less expensive. Therefore, studies of surfactant interactions have great significance in both theory and practice and a large number of investigations have recently been directed towards understanding these interactions in mixtures of surfactants (1,2,3,4,5,6,7,8,9).

In the early 1960s the ideal mixing model was developed and widely used for ideal surfactant systems (10,11,12,13,14,15,16). In 1979, Rubingh (17) developed a method to treat mixed micelle formation in nonideal mixtures based on a regular solution model. A surfactant interaction parameter for mixed micelle formation (β^M) in binary mixture of surfactants was calculated based upon the treatment. This method has been extended and applied to a wide range of investigations (18,19,20,21,22,23).

In this laboratory, we have extended the nonideal treatment to mixed monolayer formation (24,25,26,27,28,29,30) and to investigate the molecular interactions and synergism in binary mixtures of nonionic-nonionic, nonionic-anionic, anionic-anionic, zwitterionic-nonionic zwitterionic-anionic and cationic-anionic surfactants at various interfaces and in micelles.

Most of the studies of interaction between the surfactant molecules in interfacial monolayers have involved the liquid/vapor interface. Less attention has been shown to the liquid/liquid interface, and very few studies have been devoted to the solid/liquid interface.

This work extends the nonideal solution treatment of molecular interactions and synergism at the vapor/liquid interface to the solid/liquid interface. Two different treatments ("E" and "R") have been developed and used to calculate surface mole fractions (X) and interaction parameters (β) between the different surfactant molecules in the mixed interfacial monolayer.

In order to elucidate the effect of the nature of solid surface, the chemical structures and molecular environment of the surfactant molecules on the value of the interaction parameter at solid/liquid interface, β_{sl}, various kinds of surfactant mixtures in solutions of different ionic strength had been investigated at different low-surface-energy hydrophobic solid/aqueous solution interfaces. Theoretical predictions of synergism agree well with experimental

results. The effect of the interface on the mole fractions and interaction parameters is discussed and compared with that at the vapor/liquid and liquid/liquid interfaces.

I.A.2 Free Energies of Adsorption

Adsorption is the process in which the surfactant molecules redistribute between the bulk phase and the interfacial phase. The result is the formation of different surfactant concentrations in the two phases. From a thermodynamic view, the process stems from the fact that surfactant molecule has a different energy in the different phases. Adsorption is fundamental to all surface phenomena. Therefore, the thermodynamic study of adsorption is very important for both theoretical and practical purposes.

A number of different methods have been developed to calculate the standard free energy of surfactant adsorption at the vapor/aqueous solution interface using surface tension data. However, most work has concentrated on low surface pressures and the adsorption of individual surfactant at vapor/aqueous solution interface. The more practical cases at high interfacial pressure for individual or mixed surfactants have not been received their deserved attention. The available literature data on free energies of adsorption are limited to the liquid/vapor and liquid/liquid interfaces. To the best of our knowledge, data on the free energies of adsorption of mixed surfactants at the solid/liquid

interface have not yet been reported.

In order to fill the gaps, this work attempts to use a new method, based upon the Butler equation and the use of a combination of the 2-D gas and the 2-D solution models, to estimate the free energies of adsorption for ether individual or mixed surfactants at any interfacial pressure. Thermodynamic data for individual and mixed surfactants at the liquid/vapor and solid/liquid interfaces have been calculated based upon this approach. The free energy of adsorption is influenced by the nature of the solid surface and the structure of the surfactant.

I.B. Background

I.B.1 Gibbs' Adsorption

I.B.1 - 1 Gibbs Surface

Surface or interface is a difficult concept to deal with. As shown in Figure I--1, above the plane A-A' and below the plane B-B' are homogeneous bulk phases of a and b. The range between A-A' and B-B' is surface phase (also called interfacial phase). In

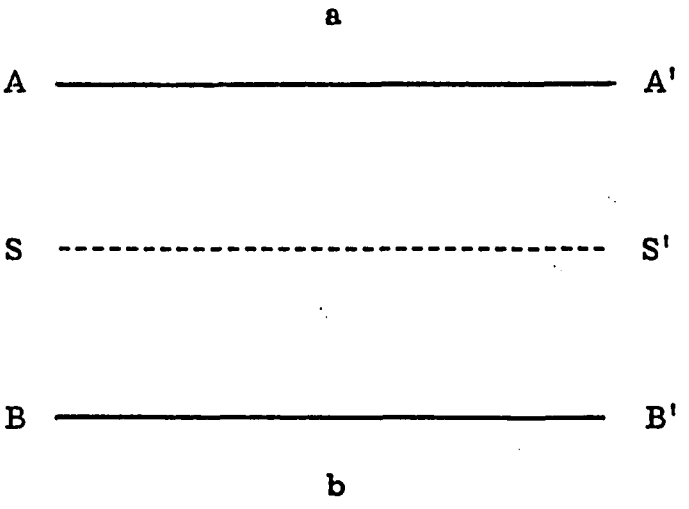

Figure I--1

this range the compositions and properties are uniform within the plane that parallels to the A-A' and B-B' planes and continuously change that along the perpendicular direction of the planes. In the actual case the boundaries between bulk and interfacial phases are not sharp. And the thickness of the surface range is usually about 1 nm or more. It is very difficult to get information of the

changes of the compositions and properties in the direction of the bulk phase.

There are some different models to be used in the thermodynamic treatments for the interfacial phase. Gibbs surface, most convenient and widely accepted model, is an imaginary surface that a plane S-S', a 1-dimensional geometry plane, is selected as the interfacial phase.

On the surface phase the compositions are described by n_i^s called surface excess. The surface excess concentration Γ_i is a surface excess per unit area and represents the adsorption of component i on the surface

$$\Gamma_i = n_i^s/A \qquad [I-1]$$

In order to fix the position of the Gibbs surface, the usual convention is to set the dividing surface S-S' such that $\Gamma_1 = 0$ and adsorption of components other than 1 is called the relative adsorption, Γ_i^1 (31). For a surface active component the surface excess concentration can be considered equal to the surface concentration without significant error.

I.B.1 -- 2 Gibbs Equation

The original scheme of a differential equation relating surface excess, n, concentration of solute, C, and the slope of plot of surface tension vs. concentration, $d\gamma/dC$, called Gibbs equation, was derived by J. W. Gibbs (32) in 1878.

The strict Gibbs equation for adsorption, obtained by use of thermodynamic concepts (33), is

$$d\gamma = - S^s dT - \Sigma \Gamma_i d\mu_i \qquad [I-2]$$

where S^s corresponds the surface phase entropy, Γ_i denotes the surface excess per unit area of component i and μ_i its chemical potential. Eq. [I-2] is one of the fundamental equations of surface chemistry.

Considering a two-component system, such as a solute in a solvent, Eq. [I-2] becomes

$$d\gamma = -\Gamma_1 d\mu_1 - \Gamma_2 d\mu_2 \qquad [I-3]$$

If the surface phase is chosen in a position that the surface excess of one component, usually solvent, is zero ($\Gamma_1 = 0$), then

$$d\gamma = - \Gamma_2^1 \, d\mu_2 \qquad [I-4]$$

At thermodynamic equilibrium of the system

$$\mu_2^s = \mu_2^b = \mu_2^o + RT \ln f C \qquad [I-5]$$

where C is the concentration and f is activity coefficient of the solute in bulk phase. In dilute solution, f is chosen as unity to a first approximation. Substituting Eq. [I-5] into Eq. [I-4] for μ gives

$$d\gamma = - \Gamma_2^1 \, RT \, d \ln C \qquad [I-6]$$

which is the form in which the Gibbs equation is generally used.

For the adsorption of 1:1 ionic solute (RM) in the absence of inorganic electrolyte, Eq. [I-3] can be expanded to:

$$d\gamma = - RT \, (\Gamma_R \, d \ln C_R + \Gamma_M \, d \ln C_M) \qquad [I-7]$$

Since the Gibbs surface is an electrically neutral phase, Γ_R is equal to Γ_M and $C_R = C_M$, which gives

$$d\gamma = - 2RT\ \Gamma_{RM}\ d \ln C_{RM} \qquad [I-8]$$

For the adsorption of 1:1 ionic solute (RM) in the presence of excess electrolyte (MY),

$$d\gamma = - RT(\Gamma_R d \ln C_R + \Gamma_M d \ln C_M + \Gamma_Y d \ln C_Y) \qquad [I-9]$$

The concentration of Y is constant and that of M (in excess) is not appreciably changed. Hence, under these conditions, Eq. [I-9] gives

$$d\gamma = - RT\ \Gamma_{RM} d \ln C_{RM} \qquad [I-10]$$

where the presence of the excess electrolyte has reduced the factor 2 of Eq. [I-8] to a factor 1.

I.B.1 -- 3 Adsorption of Mixed Surfactant

The Gibbs equation for a mixture of a nonionic or zwitterionic surfactant (R°) and an ionic surfactant (RM) in the absence of added inorganic electrolyte can be written as

$$d\gamma = - RT(\Gamma_{R^\circ} d \ln C_{R^\circ} + \Gamma_R d \ln C_R + \Gamma_M d \ln C_M) \qquad [I-11]$$

At constant mole fraction of surfactant in bulk phase, α,

$$d \ln C_{R^\circ} = d \ln C_R = d \ln C_M = d \ln C_t$$

where C_t is the total mixed surfactant concentration.

Since

$$\Gamma_t = \Gamma_{R^o} + \Gamma_R + \Gamma_M,$$

$$\Gamma_{R^o} = X_{R^o} \cdot \Gamma_t, \text{ and}$$

$$\Gamma_R = \Gamma_M = (1 - X_{R^o}) \Gamma_t,$$

where Γ_t is the total adsorption of all components and X_{R^o} is the mole fraction of R^o based only on the adsorbed surfactants at the interface. Therefore,

$$d\gamma = - RT \Gamma_t(2 - X_{R^o}) d \ln C_t \qquad [I-12]$$

For a mixture aqueous solution of an anionic (R^-M^+) and a cationic (R^+Y^-) surfactant,

$$d\gamma = -RT (\Gamma_{R^-} d \ln C_{R^-} + \Gamma_{M^+} d \ln C_{M^+} + \Gamma_{R^+} d \ln C_{R^+} + \Gamma_{Y^-} d \ln C_{Y^-})$$

Since for a neutral interface, $\Gamma_{R^-} + \Gamma_{Y^-} = \Gamma_{R^+} + \Gamma_{M^+}$, and the surface excess of the more surface-active surfactant's counter ion is zero, at constant α,

$$d\gamma = -RT\ 2X_a\Gamma_t\ d \ln C_t \qquad [I-13]$$

where X_a is the mole fraction of the more surface-active ion at the interface.

In electrolyte solution containing swamping excesses of the counter-ions (M^+ and Y^-)

$$d \ln C_{M^+} = d \ln C_{Y^-} = 0, \text{ and}$$

Eqs. [I-12] and [I-13] are changed to

$$d\gamma = -RT\ \Gamma_t d \ln C_t, \qquad [I-14]$$

which is the same as that of individual surfactant in the presence of excess electrolyte.

The average area per surfactant species, A_{av} in nm^2, when Γ_t is in mol-cm^{-2}, is then given by

$$A_{av} = 10^{14}/(N \cdot \Gamma_t) \qquad [I-15]$$

where N is Avogadro's number.

At the solid/liquid interface, the surface tension, γ_{sl}, is related to the contact angle, θ, and the surface tensions at liquid/vapor and solid/vapor, γ_{lv} and γ_{sv}:

$$\gamma_{sl} = \gamma_{sv} - \gamma_{lv} \cdot \mathrm{Cos}\theta \qquad [I-16]$$

This equation was first given by Young (34) in 1855. For a low-energy-surface solid and solutions of a nonvolatile surfactant, γ_{sv} can be considered constant without significant error. Differentiation of Eq. [I-16] gives

$$\begin{aligned} d\gamma_{sl} &= d(\gamma_{sv} - \gamma_{lv} \cdot \mathrm{Cos}\theta) \\ &= -d(\gamma_{lv} \cdot \mathrm{Cos}\theta) \end{aligned} \qquad [I-17]$$

Therefore, at the solid/liquid interface the total adsorptions of mixed surfactants of a nonionic or zwitterionic with an 1:1 ionic surfactant in the absence of excess swamping counter-ions can be calculated from

$$d\gamma_{lv} \cdot \mathrm{Cos}\theta = RT\ \Gamma_t(\ 2 - X_{R^o})d\ \ln\ C_t \qquad [I-18]$$

The total adsorption of surfactants at the solid/liquid interface for a cationic-anionic mixture system in the absence of excess inorganic electrolyte can be obtained from

$$d\gamma_{lv} \cdot \mathrm{Cos}\theta = RT\ \Gamma_t\ 2X_a d\ \ln\ C_t \qquad [I-19]$$

For a mixed surfactant system in the presence of excess swamping counter-ion the total surface adsorption of surfactants at

the solid/liquid interface is related to the adhesion tension, $\gamma_{lv}Cos\theta$, by the relationship:

$$d\gamma_{lv} \cdot Cos\theta = RT\ \Gamma_t d\ ln\ C_t \qquad [I-20]$$

These equations are similar to Eqs. [I-12], [I-13] and [I-14] at the liquid/vapor interface.

In a system where γ_{lv} and θ can be directly measured, the surface concentration, Γ, at the liquid/vapor or solid/liquid interfaces can be directly calculated from the slopes of γ_{lv} vs. log C or $\gamma_{lv} \cdot Cos\theta$ vs. log C plots.

Combining the Gibbs and Young equations, Lucassen-Reynders (35) developed an equation relating the adhesion tension to the adsorptions at the three interfaces. The contact angle is related to the L/V, L/S and S/V interfacial tension by Young's equation [I-26]. The surface adsorption at any interface can be evaluated by the Gibb's adsorption equation

$$d\gamma_{ij} = -RT\ \Gamma_{ij}\ d\ lnC \qquad [I-21]$$

where ij may be lv, ls or sv. The changes in lnC upon adding surfactant are constant over the all of three interfaces. Therefore, from Young's equation [I-16] and Eq. [I-21],

$$d(\gamma_{lv} \cdot Cos\theta)/d\gamma_{lv} = (\Gamma_{sv} - \Gamma_{sl})/\Gamma_{lv} \qquad [I-22]$$

For a low-energy surface and a nonvolatile surfactant solution Γ_{sv} can be assumed to be zero (36,37,38), which gives

$$d(\gamma_{lv} \cdot Cos\theta)/d\gamma_{lv} = -\Gamma_{sl}/\Gamma_{lv} \qquad [I-23]$$

Therefore, the slope for a plot of adhesion tension, $\gamma_{lv} \cdot Cos\theta$,

versus surface tension gives the relative adsorptions of surfactant at the solid/liquid and liquid/vapor interfaces.

I.B.2 Thermodynamic Characteristics of Adsorption

A surface active agent, which has a polar head group and a non-polar part, is always concentrated at interfaces with orientation of the hydrophilic group in the polar phase and the hydrophobic part in the non-polar or less polar phase. The strong adsorption of such materials at interfaces is termed surface activity and is related to all surface phenomena. Therefore, studies of the thermodynamic characteristics of adsorption are necessary for either theoretical or practical purposes.

J. W. Gibbs made the pioneering work over 100 years ago (32). After many scientists made great contributions in both theoretical and experimental fields. E. H. Lucassen-Reynders developed thermodynamic treatments in a systematic study (39,40,41,42). And free energies of surfactant adsorption have been calculated by many investigators, using a variety of methods.

Rodakiewicz-Nowak and Goralczyk (43,44,45,46,47,48,49) reported some thermodynamic data on cationic and anionic surfactants and their mixtures at the vapor/aqueous solution interface in the presence and absence of added inorganic salt using the Butler equation, based upon the assumption that the adsorption.

free energy (ΔG) and the partial molar area (A) are independent of π or the solution concentration of surfactant. The free energy of adsorption (ΔG_{ij}) was obtained from the experimental data by using equation

$$X^{b}_{H_2O} \exp[(-\Delta G_{H_2O} - \pi W_{H_2O})/RT] +$$
$$2f^{b}_{\pm}\{\Sigma X^{b}_{i} X^{b}_{j} \exp[(-\Delta G_{ij} - \pi W_{ij})/RT]\}^{\frac{1}{2}} = 1$$

where superscript b denotes bulk phase and W is the molar area of component at interface.

Standard free energies of adsorption (ΔG°) at the aqueous solution/vapor interface have been calculated (50,51) from the equation

$$\Delta G^{\circ} = -RT \ln[\text{Lim}_{c\to 0} (d\pi/dc)]$$

where $\text{Lim}_{c\to 0} (d\pi/dc) = \alpha$ (Traube's constant) is the slope of surface pressure (π) of the solution versus surfactant concentration (C) at very dilute surfactant concentration. Here, the hypothetical standard state is defined in that the surfactant has the environment typical of an extremely low surface concentration at unit surface pressure. Due to the very large effect of purity of the surfactant or of the solvent and the limitation of equipment the error in measuring the surface pressure of very dilute solutions is usually very large. Therefore, the utility of this equation is limited.

Mukerjee, Lucassen-Reynders and their colleagues (52,53) have calculated standard free energies of adsorption (ΔG°) of some pure and mixed surfactants at the vapor/aqueous solution interface

by use of the distribution coefficient. The distribution coefficient at infinite dilution, $\text{Lim}_{\pi \to 0} a_{ij}$,

$$\text{Lim}_{\pi \to 0} a_{ij} = [\, X_i^b X_j^b \,/\, X_i^s X_j^s \,]_{\pi=0}$$

where X_i^b, X_j^b are mole fractions of component i, j in the bulk phase and X_i^s, X_j^s are mole fractions of component i, j in the interface based on the 2-D solution model. The distribution coefficient is related to the standard free energy of adsorption of the surfactant ij by the expression:

$$\Delta G^\circ_{ij} = RT \ln a_{ij}$$

A new approach to the calculation of standard free energies of adsorption for individual surfactant solutions that is applicable to data in the high surface pressure range was described by Rosen and Aronson (54). The standard free energy of adsorption was calculated by use of the equation

$$\Delta G^\circ = 2.303\ RT \log a - \pi A_o \qquad [I\text{-}24]$$

where a is the activity of the surfactant in the bulk phase at surface pressure, π, and A_o is molar area of the surfactant in the monolayer. Here, the standard state for the interfacial phase is chosen as an interface filled with surfactants at a surface pressure of zero. Data are obtained directly from surface tension-concentration curves.

For a 1:1 electrolyte surfactant solution, the equation becomes:

$$\Delta G^\circ_{ad} = 2.303\ RT(\log C_+ + \log f_+ + \log C_- + \log f_-) - \pi A_o \qquad [I\text{-}25]$$

were the activity coefficients (f_+, f_-) can be evaluated from the Debye-Huckel equation

$$\log f = -B|Z_+ Z_-| I^{\frac{1}{2}}/(1 + 0.33\alpha I^{\frac{1}{2}}) \qquad [I-26]$$

where I is the ionic strength based upon the free ions in the system and α is the mean distance approach of the ions.

Although these various methods have been developed to calculate the free energy of adsorption, investigations to date have been limited to the liquid/air and liquid/liquid interfaces.

I.B.3 Surface Monolayers

In 1774, Benjamin Franklin (55) first reported quantitative data on the spreading of oil on a pond, and found that the oil film was only about 25 A° thick. In the 1890s, further investigations by Pockels (56) and Rayleigh (57) showed that the film was only a single molecule in thickness and a close-packed monomolecular film. But modern detailed studies of monolayers are based on the experimental contributions made by use of the technique called the Langmuir trough, and the theoretical concepts of Langmuir (58,59). The states of monolayers are classified (by analogy to three-dimensional gases, liquids and solids) into gaseous films, liquid films or solid films (60). Liquid films are classified into liquid, expanded, liquid intermediate, and liquid condensed films (61,62).

When a surface-active agent is dissolved in a liquid, the

surfactant molecules adsorb at the interface and a monomolecular layer is formed at the interface. In comparison with spread monolayers, where an insoluble or slightly soluble substance is placed at a liquid-air interface and the molecules spread over the surface to form a thin film of nm order thickness, this type of monolayer is called a Gibbs monolayer or soluble monolayer. Soluble monolayers are more common than insoluble (spread) monolayers in most interfacial phenomena. The surface concentration of a spread monolayer can be known by directly measuring the amount of chemical per unit surface area, while the surface concentration of a Gibbs monolayer is obtained indirectly by use of the Gibbs adsorption equation (Eq. [I-2]).

I.B.3 -- 1 Thermodynamics of Monolayers

The model of the interface as a monolayer is extensively used in theoretical treatments. The model assumes that the interface, s, is a single monomolecular layer linked to two homogeneous bulk phases, a and b. Using this model, we can derive an equation for the chemical potential of component i that is similar to the results obtained by applying the Gibbs surface model (63). In the monolayer, the free energy may be described as

$$G^S = F^S + PV^S - \gamma A \qquad [I-27]$$

where F^S is the Helmholtz free energy of the interface, V^S is the volume of the interface, γ is the surface tension and A is the area

of the interface. The chemical potential of component i on the interface is

$$\mu_i^s = (\partial G^s/\partial n_i^s)$$
$$= (\partial F^s/\partial n_i^s) + P\upsilon_i^s - \gamma A_i \qquad [I-28]$$

where

$$\upsilon_i^s = (\partial V^s/\partial n_i^s)$$

and

$$A_i = (\partial A/\partial n_i^s)$$

At normal pressure (P about 1 atm.) the term $P\upsilon_i^s$ is too small to compare with γA_i and is negligible. So, the chemical potential of component i can be approximately described as

$$\mu_i^s = (\partial F^s/\partial n_i^s) - \gamma A_i \qquad [I-29]$$

In the bulk phase of a perfect solution we have

$$\mu_i = \mu_i^o + RT \ln X_i \qquad [I-30]$$

and

$$F_i = G_i - PV$$
$$= n_i(\mu_i^o + RT \ln X_i - P\upsilon_i) \qquad [I-31]$$

where μ_i^o is the chemical potential of component i at the standard state defined as a monolayer of pure component i at certain pressure, P, assuming the dependence of υ_i only on T and P, and X_i is the molar fraction of component i in the solution. In the interface, by analogy,

$$F_i^s = n_i^s (\mu_i^{os} + RT \ln X_i^s - P\upsilon_i^s) \qquad [I-32]$$

From Eqs. [I-28] and [I-32]

$$\mu_i^s = \mu_i^{os} + RT \ln X_i^s - \gamma A_i \qquad [I-33]$$

This equation represences the chemical potential of component i in the interface for an ideal monolayer (meaning no interaction between the adsorbed molecules).

Although in most practical cases the thickness of the interface layer may not be that of a single molecule, the monolayer model is a simple and convenient treatment for the complex real interface and is extensively used in theoretical and practical studies, since approximately correct results can be obtained quickly.

I.B.3 -- 2 Two Approaches

Generally, two different approaches have been used to treat the monolayer of surfactants adsorbed at an interface (64).

In the first treatment, labeled the 2-D gas approach, a monolayer is regarded as a two-dimensional gas composed only of adsorbed molecules. This approach has been developed by several scientists since the early 20th century (59,62,65,66). Because of its simplicity and convenience, the approach is popular and widely used on surfactant monolayers, especially in the treatment of insoluble monolayers.

When the monolayer is a perfect 2-dimensional gas, the adsorbed molecules may be considered as point masses without interactions. The equation of state is

$$\pi A = RT \qquad [I-34]$$

where π is the surface pressure and A is the molar surface area of the adsorbed molecules, by analogy with the pressure and molar volume in a three-dimensional ideal gas. Considering the two kinds of interactions between adsorbed molecules, mutual repulsion of charged head groups and mutual attraction of hydrophobic chains, and the finite size of the adsorbed molecules, Eq. [I-34] can be modified as

$$(\pi - \pi_r - \pi_a) (A - A_o) = RT \qquad [I-35]$$

where π_r and π_a are corrections for repulsion and attraction between adsorbed molecules and A_o takes into account the finite size.

In the other approach, called the 2-D solution approach, the monolayer is treated as a special two-dimensional phase that has the same composition as the bulk phase but has different concentrations because of surface adsorption. The thermodynamic potential of component i at the interface is expressed by the Butler equation (67)

$$\mu_i^s = \mu_i^{os} + RT \ln f_i^s X_i^s - \pi A_i \qquad [I-36]$$

in which the activity coefficient, f_i^s, represences interactions between adsorbed molecules. The thermodynamics of the model have been developed by Tolman (68) and Defay (63). At thermodynamic equilibrium between bulk and surface phases, mole fractions X_i^b and X_i^s are related by the equation

$$\frac{f_i^s X_i^s}{f_i^s X_i^s} = \exp \frac{- [(\mu_i^{os} - \mu_i^{ob}) + \pi A_i]}{RT} \qquad [I-37]$$

The 2-D solution approach has been more widely used to treat soluble (69,70,71,72,73,74) and insoluble monolayers (75,76,77) because it gives a more accurate picture of the interface than the 2-D gas approach. Recently the thermodynamic characteristics and interactions between surfactants has been extensively studied by using the 2-D solution approach for mixed monolayers (39,40,41,42,43,44,45,46,47,48.49).

The qualitative interpretation of experiment data is satisfactory using both of these approaches.

I.B.4 Interaction of Surfactant Molecules in Monolayers (78)

In a binary mixed monolayer there is extra free energy, compared to that in an ideal mixed monolayer, that comes from the interaction between the different surfactant molecules.

The potential energy of the interaction between the molecules of surfactant i and surfactant j is p_{ij}. The total free energy in the monolayer for a mixture of surfactant 1 and 2

$$G^s = \Sigma p_{ij} - \gamma A$$

$$= Q_{11}p_{11} + Q_{22}p_{22} + Q_{12}p_{12} - \gamma A \qquad [I\text{-}38]$$

where Q_{ij} is the number of the interacting molecular pairs of molecule i and j.

We assume that each molecule has b interacting neighbors in the monolayer. The number of molecule 1 and 2 are NnX_1 and

NnX_2, respectively, where n is the total number of moles of surfactant 1 and 2, N is Avogadro's number, and X_1 and X_2 are the mole fractions of surfactants 1 and 2 in the monolayer. In the 2-D gas treatment, $X_1 + X_2 = 1$. The neighbors for each molecule are bX_1 of surfactant 1 and bX_2 of surfactant 2. The number of the interacted molecular pairs of surfactant 1 and 2 is

$$Q_{12} = NnX_1bX_2 = NnbX_1X_2 \qquad [I-39]$$

Similarly, for like molecules,

$$Q_{11} = 1/2\ NnX_1bX_1 = 1/2\ NnbX_1^2$$
$$Q_{22} = 1/2\ NnX_2bX_2 = 1/2\ NnbX_2^2 \qquad [I-40]$$

where the factor of 1/2 is necessary to avoid counting each contact twice.

Therefore, the monolayer free energy, G^s, is

$$\begin{aligned} G^s &= Nnb/2\ [p_{11}X_1^2 + p_{22}X_2^2 + 2p_{12}X_1X_2] - \gamma A \\ &= Nnb/2\ [p_{11}X_1(1-X_2) + p_{22}X_2(1-X_1) + \\ &\quad 2p_{12}X_1X_2] - \gamma A \\ &= Nnb/2\ (p_{11}X_1 + p_{22}X_2) + \\ &\quad Nnb[p_{12} - (p_{11} + p_{22})/2]X_1X_2 - \gamma A \end{aligned} \qquad [I-41]$$

That means that the free energy, G^s, is the sum of two terms: an ideal monolayer free energy term, $G^{id,s}$, and an extra free energy term, $G^{ex,s}$, due to the interaction between the two different surfactant molecules,

$$G^s = G^{id,s} + G^{ex,s} \qquad [I-42]$$

and

$$G^{ex,s} = Nnb\,[p_{12} - (p_{11} + p_{22})/2]X_1X_2$$
$$= n\,\beta X_1X_2$$
$$= \beta\, n_1n_2/n \qquad [I\text{-}43]$$

where

$$\beta = Nb\,[p_{12} - (p_{11} + p_{22})/2] \qquad [I\text{-}44]$$

β is a parameter that reflects the interaction between the two types of surfactant molecules and is related to the potential energies of various molecule pairs (p_{11}, p_{12} and p_{22}) and the number of interacting neighbors (b).

Differentiating [I-42] and [I-43] with respect to n_1 and n_2, respectively, we have

$$\mu_1^s = \mu^{id,s} + \beta\, X_2^2$$
$$= \mu_1^{os} + RT \ln X_1 + \beta X_2^2 - \gamma A_1$$
$$\mu_2^s = \mu^{id,s} + \beta\, X_1^2$$
$$= \mu_2^{os} + RT \ln X_2 + \beta X_1^2 - \gamma A_2 \qquad [I\text{-}45]$$

By using the relationship

$$\ln f_1 = \beta(1 - X_1)^2 = \beta X_2^2$$
$$\ln f_2 = \beta X_1^2 \qquad [I\text{-}46]$$

the Eq. [I-45] become

$$\mu_1^s = \mu_1^{os} + RT \ln f_1X_1 - \gamma A_1$$
$$\mu_2^s = \mu_2^{os} + RT \ln f_2X_2 - \gamma A_2 \qquad [I\text{-}47]$$

These thermodynamic equations are extensively used for binary mixture systems.

I.B.5 Solid Surfaces

There are many similarities between the surface layer of a solid and that of a liquid, but a very important difference is the immobility of the surface molecules of a solid. This causes difficulties in theoretical and practical studies that relate to the solid surface.

I.B.5 -- 1 Surface Free Energy of a Solid

The surface free energy or so-called free energy of surface formation is the work spent in the creation of unit area of surface by an isothermal and reversible process. The formation of a fresh surface can be divided into two steps: exposing a new surface by cleaving a substance and rearranging the surface atoms or molecules to the equilibrium position. In a liquid surface the particles reach equilibrium and a uniform, isotropic surface layer is formed in a very short time. The surface free energy (also called the surface tension) is defined (79)

$$\gamma = (\partial F/\partial A)_{T,V,rev.}$$
$$= (\partial G/\partial A)_{T,P,rev.} \qquad [I\text{-}48]$$

and the value can be directly measured experimentally. But because of the very long lifetime of a solid surface particle (for instance, 10^{32} sec. for tungsten at room temperature)(80), it is almost impossible to complete the second step in forming a solid surface. Therefore, we cannot calculate the surface tension of a

solid by using Eq. [I-48] and the direct measurement of a surface tension is not possible for an anisotropic solid surface. However, some reliable experimental surface energy values are available (81) and theoretical calculations of surface energies have been made for the simplest crystalline metals. At room temperature, the surface free energy of magnesium oxide is about 90% of the surface energy that has been determined experimentally by Jura and Garland (82).

The difference between γ_s and γ_{sv} was first emphasized by Bangham and Razouk (83). γ_{sv} is the interface tension when the solid surface is in equilibrium with the saturated vapor pressure. Therefore, that is related to the surface free energy, γ_s, by

$$\gamma_{sv} = \gamma_s - \pi_s \qquad [I-49]$$

in which π_s is the pressure of the film that covers the solid surface.

Solid surface energy is related to the contact angle. Good and Girifalco (84) developed a semiempirical model to calculate the solid surface energy in a vacuum, γ_s, using surface tension and contact angle data. Young's equation has been written as

$$\gamma_{lv} \cdot \text{Cos } \theta = \gamma_s - \gamma_{sl} - \pi_s \qquad [I-50]$$

An equation has been proposed,

$$\gamma_{sl} = \gamma_s + \gamma_{lv} - 2\,\Phi(\gamma_s\,\gamma_{lv})^{\frac{1}{2}} \qquad [I-51]$$

where the parameter, Φ, represents the molecular interactions at the interface and γ_s is the surface free energy of the solid in a vacuum.

Combining Eqs. [I-50] and [I-51] and eliminating γ_{sl}, the

solid surface tension, γ_s, can be evaluated from the following equation

$$\text{Cos } \theta = -1 + 2\,\Phi(\gamma_s/\gamma_{lv})^{\frac{1}{2}} - \pi_s/\gamma_{lv} \qquad \text{[I-52]}$$

Fowkes (85) suggested that when there are only London-van der Waals dispersion forces across the solid/liquid interface,

$$\text{Cos } \theta = -1 + 2(\gamma_s^{\,d}\,\gamma_{lv}^{\,d})^{\frac{1}{2}}/\gamma_{lv} - \pi_s/\gamma_{lv} \qquad \text{[I-53]}$$

where $\gamma_s^{\,d}$ and $\gamma_{lv}^{\,d}$ are the contributions of the dispersion forces to the solid surface energy and surface tension, respectively. Equation [I-53] is called "Good-Girifalco-Fowkes-Young" equation (86).

Zisman and Fox (87,88) introduced another important concept, the critical surface tension, γ_c, for wetting. They reported a linear relationship between the cosine of advanced contact angle of a homologous series of organic liquids on a low-surface-energy solid and their surface tensions. The function is

$$\text{Cos } \theta = 1 - b(\gamma_{lv} - \gamma_c) \qquad \text{[I-54]}$$

where γ_c is called the critical surface tension for wetting. It is the surface tension of a liquid which just wets the solid ($\theta = 0$). The critical surface tension is a useful parameter that represents the wetting behavior of a solid. In fact, the critical surface tension depends on the series of liquids used, and any interaction between the solid and the liquids would alter the value of γ_c (89). Usually the values of 18 and 24 mN/m are adopted for surfaces consisting of $-CF_2-$ and $-CH_3-$ groups, respectively (90).

For the case of using nonpolar liquids on a low-surface-energy solid such as that used by Zisman, the assumptions of $\gamma_{lv} = \gamma_{lv}^{d}$ and $\pi_s = 0$ in Eq. [I-53] are reasonable and at $\theta = 0$, gives

$$\gamma_c = \gamma_s^{d} \qquad [I-55]$$

Fowkes has verified that γ_s^{d} agrees well with γ_c experimentally (85).

I.B.5 -- 2 Nonideal Solid Surfaces (91,92)

In practical cases it is not possible to find a clean, smooth, homogeneous, rigid, isotropic solid surface. Because of the nonidealities of solid surfaces, the study of the solid/liquid interface is more difficult than that of the liquid/vapor and liquid/liquid interfaces.

At the molecular level, the heterogeneities of a solid surface are shown simply in Figure I--2. On the heterogeneous solid surface the adatom is surrounded by the smallest number of nearest neighbors and atoms in a terrace by the largest number of nearest neighbors. Atoms in kink sites have less nearest neighbors than that at step sites. Atoms in different types of surface sites have different energies that are increased with decrease in the number of nearest neighbors. Therefore, the heterogeneous solid surface is a nonuniform energy surface. Another cause of heterogeneity on a solid surface is dislocations. The motion of particle (or particles) in the crystal surface causes the point defects, edge dislocations

and screw dislocations that are high energy regions on a solid surface.

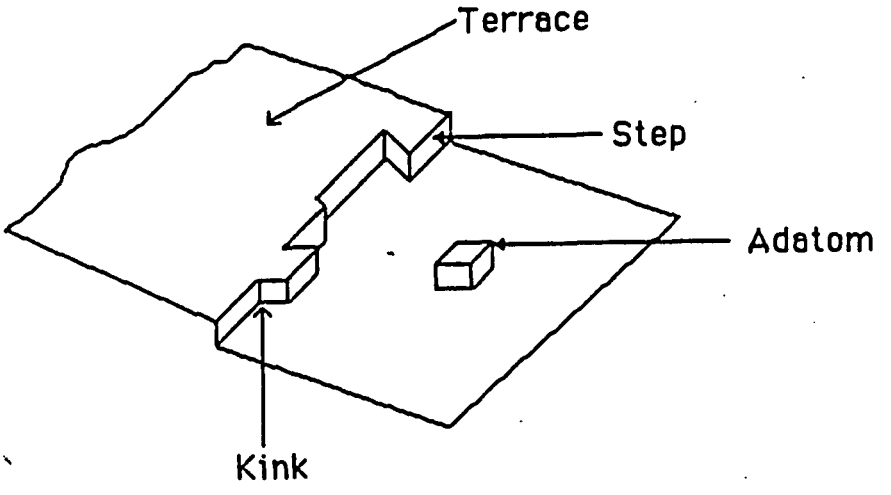

Figure I--2

There always is a layer of atoms or molecules adsorbed on a "naked" solid surface. It is in general impossible to get a clean solid surface except in a vacuum. In some cases the properties of the solid surface are tremendously changed by contaminantion by adsorbed molecules. It is worth mentioning that the polar contaminants on a nonpolar solid surface extremely influence the studies of hydrogen-bonding liquid/solid systems.

In comparison to microscale heterogeneities, macroscale roughness has even more effect on contact angles and is described by a parameter, r, called the roughness ratio

$$r = A_{true}/A_{apparent} \qquad [I\text{-}56]$$

where A_{true} is the real area of solid surface and $A_{apparent}$ is the

experimental area. The contact angle θ on a smooth solid surface and the average angle θ' on a rough surface are related to the roughness ratio, r, by Wenzel (93) as

$$\text{Cos } \theta' = r \text{ Cos } \theta \qquad \text{[I-57]}$$

Equation [I-57] shows that the roughness increases the contact angle if the contact angle θ is greater than 90° on the smooth surface and decreases the contact angle if θ is less than 90° on the smooth surface.

Distortion and swelling of a solid are also possible deviations from the ideality of a solid surface (91).

I.B.6 Contact Angles on Rigid Solid Surfaces

I.B.6 -- 1 The Thermodynamic Equation for Contact Angle

A liquid on a solid surface may spread completely over the surface or, in most cases, may remain as a drop. The angle between the liquid/solid interface and the tangent plane of the liquid/vapor interface at the three-phase line is called the contact angle. From Figure I--3, the free energy change (ΔG^s) of the surface and the area change (ΔA) of the solid surface covered by the liquid are related by the relation:

$$\Delta G^s = \Delta A(\gamma_{sl} - \gamma_{sv}) + \Delta A\gamma_{lv} \text{ Cos } (\theta + \Delta\theta) \qquad \text{[I-58]}$$

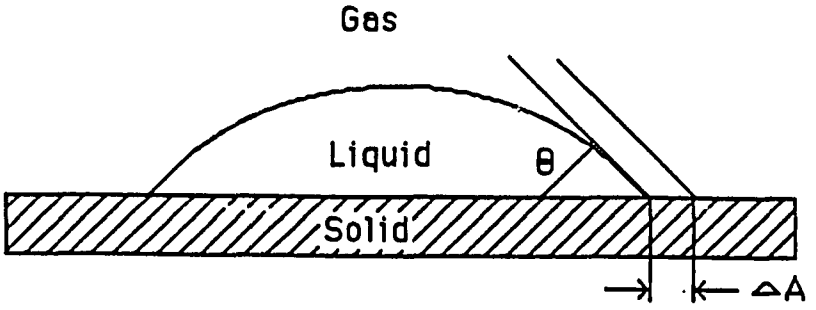

Figure I--3

When equilibrium is reached, we have

$$\mathrm{Lim}_{\Delta A \to 0}\ \Delta G^{s}/\Delta A = 0 \qquad [I\text{-}59]$$

and

$$\gamma_{sv} = \gamma_{sl} + \gamma_{lv} \cdot \mathrm{Cos}\ \theta \qquad [I\text{-}60]$$

which is known as Young's equation (34).

The term $\gamma_{lv}\mathrm{Cos}\theta$, called the "adhesion tension", suggested by Freundlich (94) (an alternative name is "wetting tension", W_{sl}^{a}) is given by

$$W_{sl}^{a} = \gamma_{lv} \cdot \mathrm{Cos}\ \theta = \gamma_{sv} - \gamma_{sl} \qquad [I\text{-}61]$$

The equation [I-60] is the most fundamental equation for the treatment of contact angle data and is in general acceptance.

I.B.6 -- 2 Measurement of Contact Angles

Various techniques have been used for measuring contact angles on a flat plate. Generally, there are two distinct methods: direct and indirect.

Measuring the contact angle directly for a sessile drop of liquid on a flat solid plate is the most convenient and widely used technique. Zisman and colleagues (95) first used the method to measure the contact angle directly through a telescope equipped with a goniometer. As the method became more and more popular, several kinds of commercial instruments for measuring the contact angle directly became available. The contact angle of a sessile liquid drop on a flat plate is now usually determined either by use of a telescope fitted with a goniometer eyepiece or by photographing the angle and then measuring it at leisure.

The method is fairly accurate and accuracy of ± 2° is commonly claimed. But a 5° discrepancy between different laboratories using this method has also been reported. This may be caused by systematic errors, such as surface structure differences between the same kind of solid, disagreement between operators, and optical illusion. Usually the polymer surface created in contact with air is homogeneous and smooth enough to yield well-defined contact angle values. Polytetrafluoroethylene (Teflon) was suggested as a satisfactory standard material by Newman and Good (96).

A self-training method was developed by Good (96) to check the goniometer readings against the contact angle values calculated from linear dimensions for spherical liquid droplets. The contact angle θ can be obtained from the dimensions of the droplet by using the equation

$$\tan \theta/2 = 2h/b \qquad [I\text{-}62]$$

where h is a height of the droplet and b is the chord of the segment of the drop that both can be obtained from the fine adjustment knobs of the instrument or measured from a photograph of the droplet. When the training method is employed, the errors due to the operators and optical illusion can be eliminated and the reproduciblity of contact angle data obtained directly from sessile drops may be better than ± 1.0° (97).

If very high accuracy is not required, the direct measuring of the contact angle from a sessile drop is one of the best and most convenient method. The advantages are requiring only very small quantities of liquid and only a few square millimeters of solid surface for the contact angle measuring.

The Wilhelmy slide technique and capillary rise method are also used to obtain contact angles on flat solid plates. The value of the contact angle can be calculated from the surface tension and the perimeter of the plate or the height of capillary rise in the methods. Usually, it is easy to obtain highly accurate values of the surface tension. Therefore, the accuracy and reproduciblity of the methods are limited only by the measuring of the plate perimeter or the capillary rise height. It is not difficult to get accurate values. Generally, an uncertainty of a few tenth of a degree was claimed for these methods, better than for the direct method. The Wilhelmy method using an electrobalance and auto-recorder can conveniently

study the change of contact angle with time. The capillary rise method with a temperature control system is particularly suitable for the measurement of the temperature dependence of contact angles. The popular acceptance of the indirect method is limited by the requirements for a large, smooth flat sample of solid and a large volume of liquid.

I.B.6 -- 3 Factors Affecting the Contact Angle

All liquids that form nonzero contact angles may show hysteresis on practically all solid surfaces. The reproduciblity of the contact angle data is directly limited by the hysteresis.

The hysteresis (H) in the contact angle is defined as the difference between the advancing (θ_a) and receding (θ_r) contact angles

$$H = \theta_a - \theta_r \qquad [I\text{-}63]$$

The major causes of hysteresis are contamination of either the liquid or the solid surface, roughness of solid surface, and surface immobility on a macromolecular scale (98). For the best reproducible contact angle, the factors causing hysteresis should be limited as much as possible. Some experimental results show that there is no contact angle hysteresis when a pure liquid is placed on a pure and smooth solid surface (99).

Advancing contact angle (θ_a) has been much more popular and is used more often than receding contact angle because the receding

angle is more sensitive to surface roughness and data on advancing angles are more reproducible.

Since 1936, after Mark's investigations (100), it has been known experimentally that the contact angle is a function of drop size when the contact angle of a liquid is measured on a solid surface by the sessile drop method. However, the effect has not been satisfactorily explained up to the present. Leja and Poling (101) suggested that the size dependence was due to gravitational effects. Unfortunately, they used a poor approximation to explain the phenomenon that the sessile drop in contact with a solid surface was treated as a spherical cap. Other investigators concluded that gravitation could not account for the drop size dependence.

An alternative explanation that a linear tension, τ, was involved in the effect was suggested by Good and Koo (97). They observed that the contact angle (advancing and receding) increases with increase in the drop size below a critical diameter that was a function of the nonuniformity of a solid surface (for example, the diameter is 3 mm for the advancing contact angle on Teflon). The relevant modification of Young's equation is

$$\gamma_{lv} \cos\theta = \gamma_{sv} - \gamma_{sl} - \tau/r \qquad [I\text{-}64]$$

where r is the radius of the sessile drop. The equation was first suggested without proof by Pethica (102). Corresponding to the effect of contact angle increasing with increase of drop size the linear tension would have a negative value. This is in contradiction

with the experimental and theoretical indication that linear tension should be small and positive. Pethica pointed out that the linear tension will have no measurable influence for macroscopic sessile drop because τ is about 10^{-5} order compare with γ_{lv} and it is negligible. The explanations of increasing hysteresis and the presence of polar impurities on the solid surface were also cited. Obviously further study of this problem is needed.

In order to avoid the influence of drop size on the experimental results, the same size drops should be employed for getting best reproduciblity of contact angle data.

That temperature does not have very great effect on contact angle was confirmed by most investigators using various solid surfaces and different organic liquids or solutions. Experimental results show that the value of $d\theta/dT$ is less than - 0.1 deg/°C in most cases (98). That may be because temperature change does not effect the value of γ_{sv} very much and has similar effect on γ_{lv} and γ_{sl}. But in some solid/liquid/liquid systems the changes due to temperature are rather large compared to that for solid/liquid/vapor systems (103).

CHAPTER II

THEORY

II.A Synergism in Binary Mixtures of Surfactants

II.A.1 Basic Equations

Based upon the 2-dimensional gas approach, the mixed monolayer can be considered as a mixture that is composed only of the different surfactants. The chemical potential, μ_1^s, of surfactant 1 at the interface can be written (104,105)

$$\mu_1^s = \mu_1^{\alpha_s} + RT \ln f_1^s X - \gamma A_1 \qquad [II-1]$$

where $\mu_1^{\alpha_s}$ is the chemical potential of surfactant 1 on the interface at a hypothetical standard state defined as a monolayer of pure surfactant 1; X is the mole fraction of surfactant 1 in the total surfactant in the mixed monolayer, f_1^s its activity coefficient and A_1 its partial molar interfacial area there; and γ is the interfacial tension.

The chemical potential, μ_1^b, of surfactant 1 in the bulk phase of the mixed solution of surfactants can be expressed as

$$\mu_1^b = \mu_1^{ob} + RT \ln C_1 f_1^b \qquad [II-2]$$

where μ_1^{ob} is the chemical potential of surfactant 1 at a standard state defined as a 1 mole solution, but behaving ideally; f_i is the activity coefficient of surfactant 1 in the solution and C_1 its molar concentration.

At equilibrium, $\mu_1^s = \mu_1^b$ and, from Eqs. [II-1] and [II-2]

$$\mu_1^{\pi s} - \mu_1^{ob} = RT \ln C_1 f_1 / (f_1^s X) + \gamma A_1 \qquad [II-3]$$

For a solution containing only surfactant 1

$$\mu_{1,o}^s = \mu_1^{\pi s} - \gamma A_1^o \qquad [II-4]$$

where A_1^o is the molar interfacial area occupied by surfactant 1 from solution of pure surfactant 1. In the bulk phase of the solution of pure surfactant 1,

$$\mu_{1,o}^b = \mu_1^{ob} + RT \ln C_1^o f_1^o \qquad [II-5]$$

where C_1^o is the molar concentration of pure surfactant 1 and f_1^o its activity coefficient.

At equilibrium, $\mu_{1,o}^s = \mu_{1,o}^b$ and from Eq.s [II-4] and [II-5],

$$\mu_1^{\pi s} - \mu_1^{ob} = RT \ln C_1^o f_1^o + \gamma A_1^o \qquad [II-6]$$

Combining Eqs. [II-3] and [II-6],

$$RT \ln \frac{C_1 f_1}{f_1^s X C_1^o f_1^o} = \gamma (A_1^o - A_1) \qquad [II-7]$$

When the concentrations of surfactants in the bulk phase are

low, $f_1 \approx f_1^o$, and Eq. [II-7] reduces to

$$\ln f_1^s = \ln \frac{C_1}{XC_1^o} - \frac{\gamma(A_1^o - A_1)}{RT} \qquad [II-8]$$

In a similar fashion, we obtain for surfactant 2 in the mixture

$$\ln f_2^s = \ln \frac{C_2}{(1 - X)C_2^o} - \frac{\gamma(A_2^o - A_2)}{RT} \qquad [II-9]$$

The activity coefficients, f_1^s and f_2^s, may be obtained, from the second term of the Margules expansion approximations (the first term being equal to zero)(106):

$$\ln f_1^s = \beta^\sigma (1 - X)^2 \qquad [II-10]$$

$$\ln f_2^s = \beta^\sigma X^2 \qquad [II-11]$$

where β^σ is a measure of the deviation of the mixture from ideality and related to the molecular interactions between surfactants 1 and 2 in the mixed monolayer at the interface. From Eqs. [II-8] and [II-10], and Eqs. [II-9] and [II-11],

$$\beta^\sigma (1 - X)^2 = \ln \frac{C_1}{XC_1^o} - \frac{\gamma(A_1^o - A_1)}{RT} \qquad [II-12]$$

and

$$\beta^\sigma X^2 = \ln \frac{C_2}{(1 - X)C_2^o} - \frac{\gamma(A_2^o - A_2)}{RT} \qquad [II-13]$$

Let

$$B_1 = \frac{\gamma(A_1^o - A_1)}{RT}$$

and

$$B_2 = \frac{\gamma(A_2^0 - A_2)}{RT}$$

Thus,

$$\beta(1 - X)^2 = \ln \frac{C_1}{XC_1^0} - B_1 \qquad \text{[II-12a]}$$

$$\beta X^2 = \ln \frac{C_2}{(1 - X)C_2^0} - B_2 \qquad \text{[II-13a]}$$

From these,

$$\frac{X^2}{(1 - X)^2} \frac{[\ln \frac{C_1}{C_1^0 X} - B_1]}{[\ln \frac{C2}{C_2^0(1 - X)} - B_2]} = 1 \qquad \text{[II-14]}$$

II.A.2 Synergism in Interfacial Tension Reduction Efficiency

The efficiency of interfacial tension reduction by surfactants in a solution of mixed surfactants can be defined as the total surfactant concentration required to produce a given interfacial tension (reduction). Synergism in this respect exists in a surfactant mixture when a given interfacial tension (reduction) can be attained at a total mixed surfactant concentration lower than that required of any components of the mixture, i.e., for solutions containing two surfactants, $C_t < C_1^o, C_2^o$.

From Eq. [II-12a] and $C_1 = \alpha C_t$, where α is the molar fraction of surfactant 1 in the total surfactant concentration,

$$\frac{\alpha C_t}{C_1^o X} = \exp\left[\beta^{\sigma}(1 - X)^2 + B_1\right] \qquad \text{[II-15]}$$

From Eq. [II-15], one condition for synergism is, therefore:

$$\frac{\alpha}{X} > \exp\left[\beta^{\sigma}(1 - X)^2 + B_1\right] \qquad \text{[II-16]}$$

When synergism exists, there will also be a minimum in the C_t versus α curve at maximum synergism. The maximum synergism in this respect is where the lowest total concentration of mixed surfactant is required to attain a given interfacial tension (reduction). This will be obtained when, mathematically,

$$\frac{dC_t}{d\alpha} = 0$$

From Eq. [II-15],

$$\ln C_t - \ln C_1^o = \ln X - \ln \alpha + \beta^{\sigma}(1 - X)^2 + B_1 \qquad \text{[II-17]}$$

Differentiating Eq. [II-17] with respect to α,

$$\frac{1}{C_t}\frac{dC_t}{d\alpha} = \frac{1}{X}\frac{dX}{d\alpha} - \frac{1}{\alpha} - 2(1 - X)\beta^{\sigma}\frac{dX}{d\alpha} + \frac{dB_1}{d\alpha}$$

Since C_t is not zero, then

$$\frac{1}{X^*}\frac{dX}{d\alpha} - \frac{1}{\alpha^*} - 2(1 - X^*)\beta^{\sigma}\frac{dX}{d\alpha} + \frac{dB_1}{d\alpha} = 0$$

or

$$\frac{dX}{d\alpha} = \frac{X^*\left(1 - \alpha^* \frac{dB_1}{d\alpha}\right)}{\alpha^*[1 - 2\beta X^*(1 - X^*)]} \qquad [II\text{-}18]$$

where α^* is the mole fraction of surfactant 1 in the total surfactant in the solution phase at the point of maximum synergism and X^* its mole fraction in the mixed monolayer at the interface.

From Eq. [II-13a] and $C_2 = C_t(1 - \alpha)$,

$$\ln C_t = \ln (1 - X) - \ln (1 - \alpha) + \ln C_2^{\,o} + \beta^{\sigma} X^2 + B_2 \qquad [II\text{-}19]$$

Differentiating Eq. [II-19] with respect to α,

$$\frac{1}{C_t}\frac{dC_t}{d\alpha} = \frac{-1}{(1 - X)}\frac{dX}{d\alpha} + \frac{1}{(1 - \alpha)} + 2\beta^{\sigma}\frac{dX}{d\alpha} + \frac{dB_2}{d\alpha}$$

At the point of maximum synergism, i.e., when $dC_t/d\alpha = 0$,

$$\frac{dX}{d\alpha} = \frac{(1 - X^*)\left[1 + (1 - \alpha^*)\frac{dB_2}{d\alpha}\right]}{(1 - \alpha^*)[1 - 2\beta X^*(1 - X^*)]} \qquad [II\text{-}20]$$

Here

$$\frac{dB_1}{d\alpha} = \frac{d}{d\alpha}\left[\frac{\gamma(A_1^{\,o} - A_1)}{RT}\right]$$

$$\frac{dB_2}{d\alpha} = \frac{d}{d\alpha}\left[\frac{\gamma(A_2^{\,o} - A_2)}{RT}\right]$$

At constant γ, $A_1^{\,o}$ and $A_2^{\,o}$ are constants, thus

$$\frac{dB_1}{d\alpha} = \frac{-\gamma}{RT}\left(\frac{dA_1}{d\alpha}\right)$$

and $$= \frac{-Y}{RT}\left(\frac{dA_2}{d\alpha}\right)$$

$$\frac{dB_2}{d\alpha} = \frac{-Y}{RT}\left(\frac{dA_2}{d\alpha}\right)$$

At the point of maximum synergism,

$$\left(\frac{\partial A_1}{\partial \alpha}\right)_{\alpha = \alpha^*} = 0$$

and

$$\left(\frac{\partial A_2}{\partial \alpha}\right)_{\alpha = \alpha^*} = 0$$

Therefore, combining Eqs. [II-18] and [II-20], we have

$$X^* = \alpha^* \qquad \text{[II-21]}$$

indicating that at the point of maximum synergism in this respect, the mole fraction of either surfactant in the total surfactant at the monolayer equals its mole fraction in the total surfactant in the solution phase.

Combining Eqs. [II-21] and [II-16], knowing that $(1 - X)^2 > 0$, $A_1^o > A_1$ and $A_2^o > A_2$, we obtain the result that, for synergism to exist, β^σ must be negative.

Subtracting Eq. [II-13a] from Eq. [II-12a] and substituting the relationships, $C_1 = \alpha C_t$ and $C_2 = (1 - \alpha)C_t$, we obtain

$$\frac{\alpha(1 - X)C_2^o}{(1-\alpha)XC_1^o} = \exp\left[\beta^\sigma(1 - 2X) + (B_1 - B_2)\right]$$

At maximum synergism, $X^* = \alpha^*$, and

$$\ln \frac{C_1^o}{C_2^o} = \beta^\sigma(1 - 2X^*) + (B_1 - B_2) \qquad [II\text{-}22]$$

Since $|1 - 2X| < 1$ (i.e., $0 < X < 1$), we obtain a second condition for synergism in this respect:

$$|\ln (C_1^o/C_2^o) + (B_1 - B_2)| < |\beta^\sigma|$$

From Eq. [II-22],

$$\alpha^* = X^* = \frac{\ln \frac{C_1^o}{C_2^o} + \beta^\sigma + (B_1 - B_2)}{2\beta^\sigma} \qquad [II\text{-}23]$$

Substituting Eq. [II-23] into Eq. [II-12a],

$$C_{t,min} = C_1^o \exp\left\{\frac{[\beta^\sigma - \ln \frac{C_1^o}{C_2^o} - (B_1 - B_2)]}{4\beta^\sigma} + B_1\right\} \qquad [II\text{-}24]$$

where $C_{t,min}$ is the minimum total mixed surfactant concentration in the solution phase required to produce a given value of γ.

If surfactant 1 represents the more interfacial-active component, then the limiting condition for synergism in this respect is when

$$C_{t,lim} = C_1^o$$

Substituting this and $C_1 = \alpha_{lim} C_{t,lim}$ into Eq. [II-12a],

$$\alpha_{lim} = X_{lim} \exp [\beta^\sigma(1 - X_{lim})^2 + B_1] \qquad [II\text{-}25]$$

where α_{lim} is the limiting (minimum) mole fraction of surfactant 1 in the solution phase at which synergism exists and X_{lim} its mole fraction at the interface monolayer.

Introducing $C_{t,lim} = C_1^o$, $C_2 = (1 - \alpha_{lim})C_{t,lim}$, and Eq. [II-25] into Eq. [II-13a], we obtain:

$$\{1 - X_{lim} \exp [\beta^\sigma(1 - X_{lim})^2 + B_1]\}C_1^o = C_2^o(1 - X_{lim}) \exp (\beta^o X_{lim}^2 + B_2)$$

or

$$\frac{1 - X_{lim} \exp [\beta^\sigma(1 - X_{lim})^2 + B_1]}{1 - X_{lim}} = \frac{C_2^o}{C_1^o} \exp (\beta^\sigma X_{lim}^2 + B_2) \quad \text{II-26]}$$

Eq. [II-26] can be solved numerically for X_{lim} when C_1^o, C_2^o and β^σ are known. X_{lim} is introduced into Eq. [II-25] to yield α_{lim}.

II.A.3 Two Assumptions for the Molar Area of Surfactant in the Mixture

Two different treatments can be used to calculate surface mole fractions (X) and interaction parameters (β^σ) between different surfactant molecules in mixed interfacial monolayers. One treatment, which we shall designate treatment "E", is based upon the assumption that the average molar area of surfactant in the mixed system is not significantly different from that in the individual solutions. The second treatment, which was used on systems where it was known that molar areas in the mixed system are considerably different from those in the individual solutions (30), and which we designate treatment "R", is based upon the assumption that the ratio of the molar areas of the two surfactants in the mixed

monolayer is equal to that in the individual monolayers.

If the assumption is made that the area occupied by a mole of surfactant in the mixed monolayer of the mixture is not significantly different from that in a monolayer of the individual surfactant, i.e.,

$$A_1 \simeq A_1^o$$

and

$$A_2 \simeq A_2^o$$

then

$$B_1 = B_2 = 0$$

Eqs. [II-12] and [II-14] then become

$$\beta^\sigma = \frac{\ln \frac{C_1}{X C_1^o}}{(1 - X)^2} \qquad \text{[II-27]}$$

and

$$\frac{X^2}{(1 - X)^2} \frac{\ln \frac{C_1}{X C_1^o}}{\ln \frac{C_2}{(1 - X) C_2^o}} = 1 \qquad \text{[II-28]}$$

Eq. [II-28] can be solved numerically for X when C_1, C_2, C_1^o and C_2^o are known from experimental data. Substituting X and the relevant experimental quantities into Eq. [II-27] permits the evaluation of β^σ, the parameter related to molecular interactions between the two surfactants in the monolayer.

The minimum total mixed surfactant concentration to produce a given interfacial tension, $C_{t,lim}$, can be obtained from

$$C_{t,lim} = C_1^0 \exp \frac{\beta^\sigma - \ln \frac{C_1^0}{C_2^0}}{4\beta^\sigma} \qquad [II\text{-}29]$$

The limiting mole fraction of surfactant 1 in the solution phase and its mole fraction at the interface monolayer can be calculated from

$$\alpha_{lim} = X_{lim} \exp [\beta^\sigma (1 - X_{lim})^2] \qquad [II\text{-}30]$$

and

$$\{1 - X_{lim} \exp [\beta^\sigma (1 - X_{lim})^2]\} C_1^0 = C_2^0 (1 - X_{lim}) \exp (\beta^\sigma X_{lim}^2) \qquad [II\text{-}31]$$

Eqs. [27] and [28], which we have designated treatment "E", have been extensively used for nonionic-nonionic, nonionic-ionic, nonionic-betaine and betaine-ionic mixture systems (24,25,26,27,28,29).

If instead, the assumption is made that the ratio of the partial molar areas of the two surfactants in the mixed monolayer equals the ratio of the molar areas of the two individual surfactants at the same interfacial tension, i.e.,

$$\frac{A_1}{A_2} = \frac{A_1^0}{A_2^0} \qquad [II\text{-}32]$$

Equation [II-32] implies that A_1 is same fraction, k, of A_1^0, due to reduction of the repulsion between the ionic head groups and that A_2 is this same fraction of A_2^0, because of the mutual neutralization of charge by the oppositely-charged head groups in the mixed film. That is $A_1 = kA_1^0$ and $A_2 = kA_2^0$.

We have the relationship,

$$XA_1 + (1 - X)A_2 = A_{av} \qquad [II\text{-}33]$$

From Eqs. [II-32] and [II-33],

$$A_1 = \frac{A_{av}A_1^0}{XA_1^0 + (1 - X)A_2^0}$$

and

$$A_2 = \frac{A_{av}A_2^0}{XA_1^0 + (1 - X)A}$$

From these,

$$B_1 = \frac{Y(A_1^0 - A_1)}{RT} = \frac{YA_1^0\left[1 - \frac{A_{av}}{XA_1^0 + (1 - X)A_2^0}\right]}{RT} \qquad [II\text{-}34]$$

and

$$B_2 = \frac{Y(A_2^0 - A_2)}{RT} = \frac{YA_1^0\left[1 - \frac{A_{av}}{XA_1^0 + (1 - X)A_2^0}\right]}{RT} \qquad [II\text{-}35]$$

Eqs. [II-12] and [II-14] then become:

$$\beta^{\sigma} = \frac{\ln\frac{C_1}{C_1^0 X} - \frac{YA_1^0}{RT}\left[1 - \frac{A_{av}}{XA_1^0 + (1 - X)A_2^0}\right]}{(1 - X)^2} \qquad [II\text{-}36]$$

and

$$\frac{X^2}{(1-X)^2}\,\frac{\ln\dfrac{C_1}{C_1^{o}X}-\dfrac{\gamma A_1^{o}}{RT}\left[1-\dfrac{A_{av}}{XA_1^{o}+(1-X)A_2^{o}}\right]}{\ln\dfrac{C_2}{C_2^{o}(1-X)}-\dfrac{\gamma A_2^{o}}{RT}\left[1-\dfrac{A_{av}}{XA_1^{o}+(1-X)A_2^{o}}\right]}=1 \qquad \text{[II-37]}$$

Since C_1^{o}, A_1^{o}, C_2^{o}, A_2^{o}, C_1, C_2 and A_{av} can be obtained from experimental data, the mole fraction of surfactant 1 at the interfacial monolayer, X, can be solved numerically from Eq. [II-37]. Substituting X into Eq. [II-36], the interaction parameter, β^{σ}, can be obtained.

Since B_1 and B_2 can be calculated from Eqs. [II-34] and [II-35] based upon experimental data, Eqs. [II-24], [II-26] and [II-25] can be solved for $C_{t,lim}$, X_{lim} and α_{lim}.

It is apparent from a comparison of Eqs. [II-27], [II-28] with Eqs. [II-36], [II-37] that as the quantity, $1 - A_{av}/[XA_1^{o} + (1 - X)A_2^{o}]$, which we shall call the "packing deviation factor", decreases, the two sets of equations become more and more similar and that when the quantity equals zero, the two sets of equations are the same. When the "packing deviation factor" is positive, then β^{σ}_R will be more negative then β^{σ}_E; when it is negative, then β^{σ}_R will be more positive than β^{σ}_E. The difference between β^{σ}_E and β^{σ}_R should also decrease with decrease in the value of γ.

In binary surfactant mixture systems containing swamping excesses of electrolyte with common ions, the surface excess concentrations of surfactant 1 and 2, Γ_1 and Γ_2, respectively, are

given by the Hutchinson method (107)

$$\Gamma_1 = \frac{-1}{RT}\left(\frac{\delta \gamma}{\delta \ln C_1}\right)_{C_2} \qquad [II-38]$$

and

$$\Gamma_2 = \frac{-1}{RT}\left(\frac{\delta \gamma}{\delta \ln C_2}\right)_{C_1} \qquad [II-39]$$

where γ is the interfacial tension of the mixed surfactant solution, and C_1 and C_2 are the molar concentrations of surfactant 1 and 2. The mole fractions of surfactants 1 and 2 in the interfacial monolayer are related to their relative adsorptions by the expressions:

$$X_1 = \frac{\Gamma_1}{\Gamma_1 + \Gamma_2} \quad \text{and} \quad X_2 = \frac{\Gamma_2}{\Gamma_1 + \Gamma_2} \qquad [II-40]$$

This permits comparison of X values, obtained by this method, with those obtained by treatments "E" and "R".

II.A.4 Synergism in S/L Interfacial Tension Reduction Efficiency

For a hydrophobic (low-energy-surface) solid, γ_{sv} may be considered to be constant with change in the concentration of surfactant in the aqueous phase. From Young's equation,

$$\gamma_{sl} = \gamma_{sv} - \gamma_{lv}\text{Cos}\theta \qquad [II-41]$$

the surfactant solution at the same value of $\gamma_{lv}\text{Cos}\theta$ will have the

same value of γ_{sl} and can consequently be used to evaluate the quantities in Eq. [II-37]. C_1^o, A_1^o, C_2^o, A_2^o, C_1, C_2 and A_{av} can be obtained from plots of $\gamma_{lv}\text{Cos}\theta$ versus log C_t, the total molar concentration of surfactant in the solution phase, for the two pure surfactants and their mixtures by selecting values at the same $\gamma_{lv}\text{Cos}\theta$ product in all cases.

γ_{sl} for a low-energy-surface solid can be evaluated from Eq. [II-41] by assuming that γ_{sv} can be approximated by γ_c, the critical surface tension (90). This permits Eq. [II-37] to be solved numerically for X, the mole fraction of surfactant 1 in the S/L interfacial monolayer.

Substituting X and the relevant experimental quantities into Eq. [II-36] permits the evaluation of β^{σ}_{sl}, the parameter related to molecular interactions between the two surfactants in the S/L interfacial monolayer.

Synergism in S/L interfacial tension reduction efficiency exists in a solution of mixed surfactants in contact with a solid when a given S/L interfacial tension (reduction) can be obtained at a total mixed surfactant concentration in the solution phase lower than that required of any component of the mixture. Since for a hydrophobic (low-energy-surface) solid, it can be assumed that γ_{sv} is a constant, from Young's equation, Eq. [II-41], the value of $\gamma_{lv}\text{Cos}\theta$, the "adhesion tension", determines the value of γ_{sl}. Synergism in S/L interfacial tension reduction efficiency will therefore be present

in the system if it can attain a given value of $\gamma_{lv}Cos\theta$ at a total surfactant concentration lower than that required of either component of the mixture, i.e., for solutions containing two surfactant, $C_t < C_1^o, C_2^o$.

$C_{t,min}$ is the minimum total mixed surfactant concentration in the solution phase to produce a given value of $\gamma_{lv}Cos\theta$. Since, for hydrophobic (low-energy-surface), $C_{t,min}$ is also the minimum mixed surfactant concentration required to produce a given S/L interfacial tension, it can be calculated from Eq. [II-24]. Similarly α_{lim} is the limiting (minimum) mole fraction of surfactant 1 in the solution phase at which synergism exists and X_{lim} its mole fraction in the S/L interfacial monolayer. α_{lim} and X_{lim} can be obtained from Eqs. [II-25] and [II-26].

II.B Free Energy of Adsorption at an Interface

The two-dimensional solution approach has been used more extensively than the 2-D gas approach to treat many surface phenomena and to study theoretically (41,71,108) because it is a more accurate picture of the interface. In the 2-D solution approach the chemical potential of component i at the interface can be expressed by the equation (67)

$$\mu_i^s = \mu_i^{os} + RT \ln f_i^s X'^s_i + \pi A_i \qquad [II-42]$$

where μ_i^{os} is the standard chemical potential of component i at S/L interface with standard state defined as a pure component i, X'^s_i is mole fraction of the component i in the total surfactant and solvent in the surface layer, f_i^s its activity coefficient, π is the interfacial pressure and A_i is the partial mole area of component i at the interface.

In the bulk phase

$$\mu_i^b = \mu_i^{ob} + RT \ln f_i^b X'^b_i \qquad [II-43]$$

where the μ_i^{ob} is the chemical potential of the pure i'th species in the bulk phase, f_i^b and X'^b_i are the activity coefficient and mole fraction of surfactant i in the bulk phase.

The thermodynamic condition at equilibrium between the interfacial phase and the bulk phase is

$$\mu_i^s = \mu_i^b$$

From Eqs. [II-42] and [II-43],

$$\mu_i^{os} - \mu_i^{ob} + RT \ln \frac{f_i^s}{f_i^b} = RT \ln \frac{X_i'^b}{X_i'^s} - \pi A_i \qquad [II-44]$$

The standard free energy of adsorption of i'th component at infinite dilution is

$$\Delta G_i^o = \mu_i^{os} - \mu_i^{ob} \qquad [II-45]$$

And the extra free energy of adsorption at a given interfacial pressure due to the interactions between the components and related to the activity coefficients is

$$\Delta G_i^E = RT \ln \frac{f_i^s}{f_i^b} \qquad [II-46]$$

At infinite dilution the activity coefficients (f_i^b, f_i^s) are unity and the surface pressure (π) tends to zero. The extra free energy of adsorption is zero. The standard free energy of adsorption is related to the distribution coefficient (a_i) at infinite dilution (75) i.e.

$$\Delta G_i^o = RT \, \mathrm{Lim}_{\pi \to 0} \mathrm{Ln} \, X'^b_i / X'^s_i$$

$$= RT \ln a_{i \, \pi \to 0}$$

From Eqs. [II-44], [II-45] and [II-46], the free energy of adsorption of the i'th component at a given interfacial pressure is:

$$\Delta G_i = \Delta G_i^o + \Delta G_i^E$$

$$= RT \ln \frac{X_i'^b}{X_i'^s} - \pi A_i \qquad [II-47]$$

Thus the mole fraction of the component i at the interface is related to the free energy of adsorption by the expression:

$$X_i^{'s} = X_i^{'b} \exp \frac{-\Delta G_i - \pi A_i}{RT} \qquad [II-48]$$

The Gibbs' surface is chosen as the interface where the surface excess of solvent ($\Gamma_{solvent}$) is equal to zero. Therefore the free energy of adsorption of water in the aqueous solution is almost zero (109). According to the same idea, the area per molecule of water in the interface is 9.7 A^{o2} (molar area of water = 58.2 x 10^3 m^2), based on the molecular dimensions of bulk water.

The mole fraction of water at interface is related to the mole fraction of water in bulk phase ($X'^{b}_{H_2O}$) and surface pressure through equation:

$$X'^{s}_{H_2O} = X'^{b}_{H_2O} \exp \frac{-\pi \times 58.2 \times 10^3}{RT} \qquad [II-49]$$

Since the Gibbs' surface is an electroneutral surface, only electroneutral combinations can be considered. From Eq. [II-47], the free energy of adsorption of any electroneutral combination should be expressed:

$$\Delta G_{ij} = RT \ln \frac{X_i^{'b} X_j^{'b}}{X_i^{'s} X_j^{'s}} - \pi A_{ij} \qquad [II-50]$$

At the interface of an individual cationic (R^+Y^-) or anionic

(R^-M^+) surfactant solution:

$$X'^{s}_{H_2O} + X'^{s}_{R^+} + X'^{s}_{Y^-} = 1$$

or

$$X'^{s}_{H_2O} + X'^{s}_{R^-} + X'^{s}_{M^+} = 1 \qquad [II-51]$$

Following the electroneutrality condition of the interface, we have:

$$X'^{s}_{R^+} = \frac{1 - X'^{s}_{H_2O}}{2}$$

$$X'^{s}_{R^-} = \frac{1 - X'^{s}_{H_2O}}{2} \qquad [II-52]$$

Using the Gibbs' adsorption theorem, the partial mole surface area of cationic or anionic surfactant can be obtained from experimental data as follows:

$$\Gamma(R^+Y^-) = \frac{1}{nRT} \frac{-d\gamma}{d \ln C_{(R^+Y^-)}}$$

or

$$\Gamma(R^-M^+) = \frac{1}{nRT} \frac{-d\gamma}{d \ln C_{(R^-M^+)}}$$

where $\Gamma_{(R^+Y^-)}$ or $\Gamma_{(R^-M^+)}$ are surface excess concentration of R^+Y^- or R^-M^+ pairs and coefficient n is 1 or 2 in presence or absence of added excess inorganic salt.

And $$A(R^+Y^-) = \frac{1}{\Gamma(R^+Y^-)}$$

or

$$A(R^- M^+) = \frac{1}{\Gamma(R^- M^+)} \qquad [II-53]$$

At the interface of a solution of a mixture of cationic (R^+Y^-) and anionic (R^-M^+) surfactants

$$X'^{s}_{H_2O} + X'^{s}_{R+} + X'^{s}_{Y-} + X'^{s}_{R-} + X'^{s}_{M+} = 1 \qquad [II-54]$$

In the case where the cationic surfactant is more active than the anionic surfactant, i.e., $X_{R+} > 0.5$ (where X_{R+} is the mole fraction at the interface, using the 2-D gas model) we have:

$$X'^{s}_{M+} = 0 \quad \text{and} \quad X'^{s}_{R+} = X'^{s}_{Y-} + X'^{s}_{R-}$$

therefore Eq. [II-54] gives

$$X'^{s}_{R+} = \frac{1 - X'^{s}_{H_2O}}{2} \qquad [II-55]$$

Similarly, in the case where the anionic surfactant is more active, i.e., $X_{R-} > 0.5$,

$$X'^{s}_{Y-} = 0 \quad \text{and} \quad X'^{s}_{R-} = X'^{s}_{R+} + X'^{s}_{M+}$$

and

$$X'^{s}_{R-} = \frac{1 - X'^{s}_{H_2O}}{2} \qquad [II-56]$$

We now make the reasonable assumption that the ratio of the two surface active ions of the interface is the same, irrespective of whether the 2-D gas or the 2-D solution treatment is used:

$$\frac{X^{'s}_{R^+}}{X^{'s}_{R^-}} = \frac{X_{R^+}}{X_{R^-}} = \frac{X_{R^+}}{1 - X_{R^+}} \qquad [II-57]$$

Using this assumption in Eqs. [II-55] and [II-56] for the more active cationic surfactant and more active anionic surfactant, respectively, produces:

$$X^{'s}_{R^-} = \frac{1 - X_{R^+}}{X_{R^+}} \frac{1 - X^{'s}_{H_2O}}{2} \qquad [II-58]$$

and

$$X^{'s}_{R^+} = \frac{X_{R^+}}{1 - X_{R^+}} \frac{1 - X^{'s}_{H_2O}}{2} \qquad [II-59]$$

The molar surface area of mixed surfactant solution at the air/aqueous solution interface can be obtained from the Gibbs' surface excess concentration:

$$\Gamma_{mix} = \frac{-1}{nRT} \left(\frac{dY}{d \ln C_{mix}} \right)_{\alpha}$$

where n equal 1 or 2X, X is mole fraction of more surface active surfactant, in presence or absence of extra inorganic electrolyte.

And

$$A_{mix} = \frac{1}{\Gamma_{mix}} \qquad [II-60]$$

Similarly, at the solid/aqueous solution interface the molar

surface areas of individual and mixed surfactant solutions are:

$$\Gamma_{sl} = \frac{-1}{nRT} \frac{d\gamma_{sl}}{d \ln C}$$

$$= \frac{-1}{nRT} \frac{d(\gamma_{sv} - \gamma_{lv} \cos\theta)}{d \ln C}$$

$$= \frac{1}{nRT} \frac{d(\gamma_{lv} \cos\theta)}{d \ln C}$$

$$A_{sl} = \frac{1}{\Gamma_{sl}} \qquad \text{[II-61]}$$

and

$$\Gamma_{sl,mix} = \frac{-1}{nRT} \frac{d\gamma_{sl}}{d \ln C_{mix}}$$

$$= \frac{1}{nRT} \frac{d(\gamma_{lv} \cos\theta)}{d \ln C_{mix}}$$

$$A_{sl,mix} = \frac{1}{\Gamma_{sl,mix}} \qquad \text{[II-62]}$$

respectively, where the assumption of constant γ_{sv} is made for a low-energy-surface solid.

In the case of more active cationic surfactant, the molar surface areas A_{R+R-} and A_{R+Y-} of mixed surfactant solution are

related to A_{mix} through the equation

$$X_{R^+R^-} A_{R^+R^-} + X_{R^+Y^-} A_{R^+Y^-} = A_{mix} \qquad [II-63]$$

Since number of R^+R^- and R^+Y^- pars is equal to the number of R^- and Y^-, respectively, and $X^s_{Y^-} + X^s_{R^-} = X^s_{R^+}$, from Eq. [II-57] the mole fraction of R+R- and R+Y- at interface of mixture solution are

$$X_{R^+R^-} = \frac{X'^s_{R^-}}{X'^s_{R^-} + X'^s_{R^+}}$$

$$= \frac{1 - X_{R^+}}{X_{R^+}} \qquad [II-64]$$

and

$$X_{R^+Y^-} = \frac{X'^s_{Y^-}}{X'^s_{R^+} + X'^s_{Y^-}}$$

$$= 1 - \frac{1 - X_{R^+}}{X_{R^+}}$$

$$= \frac{2X_{R^+} - 1}{X_{R^+}} \qquad [II-65]$$

respectively.

Combining Eqs. [II-63], [II-64] and [II-65]

$$A_{R^+R^-} = \frac{A_{mix} - (2 - \frac{1}{X_{R^+}}) A_{R^+Y^-}}{\frac{1 - X_{R^+}}{X_{R^+}}}$$

$$= \frac{A_{mix} X_{R^+} - (2X_{R^+} - 1) A_{R^+Y^-}}{1 - X_{R^+}} \qquad [II-66]$$

where A_{mix} and $A_{R^+Y^-}$ are the molar surface areas of the mixed surfactant and pure R^+Y^- solution at the interface, obtained from experimental data. Similarly, the molar surface area of R^+R^- in the case of a more active anionic surfactant is:

$$A_{R^+R^-} = \frac{A_{mix} X_{R^-} - (2X_{R^-} - 1) A_{R^-M^+}}{1 - X_{R^-}} \qquad [II-67]$$

The surface pressure at the air/aqueous solution interface is

$$\pi_{lv} = \gamma^{\circ}_{lv} - \gamma_{lv} \qquad [II-68]$$

where γ°_{lv} is the surface tension of pure water. Similarly, the interfacial pressure at the solid/aqueous solution interface is

$$\pi_{sl} = \gamma^{\circ}_{sl} - \gamma_{sl} \qquad [II-69]$$

where γ°_{sl} is interfacial tension at the solid/pure water interface. Using Young's equation, $\gamma_{sl} + \gamma_{lv} \text{ Cos } \theta = \gamma_{sv}$, in Eq. [II-69] yields

$$\pi_{sl} = \gamma^{\circ}_{sv} - \gamma^{\circ}_{lv} \text{ Cos } \theta^{\circ} - \gamma_{sv} + \gamma_{lv} \text{ Cos } \theta$$

$$= \gamma_{lv} \text{ Cos } \theta - \gamma^{\circ}_{lv} \text{ Cos } \theta^{\circ} \qquad [II-70]$$

in which the assumption that $\gamma^{\circ}_{sv} = \gamma_{sv}$ is reasonable and θ° is the contact angle at the solid/pure water interface. Therefore, from experimental data, the free energies of adsorption of the individual and mixed surfactants at various interfacial pressures can be evaluated by using Eqs. [II-47] and [II-50], respectively.

CHAPTER III

EXPERIMENTAL

III.A Materials

III.A.1 Surface-Active Agents

1 - 1 Purchased Surfactants

Sodium octanesulfonate, $C_8H_{17}SO_3Na$ (C_8SO_3Na), decanesulfonate, $C_{10}H_{21}SO_3Na$ ($C_{10}SO_3Na$), and dodecanesulfonate, $C_{12}H_{25}SO_3Na$ ($C_{12}SO_3Na$) all were obtained from Research Plus, Inc., Bayonne, NJ. The elemental analysis and theoretical values are shown in Table A - 1.

Sodium dodecyl sulfate, $C_{12}H_{25}SO_4Na$ ($C_{12}SO_4Na$), purity better than 99%, was purchased from Research Plus, Inc., Bayonne,

NJ.

N-Dodecyloctaethyleneglycol, $C_{12}H_{25}(OC_2H_4)_8OH$ ($C_{12}(EO)_8$), was purchased from Nikko Chemical Co., Tokyo, Japan. The purity is greater than 98%, as indicated by gas chromatography.

Table A - 1

Elemental Analyses of Sodium Alkyl Sulfonates

Chemical		C %	H %	S %
C_8SO_3Na	Theoretical	44.43	7.92	14.82
	Found	44.66	8.05	14.88
$C_{10}SO_3Na$	Theoretical	49.14	8.69	13.13
	Found	49.40	8.71	13.28
$C_{12}SO_3Na$	Theoretical	52.92	9.25	11.77
	Found	53.06	9.43	11.36

1 - 2 Synthesized Surfactants

1 - 2.1 Preparation of N-Alkyl Pyridinium Bromides, $C_nH_{2n+1}(C_5H_5N)Br$

Three homologous, in which n = 8 (C_8NBr), n = 10 ($C_{10}NBr$) and n = 12 ($C_{12}NBr$), were synthesized by the SN_2 nucleophilic substitution reaction of the appropriate 1-bromoalkane with pyridine.

$$C_nH_{2n+1}Br + C_5H_5N \dashrightarrow C_nH_{2n+1}C_5H_5N^+Br^-$$

1 - 2.1.1 N-Octylpyridinium Bromide, C_8H_{17}-$(C_5H_5N^+)Br^-$

Two methods were used to prepare n-octylpyridinium bromide (C_8NBr):

Method A

1-Bromooctane (Aldrich, 99% purity by I.R. and G.C.), 50 g (0.26 mole), was mixed with twenty molar per cent excess of pyridine (J. T. Baker, assay 99.9% by G.C., dried over KOH). The mixture was headed under reflux at 115 °C for 24 hours (110), during which time the color of the mixture changed to dark brown.

Method B

The mixture was allowed to stand at room temperature with occasional shaking (8). The mixture originally contained two separate phases which, after 20 days, changed to one brown phase.

The excess pyridine in the crude product was stripped off at reduced pressure, using a rotary evaporator. The residue was dissolved in 100 ml of a hot mixture of acetone and tetrahydrofuran

(V/V, 1:1) and crystallized in a "dry ice" cooling bath. The crystals were dissolved in 180 ml of hot methanol and decolorized by using G-60 activated carbon (Darco, ICI America Inc.). After the mixture had been filtered, the methanol was removed from the filtrate. The white residue was recrystallized repeatedly once from acetone and four times from 2-butanone. The white crystals were dried in vacua over phosphorus pentoxide at room temperature for 4 days to constant weight. The products weighed 34.2 g and 39.6 g (48.5% and 56.2% of the theoretical yield) for method A and method B, respectively. The elemental analysis results are shown in Table A - 2.

1 - 2.1.2 N-Decylpyridinium Bromide, $C_{10}H_{21}$-($C_5H_5N^+$)Br^-

1-Bromodecane (Aldrich, 98%), 32.0 g (0.145 moles), and pyridine (J. T. Baker, assay 99.9% by G.C., dried over KOH), 13.7 g (0.173 moles) were mixed.

The color of the crude products, obtained by method A was tan. By method B the mixture changed to a light yellow phase at the fourteenth day.

The procedure for recrystallization and decolorization was the same as that used for n-octylpyridinium bromide. The yields of a white, crystal product were 23.9 g (55.0% of the theoretical) and 26.2 g (60.2% of the theoretical yield) for method A and method B, respectively.

The modified two-phase dye transfer titration method, developed by Li and Rosen (111) using 2 : 3 (V/V) chloroform :

1-nitropropane as the organic phase and a multiple extraction-titration technique, was used to check the purity of the product using sodium dodecanesulfonate solution of known concentration. Details of the procedure are given in the Purification and Concentration Determination of Surfactant Solution section, below. The purity of the n-decylpyridinium bromide ($C_{10}NBr$) was 100.2%. The elemental analysis results are listed in Table A - 2.

1 - 2.1.3 N-Dodecylpyridinium Bromide, $C_{12}H_{21}$-$(C_5H_5N^+)Br^-$

The procedure was similar to that used for n-octylpyridinium bromide and n-decylpyridinium bromide.

The reaction mixture was 1-bromododecane (Humphrey, 97% purity), 31.0 g (0.124 moles), and twenty molar per cent excess pyridine (J. T. Baker, assay 99.9% by G.C., dried over KOH).

The colors of crude products were brown and light brown by method A and B, respectively. By method B, the mixture changed to a homogeneous phase after only ten days.

After removal of the excess pyridine under reduced pressure the crude products were crystallized from acetone and then decolorized by use of G-60 activated carbon. The white solid residue was recrystallized four times from methyl ethyl ketone. The product was dried in vacuo over phosphorus pentoxide for four days at room temperature.

The yields of products were 24.9 g (61.2% of the theoretical) and 26.6 g (65.4% of the theoretical yield) by method A and B, respectively. The purity of n-dodecylpyridinium bromide ($C_{12}NBr$)

was 99.8%, by the usual 2-phase dye transfer titration with sodium dodecylsulfonate solution using acidic mixed indicators (112). Details of the technique are given in the Purification and Concentration Determination of Surfactant Solutions section, below.

The elemental analysis results are listed in Table A - 2.

Table A - 2

Elemental Analyses of Alkylpyridinium Bromides

Chemical		C %	H %	N %
C_8NBr	Theoretical	57.36	8.15	5.15
	Found	57.36	8.32	5.53
$C_{10}NBr$	Theoretical	60.00	8.73	4.66
	Found	59.96	8.70	4.62
$C_{12}NBr$	Theoretical	62.19	9.21	4.27
	Found	62.16	9.13	4.11

1 - 2.2 Preparation of N-Alkyltrimethylammonium Bromides, $C_nH_{2n+1}N^+(CH_3)_3Br^-$

Two homologues, in which n = 12 (C_{12}TMABr) and n = 14 (C_{14}TMABr), were synthesised by SN_2 nucleophilic substitution, using the appropriate 1-bromoalkane and trimethylamine.

$$C_nH_{2n+1}Br + N(CH_3)_3 \dashrightarrow C_nH_{2n+1}N^+(CH_3)_3Br^-$$

1 - 2.2.1 N-Dodecyltrimethylammonium Bromide, $C_{12}H_{25}N^+(CH_3)_3Br^-$

1-Bromododecane (Aldrich, 98% purity), 45.0 g (0.203 mole), was mixed with a twenty five percent excess of thirty three per cent trimethylamine in ethanol (Fluka). The reaction mixture was heated under reflux for twelve hours.

The ethanol and excess trimethyl amine were evaporated by rotary evaporator under reduced pressure. The white residue was dissolved in 75 ml of hot acetone and then crystallized in a "dry ice" cooling bath. The solid was recrystallized five times from methyl ethyl ketone. The white product was dried over phosphorus pentoxide in vacuo for four days to constant weight. The yield of n-dodecyltrimethylammonium bromide was 32.0 g (56.3% of the theoretical yield).

The purity of the product was 99.5%, by titration with sodium dodecanesulfonate solution of known concentration, using the regular 2-phase dye transfer titration technique and acidic mixed indicator (112).

1 - 2.2.2 N-Tetradecyltrimethylammonium Bromide, $C_{14}H_{25}N^{+}(CH_3)_3Br^{-}$

The procedure was same as that used for n-dodecyltrimethylammonium bromide.

1-Bromotetradecane (Humphrey, 97% purity), 55.5 g (0.200 moles), was mixed with twenty five molar percent excess trimethyl amine. After ten hours of refluxing a light yellow crude product was formed. Crystallization of the crude product once from acetone and four times from methyl ethyl ketone yielded 38.8 g of a white crystalline product (57.7% of the theoretical yield).

The purity of n-tetradecylammonium bromide was 99.8%, as determined by the usual two phase titration with sodium dodecanesulfonate solution, using acidic mixed indicator.

1 - 2.3 Preparation of N-Dodecyl, N-Benzyl, N-Methylglycine, $C_{12}H_{25}N^{+}(CH_2C_6H_5)(CH_3)CH_2COO^{-}$

N-Dodecyl, N-benzyl, N-methylglycine, (C_{12}BMG), was synthesized in this laboratory (113) by heating the mixture of N-methylbenzylamine (200% molar excess) and sodium chloroacetate in 95% ethanol at reflux temperature of 60 °C. The purity of C_{12}BMG is not less than 98%.

1 - 3 Purification and Concentration Determination of Aqueous Surfactant Solutions for Surface Tension and Contact Angle Measurements

Aqueous solutions of surfactants, used for surface tension and contact angle measurements, were prepared with quartz-condensed water. All solutions of surfactant (except C_8SO_3Na) at a concentration below their critical micelle concentration (C.M.C.) were further purificated by passing them three times through high-density chromatographic columns of octadecylsilanized silica gel (SEP-PAK C_{18} Cartridge, Water Associates, Milford, MA) (114) to remove any traces of impurities more interfacial active than the parent compound. C_8SO_3Na was purified by extracting it with ethyl ether for 48 hours.

The solutions of the individual surfactants reached equilibrium surface tension (when the difference between two succession readings, taken at ten to fifteen minutes intervals between readings, was less than 0.1 $mN\text{-}m^{-1}$) within one hour. There was no minimum in the surface tension versus logarithm concentration curve in the region of the C.M.C. for any of the surfactants.

The concentration of the C_8SO_3Na solution was determined by accurately weighing the ethyl ether-extracted chemical (dried in vacuo over phosphorus pentoxide to constant weight) to 0.1 mg and preparing the solution in a volumetric flask.

Two-phase titration using acidic mixed indicator was used to determine the concentration of the other ionic surfactant solutions, after passage through the SEP-PAK columns first. The titration is based upon the transfer of dye-anionic surfactant complex between aqueous phase and organic phase. The organic-soluble complex of an anionic surfactant with a basic dye is distroyed by the cationic surfactant and the dye is released into the water phase and the complex of anionic and cationic surfactants enters the organic phase (chloroform, or mixture of chloroform and 1-nitropropane).

The multiple extraction, two phase dye transfer technique, developed by Li and Rosen (111) was used to determine surfactant concentration of $C_{10}SO_3Na$ solutions. The solution was titrated with the cationic surfactant solution, Hyamine 1622, of known concentration, using acidic mixed indicator (see below). To ten ml of the anionic surfactant solution of the unknown concentration solution (approximately 2 ~ 3 X 10^{-3} M) in a 150-ml separatory funnel were added ten ml of acidic mixed indicator solution and fifteen ml of a 2:3 V/V mixture of chloroform (AR, Fisher Scientific Co., Fair Lawn, NJ) and 1-nitropropane (AR, Eastern Chemical, Hauppauge, NY). This mixture was titrated with the Hyamine 1622 solution, with vigorous shaking after each addition, until the organic layer showed a light grey color without trace of pink color (the end point). Then the lower (organic) layer was drained through the stopcock at the bottom of the funnel. To the aqueous solution in the funnel was added another 15 ml of the organic

mixture and the whole was shaken well. Titration with same Hyamine solution was continued to a new end point. The organic layer was again withdrawn. After titration and removal of the organic layer a third time no additional Hyamine solution was required to reach the end point. The concentration of $C_{10}SO_3Na$ solution was determined from the total consumption of the Hyamine solution.

The usual (single) titration procedure was used to determine the concentrations of $C_{12}SO_3Na$ and $C_{12}SO_4Na$ solutions. Ten ml of approximately 2 ~ 3 X 10^{-3} M $C_{12}SO_3Na$ or $C_{12}SO_4Na$ solution was pipetted into a 250 ml, glass-stoppered, Erlenmeyer flask. 15 ml of chloroform and 10 ml of acidic mixed indicator were added to the solution. Hyamine solution of known concentration was titrated into the anionic surfactant solution with vigorous shaking after each addition, until the end point was reached. The concentration of anionic surfactant solution was calculated from the volume and concentration of the Hyamine solution.

The procedure used to determine the concentrations of cationic surfactant (C_{12}TMABr and C_{14}TMABr) solutions, was the same as that used for the $C_{12}SO_3Na$ solution, except that the anionic surfactant ($C_{12}SO_3Na$) of known concentration was used to check the cationic surfactant solution of unknown concentration.

The standard cationic surfactant solution, used to titrate the anionic surfactant solutions, was prepared by using

diisobutylphenoxyethoxyethyl dimethyl benzyl ammonium chloride (Hyamine 1622) (98.8% purity, Rohm and Haas Co., PA). The purity of Hyamine 1622 was determined by titrating against sodium dodecyl sulfate (BDH Chemical, Ltd., Poole, England). On the basis of this, the molar absorptivity of the sample of Hyamine 1622 was determined to be 1266 $L\text{-}mol^{-1}\text{-}cm^{-1}$ at wavelength of 269.5 nm. The concentration of all subsequent Hyamine solutions were checked by ultraviolet absorbance and the above value of the molar absorptivity was used. The solution was prepared with deionized distilled water and had a concentration of approximate 1 $X10^{-3}$ molarity.

The acidic mixed indicator was made from dimidium bromide (Burroughs Wellcome Co., Ltd., London, England) and Erioglaucine (also called Disulphine Blue V) (BDH Chemical Ltd., Poole, England) (113,115). Weigh 0.5 ± 0.005g of dimidium bromide into a 50 ml beaker and weigh Disulphine Blue V, 0.25 ± 0.005 g, into another 50 ml beaker. Add 25 ml of 10% (volume) hot ethanol in water to each beaker. Stir the solutions to dissolve the dye, then transfer them to a 250 ml volumetric flask and dilute to the mark with the hot 10% ethanol solution. This solution was saved as stock solution in a brown bottle. Transfer 20 ml of the above stock solution, 200 ml of deionized distilled water and 20 ml of 2.5 M sulfuric acid into a 500 ml graduated flask and shake it well, then dilute to 500 ml with distilled water. This is the acidic mixture indicator used for the two-phase titration of cationic or anionic

surfactant solutions.

The concentrations of aqueous solutions of C_8NBr, $C_{10}NBr$, $C_{12}NBr$ and $C_{12}BMG$ were measured by ultraviolet absorbance. The molar absorptivities (ε) and maximum absorption wavelengths (λ_{max}), in aqueous solution without inorganic electrolyte, are shown in Table A - 3.

The concentration of $C_{12}(EO)_8$ solutions, after purification through SEP-PAK columns, was determined from standard curves of surface tension versus logarithm concentration of pure $C_{12}(EO)_8$ solutions measured in this laboratory (110).

Table A - 3

Molar Absorptivities and Maximum Absorption Wavelengths of C_nNBr and $C_{12}BMG$

Compound	Solvent	Maximum Absorption Wavelength λ(nm)	Molar Absorptivity $\varepsilon X10^{-3}$ ($L\text{-}mol^{-1}\text{-}cm^{-1}$)
C_8NBr	H_2O	259	3.910
$C_{10}NBr$	H_2O	259	3.960
$C_{12}NBr$	H_2O	259	4.020[a]
$C_{12}BMG$	H_2O	263	0.334[b]

a. Value shown in Ref. (110):

$C_{12}NBr$--$3.88X10^3$; $C_{12}NCl$--$4.08X10^3$

Value shown in J. Colloid Interface Sci., 1966, 21,522:

$C_{12}NCl$--$4.09X10^3$; $C_{12}NBr$--$3.82X10^3$;

$C_{12}NI$--$4.29X10^3$ at 260 nm.

b. Value shown in Ref. (110): $3.55X10^2$.

III.A.2 Water and Inorganic Salts

The water used for the preparing of surfactant solutions was deionized first and then distilled twice (the last distillation being from alkaline $KMnO_4$ solution, through a three-foot high Vigreaux column with quartz condenser and receiver). The specific conductivity of the quartz-condensed water is 1.1 $X10^{-6}$ mho-cm^{-1} at 25 °C and the value of pH is about 5.8.

Sodium bromide (assay 100.5%, J. T. Baker Chemical Co., Phillipsburg, NJ) and sodium chloride (100.00% standard, Thom Smith Chemist, Beulah, MI), using to adjust the ionic strength of surfactant solutions, were baked over six hours in a porcelain casserole at red head to remove traces of organic compounds. In order to ensure the absence of traces of surface-active impurities the surface tensions of aqueous solutions of the baked salts were checked. The surface tensions of 0.1 N NaCl and 0.1 N NaBr aqueous solution are 72.3 mN-m^{-1} and 72.2 mN-m^{-1} at 25 °C.

III.A - 3 Treatments of Solid Surface

Low-energy solid surfaces were made from Teflon (0.25 mm thickness, E. I. du Pont de Nemous & Co., Wilmington, DEL), Parafilm ("M" Laboratory film, American Can Co., Greenwith, CT) and Polyethylene (0.12 mm thickness, Scotch 3M, St. Paul, MN) tapes, cut as rectangular pieces (1.2 x 2.5 cm^2) and pressed onto clean microscope slides. The surfaces of Teflon and Polyethylene

were brushed gently with a detergent solution and then rinsed repeatedly with tap water, shaken free of any water drops and rinsed first with n-hexane (AR, Fisher Scientific, Fair Lawn, NJ) and then with methanol (Spectranalyzed, Fisher Scientific, Fair Lawn, NJ). Finally, the surfaces were rinsed with deionized distilled water and then with quartz-condensed water. Parafilm was used after removal from the roll, without further cleaning treatment. All surfaces were dried over phosphorus pentoxide in a desiccater for twelve hours before the measurement of contact angles.

The contact angles of the quartz-condensed water at the Teflon, Parafilm and polyethylene surfaces were 111.9°, 112.5° and 93.3°, respectively. The contact angles at Teflon and polyethylene surfaces are agreed well with literature values of 112° for Teflon (116) and 94° for polyethylene (117). The contact angle on Parafilm is higher than the value of 110° for paraffin (116,118). This means the Parafilm surface has a lower energy than that of paraffin.

The effects of pretreatments of the solid surface on contact angles are shown in Tables A - 4 and A - 5.

Table A - 4

The Effect of Pretreatments on Contact Angle Measurements at the Teflon Surface

	PRETREATMENT	CONTACT ANGLE
a.	None	100.2°
b.	Rinse with detergent solution and then with quartz-condensed water and equilibrate over water 12 hours	110.1°
c.	Rinse with detergent solution then with quartz water and dry over P_2O_5 for 12 hours	110.4°
d.	Rinse with detergent solution then successively with n-hexane, methanol and quartz water and equilibrate over water for 12 hours	111.3°
e.	Rinse with detergent solution then successively with n-hexane, methanol and quartz water and dry over P_2O_5 for 12 hours	111.9°

Table A - 5

The Effect of Pretreatments on Contact Angle Measurements at the Parafilm Surface

	PRETREATMENT	CONTACT ANGLE
a.	None	112.5°
b.	Equilibrate over water for 12 hours	112.1°
c.	Rinse with quartz water and equilibrate over water for 12 hours	112.1°
d.	Rinse successively with n-hexane, methanol and quartz water and equilibrate over water for 12 hours	112.3°
e.	Dry over P_2O_5 for 12 hours	112.5°
f.	Rinse successively with n-hexane, methanol and quartz water and dry over P_2O_5 for 12 hours	112.6°
g.	Rinse with detergent solution and quartz water and dry over P_2O_5 for 12 hours	112.5°

It is clear from the data in Tables A - 4 and A - 5 that the equilibration over water decreases the contact angle, but the change is within the experimental error (±1°) and is consequently negligible. The data in Table A - 5 show that the cleaning process does not effect on the contact angle of Parafilm and the original paper-covered Parafilm is clean. The original surface of the Teflon was contaminated and the satisfactory contact angle, comparing with the literature value, could be obtained only through a certain pretreatment process.

III.B Measurements of Surface Tension and Contact Angle

III.B.1 Surface Tension Measurements

The Wilhelmy slide method, contributed by L. Wilhelmy (119) in 1863, was used to measure all surface tensions. The slide was made of an approximately 5 cm perimeter platinum rectangle plate (0.1 mm thickness), sandblasted to be completely wetted (zero contact angle) by all solutions. The calibration of the slide was checked with fresh quartz-condensed water each day that the surface tension was measured. Because the weight per cent of surfactant in all solutions (except a few points of C_8SO_3Na and C_8NBr) was less than one per cent, the density of the surfactant solution was considered to be that of the quartz-condensed.

The platinum plate was suspended, by use of a cotton string, under loop B of a Chan RG Electrobalance (CHAN Division, Ventron Instruments Corp., Paramount, CA), with a maximum capacity of 500 mg and an accuracy of 0.05 mg. A jacketed dish, holding the surfactant solution, was maintained at constant temperature by circulation of constant temperature water pumped from a bath that consisted of an immersion heater, a copper cooling coil attached to the cold tap water and a thermistor connected to a proportional temperature controller (YSI Model 72, Yellow Springs Instrument Co., Inc., Yellow Spring, OH) to adjust temperature of the water bath at the desired temperature ± 0.02 °C. A microscope jack was used to regulate the height of the surfactant solution. A chart recorder, 1 mv span, (Electronik 194, Honeywell, Fort Washington, PA) was used to record the data from the Electrobalance.

The procedure for surface tension measurement by using the Electrobalance is as follows:

1. Adjust the Electrobalance and the recorder (for the process details see below).
2. Regulate the water bath to the desired temperature by using the temperature controller.
3. Pour about 50 ml of the surfactant solution into the jacketed dish. Turn on the pump to circulate the water and equilibrate the solution to the bath temperature.
4. Rinse the platinum plate with quartz-condensed water and heat

the plate in the outer cone of a Bunsen burner flame to red heat.

5. Suspend the plate from a cotton string attached to the loop B of the Electrobalance and adjust to read zero.
6. Slowly raise the jacketed dish with the coarse adjustment knob of the microscope jack until the edge of the plate is within 0.5 mm of the solution surface, then carefully raise the dish by using the fine adjustment knob until the plate just touches the solution surface and note the position of the plate on the adjustment knob scale. For measuring the surface tension, the solution must be at this same position.
7. Continue raising the dish to submerge the plate completely in the solution for a few seconds, then lower the dish until half the height of the plate is submerged in the solution and keep this position between surface tension readings.
8. After about 15 minutes lower the dish to its original position (were the lower edge of the plate just touched the surface of the solution) and turn the mass dial of the Electrobalance until the recorder reads zero. The value can be read from the mass dial knob and converted to surface tension by using the plate constant obtained from fresh quartz-condensed water each day that a measurement is made.
9. After ten to twelve minutes repeat the steps 7 and 8 until the difference between two successive readings are within 0.1 $mN\text{-}m^{-1}$.

The process for adjusting the Electrobalance and the recorder is as the following:

1) Turn on the power of the Electrobalance and the recorder and warm up for 30 minutes.
2) Set the span range of the recorder on 1 mv and zero the recorder, if necessary, by using the zero adjusting knob.
3) Set the Recorder Range switch to "Z", Factor to 1 and Filter control to 2.
4) Set both tabs of the Mass Dial Range control and the Recorder Range control to the letter B and then set the Mass Range switch to 500 mg.
5) Place a stirrup and a pan on loop B. Suspend the platinum plate on the string attached to the stirrup under loop B.
6) Place a stirrup and a pan on loop C. Add tare weight that is equal to one fifth of the weight of the plate and the string to this pan.
7) Set the Mass dial to 0.000 and turn the Recorder Range switch to 50. The recorder should read near zero. (Adjust the recorder reading to near zero by adding or removing the weight on the pan of loop C). Zero the recorder with the Set 0/10.
8) Add 250 mg calibrating weights on pan under loop B. Set Recorder Range switch to 50 and Mass dial to 5.000. Adjust the recorder reading to zero by using Set 5. Then set Mass dial to 4.000. The recorder should read full scale. Adjust,

if need, recorder reading to full scale with Calibrate Recorder knob.

9) Set Recorder Range switch to 100. The reading of recorder should be zero and half scale when the Mass dial was 5.000 and 4.000, respectively. The adjusting process is same as step 8).

10) Remove 250 mg calibrating weight from the pan of loop B. Set Mass dial to 0 and Recorder Range switch to 50 and 100, recheck the zero reading on recorder. Adjust the reading, if necessary, as in step 7).

11) Repeat steps 7), 8), 9) and 10) until there is no further adjustment for the recorder reading. The Electrobalance is now ready for surface tension measurement.

III.B - 2 Contact Angle Measurements

The procedure for contact angle measurements using Ramehart Goniometer is the following:

1) Place a piece of microscope slide on the platform of the Chamber. Position and focus the slide corner on the extreme right of the slide. Move the Chamber, using Cross-Travel dial, and view the extreme left of the slide. The "base line" of the slide should be same position. Use both left and right side jacking screws under the Chamber to achieve the left to right leveling.

2) A similar procedure is used to adjust the optical axis leveling, but using the far side and near side jacking screw under the Chamber. (In order to obtain accurate contact angles the precise optical axis leveling is very important.)

3) Optimize illumination by positioning the illuminator and focus the illumination beam until a sharp edge of the solution drop is obtained.

4) Adjust the temperature of the Chamber to a desired temperature by circulating the bath water through the supply fittings on the base of the Chamber.

5) Place a sample of the solution or liquid being tested in the Chamber to saturate the vapor phase. This is to prevent evaporation of solvent from the drops on which contact angles are being measured [see 7), below].

6) Place a microscope slide with the rectangular piece of solid tape on the platform of the Chamber. Recheck the left to right leveling and optical axis leveling of the microscope slide [steps 1) and 2)].

7) Deposit four drops of the solution on the solid surface by using a micrometer syringe. Add a little more solution to each drop and let the solution on the needle tip just touch the top surface of the original drop to ensure forming advancing contact angle. The diameter of the drop should be about 2.5 ~ 3.0 mm.

8) After ten minutes refocus the microscope to an edge of the

drop. Slowly rotate the measuring cross-line and adjust position by using the cross-travel knob to attain the tangency between the cross-line and the drop profile at the base of the solution drop. Directly read contact angle from the "measuring" reticle at six o'clock position. Measure on both sides of each of the four drops. The average value of the eight measurements is taken as the contact angle of the solution on the solid surface.

The advancing contact angle reproduciblity was within 1° at L/T and L/Para interfaces and 1.5° at L/Poly interface.

CHAPTER IV

RESULTS AND DISCUSSION

IV.A Surfactant Molecular Interactions in the Mixed Monolayer

IV.A.1 Treatments "E" and "R"

Molecular interactions and synergism have been extensively studied in this laboratory (24,127,25,26,27,28,29,30). Positive synergism is due to attractive interaction between the two surfactants, i.e. when the mixed system shows a negative deviation from ideality and the interaction parameter (β) is negative. The larger the negative value of β, the stronger the attractive interaction between the different surfactant molecules. Since interaction between the surfactants should affect the adsorption of surfactant at the interface, the molar area of surfactant should be different in the mixed system from that in the individual, and the stronger the interaction (the more negative the β value) the greater should be the difference.

Data in this laboratory show (24,25,28,30,120) that molecular interaction between two surfactants in aqueous solution decreases in the order: cationic-anionic >> betaine-anionic > POE nonionic-ionic(cationic or anionic) > betaine-cationic > POE nonionic-betaine > POE nonionic-POE nonionic. Attractive interaction between cationic and anionic surfactant molecules should therefore significantly decrease the molar area of surfactant in the mixed system. Holland (104) using the results of Corkill (121), found that the molar area of the surfactants in a 1:1 molar mixture of decyltrimethylammonium bromide and sodium decyl sulphate in presence of excess inorganic electrolyte was about seventy percent of the area for the corresponding unmixed components.

The purpose here is to compare the results obtained by using the two different treatments ("R" and "E") ,the treatment "R" based upon the assumption that the ratio of partial molar areas of the two surfactants in the mixed monolayer equals the ratio of the molar monolayer areas of the two individual surfactants at the same interfacial tension and the treatment "E" based upon the assumption that the area occupied by the surfactant in the mixed monolayer is not significantly different from that in a monolayer of the individual surfactant, for cationic-anionic surfactant mixed monolayers at the air/aqueous solution and the hydrophobic solid/aqueous solution interfaces. Three mixed systems have been investigated: octyl pyridinium bromide-dodecanesulfonate, C_8NBr-$C_{12}SO_3Na$, dodecyl pyridinium bromide-decanesulfonate, $C_{12}NBr$-$C_{10}SO_3Na$, and

tetradecyl trimethyl ammonium bromide-octanesulfonate, C_{14}TMABr-C_8SO_3Na. In order to compare the results, all surfactant solutions (except a few points in the curves of individuals of C_8NBr and C_8SO_3Na), individual and mixed, had the same 0.1 N ionic strength, adjusted with sodium bromide. The mole fractions (X) of cationic surfactant in the interfacial monolayer varied from 0.3 to 0.8. The mole fractions of adsorbed surfactant in the mixed monolayers, calculated by these two treatments, were compared to the mole fractions calculated by use of the Hutchinson method (107) based upon the Gibbs adsorption equation. Interaction parameters (β) between the two kinds of surfactants in the mixed monolayer were also calculated from surface tension and contact angle measurements, using the two different treatments.

Figure 1 shows plots of surface tension (γ_{lv}) versus logarithm of C_8NBr molar concentration for C_8NBr-$C_{12}SO_3Na$ mixtures at constant $C_{12}SO_3Na$ concentration; Figure 2 shows the plots of γ_{lv} vs. log molar concentration of $C_{12}SO_3Na$ (log $C_{C_{12}SO_3Na}$) for these mixtures at constant concentration of C_8NBr. The adhesion tension ($\gamma_{lv}\cos\theta$) vs. log C_{C_8NBr} curves for C_8NBr-$C_{12}SO_3Na$ mixtures at constant concentration of $C_{12}SO_3Na$ at the Teflon/aqueous solution interface (L/T) and Parafilm/aqueous (L/Para) interface are shown in Figures 3 and 5, respectively. The $\gamma_{lv}\cos\theta$ - log $C_{C_{12}SO_3Na}$ curves for these mixtures at constant concentration of C_8NBr on the L/T and L/Para interfaces are shown in Figures 4 and 6.

Plots of surface tension (or adhesion tension) vs. the

logarithm of total surfactant molar concentration at constant molar fraction (α) for C_8NBr-$C_{12}SO_3Na$ mixtures are shown in Figures 7, 8 and 9 at the L/V, L/T and L/Para interfaces.

Figures 10, 12 and 14 show the plots of γ_{lv} (or $\gamma_{lv}Cos\theta$) vs. log $C_{C_{12}NBr}$ for $C_{12}NBr$-$C_{10}SO_3Na$ mixtures at constant $C_{10}SO_3Na$ concentration at L/V, L/T and L/Para interfaces, respectively. The curves of γ_{lv} (or $\gamma_{lv}Cos\theta$) vs. log $C_{C_{10}SO_3Na}$ for same mixture system at constant $C_{12}NBr$ concentration at the L/V, L/T and L/Para interfaces are shown in Figures 11, 13 and 15.

Plots of γ_{lv} (or $\gamma_{lv}Cos\theta$) vs. log C_t for this mixture system are shown in Figures 16, 17 and 18 at the L/V, L/T and L/Para interfaces, respectively. In each figure, surfactant 1 is $C_{12}NBr$ and the values of α are 0.2276, 0.5000, 0.7714 and 1. The plots for individual $C_{10}SO_3Na$ are shown in Figure 42, 44 and 46 at the L/V, L/T and L/Para interfaces.

For $C_{14}TMABr$-C_8SO_3Na mixtures, Figure 19 shows the plots of γ_{lv} vs. log $C_{C_{14}TMABr}$ at constant concentration of C_8SO_3Na; Figure 20 shows the plots of γ_{lv} vs. log $C_{C_8SO_3Na}$ at constant concentration of $C_{14}TMABr$. Figures 21 and 23 show the plots of $\gamma_{lv}Cos\theta$ vs. log $C_{C_{14}TMABr}$ in presence of constant concentration of anionic surfactant at the L/T and L/Para interfaces. Curves of $\gamma_{lv}Cos\theta$ vs. log $C_{C_8SO_3Na}$ in presence of constant concentration of cationic surfactant are shown in Figures 22 and 24 at the L/T and L/Para interfaces, respectively.

Figures 25 and 26, 27 show γ_{lv}-log C_t and γ_{lv}Cosθ-log C_t curves for $C_{12}SO_3Na$ and C_{14}TMABr-C_8SO_3Na mixed solutions at a fixed value of α, the mole fraction of cationic surfactant in the solution phase on a surfactant only basis, at the L/V and L/T, L/Para interfaces. In each figure, surfactant 1 is the cationic surfactant (C_{14}TMABr) and the values of α are 0, 0.4000, 0.6923, and 0.8836. Plots of γ_{lv}-log C and γ_{lv}Cosθ-log C for C_{14}TMABr are shown in Figure 42, 44 and 46 at the L/V, L/T and L/Para.

Surface excess concentrations of cationic and anionic surfactants at the mixed monolayer were calculated from the experimental data, using Eqs. [II-38] and [II-39]. Mole fractions of the cationic surfactant (X_H), based upon Hutchinson method, were calculated by using equation [II-40].

The surface mole fractions (X_E) and interaction parameters (β_E), using treatment "E", were calculated from Eqs. [II-28] and [II-27]; the corresponding values, X_R and β_R, using treatment "R", were obtained from Eqs. [II-37] and [II-36]. C_1^o, A_1^o, C_2^o, A_2^o, $C_1(= \alpha C_t)$, $C_2[= (1 - \alpha)C_t]$ and A_{av} can be obtained from plots of γ_{lv} (or γ_{lv}Cosθ) versus log C_t, the total molar concentration of surfactants in the solution phase, for the two individual surfactants and their mixtures by selecting values at the same interfacial tension in all cases.

In electrolyte solutions containing swamping excesses of surfactant counter-ion, the total surface excess concentration of

mixed surfactant at the interface, Γ_t, is obtained by using Eq. [I-14]. The average area per surfactant species at the interface A_{av}, in nm^2, was calculated by use of Eq. [I-15].

The mole fractions, X_H, X_R and X_E, the molecule interaction parameters, β_R and β_E, and relevant interfacial tension, γ_{lv} or γ_{sl}, are listed in Tables A - 6, 7, 8, 9, 10, 11, 12, 13 and 14 for the three mixed systems at the L/V, L/T and L/Para interfaces, respectively. γ_{sl} was evaluated from Eq. [II-41] by assuming that the solid-vapor interfacial tension, γ_{sv}, is equal to the critical surface tension, γ_c, for the low-energy solid surface, using γ_c equal to 18, and 24 $mN\text{-}m^{-1}$ for Teflon and Parafilm (90), respectively.

1 - 1 Surface Mole Fraction, X, and Interaction Parameter, β, Values

C_8NBr - $C_{12}SO_3Na$ System

Tables A - 6, 7 and 8 list the values of X and β for the C_8NBr - $C_{10}SO_3Na$ mixture system at the L/V, L/T and L/Para interfaces, respectively. The value of X_H, the mole fraction of C_8NBr as calculated by the Hutchinson method, varies from 0.32 to 0.39 as α changes from 0.23 to 0.77 at all three interfaces. This means that the more active surfactant ion ($C_{12}SO_3^-$) occupies a dominant position at the interfaces in the presence of excess inorganic salt (45,49). X_R, based on treatment "R", shows very

good agreement with the experimental value X_H, the average difference between them being 3%, 2% and 1% at the L/V, L/T and L/Para interfaces, respectively. Comparison of X_H and X_E, based on treatment "E", shows an average difference of 14%, 20% and 16% at the L/V, L/T and L/Para interfaces. X_E could not be calculated at a high interfacial tension at the L/T interface. At constant α, X_H and X_R remain constant with increase in surface or interface tension, while X_E decreases with increase in the interfacial tension at all three interfaces. X_E of the less surface active surfactant is always smaller than X_H and X_R at the various interfacial tension and α values on all three interfaces.

The average value of the interaction parameter (β_R), calculated from Eq. [II-36], is -19.5, -14.1 and -15.3 at the L/V, L/T and L/Para interfaces, respectively. Variations are less than 3% from the average at the different α or interfacial tension values. Therefore, it appears that the value of the interaction parameter, as calculated by equations [II-37] and [II-36], is not affected by change in the interfacial tension or the mole fraction of the bulk phase. This is consistent with previous data (25,27), calculated by equations [II-28] and [II-27] at the L/V interface for nonionic-nonionic and nonionic-ionic mixture systems.

For this cationic-anionic surfactant mixture, however, the absolute values of β_E decrease with increase in interfacial tension at the three interfaces. At the L/T interface, the β_E value at lowest interfacial tension, 15.9 $mN\text{-}m^{-1}$, is about double that at the high

interfacial tension, 33.3 $mN\text{-}m^{-1}$, and there are only about 20% and 30% change in β_E value between corresponding interfacial tension at the L/V and L/Para interfaces.

At low interfacial tensions (saturated adsorption), the work term, $\gamma(A_1^o - A_1)$, is 5.0 $KJ\text{-}mol^{-1}$, 2.8 $KJ\text{-}mol^{-1}$ and 2.6 $KJ\text{-}mol^{-1}$ at the L/V, L/T and L/Para interfaces, respectively, while the nonideal interaction term, $RT\beta_R(1 - X)^2$, is 19.8 $KJ\text{-}mol^{-1}$, 13.5 $KJ\text{-}mol^{-1}$ and 16.0 $KJ\text{-}mol^{-1}$ at the L/V, L/T and L/Para interfaces. Obviously the work term is not negligible in the calculation of surface molar fractions and interaction parameters of surfactants in the monolayer. Due to the omission of the contribution of the work term, the average value of β_E is only 53%, 56% and 63% of β_R at the L/V, L/T and L/Para interfaces, respectively.

Table A - 6

Surface Mole Fraction & Surfactant Interaction Parameter Values, C_8NBr-$C_{12}SO_3Na$ (0.1 N NaBr); L/V Interface

γ_{lv}	X_H	X_R	X_E	β_R	β_E
		α = 0.2286			
35.8	0.33	/	/	/	/
40.7	0.32	/	/	/	/
45.3	0.32	0.33	0.25	-19.2	-11.8
49.6	0.31	0.33	0.25	-19.3	-11.3
53.6	0.31	0.33	0.25	-19.6	-10.8
		α = 0.5000			
35.9	0.35	/	/	/	/
45.2	0.35	0.36	0.30	-19.3	-12.1
49.6	0.35	0.36	0.30	-19.4	-11.6
53.7	0.35	0.36	0.30	-19.7	-11.0
57.5	0.35	0.36	0.30	-19.6	-10.4
61.3	0.35	0.36	0.29	-19.3	-9.7
		α = 0.7714			
40.0	0.38	/	/	/	/
44.7	0.38	0.39	0.35	-19.5	-12.5
49.2	0.38	0.39	0.35	-19.5	-11.8
53.4	0.39	0.39	0.35	-19.8	-11.3
57.2	0.39	0.39	0.35	-19.4	-10.7

Table A - 7

Surface Mole Fraction & Surfactant Interaction Parameter Values, C_8NBr-$C_{12}SO_3Na$ (0.1 N NaBr); L/T Interface

γ_{sl}	X_H	X_R	X_E	β_R	β_E
		α = 0.2286			
15.9	0.32	0.31	0.26	-14.2	-10.4
20.1	0.32	0.31	0.25	-14.3	-9.4
24.9	0.32	0.31	0.21	-13.9	-7.6
29.5	0.32	0.32	0.15	-14.2	-5.3
33.0	0.32	0.32	/	-15.7	/
		α = 0.5000			
15.6	0.34	0.34	0.31	-14.4	-10.9
20.6	0.34	0.35	0.30	-14.1	-9.2
24.9	0.34	0.35	0.28	-14.0	-8.1
29.0	0.33	0.36	0.26	-14.3	-6.8
33.3	0.33	0.36	0.21	-14.1	-4.6
		α = 0.7714			
20.2	0.38	0.38	0.35	-14.3	-9.7
24.6	0.38	0.39	0.35	-14.0	-8.4
28.8	0.38	0.39	0.34	-14.2	-7.1
33.2	0.39	0.40	0.31	-14.2	-5.3

Table A - 8

Surface Mole Fraction & Surfactant Interaction Parameter Values, C_8NBr-$C_{12}SO_3Na$ (0.1 N NaBr); L/Para Interface

γ_{sl}	X_H	X_R	X_E	β_R	β_E
		α = 0.2286			
15.0	0.32	/	/	/	/
19.7	0.32	0.31	0.25	-15.0	-11.0
24.2	0.32	0.31	0.25	-15.3	-10.2
28.2	0.32	0.32	0.24	-15.5	-9.4
32.8	0.32	0.32	0.22	-15.1	-8.1
		α = 0.5000			
19.7	0.34	0.34	0.30	-15.1	-11.3
24.0	0.34	0.35	0.30	-15.5	-10.6
28.5	0.34	0.35	0.29	-15.6	-9.7
32.7	0.35	0.35	0.29	-15.1	-8.7
37.2	0.35	0.35	0.27	-15.2	-7.1
		α = 0.7714			
19.2	0.38	0.38	0.35	-15.1	-11.6
24.1	0.38	0.38	0.35	-15.4	-10.6
27.9	0.38	0.38	0.34	-15.5	-9.8
32.8	0.39	0.38	0.34	-15.0	-8.8
37.1	0.39	0.39	0.34	-15.4	-7.4

$C_{12}NBr$ - $C_{10}SO_3Na$ System

Tables A - 9, 10 and 11 list the mole fractions and interaction parameters for $C_{12}NBr$-$C_{10}SO_3Na$ mixtures at the L/V, L/T and L/Para interfaces, respectively. $C_{12}NBr$ is a little more surface active than $C_{10}SO_3Na$, since it has a longer carbon chain length. Therefore, at all three interfaces the surface mole fraction of $C_{12}NBr$ is slightly larger than 0.5, for the entire range of α from 0.23 to 0.77. The surface mole fraction, X_R, again shows better agreement with the value of X_H than does X_E. The average difference between X_R and X_H is 3%, 5% and 5% at the L/V, L/T and L/Para interfaces, while the average difference between X_E and X_H is 11% at all three interfaces. X_H and X_R are almost constant at constant α. X_E shows a slight increase with increased interfacial tension and is always larger than the corresponding X_H and X_R values at all three interfaces. The deviation of X_E from X_H in this system is less than that of other two mixed systems. This is because the X value is close to 0.5 and $(A_1^o - A_1)$ and $(A_2^o - A_2)$ are similar in value. Mathematically, there is no difference between Eqs. [II-28] and [II-37] when X = 0.5 and $A_1^o - A_1 = A_2^o - A_2$. But the effect of the work term, $\gamma(A_i^o - A_i)$, is apparent from the values of the interaction parameters. β_E shows a variation up to 30% between the lowest and the highest interfacial tensions at the same α at all three interfaces. While the variation of $\beta_)$ is 3%, 5% and 7% from the average value is -19.7, -14.2 and -15.5 at the L/V, L/T and L/Para interfaces, respectively. The average value of β_E

is only 56%, 68% and 67% of β_R at the L/V, L/T and L/Para interfaces. $\gamma(A_1^o - A_1)$ and $RT\beta_R(1 - X)^2$ are 3.7 KJ-mol^{-1} and -9.9 KJ-mol^{-1} at the L/V interface, 1.9 KJ-mol^{-1} and 6.5 KJ-mol^{-1} at the L/T interface, 2.0 KJ-mol^{-1} and 7.1 KJ-mol^{-1} at the L/Para interface.

Table A - 9

Surface Mole Fraction & Surfactant Interaction Parameter Values, $C_{12}NBr$-$C_{10}SO_3Na$ (0.1 N NaBr); L/V Interface

γ_{lv}	X_H	X_R	X_E	β_R	β_E
		α = 0.2286			
37.3	0.52	/	/	/	/
42.4	0.52	0.52	0.54	-19.2	-13.5
47.5	0.51	0.52	0.54	-19.5	-12.8
52.5	0.51	0.52	0.55	-19.7	-12.0
57.1	0.51	0.52	0.55	-19.9	-11.3
		α = 0.5000			
39.3	0.53	0.55	0.57	-19.2	-13.8
44.7	0.53	0.55	0.58	-19.4	-12.9
49.8	0.52	0.55	0.59	-19.7	-12.2
54.4	0.53	0.55	0.60	-19.7	-11.5
58.8	0.53	0.55	0.61	-19.9	-10.7
62.7	0.53	0.56	0.62	-20.3	-9.7
		α = 0.7714			
41.9	0.56	0.58	0.62	-19.4	-12.9
46.6	0.56	0.58	0.63	-19.8	-12.3
51.6	0.56	0.58	0.64	-19.8	-11.5
56.4	0.56	0.58	0.65	-19.7	-10.8
60.2	0.59	0.58	0.66	-20.4	-10.0

Table A - 10

Surface Mole Fraction & Surfactant Interaction Parameter Values, $C_{12}NBr$-$C_{10}SO_3Na$ (0.1 N NaBr); L/T Interface

γ_{sl}	X_H	X_R	X_E	β_R	β_E
		α = 0.2286			
18.0	0.52	0.53	0.54	-13.8	-11.2
22.2	0.53	0.53	0.54	-14.0	-10.6
26.4	0.53	0.53	0.55	-14.2	-9.8
30.5	0.53	0.53	0.55	-14.8	-9.0
34.1	0.52	0.53	0.56	-14.9	-8.3
		α = 0.5000			
15.2	0.54	0.57	0.58	-13.8	-11.6
19.8	0.55	0.57	0.59	-13.8	-10.8
23.9	0.54	0.57	0.60	-14.2	-10.2
27.8	0.54	0.57	0.60	-14.5	-9.5
32.2	0.54	0.57	0.61	-14.8	-8.4
		α = 0.7714			
17.0	0.56	0.61	0.64	-13.5	-10.8
21.0	0.56	0.61	0.64	-13.7	-10.3
25.4	0.56	0.61	0.65	-13.9	-9.4
29.6	0.55	0.61	0.67	-14.3	-8.5
33.6	0.56	0.61	0.69	-14.8	-7.5

Table A - 11

Surface Mole Fraction & Surfactant Interaction Parameter Values, $C_{12}NBr$-$C_{10}SO_3Na$ (0.1 N NaBr); L/Para Interface

γ_{sl}	X_H	X_R	X_E	β_R	β_E
		α = 0.2286			
19.7	0.54	0.54	0.54	-15.1	-12.0
24.4	0.53	0.54	0.55	-15.1	-11.3
28.6	0.53	0.54	0.55	-15.6	-10.6
33.1	0.54	0.54	0.55	-16.2	-9.8
36.8	0.53	0.54	0.55	-16.6	-9.2
		α = 0.5000			
21.2	0.54	0.57	0.59	-15.1	-11.7
25.6	0.54	0.57	0.59	-15.2	-11.1
29.9	0.54	0.57	0.60	-15.8	-10.4
34.4	0.54	0.57	0.61	-16.3	-9.4
38.6	0.54	/	/	/	/
		α = 0.7714			
18.3	0.55	0.61	0.63	-14.9	-11.8
23.3	0.56	0.61	0.64	-14.7	-10.8
27.6	0.56	0.61	0.65	-15.2	-10.1
31.8	0.56	0.61	0.66	-15.7	-9.5
36.2	0.57	0.61	0.67	-15.9	-8.4

C_{14}TMABr-C_8SO_3Na System

Tables A - 12, 13 and 14 list the values of X_H, X_R, X_E and β_R and β_E at the L/V, L/T and L/Para interfaces, respectively. The X_H values of C_{14}TMABr vary from about 0.7 to 0.8 as the value of α is changed from 0.4 to 0.9 on all three interfaces, in agreement with the greater surface activity of C_{14}TMABr than C_8SO_3Na. The mole fraction values, X_H and X_R, show good agreement with each other, the average differences being 3%, 1% and 2% at the L/V, L/T and L/Para interfaces, respectively. The average differences between X_E and X_H are 10%, 13% and 10% at the L/V, L/T and L/Para interfaces. At the L/T interface, X_E cannot be calculated at high interfacial tension or large α values. X_E is always higher than the corresponding values of X_H and X_R at all three interfaces. The values of X_H and X_R show a slight increase with increase in the interfacial tension at constant α and the average β_R values of -13.5, -10.8 and -11.4 at the L/V, L/T and L/Para interfaces are somewhat smaller than expected (when compared with the values for the C_{12}TMABr-$C_{10}SO_3Na$ system). Both of these may be caused by nonionic or short chain homolog impurities in C_8SO_3Na, due to the inability to purify it by the reverse chromatographic technique because of the lack of an analytical method for determining its concentration in the effluent. The value of β_E again decreases with incease in interfacial tension, similar to that observed in the C_8NBr-$C_{12}SO_3Na$ and C_{12}NBr-$C_{10}SO_3Na$ systems, but the variation is a little better (slightly less

than 30%). The average value of β_E is about 71%, 63% and 66% of β_R at the L/V, L/T and L/Para interfaces. $\gamma(A_1^o - A_1)$ is 2.2 KJ-mol^{-1}, 1.3 KJ-mol^{-1} and 1.3 KJ-mol^{-1}; $RT\beta_R(1 - X)^2$ is 3.0 KJ-mol^{-1}, 1.7 KJ-mol^{-1} and 1.9 KJ-mol^{-1} at the L/V, L/T and L/Para interfaces, respectively. Comparing it with $RT\beta_R(1 - X)^2$, the work term maks a considerable contribution to the value of the surface mole fraction and interaction parameter of the surfactants in the monolayer.

It is apparent from the above results that, for cationic-anionic mixed systems, treatment "R", which uses equations [II-37] and [II-36], yields values that are in close agreement with those calculated from the Gibbs adsorption equation by use of equations [II-38], [II-40], while treatment "E", based upon equations [II-28] and [II-27], yields values that deviate more. In addition, treatment "R" yields X_R and β_R values that show changes of only a few percent when γ (or $\gamma_{lv}Cos\theta$) or α is varied over the complete range investigated here; the changes in the values obtained by treatment "E" are considerably larger. In agreement with the differences between the equations for treatment "E" and "R", the differences between the values of X and β obtained from the two treatments increase with increase in the interfacial tension.

Table A - 12

Surface Mole Fraction & Surfactant Interaction Parameter Values, $C_{14}TMABr$-C_8SO_3Na (0.1 N NaBr); L/V Interface

γ_{lv}	X_H	X_R	X_E	β_R	β_E
		α = 0.4000			
42.8	0.67	0.70	0.76	-14.2	-10.2
47.2	0.68	0.70	0.79	-14.3	-9.1
51.3	0.71	0.70	0.79	-14.1	-9.0
55.0	0.73	0.70	0.80	-14.0	-8.8
58.4	0.73	0.71	0.81	-13.5	-8.5
		α = 0.6923			
42.6	0.73	0.74	0.83	-14.0	-9.3
46.8	0.76	0.74	0.84	-13.7	-8.8
50.5	0.79	0.75	0.85	-13.1	-8.5
54.0	0.80	0.76	0.86	-13.0	-8.3
57.5	0.80	0.75	0.88	-13.2	-7.8
60.6	0.80	0.75	0.88	-13.7	-7.6
		α = 0.8836			
41.3	0.82	0.78	0.89	-13.3	-8.8
45.2	0.82	0.78	0.91	-13.0	-8.0
48.9	0.83	0.79	0.92	-13.0	-7.8
52.2	0.83	0.80	0.92	-13.0	-7.9

Table A - 13

Surface Mole Fraction & Surfactant Interaction Parameter Values, $C_{14}TMABr-C_8SO_3Na$ (0.1 N NaBr); L/T Interface

γ_{sl}	X_H	X_R	X_E	β_R	β_E
		α = 0.4000			
23.6	0.76	0.75	0.82	-11.1	-8.0
27.6	0.78	0.75	0.85	-11.0	-7.3
31.8	0.78	0.75	0.88	-10.8	-5.9
35.3	0.78	0.76	0.90	-10.9	-6.1
38.6	0.78	0.77	/	-10.2	/
		α = 0.6923			
18.9	0.78	0.80	0.87	-10.8	-7.9
22.3	0.80	0.79	0.89	-10.9	-7.6
26.1	0.81	0.80	0.92	-11.0	-6.6
29.9	0.81	0.80	0.98	-11.0	-5.0
34.0	0.81	0.80	/	-10.8	/
37.3	0.81	0.81	/	-10.8	/
		α = 0.8836			
17.4	0.83	0.85	/	-10.3	/
20.9	0.85	0.84	/	-10.7	/
24.1	0.85	0.84	/	-11.0	/
28.1	0.85	0.84	/	-10.9	/
32.3	0.85	0.85	/	-10.5	/

Table A - 14

Surface Mole Fraction & Surfactant Interaction Parameter Values, $C_{14}TMABr-C_8SO_3Na$ (0.1 N NaBr); L/Para Interface

γ_{sl}	X_H	X_R	X_E	β_R	β_E
		α = 0.4000			
23.8	0.76	0.74	0.80	-12.1	-8.9
27.8	0.76	0.74	0.81	-12.0	-8.6
33.0	0.77	0.74	0.82	-11.9	-7.9
35.7	0.77	0.74	0.83	-11.8	-7.4
39.9	0.77	0.75	0.85	-11.4	-6.7
		α = 0.6923			
22.3	0.79	0.79	0.86	-11.9	-8.7
26.6	0.81	0.79	0.88	-11.8	-7.9
30.3	0.81	0.79	0.89	-11.7	-7.6
34.3	0.82	0.79	0.90	-11.5	-7.0
38.0	0.81	0.81	0.92	-10.9	-6.4
		α = 0.8836			
20.5	0.82	0.82	0.93	-12.0	-7.9
24.9	0.83	0.83	0.97	-11.8	-6.8
28.5	0.84	0.83	0.97	-11.3	-6.2
32.3	0.84	0.83	/	-11.2	/

1 - 2 Factors Affecting the Deviation Between X_R and X_E; β_R and β_E

As shown in Tables A - 6 ~ 14, the deviation of X_E and β_E from X_R and β_R, respectively, increases with increase in the interfacial tension. This is because: 1) the change in slope of the γ_{lv}-log C_t (or γ_{lv}Cosθ-log C_t) curve with increase in interfacial tension is larger for a solution of an individual surfactant then for a mixed surfactant solution in these systems, therefore $(A_i^o - A_i)$ increases with increase in interfacial tension; 2) the value of $\gamma(A_i^o - A_i)$ increases with increase in γ. Therefore the $\gamma(A_i^o - A_i)$ term makes a greater contribution to the calculation of the surface mole fraction and interaction parameter as the interfacial tension increases.

In all the systems, the absolute value of β_E decreases with increase in interfacial tension at a fixed α value at all three interfaces. The decrease is in order: air/aqueous < Parafilm/aqueous < Teflon/aqueous and reflects the order of increasing change in $(A_i^o - A_i)$ with increase in the interfacial tension. This can be extended to explain the fair agreement between X values calculated by using Eq. [II-28], treatment "E", and Eq. [II-40], Hutchinson method, in nonionic-nonionic and nonionic-anionic systems (25). In those systems the interaction between surfactant molecules in the monolayer is very weak (small absolute value of β) and the changes of the area per surfactant in

the mixed and individual systems is so small that it produces no significant effect on the X and β values.

Tables A - 15.1 and 15.2 list average values of β_R and β_E, their absolute difference $|\beta_R - \beta_E|$, the work term $\gamma(A_1^o - A_1)$, and the packing deviation factor, $1 - A_{av}/[XA_1^o + (1 - X)A_2^o]$, which measures the degree of change in the area per surfactant molecule in the monolayer from an individual surfactant to a mixed surfactant system. Included are data from other investigations and other investigators. It is apparent from the data in Table A - 15.1 that the larger the value of $\gamma(A_1^o - A_1)$, the larger the value of $|\beta_R - \beta_E|$. It is also clear from the data in Table A - 15.2 that in general, and irrespective of the interface, the value of the packing deviation factor increases with increase in the attraction interaction between the two surfactants, i.e., with larger negative values of β_R and β_E. Other investigators have also observed this decrease in the average area per surfactant molecule at the interface when intermolecular attraction is large. Lucassen-Reynders (53) found that the area per ionic surfactant at the L/V interface in C_{12}TMABr-$C_{12}SO_4Na$ aqueous mixtures without excess inorganic electrolyte was only about half of that for solutions of the individual surfactants. We obtained similar results from Rodakiewicz-Nowak's (44) experimental data on the C_{12}TMABr-C_{10}SNa mixed system. As the ionic strength increases, the packing deviation factor decreases; for the C_{12}TMABr-$C_{10}SO_3Na$ system at the L/V interface the factor is 0.50 and 0.30 in aqueous solution and 0.1 N NaBr, respectively.

Increased electrolyte counter ion decreases the attractive interaction between the cationic and anionic head groups in the interfacial monolayer, decreasing the absolute value of β and decreasing the packing deviation factor. Similar results were obtained by other investigaters. Holland (104) indicated that the area per ionic surfactant is about 70% of that for the corresponding unmixed components for the $C_{10}TMABr$-$C_{10}SO_4Na$ system in 0.05 N NaBr. The packing deviation factor in a spread film of octadecyldimethylamine oxide-sodium dodecyl sulfate mixture in 0.01 N NaCl at PH = 5.5 (HCl) is about 0.65 (at high surface pressure), calculated from Rosano's data (129). These are in agreement with our results.

The data in Table A - 15.2 also indicate that for all the interfaces investigated here the variation of β_E from β_R increases with increase in the packing deviation factor. Thus, when attractive interaction between the two surfactants is large, the packing deviation factor and the $|\beta_R - \beta_E|$ values are large. When intermolecular attraction is relatively weak ($\beta_R < 6$), for example in nonionic-nonionic or nonionic-ionic mixtures, the packing deviation factor is small and the difference between β_R and β_E is negligible. In this case the error in the assumptions that $A_1^o \simeq A_1$ and $A_2^o \simeq A_2$ is less than 10% and treatment "E" can be used to calculate the surface mole fractions and the interaction parameters without significant error.

Table A - 15.1

Factors Affecting β_R, β_E, and Their Difference

System	Interface	β_R	β_E	$\lvert\beta_R-\beta_E\rvert$	$\gamma(A_1^o-A_1)$ KJ-mol^{-1}
$C_{12}TBr$-$C_{12}SO_4Na$	L/V[a]	-38.4	-27.4	11.0	6.7
H_2O	L/T	-30.6	-20.4	10.2	5.7
	L/Poly	-26.7	-17.2	9.5	4.9
$C_{12}TBr$-$C_{10}SNa$	L/V[b]	-35.6	-22.7	12.9	7.8
H_2O	L/T	-28.8	-17.9	10.9	6.1
	L/Poly	-26.6	-16.9	9.7	5.8
$C_{12}TBr$-$C_{10}SNa$	L/V	-19.6	-13.3	6.3	4.1
0.1 NaBr	L/T	-14.1	-11.0	3.1	1.8
	L/Para	-15.3	-12.2	3.1	1.7
C_8NBr-$C_{12}SNa$	L/V	-19.5	-11.2	8.3	5.0
0.1 NaBr	L/T	-14.1	-7.9	6.2	2.8
	L/Para	-15.3	-9.6	5.7	2.6
$C_{12}NBr$-$C_{10}SNa$	L/V	-19.7	-11.9	7.8	4.3
0.1 NaBr	L/T	-14.2	-9.7	4.5	2.3
	L/Para	-15.5	-10.4	5.1	2.4
$C_{14}TBr$-C_8SNa	L/V	-13.5	-8.6	4.9	2.3

0.1 NaBr	L/T	-10.8	-6.8	4.0	1.3
	L/Para	-11.2	-7.5	3.7	1.3
C_{12}BMG-C_{12}SNa	L/V	-8.3	-5.4	2.9	2.2
0.1 NaBr	L/T	-6.2	-4.9	1.3	1.2
	L/Para	-6.9	-5.1	1.8	1.2
	L/Poly	-3.2	-3.3	0.1	-0.2
$C_{12}(EO)_8$-$C_{12}SO_4Na$	L/V[c]	-3.7	-3.5	0.2	0.2
Na 0.1 NaCl	L/T	-2.9	-2.6	0.3	0.2
$C_{12}(EO)_8$-$C_{12}SO_4Na$	L/V[c]	-3.3	-3.1	0.2	0.6
Na 0.5 NaCl	L/T	-2.7	-2.5	0.2	0.6
$C_{12}(EO)_8$-C_{12}SNa	L/V[c]	-2.7	-2.6	0.1	0.5
0.1 NaCl	L/T	-2.1	-2.0	0.1	0.6
$C_{12}(EO)_8$-C_{12}SNa	L/V[c]	-2.0	-2.0	0.0	-0.1
0.5 NaCl	L/T	-1.7	-1.6	0.1	0.1

a.-Ref.(53) b.-Ref.(44) c.-Ref.(27)

Table A - 15.2

Factors Affecting β_R, β_E, and Their Difference

System	Interface	β_R	β_E	$\lvert\beta_R-\beta_E\rvert$	N^d
$C_{12}TBr$-$C_{12}SO_4Na$	L/V[a]	-38.4	-27.4	11.0	0.48
H_2O	L/T	-30.6	-20.4	10.2	0.47
	L/Poly	-26.7	-17.2	9.5	0.36
$C_{12}TBr$-$C_{10}SNa$	L/V[b]	-35.6	-22.7	12.9	0.50
H_2O	L/T	-28.8	-17.9	10.9	0.48
	L/Poly	-26.6	-16.9	9.7	0.41
$C_{12}TBr$-$C_{10}SNa$	L/V	-19.6	-13.3	6.3	0.30
0.1 NaBr	L/T	-14.1	-11.0	3.1	0.28
	L/Para	-15.3	-12.2	3.1	0.27
C_8NBr-$C_{12}SNa$	L/V	-19.5	-11.2	8.3	0.31
0.1 NaBr	L/T	-14.1	-7.9	6.2	0.32
	L/Para	-15.3	-9.6	5.7	0.31
$C_{12}NBr$-$C_{10}SNa$	L/V	-19.7	-11.9	7.8	0.32
0.1 NaBr	L/T	-14.2	-9.7	4.5	0.28
	L/Para	-15.5	-10.4	5.1	0.31
$C_{14}TBr$-C_8SNa	L/V	-13.5	-8.6	4.9	0.18
0.1 NaBr	L/T	-10.8	-6.8	4.0	0.17

	L/Para	-11.2	-7.5	3.7	0.16
C_{12}BMG-C_{12}SNa	L/V	-8.3	-5.4	2.9	0.13
0.1 NaBr	L/T	-6.2	-4.9	1.3	0.14
	L/Para	-6.9	-5.1	1.8	0.14
	L/Poly	-3.2	-3.3	0.1	-0.02
$C_{12}(EO)_8$-$C_{12}SO_4Na$	L/V[c]	-3.7	-3.5	0.2	0.01
Na 0.1 NaCl	L/T	-2.9	-2.6	0.3	0.02
$C_{12}(EO)_8$-$C_{12}SO_4Na$	L/V[c]	-3.3	-3.1	0.2	0.04
Na 0.5 NaCl	L/T	-2.7	-2.5	0.2	0.06
$C_{12}(EO)_8$-C_{12}SNa	L/V[c]	-2.7	-2.6	0.1	0.03
0.1 NaCl	L/T	-2.1	-2.0	0.1	0.06
$C_{12}(EO)_8$-C_{12}SNa	L/V[c]	-2.0	-2.0	0.0	-0.01
0.5 NaCl	L/T	-1.7	-1.6	0.1	0.01

a.-Ref.(53) b.-Ref.(44) c.-Ref.(27)

d. $N = 1 - A_{av}/[XA_1^o + (1 - X)A_2^o]$

1 -3 Conclusions

1. The work term, $\gamma(A_1^{o} - A_1)$, due to the change in area per surfactant molecule at the interface resulting from intermolecular attraction in the mixed monolayer, cannot be neglected for the calculation of interfacial mole fractions and interaction parameters in cationic-anionic surfactant mixtures.

2. A treatment "R", based upon the assumption that the ratio of the partial molar areas of the two surfactants in the mixed monolayer equals the ratio of the molar areas of the two individual surfactants at the same interfacial tension, gives mole fraction values of the surfactants at the interface that are in very good agreement with those obtained by use of the Hutchinson method based upon the Gibbs adsorption equation, at both the liquid/vapor and liquid/hydrophobic solid interfaces.

3. The value of the interaction parameter (β_R) between the surfactants in the mixed monolayer, obtained by treatment "R", is essentially constant with change in either the ratio of the two surfactants in the solution phase or the interfacial tension at the air/aqueous solution, Teflon/aqueous solution, or Parafilm/aqueous solution interfaces.

4. Treatment "E", based upon the assumption of equal surfactant areas in the mixed and individual surfactant films, gives interfacial mole fractions and interaction parameters for mixed monolayer formation that deviate from those obtained by treatment "R". The deviation increases with increase in interfacial tension

and in the degree of change in surfactant area at the interface. The latter increases with increase in the strength of the interaction between the two surfactants.

5. When interaction between the two surfactants in the mixed monolayer is relatively weak, the two treatments yield essentially the same interfacial mole fraction and interaction parameter values.

IV.A.2 Factors Affecting the Interaction Parameter at Liquid/Hydrophobic Solid Interface

The interaction between the two surfactant molecules at the interfacial monolayer, as measured by the value of β, is affected by microenviromental factors, such as the nature of the interface and the ionic strength of the solution, and the chemical structures of the surfactants such as the number of carbon atoms in the hydrophobic groups of the surfactants and the nature of the hydrophilic groups of the surfactants.

2 - 1 Effect of the Nature of the Hydrophobic Surface

Plots of adhesion tension vs. log of total molar surfactant concentration (log C_t) for C_{12}BMG, $C_{12}SO_3Na$ and their mixtures in aqueous solution without excess inorganic electrolyte are shown in Figures 28, 29 and 30 at the L/T, L/Para and L/Poly interfaces, respectively. C_{12}BMG is chosen as surfactant 1 and the values of α are 0, 0.0134, 0.0276, 0.0884, 0.3274, 0.6864, 0.9448 and 1. The values of the surface tension are taken from reference (28). For this zwitterionic-anionic mixed system in aqueous solution, in the absence of added inorganic electrolyte, the total surface excess concentration was obtained by use of Eq. [I-12]. Eqs. [I-6] and [I-8] were used to calculate the surface excess concentrations of the individual zwitterionic (C_{12}BMG) and anionic ($C_{12}SO_3Na$) surfactants.

Figure 31 shows the surface tension, γ_{lv}, versus log C_t for $C_{12}BMG$, $C_{12}SO_3Na$ and their mixtures in aqueous sodium bromide solution of 0.1 N total ionic strength (IS). Plots of log C_t for these solutions vs. the adhesion tension, $\gamma_{lv}Cos\ \theta$, at the L/T, L/Para and L/Poly interfaces are shown in Figures 32, 33 and 34, respectively. In each figure, surfactant 1 is $C_{12}BMG$ and the values of molar fraction in bulk phase, α, are 0, 0.0204, 0.0849, 0.355, 0.693, 0.919 and 1.

For a cationic-anionic mixture system, $C_{12}TMABr$-$C_{10}SO_3Na$, the curves of surface tension (or adhesion tension) vs. log C_t in 0.1 N IS (NaBr) aqueous solution are plotted in Figures 35, 36 and 37 at the L/V, L/T and L/Para interfaces, respectively. In these figures, surfactant 1 is $C_{12}TMABr$ and the α values are 0, 0.5000 and 1. Figures 38 and 39 show the $\gamma_{lv}Cos\ \theta$ vs. log C_t curves for the same mixed system in aqueous solution in the absence of excess inorganic salt, where α are 0, 0.500 and 1, at the L/T and L/Poly interfaces. The surface tension, γ_{lv}, data are from reference (44). Equations [I-14] and [I-13] were used to calculate the total surface excess concentrations for the cationic-anionic mixed systems in the presence and absence of excess inorganic electrolyte, respectively.

Figures 40 and 41 show $\gamma_{lv}Cos\theta$ - log C_t curves for $C_{12}TMABr$, $C_{12}SO_4Na$ and their mixtures in aqueous solution in the absence of excess inorganic electrolyte on Teflon and polyethylene, respectively. The γ_{lv} data were obtained from reference (53). In

each figure, surfactant 1 is $C_{12}SO_4Na$ and the α values are 0, 0.500, 0.667 and 1.

Table A - 16 lists the values of the average area per surfactant species, A_{av}, at the interfacial mixed monolayer, the total surface excess concentration, Γ_t, and the relevant interaction parameter for mixed monolayer formation (β_{lv}, for the L/V interface; β_{sl} for the L/T, L/Para and L/Poly interfaces) for the C_{12}BMG-$C_{12}SO_3Na$ and C_{12}TMABr-$C_{10}SO_3Na$ mixed systems in the absence and presence of added inorganic electrolyte and C_{12}TMABr-$C_{12}SO_3Na$ in the absence of excess inorganic electrolyte. In order to permit comparison, the values are given at the same mole fraction in the bulk phase.

It is clear from the data in Table A - 16 that the nature of the interface does have a major effect on the degree of interaction of the two surfactants in the interfacial monolayer. The attraction interaction between the two surfactant molecules decreases (shows less negative β values) in the order: L/V > L/Para > L/T > L/Poly. The values of the total surface excess concentration, Γ_t, show that the adsorption of surfactants decreases in the same order: L/V > L/Para > L/T > L/Poly. This is reasonable since the average area per surfactant increases with decrease in Γ_t and the interaction between the surfactants would be expected to decrease with increase in the distance between the surfactant molecules.

However, the trend with the change in the area per molecule

is not uniform. The difference between the interaction parameters ($\Delta\beta$) at the L/Para interface and L/V interfaces is much larger than the difference in the area per molecule between those interfaces, compared with those at the L/Para and L/T interfaces. Possibly the cohesive force between the hydrocarbons of the Parafilm surface and hydrocarbon chains of the surfactants reduces the interaction between the hydrocarbon chains of the two different surfactants, while the "mutual phobicity" between the fluorocarbons of the Teflon surface and the hydrocarbon chains of the surfactants causes the hydrocarbon chains of the different surfactants to be closely packed and the interaction parameter between them to be greater. Therefore the interaction parameter at the Teflon/aqueous interface, compared with that at the Parafilm/aqueous interface, is larger than that expected based upon the area per surfactant molecule.

The surface excess concentration at the L/Para interface is slightly less than that at the L/V interface. This is in agreement with E. H. Lucassen-Reynders's data (35) and G. Zografi's results (123) for the adhesion tension vs. surface tension of various aqueous surfactant and polymer solutions. Data (29) in this laboratory have shown that the value of the interaction parameter for mixed monolayer formation at the aqueous solution/hydrocarbon interface is less negative than that for the same system at the L/V interface.

Table A - 16

Effect of the Interface on β and A_{av} Values

System	Interface	α	β	Γ_t mol-cm^{-2}x10^{10}	A_{av} nm^{-2}
C_{12}BMG-$C_{12}SO_3Na$	L/V	0.686	-6.6	3.7	0.45
H_2O	L/T	0.686	-4.7	2.8	0.59
	L/Para	0.686	-5.0	3.4	0.49
	L/Poly	0.686	-1.9	2.4	0.70
C_{12}BMG-$C_{12}SO_3Na$	L/V	0.355	-8.3	3.9	0.43
0.1 N IS (NaBr)	L/T	0.355	-6.2	3.5	0.47
	L/Para	0.355	-6.7	3.7	0.45
	L/Poly	0.355	-3.2	2.7	0.62
C_{12}TMABr-$C_{10}SO_3Na$	L/V	0.500	-19.6	5.2	0.32
0.1 N IS (NaBr)	L/T	0.500	-14.1	4.1	0.40
	L/Para	0.500	-15.3	4.4	0.38
C_{12}TMABr-$C_{10}SO_3Na$	L/V	0.500	-35.6	5.9	0.28
H_2O	L/T	0.500	-28.8	4.6	0.36
	L/Poly	0.500	-26.6	3.0	0.56
C_{12}TMABr-$C_{12}SO_4Na$	L/V	0.500	-38.4	6.1$_5$	0.27
H_2O	L/T	0.500	-30.6	3.8	0.44
	L/Poly	0.500	-26.7	3.0	0.55

The larger values of A_{av} at the L/Poly interface than at the L/V interface is consistent with previous data on insoluble monolayers of individual surfactants, indicating that they are less closely packed at the hydrocarbon/water interface than at the air/water interface (124). Compared with that on Parafilm, the area per surfactant molecule on polyethylene is larger than expected. This is because polyethylene has been shown to exhibit some polar character. This was shown by E. D. Goddard and coworker from wetting studies using pure liquids (125).

The intermediate value for the L/T interface possibly reflects the mutual phobicity of hydrocarbon chains and fluorocarbon surfaces pointed out by P. Mukerjee and colleagues (126,127,128) from several different respect studies of fluorocarbon and hydrocarbon surfactants and other investigators (129,130,131). This would result in less adsorption of hydrocarbon surfactant at a L/T interface than that at a L/Para interface. P. Mukerjee (132) calculated that the free energy of adsorption per mole methylene group ($-CH_2-$) was -820 Cal-mol^{-1} at the hexane/water interface and -690 Cal-mol^{-1} at the perfluorohexane/water interface.

2 - 2 Effect of the Number of Carbon Atoms in Mixed Systems

Figure 42 shows plots of surface tension versus logarithm of surfactant concentration (in mol-dm^{-3}) for $C_{10}NBr$, $C_{10}SO_3Na$ and $C_{14}TMABr$ at the L/V interface. Plots of surface tension vs. logarithm of total surfactant concentration for the cationic-anionic mixtures, all equimolar concentrations of cationic and anionic in the bulk phase (i.e., $\alpha = 0.5$) are shown in Figure 43. Figures 44, 45, 46 and 47 show the adhesion tension ($\gamma_{lv}Cos\theta$) vs. logarithm of the concentration for the individual surfactants and the equimolar cationic-anionic surfactant mixtures at the L/T and L/Para interfaces, respectively.

The interaction parameters (β) of the surfactants in the interfacial monolayers were calculated by use of Eq. [II-36]. Eq. [II-37] was used to obtain the surface mole fraction of cationic surfactant at γ_{lv} = 45 mN-m^{-1} at the L/V interface and at γ_{sl} = 22 mN-m^{-1} at the L/T and L/Para interfaces, respectively. The minimum average area per surfactant molecule (A_{av}), in nm^{-2}, was calculated by use of Eq. [I-15], with the total surface excess concentration, Γ_t, obtained by use of Eq. [I-14] for the system in the presence of excess electrolyte from the linear part of the curve of surface tension or (adhesion tension) vs. log C_t.

Table A - 17

Values of β, X, and A_{av} for C_nNBr-C_mSO_3Na Mixtures at α = 0.5 in Aqueous Solution of 0.1 IS (NaBr) at the L/V Interface: γ_{lv} = 45 $mJ\text{-}m^{-1}$

n	m	X	A_{av} nm^{-2}	β
8	10	0.41	0.37	-19.5
10	10	0.48	0.33	-20.7
12	10	0.54_5	0.31_5	-19.7
8	12	0.36	0.36_5	-19.5_5
10	12	0.43	0.33_5	-20.1
12	12	0.49	0.30	-20.9

Table A - 18

Values of β, X, and A_{av} for C_nNBr-C_mSO_3Na Mixtures at α = 0.5 in Aqueous Solution of 0.1 IS (NaBr) at the L/T Interface: γ_{sl} = 22 $mJ\text{-}m^{-1}$

n	m	X	A_{av} nm^{-2}	β
8	10	0.42	0.43	-14.2
10	10	0.50	0.37	-16.1
12	10	0.57.	0.35	-14.5
8	12	0.36	0.42	-14.1
10	12	0.43_5	0.38_5	-14.6
12	12	0.50	0.31_5	-16.7

Table A - 19

Values of β, X, and A_{av} for C_nNBr-C_mSO_3Na Mixtures at α = 0.5 in Aqueous Solution of 0.1 IS (NaBr) at the L/Para Interface: γ_{sl} = 22 $mJ\text{-}m^{-1}$

n	m	X	A_{av} nm^{-2}	β
8	10	0.42	0.39	-15.4
10	10	0.49	0.35	-16.9
12	10	0.57.	0.32	-15.7
8	12	0.35	0.37	-15.3
10	12	0.42_5	0.36	-15.7
12	12	0.50	0.31	-17.3

Table A - 17, 18 and 19 list the values of β, X and A_{av} for C_nNBr-C_mSO_3Na mixtures where n equals 8, 10, or 12 and m equals 10 or 12, and α = 0.5 in aqueous solutions of 0.1 N IS (NaBr) at the L/V, L/T and L/Para interfaces, respectively.

The data in Tables A - 17, 18 and 19 show that at all three interfaces investigated here the attractive interaction between the surfactants in the monolayer increases slightly (more negative value of β) with increase in the carbon number of either the cationic surfactant or anionic surfactant. This is because the electrostatic attractive force between the cationic and anionic heads is the dominant contribution to the interaction, compared to the Van der Waals attractive force between the hydrocarbon chains. There is a somewhat stronger interaction when both the cationic and anionic surfactants that have the same number of carbon atoms in their alkyl chains. This phenomenon was also observed in this laboratory (27) for nonionic-cationic and nonionic-anionic mixed systems in the presence of excess electrolyte at the L/V interface. For the same mixture of surfactants, the interaction decreases in the order: air/aqueous > Parafilm/aqueous > Teflon/aqueous interface and the area per surfactant molecule is just reverse, as observed for other systems.

As shown by the data in Tables A - 17, 18 and 19, at all three interfaces the β values become more negative with decrease in the average area per surfactant molecule in the mixed monolayer. The average area per surfactant molecule decreases with increase in

the individual and total carbon atom number of the cationic and anionic surfactants. A_{av} shows a minimum value when the cationic and anionic surfactants have equal chain length and this is consistent with the fact that the maximum interaction between two surfactants occurs when the two surfactants have same number of carbon atoms in their alkyl chains. O. Shibata (133) and D. O. Shah (134) observed the condensing effect on a mixed film when the two surfactants have equal chain length. Shah suggested that the portion of the molecules above the height of the adjacent molecules for a mixture containing different chain lengths possessed thermal motion (vibration, oscillation and rotation) and this thermal disturbance would be propagated along the chain for a considerable length toward the polar head part. The mixed monolayer would be expanded and have a greater average area per molecule. Therefore, the absolute β value will be decreased by this thermal motion as a result of the increased distance between the interacting surfactant molecules. The greater interaction between two surfactants having the same chain length can then be explained by the absence of this thermal motion factor.

2 - 3 Effect of the Ionic Strength of the Solution

Figure 48 shows the curves of adhesion tension vs. log C_t for $C_{12}(EO)_8$, $C_{12}SO_4Na$ and their mixtures in quartz-condensed water and in 0.1 N and 0.5 N total ionic strengths adjusted with NaCl, at

the L/T interface. The corresponding γ_{lv} values were obtained from the data of reference (27).

Table A - 20 lists the values of β and A_{av} for these nonionic-anionic systems, $C_{12}(EO)_8$-$C_{12}SO_3Na$ and $C_{12}(EO)_8$-$C_{12}SO_4Na$ at the L/T interface, for the zwitterionic-anionic system, C_{12}BMG-$C_{12}SO_3Na$, in quartz-condensed water and in 0.1 N IS (NaBr) at the L/T, L/Para and L/Poly interfaces, and for the cationic-anionic system, C_{12}TMABr-$C_{10}SO_3Na$, in quartz-condensed water at the L/T and L/Poly interfaces and in the 0.1 N IS (NaBr) at the L/T and L/Para interfaces.

Table A - 20

Effect of the Ionic Strength of Surfactant Solution on β and A_{av} values

System	Interface	Medium	A_{av} nm^{-2}	β
$C_{12}(EO)_8$-$C_{12}SO_3Na$	L/T	H_2O	0.82	-1.1
		0.1N IS (NaCl)	0.58	-2.1
		0.5N IS (NaCl)	0.54	-1.7
$C_{12}(EO)_8$-$C_{12}SO_4Na$	L/T	H_2O	0.78	-1.7
		0.1N IS (NaCl)	0.57	-2.9
		0.5N IS (NaCl)	0.53	-2.7
C_{12}BMG-$C_{12}SO_3Na$	L/T	H_2O	0.56	-4.5
		0.1N IS (NaBr)	0.47	-6.2
	L/Para	H_2O	0.49	-4.8
		0.1N IS (NaBr)	0.44_5	-6.7
	L/Poly	H_2O	0.70	-1.6
		0.1N IS (NaBr)	0.62	-3.1
C_{12}TMABr-$C_{10}SO_3Na$	L/T	H_2O	0.39	-28.8
		0.1N IS (NaBr)	0.40	-14.1
	L/Poly	H_2O	0.59	-26.6
	L/Para	0.1N IS (NaBr)	0.38	-15.3

The data in Table A - 20 indicate that the surfactant interaction in the two nonionic-anionic systems increases with increase in the ionic strength of the solution to 0.1 N IS, but decreases with further increase in the ionic strength to 0.5 N IS. These results are consistent with those obtained in this laboratory at the L/V interface (27).

The electrostatic component of the attractive interaction between the surfactant molecules in the interfacial monolayer would be expected to decrease with increase in the ionic strength of the solution due to compression of the electrical double layer surrounding the ionic head groups. The explanation for the interaction increase with increase in ionic strength to 0.1 N IS is that some of the oxygen in the polyoxyethylene chain forms a complex with the sodium ion, in a manner similar to a crown ether (135), producing a positive charge on the nonionic surfactant. This causes interaction of the nonionic surfactant with the anionic surfactant as a partial cationic-anionic interaction. This is consistent with previous investigations in this laboratory showing that polyoxyethylenated nonionic surfactants have a stronger interaction with anionic surfactants at the L/V interface than with cationic surfactants with the same number of carbon atoms in the hydrophobic chain (25). It was also found that the interaction for $C_{12}(EO)_8$-$C_{12}SO_3Na$ system in 0.1 N IS (NaCl) at the L/V interface decreases (shows a less negative β value) with increase in pH of the solution (27). The formation of a complex between surfactants

having a crown ether attached to a long-chain alkyl group and alkali ions has been investigated by Okahara and coworkers (135). The logarithm of the complexing stability constant for octyl 18-crown-6 and potassium chloride is 1.7. The additive of an anionic surfactant tremendously favors the formation of the complex. The log of the constant for $C_{12}(EO)_8Na^+$ is about 7 in presence of $C_{12}SO_3Na$ (136). These data all suggest that polyoxyethylenated nonionic surfactants can form a cationic complex with sodium ion in aqueous solution, in the presence of an anionic surfactnt.

As the ionic strength is further increased to 0.5 N, the interaction decreases. This is because the usual decrease in electrostatic interaction between surfactants as a result of increase in ionic strength overcomes the increase due to increased complex formation with increase in sodium ion concentration (the complex is saturated with sodium ion and only increases slightly with the increase of the concentration of sodium ion). The values of average area per surfactant are consistent with the results. As the ionic strength changes to 0.1 N, the A_{av} values change significantly because 1) the formed complex increases the interaction with the anionic surfactant and 2) the increasing ionic strength lowers the repulsion between remaining charge on similarly charged surfactant molecules. The A_{av} value is only decreased slightly with further increase in ionic strength because the repulsive force between the surfactants having similarly charged head groups has already been decreased by the increase in ionic strength.

The β values for the C_{12}BMG-$C_{12}SO_3Na$ system at the L/T, L/Para and L/Poly interfaces become more negative as the ionic strength of the solution is increased to 0.1 N IS. The reason is similar as that for the nonionic-anionic systems. In a manner similar to the formation of a salt, $C_{12}H_{25}N(CH_3)_2OH^+ \cdot C_{12}SO_3^-$, between N,N-dimethyldodecylamine oxide and potassium dodecanesulfonate, postulated by Rosen et al (137), the hypothesis of a protonated betaine, $C_{12}BMGH^+$, in the presence of a small concentration of proton (pH = 5.85) was used to explain the high interaction between C_{12}BMG and $C_{12}SO_4Na$ at the L/V interface. And it is proved by the elemental analysis of the crystalline precipitate between C_{12}BMG and $C_{12}SO_3Na$ (138). In the case of C_{12}BMG, no complex can be formed with sodium ion, since sodium ion is not an acidic ion. Therefore the large decrease in average area per surfactant molecule with increase in ionic strength to 0.1 N probably is the cause of the increase in the interaction.

For the cationic-anionic surfactant mixture, C_{12}TMABr-$C_{10}SO_3Na$, the β value is tremendously changed (to less negative β value) with increase of ionic strength to 0.1 N IS, as expected. As mentioned before, the electrostatic attractive force between the cationic and anionic heads is the dominant contribution to the interaction of surfactants. The electrostatic force significantly decreases with increase in the ionic strength of the solution. The β value in 0.1 N IS is about half of that in the absence of added electrolyte at the L/T interface. This is consistent with that at the

L/V interface [β is -35.6 for C_{12}TMABr-$C_{10}SO_3Na$ in quartz-condensed water and is -19.7 for the same system in 0.1 N IS (NaBr)].

2 - 4 Effect of Surfactant Structure

Table A - 21 lists the interaction parameters and average areas per surfactant molecule at the various liquid/hydrophobic solid interfaces for nonionic-anionic, zwitterionic-anionic and cationic-anionic mixture systems in the absence and presence of excess inorganic electrolyte.

For the systems of $C_{12}(EO)_8$-$C_{12}SO_3Na$, C_{12}BMG-$C_{12}SO_3Na$ and C_{12}NBr-$C_{12}SO_3Na$ at the same ionic strength (0.1 N NaBr), the hydrophobic chain length was constant for all surfactants and the same anionic surfactant was used. The data in Table A - 21 show that the interaction between the surfactants is affected by the nature of the head groups of the two surfactants and that it increases with increase in electrostatic interaction in the order: polyoxyethylenated nonionic-anionic < zwitterionic-anionic < cationic-anionic. This is the same order as was found at the L/V interface and in mixed micelle formation in aqueous solution (120).

Table A - 21

Effect of Surfactant Structure on β Values

System	Mediun	Interface	A_{av} nm^{-2}	β
$C_{12}(EO)_8$-$C_{12}SO_3Na$	0.1N IS(NaCl)	L/T	0.58	-2.1
C_{12}BMG-$C_{12}SO_3Na$	0.1N IS(NaBr)	L/T	0.47	-6.2
		L/Para	0.44_5	-6.7
		L/Poly	0.62	-3.1
C_{12}NBr-$C_{12}SO_3Na$	0.1N IS(NaBr)	L/T	0.31_5	-16.7
		L/Para	0.31	-17.3
$C_{12}(EO)_8$-$C_{12}SO_4Na$	0.1N IS(NaCl)	L/T	0.57	-2.9
C_{12}TMABr-$C_{12}SO_4Na$	H_2O	L/T	0.44	-30.6
		L/Poly	0.55	-26.7
C_{12}TMABr-$C_{10}SO_3Na$	H_2O	L/T	0.46	-28.8
		L/Poly	0.56	-26.6
C_{12}TMABr-$C_{10}SO_3Na$	0.1N IS(NaBr)	L/T	0.51	-14.1
		L/Para	0.49	-15.3
C_{12}NBr-$C_{10}SO_3Na$	0.1N IS(NaBr)	L/T	0.35	-14.2
		L/Para	0.32	-15.5

Comparing the β values of $C_{12}(EO)_8$-$C_{12}SO_3Na$ with $C_{12}(EO)_8$-$C_{12}SO_4Na$ in aqueous 0.1 N IS (NaCl) and that between C_{12}TMABr-$C_{10}SO_3Na$ and C_{12}TMABr-$C_{12}SO_4Na$ in quartz-condensed water, the data show that the interactions of cationics or nonionics with alkyl sulfates are somewhat stronger than those with the corresponding sulfonates.

The previous data at the L/V interface (27) for polyoxyethylenated nonionic-anionic systems shown this same phenomenon and the greater polarizability of the sulfate group than the sulfonate group, due to the oxygen atom between carbon and sulphur, was used as a explanation. This can be also used here to explain the data at the liquid/hydrophobic solid interfaces.

The data in Table A - 21 also show that the interaction between C_{12}NBr and $C_{12}SO_3Na$ is similar as that between C_{12}TMABr and $C_{12}SO_3Na$. But the smaller A_{av} of the former would be expected to produce stronger interaction. The similar values of β suggest that the contribution of the smaller distance between the surfactant molecules is counteracted by the effect of positive charge dispersion in the pyridine ring, due to the conjugated electrons.

Based upon our data, we may conclude that the order of increased interaction between surfactant molecules in mixed monolayers at the liquid/hydrophobic solid interface is similar as that at the liquid/air interface and in the mixed micelle (24): i.e., polyoxyethylenated (POE) nonionic-POE nonionic < POE nonionic-

betaine < betaine-cationic < POE nonionic-ionic (cationic, anionic) << betaine-anionic << cationic-anionic. Therefore the possibility of synergism existing at liquid/hydrophobic solid interface is primarily in cationic-anionic mixture systems and then in betaine-anionic mixture systems.

2 - 5 Conclusions

1. The interface does have a major effect on the value of β, the interaction parameter for mixed monolayer formation. Attractive interaction between the two surfactants in the mixture decreases with change in the nature of the interface in order: L/V > L/Para > L/T > L/Poly. The average area per surfactant molecule at the interface increases in the same order.

2. For binary mixtures of surfactants with straight alkyl chain hydrophobic groups the interaction increases with increase in the carbon number of either surfactant and the maximum interaction occurs when their alkyl chains contain the same number of carbon atoms.

3. For cationic-anionic surfactant mixture systems the interaction between the different surfactant molecules in the monolayer decreases with increase in ionic strength of the solution phase to 0.1 N. The increase in interaction with increase in ionic strength for polyoxyethylenated nonionic-anionic mixture systems is due to cationic complex formation between oxygen of the

polyoxyethylene chains and alkali ion.

4. The nature of the chemical structures of the hydrophilic groups of the two surfactants has a significant effect on the extent of interaction between them. In general, the interaction decreases in the order: cationic-anionic >> betaine-anionic >> polyoxyethylenated nonionic-anionic.

IV.A.3 Synergism at the Liquid/Hydrophobic Solid Interface

In all wetting processes, the solid/liquid interface is increased. Since work is required to create additional interface, it is important, for the purposes of facilitating a wetting process, to reduce the value of γ_{sl}. It is also useful to know the concentration of surfactant in the liquid phase required to obtain a given value of γ_{sl} (reduction). When mixtures of surfactants are used, it is important to know whether the mixture will decrease γ_{sl} more efficiently or less efficiently than the individual surface-active components of the mixture.

3 - 1 Synergism in Interfacial Tension Reduction Efficiency at the Liquid/Hydrophobic Solid Interface

The efficiency of surface tension reduction by a surfactant is defined by Rosen (139) as the solution phase concentration required to produce a given surface tension (reduction). Synergism in interfacial tension reduction efficiency at a liquid/hydrophobic solid interface is present in a solution of mixed surfactants in contact with a hydrophobic solid when a given S/L interfacial tension (reduction) can be obtained at a total mixed surfactant concentration in the solution phase lower than that required of any component of the mixture.

The surfactant interaction parameters, β, and values of

ln C_1^o/C_2^o + (B_1 - B_2) for various mixtures in aqueous solution in the absence of added electrolyte and at 0.1 N IS (NaBr or NaCl) at the L/T, L/Para and L/Poly interfaces, together with the solid-liquid interfacial tension, γ_{sl}, values at which they were taken, are listed in Table A - 22. β values were calculated by substituting X, obtained by numerically solving Eq. [II-37], into equation [II-36]. In order to permit intercomparisons of the results from different interfaces, the value of γ_{sl} was kept constant. γ_{sl} was evaluated from Eq. [II-41] by assuming that the solid-vapor interfacial tension, γ_{sv}, is equal to the critical surface tension, γ_c, for low-energy solid surface and using γ_c equal to 18, 24 and 31 $mN\text{-}m^{-1}$ for Teflon, Parafilm and polyethylene (90), respectively. The areas per surfactant molecule in monolayers of the individual surfactants, A_1^o and A_2^o, and the average area per surfactant molecule in the mixed monolayers, A_{av}, were calculated from the surface excess concentration, Γ, by using Eq. [I-15]. In electrolyte solutions containing a swamping excess of counter-ion in common with the surfactant, the surface excess concentrations of the individual surfactants, Γ_1^o and Γ_2^o, and the total surface excess concentration of their mixture Γ_t, could be obtained by using Eqs. [I-10] and [I-14], respectively. The relative values of C_1^o, C_2^o, C_1 and C_2 were obtained from the plots of $\gamma_{lv}\cos\theta$ vs. log C in Figures 28 ~ 30, 32 ~ 39 and 49.

The surface tension data of $C_{12}(EO)_8$-$C_{12}SO_3Na$ in the aqueous solution without inorganic electrolyte and with excess

electrolyte (sodium chloride) of 0.1 N and 0.5 N total ionic strength were taken from reference (27).

Plots of ln C_t, the napierian logarithm of total concentration of mixed surfactants to yield a interfacial tension of 40 mN-m^{-1} at the L/V interface and 18 mN-m^{-1} at the liquid/solid interfaces, versus the molar fraction of C_{12}BMG in the total surfactant in the bulk phase for the C_{12}BMG-$C_{12}SO_3Na$ mixed system in 0.1 N IS (NaBr) aqueous solution at the L/V, L/T, L/Para and L/Poly interfaces are shown in Figures 50, 51, 52 and 53, respectively.

Figures 54, 55 and 56 show the curves of ln C_t, given a interfacial tension of 45 mN-m^{-1} and 24 mN-m^{-1} at the L/V and L/S interfaces, vs. α for the C_8NBr-$C_{12}SO_3Na$ mixture system in the presence of excess NaBr of total 0.1 N ionic strength at the L/V, L/T and L/Para interfaces, respectively.

It is apparent from the data in Table A - 22 that the synergism in interfacial tension reduction efficiency for C_{12}TMABr-$C_{10}SO_3Na$ and C_{12}BMG-$C_{12}SO_3Na$ mixed systems is predicted by the conditions of 1) β being negative 2) $|\ln C_1^o/C_2^o + (B_1 - B_2)| < |\beta|$, and it is found experimentally in the absence or presence of excess inorganic electrolyte at the L/T, L/para and L/Poly (except for C_{12}BMG-$C_{12}SO_3Na$ in the absence of added inorganic electrolyte) interfaces.

Table A - 22

Synergism in Interfacial Tension Reduction Efficiency at Various Interfaces

System	Interface	γ_{sl} mN-m^{-1}	M[a]	β	Predi.	Exp.
C_{12}TMABr-$C_{10}SO_3Na$	L/T	24	-1.36	-28.8	Yes	Yes
H_2O	L/Poly	24	-1.16	-26.6	Yes	Yes
C_{12}TMABr-$C_{10}SO_3Na$	L/T	24	-2.42	-14.1	Yes	Yes
0.1 N (NaBr)	L/Para	24	-2.40	-15.3	Yes	Yes
C_{12}BMG-$C_{12}SO_3Na$	L/T	18	-2.45	-6.2	Yes	Yes
0.1 N (NaBr)	L/Para	18	-2.32	-6.7	Yes	Yes
	L/Poly	18	-2.10	-3.1	Yes	Yes
C_{12}BMG-$C_{12}SO_3Na$	L/T	18	-4.34	-4.5	Yes	Yes
H_2O	L/Para	18	-4.31	-4.8	Yes	Yes
	L/Poly	18	-4.28	-1.6	No	No
$C_{12}(EO)_8$-$C_{12}SO_3Na$	L/T	17	-3.98	-2.1_5	No	No
0.1 N (NaCl)						
$C_{12}(EO)_8$-$C_{12}SO_3Na$	L/T	17	-5.50	-1.1	No	No
H_2O						

a. $M = \ln C_1^o/C_2^o + (B_1 - B_2)$

Table A - 22 also lists the data for $C_{12}(EO)_8$-$C_{12}SO_3Na$ mixtures in 0.1 N IS (NaCl) and aqueous solution without excess electrolyte at the L/T interface and C_{12}BMG-$C_{12}SO_3Na$ in aqueous solution without electrolyte at the L/Poly interface. These systems do not show synergism in interfacial tension reduction efficiency experimentally. And it is coincident with criterions for synergism. Although the values of β are negative (the first condition is satisfied) the values of $|\ln C_1^o/C_2^o + (B_1 - B_2)|$ is larger than that of $|\beta|$, the second condition is not satisfied.

It is noteworthy that, in all systems investigated (except C_{12}BMG-$C_{12}SO_3Na$ in absence of electrolyte at L/Poly interface), there was a consistency between synergism (or lack thereof) at the aqueous solution/air interface and at the aqueous solution/hydrophobic solid interfaces.

Table A - 23 lists some values of the minimum total mixed surfactant concentration for synergism to exist, $C_{t,lim}$, the mole fraction of surfactant 1 in the total surfactant in the bulk phase at the point of maximum synergism, α^*, and the minimum mole fraction of surfactant 1 in the total surfactant in the bulk phase at which synergism exists, α_{lim}, for the C_{12}BMG-$C_{12}SO_3Na$ system in 0.1 N IS (NaBr) at the L/V, L/T, L/Para and L/Poly interfaces. The calculated values were obtained by using Eqs. [II-24], [II-23] and [II-25], [II-26] and the experimental values were obtained from the

corresponding Figures 31, 32, 33 and 34. There is good agreement between calculated and experimental values. The difference between experimental and calculated values at the L/Poly interface is a little larger than that at the L/V, L/T and L/Para interfaces. This is consistent with the observation that the contact angle reproduciblity at the L/Poly interface is lower than that at the L/T and L/Para interfaces.

Table A - 23

Values of $C_{t,min}$, α^* and α_{lim} for $C_{12}BMG$-$C_{12}SO_3Na$ Mixture at 25 °C, IS = 0.1 N (NaBr).

Interface	γ mN-m^{-1}		$C_{t,min}$ mol-dm^{-3}	α^*	α_{lim}
L/V	45	Experimental	4.9×10^{-5}	0.68	0.23
		Calculated	4.7×10^{-5}	0.66	0.22
L/T	18	Experimental	8.5×10^{-5}	0.73	0.29
		Calculated	8.9×10^{-5}	0.70	0.29
L/Para	18	Experimental	9.3×10^{-5}	0.70	0.24
		Calculated	8.9×10^{-5}	0.67	0.23
L/Poly	18	Experimental	5.4×10^{-5}	0.82	0.43
		Calculated	6.3×10^{-5}	0.84	0.47

The experimental and calculated values of $C_{t,min}$ and α^* for the cationic-anionic surfactant system (C_8NBr-$C_{12}SO_3Na$) in 0.1 N IS (NaBr) are listed in Table A - 24. The agreement between calculated values and experimental results for this system is even better than that for zwitterionic-anionic mixture system.

For all the investigated systems (cationic-anionic, zwitterionic-anionic, nonionic-anionic surfactant mixtures in the absence or presence of excess inorganic electrolyte) the predicted, based upon nonideal solution theory, synergism in interfacial tension reduction efficiency (or lack thereof) and experimental results show good agreement at the aqueous solution/hydrophobic solid interfaces. There is also good agreement between calculated values and experimental results for $C_{t,min}$, α^* and α_{lim} in the systems where synergism exists.

Table A - 24

Values of $C_{t,min}$ and α^* for C_8NBr-$C_{12}SO_3Na$ Mixture at 25 °C, IS = 0.1 N (NaBr).

Interface	γ mN-m^{-1}		$C_{t,min}$ mol-dm^{-3}	α^*
L/V	45	Experimental	3.7×10^{-4}	0.35
		Calculated	3.7×10^{-4}	0.34
L/T	18	Experimental	3.9×10^{-4}	0.33
		Calculated	4.3×10^{-4}	0.35
L/Para	18	Experimental	3.8×10^{-4}	0.34
		Calculated	4.0×10^{-4}	0.34

3 - 2 Conclusions

1. The nonideal solution treatment of molecular interaction in binary mixtures of surfactants can be used at the liquid/hydrophobic solid interfaces. This permits the calculation of β, a parameter related to the molecular interactions between the two surfactants, and X, the mole fraction of surfactant 1 in the total surfactant in the mixed monolayer at that interface.

2. The conditions under which synergism in interfacial tension reduction efficiency will exist at that interface are: 1) β is negative; 2) the absolute value of β is larger than $|\ln C_1^o/C_2^o + (B_1 - B_2)|$. There is good agreement between predicted and experimental results for synergism (or lack thereof) at the liquid/hydrophobic solid interface.

3. The equations that have been derived for the calculation of minimum total mixed surfactant concentration in the solution phase required to produce a given value of interfacial tension, $C_{t,min}$, the limiting (minimum) mole fraction of surfactant 1 in the total surfactant in the solution phase at which the synergism exists, α_{lim}, and the mole fraction of surfactant 1 in the total surfactant in the bulk phase at the point of the maximum synergism, α^*, give calculated values for these quantities that agree well with the experimental results.

IV.B Thermodynamic Characteristics of Surfactants in Interfacial Monolayers

IV.B.1 The Standard Free Energy of Adsorption of Individual Surfactants

The standard free energy of adsorption for individual surfactants was calculated by use of equation [I-25]. The minimum area per molar surfactant, $A_{min.}$, was calculated from the slope of γ_{lv} (or $\gamma_{lv}Cos\ \theta$) vs. log C curve at the linear part. The adhesion tension corresponding to π = 20 mN-m^{-1} is -6.97, -7.55 and 16.23 mN-m^{-1} at the L/T, L/Para and L/Poly interfaces, respectively. The Debye-Huckel equation , Eq. [I-26], was used to evaluate the activity coefficients in which I is the ionic strength based on the free ions in the solution, α is the mean distance approach of the ions (taken as 0.6 for the surfactant and 0.3 for the counterions) (140) and B is related the dielectric constant of solvent and is 0.509 for quartz-condensed water at 25 °C.

The standard free energy of adsorption for nonionic ($C_{12}(EO)_8$), zwitterionic ($C_{12}BMG$), anionic ($C_{12}SO_3Na$, $C_{12}SO_4Na$) and cationic surfactants ($C_{12}TMABr$), each containing a straight-chain C_{12} hydrophobic group, in different ionic strength solutions, at various interfaces, are listed in Table A - 25. At all three different ionic strengths the standard free energies of adsorption for the nonionic surfactant ($C_{12}(EO)_8$) are almost constant (the

deviation is within the experimental error) at the L/V and L/T interfaces. The data for the zwitterionic surfactant (C_{12}BMG) at the L/V, L/T, L/Para and L/Poly interfaces also show ionic strength independence. But for the ionic (anionic and cationic) surfactants, the values calculated in the absence of added inorganic electrolyte are more somewhat negative than that in the presence of extra electrolyte at all the investigated interfaces. The value of the standard free energy of adsorption, using activity coefficients, should be constant with change in the ionic strength of the solution. The more negative ΔG^{o}_{ad} value in the absence of added electrolyte is due to the assumption that the surface concentration of surfactant counter-ion is equal to that of surfactnat ion in the monolayer. The higher value of ΔG^{o}_{ad} indicates that the surface concentration of counterion is lower than that of surfactant ion in the monolayer in the absence of added electrolyte. This is consistent with the concept of the electrical double layer containing a diffuse region of counterion extending into the solution phase. Therefore, the values, calculated in the presence of excess electrolyte, are more reliable than those obtained in the absence of added electrolyte.

Table A - 25

The Standard Free Energy of Adsorption in Different Ionic Strength Solutions at Various Interfaces

System	Medium	Interface	ΔG^{o}_{ad} KJ-mole^{-1}
C_{12}BMG	H_2O	L/V	-42.2
		L/T	-43.2
		L/Para	-44.7
		L/Poly	-41.0
	0.1N IS (NaBr)	L/V	-42.6
		L/T	-43.0
		L/Para	-44.2
		L/Poly	-41.2
$C_{12}(EO)_8$	H_2O	L/V	-47.6
		L/T	-47.4
	0.1N IS (NaCl)	L/V	-48.0
		L/T	-47.3
	0.5N IS (NaCl)	L/V	-48.1
		L/T	-46.8
$C_{12}SO_3Na$	H_2O	L/V	-53.7
		L/T	-56.5

		L/Para	-57.6
		L/Poly	-54.8
	0.1N IS (NaBr)	L/V	-51.7
		L/T	-52.4
		L/Para	-53.4
		L/Poly	-51.5
$C_{12}SO_4Na$	H_2O	L/V	-54.0
		L/T	-58.3
	0.1N IS (NaCl)	L/V	-52.3
		L/T	-53.5
$C_{12}TMABr$	H_2O	L/V	-52.4
		L/T	-56.6
	0.1N IS (NaBr)	L/V	-51.6
		L/T	-52.4

The difference in the value in the absence and in the presence of excess electrolyte, ΔG^{o}_{ad}, is 1 ~ 2 KJ-mol^{-1} at the L/V interface, which means that the surfactant ion/counterion ratio in the monolayer is slightly larger than 1. At the L/S interfaces the difference is raised up to about 4 KJ-mol^{-1}. The larger difference at the L/S interfaces may reflect the smaller electrical charge density at those interface, compared with that at the L/V interface, as evidenced by the larger area per surfactant molecule at the L/S interfaces. As the electrical charge density decreases, the surfactant ion/counterion ratio should become larger, producing a larger ΔG^{o}_{ad} value.

For all the investigated surfactants except $C_{12}(EO)_8$, the standard free energy is changed to a more negative value in the order: L/V ~ L/Poly → L/T → L/Para. The more negative values at liquid/hydrophobic solid interfaces reflect stronger adsorption than that at the L/V interface. More negative ΔG^{o}_{ad} values at hydrocarbon organic liquid/aqueous solution interfaces have been obtained in this laboratory for $C_{12}SO_4Na$ and $C_{12}BMG$. Mukerjee's data (52) show that the free energies of adsorption for hydrocarbon and fluorocarbon surfactants at the L/V interface are less negative values than that at the hexane/water and perfluorohexane/water interfaces, respectively. The probable explanation is that besides the hydrophobic chain interactions of the surfactant molecule there exist van der Waals interactions between the hydrophobic solid surface and the hydrophobic chains of the surfactant. Another

reason is that the repulsion force between similarly-charged the head groups of the adsorbed surfactant, decreases with increase in the distance between them. Therefore, the free energy of adsorption should be more negative with the increase in the area per surfactant molecule from the L/V interface to the L/S interfaces. The smallest values at the L/Poly interface is due to the partial polar property of the solid surface. The mutual phobicity (126,127,128,129,130,131) between the hydrocarbon chains of the surfactant molecules and the fluorocarbon solid surface causes the intermediate values at the L/T interface. The comparable data at S/L interfaces are limited.

The standard free energies of adsorption for $C_{12}(EO)_8$ show similar values at the L/V and the L/T interfaces at various ionic strengths. For nonionic surfactants the head repulsive force change with the distance between the adsorbed surfactant molecules makes no contribution to the ΔG^{o}_{ad} value.

Tables A - 26, 27 and 28 list the standard free energies of adsorption and the changes ($\Delta\Delta G^{o}_{ad}$) in ΔG^{o}_{ad} upon adding two methylene groups ($-CH_2-$) to a hydrocarbon chain in homologous series of anionic and cationic surfactants at the L/V, L/T and L/Para interfaces, respectively.

From the data in Table A - 26, $\Delta\Delta G^{o}_{ad}$ per methylene group at the L/V interface is -3.1 KJ-mol^{-1} is not dependent on the head group. Previous studies (141) have shown that $\Delta\Delta G^{o}_{ad}$ values for

moderate to high chain lengths are likely to be independent of head-group effects. The value of -3.1 KJ-mol^{-1} per methylene group adsorption is in good agreement with the values of -3.05 ~ -3.15 KJ-mol^{-1} for N-alkyl, N-benzyl, N-methylglycines and N-alkyl, N-benzyl, N-methyltaurines (110) and for long-chain alcohols and 1,3-diols (54) at the L/V interface.

At the L/T and L/Para interfaces the values of $\Delta\Delta G^{o}_{ad}$, show in Table A - 27 and 28, are smaller than the corresponding values at the L/V interface and decrease with increase of the length of hydrophobic chains. Both of these indicate that a "steric inhibition" effect exists in adsorption at the L/S interfaces. The less negative values of $\Delta\Delta G^{o}_{ad}$ at the L/T interface, compared with that at the L/Para interface, is due to the mutual phobicity effect between hydrocarbon chains of surfactant molecule and fluorocarbon solid surface, causing the contribution of hydrophobic interactions between hydrocarbon chains and hydrophobic surface upon adding methylene groups to the long-chain in the former case to be less than in the latter. Unlike the case at the L/V interface, here the $\Delta\Delta G^{o}_{ad}$ values appear to be dependent on the head group of surfactants and/or on the length of the hydrophobic group. Perhaps the increased repulsion between similarly-charged head groups which accompanies the decrease in area per surfactant molecule with increased chain length is not counter balanced as much, in the case of the L/T or L/Para interfaces, by chain-chain interactions because of bending of the chains. Note: somewhat

larger area per surfactant at the L/T and L/Para interfaces, compared to that at the L/V interface. In case of the L/T interface there is also the "mutual phobicity" of the fluorocarbon and hydrocarbon chains which might decrease the $\Delta\Delta G^{o}_{ad}$ per methylene group even more.

Table A - 26

The Standard Free Energies of Adsorption of Surfactants in 0.1 N IS (NaBr) at the L/V Interface

System	$A_{min.}$ nm^2	ΔG^o_{ad} $KJ\text{-}mol^{-1}$	$\Delta\Delta G^o_{ad}$ $KJ\text{-}mol^{-1}$
C_8NBr	0.61	-40.7	
			-6.3
$C_{10}NBr$	0.57	-47.0	
			-6.3
$C_{12}NBr$	0.53	-53.3	
$C_{10}SO_3Na$	0.43	-45.5	
			-6.2
$C_{12}SO_3Na$	0.42	-51.7	
$C_{12}TMABr$	0.51	-51.5	
			-6.2
$C_{14}TMABr$	0.47	-57.7	

Table A - 27

The Standard Free Energies of Adsorption of Surfactants in 0.1 N IS (NaBr) at the L/T Interface

System	$A_{min.}$ nm^2	ΔG^o_{ad} $KJ\text{-}mol^{-1}$	$\Delta\Delta G^o_{ad}$ $KJ\text{-}mol^{-1}$
C_8NBr	0.76	-44.3	
			-5.6
$C_{10}NBr$	0.70	-49.9	
			-4.8
$C_{12}NBr$	0.63	-54.7	
$C_{10}SO_3Na$	0.55	-47.2	
			-5.2
$C_{12}SO_3Na$	0.53	-52.4	
$C_{12}TMABr$	0.59	-52.4	
			-4.2
$C_{14}TMABr$	0.50	-56.6	

Table A - 28

The Standard Free Energies of Adsorption of Surfactants in 0.1 N IS (NaBr) at the L/Para Interface

System	$A_{min.}$ nm^2	ΔG^o_{ad} $KJ\text{-}mol^{-1}$	$\Delta\Delta G^o_{ad}$ $KJ\text{-}mol^{-1}$
C_8NBr	0.69	-44.3	
			-5.9
$C_{10}NBr$	0.67	-50.2	
			-5.2
$C_{12}NBr$	0.56	-55.4	
$C_{10}SO_3Na$	0.52	-47.8	
			-5.6
$C_{12}SO_3Na$	0.50	-53.4	
$C_{12}TMABr$	0.54	-52.9	
			-5.0
$C_{14}TMABr$	0.48	-57.9	

IV.B.2 The Free Energy of Adsorption of Mixed Surfactants

The plots of surface tension (or adhesion tension) versus logarithm of total surfactant concentration (in mol-dm^{-3}) for the six cationic-anionic mixtures of C_nNBr-C_mSO_3Na (n = 8, 10, 12; m = 10, 12), all at equimolar concentrations of cationic and anionic in the bulk phase (i.e., α = 0.5), in 0.1 N IS (NaBr) aqueous solution at the L/V, L/T and L/Para interfaces are shown in Figure 23 ~ 28.

The difference between the free energy of adsorption, calculated from Eq. [II-50], and a standard free energy of adsorption is that the former contains the extra free energy of adsorption due to the interactions between the components and related to the activity coefficients in the bulk phase and in the interfacial monolayer.

In case of the cationic-anionic mixed systems, the very small total bulk phase concentrations, made the change in the activity coefficients in the bulk phase with change in the mole fraction negligible. Therefore, the main deviation is caused by the change in activity coefficients at the interface (f^s). In order to obtain comparable free energies of adsorption for mixed surfactants, a fixed ratio of the two surfactants in the monolayer should be specified as a standard state, for example, equimolar.

In the case where the interaction of the surfactants with the solvent are neglected, the activity coefficients in the mixed

monolayer, entirely due to interactions of the two surfactants, may be evaluated from the second term of the Margules expansion (Eqs. [II-10] and [II-11]). The value of ln $f_1^s f_2^s$ is a function of the interfacial mole fraction, X, equal to $\beta(1 - 2X + 2X^2)$. Table A - 29 lists the values of X and $\beta(1 - 2X + 2X^2)$ for six equimolar mixed systems, C_nNBr-C_mSO_3Na, at the L/V interface. The data show that the value of $\beta(1 -2X + 2X^2)$ is not very sensitive to the value of X and the maximum deviation is 8% for the system of C_8NBr-$C_{12}SO_3Na$. Therefore, data calculated using equimolar bulk phase concentrations instead of the equimolar ratio in the monolayer should not have significant error and are comparable.

From the experimental data at equimolar bulk phase concentrations, the free energies of adsorption of the mixed surfactants at the various interfaces have been calculated by using Eq. [II-50] in the range where the interface is saturated with surfactants. Here the assumption that the free energy of adsorption of water (ΔG_{H_2O}) is equal to zero was used (109). Based upon the Gibbs surface definition ($\Gamma_{H_2O} = 0$), the standard free energy of adsorption of water ($\Delta G^o_{H_2O}$) should be zero. The portion of free energy of adsorption of water, corresponding to the difference in its activity coefficients in the surface and bulk phases is so small (43,44,45,47,48) that it does not essentially affect the value of the adsorption free energy and is negligible compared to the work term (πA) of water.

Table A - 29

The Values of X and $\beta(1 - 2X + 2X^2)$ for the Mixed System, C_nNBr-C_mSO_3Na, at the L/V Interface in 0.1 N IS (NaBr)

n	m	x	$\beta(1 - 2X + 2X^2)$
8	10	0.413	0.515β
10	10	0.483	0.501β
12	10	0.545	0.504β
8	12	0.356	0.541β
10	10	0.428	0.510β
12	10	0.491	0.500β
Standard State		0.500	0.500β

The data shown in Table A - 30, 31 and 32 are the free energies of adsorption (ΔG) per mole of mixed surfactants, calculated by using Eq. [II-50], and the adsorption free energy changes for two methylene groups ($\Delta\Delta G$) for the equimolar cationic-anionic mixture systems at the L/V, L/T and L/Para interfaces, respectively.

The free energies of adsorption of the C_8NBr-$C_{10}SO_3Na$ and $C_{10}NBr$-$C_{10}SO_3Na$ mixed systems in 0.1 N IS (NaBr) at the L/V interface are -53.6 KJ/mole and -59.6 KJ/mole and the literature values (49) are -57.0 KJ/mole and -63.3 KJ/mole for the C_8NCl-$C_{10}SO_3Na$ and $C_{10}NCl$-$C_{10}SO_3Na$ systems in 0.1 N NaBr aqueous solution. We can not find literature data to compare with our results at the solid/aqueous solution interface.

The values of the free energy of adsorption are similar for the same mixture system at all three interfaces investigated. This is agreement with results (142) for the nonionic surfactants, N-alkyl-2-pyrrolidones. Although the area per surfactant is different at the L/V, L/T and L/Para interfaces, there are similar values of the standard free energy of adsorption at these three interfaces. This is because in these mixed systems the formation of a cation-anion pair (R^+R^-) in the monolayer causes the adsorption of these cationic-anionic mixtures to resemble the adsorption of a nonionic surfactant. There is no effect of electrical repulsion between similarly-charged head groups on the free energy of adsorption for

the non-charged surfactant pair. And the contribution of the hydrophobic interaction between the hydrocarbon chain and the hydrophobic solid surface is offset by the "steric inhibition" of adsorption at the L/S interfaces. This is consistent with the case of the nonionic surfactant ($C_{12}(EO)_8$), mentioned in the above section. The slightly smaller value of the adsorption free energy at the L/T interface than at the L/V and L/Para interfaces is because of the effect of the mutual phobicity of the hydrocarbon chains and the fluorocarbon surface.

In the mixed systems there is the same linear relationship between the total carbon atom number (of cation plus anion) and the free energy of adsorption as in the individual surfactants at the air/aqueous interface. The slopes are -3.5 KJ-mole^{-1} per -CH_2- increase in the alkyl sulfonate and -3.1 KJ-mole^{-1} per -CH_2- increase in the alkyl pyridinium salts. Goralczyk's values (49) are -3.6 KJ-mole^{-1} for alkyl sulfonate and -3.3 KJ-mole^{-1} for alkyl pyridinium salts, obtained by using a different approach.

At the L/T and L/Para interfaces, the increment, $\Delta\Delta G(R^-)$, on adding a methylene group to a alkylsulfonate is -3.2 KJ-mol^{-1} and -3.1 KJ-mol^{-1}, respectively, and for the same addition to the alkylpyridinium salts is -2.7 ~ -2.5 and -2.9 ~ -2.7 KJ-mol^{-1}, respectively. These follow the results at the L/V interface, in that the addition of a -CH_2- to the alkylpyridinium is less negative than the addition to the alkylsulfonate. At present, this cannot be

explained. However, the less negative increments at the L/T and L/Para interfaces than at the L/V interface, indicate that adsorption of a longer chain length at the L/V interface is more favour than at the L/S interfaces. An explanation is that at the L/S interface hydrocarbon chains are partially bent and cannot be so close-packed as at the L/V interface.

Table A - 30

The Free Energies of Adsorption and the Changes of Two Methylene Groups at the L/V Interface for Equimolar Mixture of C_nNBr-C_mSO_3Na, in 0.1 N IS (NaBr)

m/n		8	10	12
	$-\Delta\Delta G(R^+)$	6.0	6.1	
10	$-\Delta G(R^+R^-)$	53.6	59.6	65.7
	$-\Delta\Delta G(R^-)$	6.9	6.9	6.9
	$-\Delta\Delta G(R^+)$	6.0	6.1	
12	$-\Delta G(R^+R^-)$	60.5	66.5	72.6

Unit: $[\Delta G] = KJ\text{-}mol^{-1}$

Table A - 31

The Free Energies of Adsorption and the Changes of Two Methylene Groups at the L/T Interface for Equimolar Mixture of C_nNBr-C_mSO_3Na, in 0.1 N IS (NaBr)

m/n		8	10	12
	$-\Delta\Delta G(R^+)$	5.3	4.9	
10	$-\Delta G(R^+R^-)$	53.5	58.8	63.7
	$-\Delta\Delta G(R^-)$	6.3	6.4	6.4
	$-\Delta\Delta G(R^+)$	5.3	4.9	
12	$-\Delta G(R^+R^-)$	59.8	65.2	70.1

Unit: $[\Delta G] = KJ\text{-}mol^{-1}$

Table A - 32

The Free Energies of Adsorption and the Changes of Two Methylene Groups at the L/Para Interface for Equimolar Mixture of C_nNBr-C_mSO_3Na, in 0.1 N IS (NaBr)

m/n		8	10	12
	$-\Delta\Delta G(R^+)$	5.8	5.4	
10	$-\Delta G(R^+R^-)$	54.3	60.1	65.5
	$-\Delta\Delta G(R^-)$	6.1	6.2	6.3
	$-\Delta\Delta G(R^+)$	5.9	5.5	
12	$-\Delta G(R^+R^-)$	60.4	66.3	71.8

Unit: $[\Delta G] = KJ\text{-}mol^{-1}$

IV.B.3 Conclusions

1. The results show that the standard free energy of adsorption depends on the nature of the interface and decreases in the order: L/V → L/Poly → L/T → L/Para. The value of - 3.1 KJ-mole^{-1} for adsorption per methylene group at the L/V interface is independent of the head group of the surfactant and the length of its hydrophobic group in the C_8 ~ C_{14}. At the S/L interfaces the standard free energy of adsorption per methylene group (-2.8 ~ -2.1 and -2.9 ~ -2.5 KJ-mol^{-1} at the L/T and L/Para interface, respectively) decreases with increase in the carbon chain length and is smaller than the corresponding value at the L/V interface

2. The free energy of adsorption of cationic-anionic pairs (R^+R^-) was calculated by a new method. A linear relationship between the total carbon atom number and the free energy of adsorption was found at the L/V interface. The behaviour of a cationic-anionic surfactant pair (R^+R^-) is much like that of a nonionic surfactant and is not sensitive to the nature of the (low free energy) interfaces investigated. All results, the free energies of adsorption for mixed surfactant systems obtained by use of new method, are consistent with the data of standard free energy of adsorption calculated using the Rosen-Aronson approach, in that $\Delta\Delta G$ ($-CH_2-$) is constant at the L/V interface and decreases with increase of carbon chain length at the L/T and L/Para interfaces and the slightly less negative value of ΔG at the L/T interface than at the L/V and L/Para interfaces.

IV.C.1 The Relative Adsorption of Surfactants to the Solid/Liquid and the Liquid/Vapor Interfaces

The plots of adhesion tension, $\gamma_{lv}Cos\theta$, versus surface tension, γ_{lv}, for anionic surfactants $C_{10}SO_3Na$ and $C_{12}SO_3Na$, cationic surfactant $C_{12}TMABr$ and zwitterionic surfactant $C_{12}BMG$, on Teflon, Parafilm and polyethylene, all at constant ionic strength of 0.1 N (NaBr), except for $C_{12}TMABr$ on polyethylene, are show in Figures 57, 58, 59 and 60, 61, 62.

Figures 63, 64 and 65 show the plots on Teflon for individual surfactant solutions of C_nNBr and C_8SO_3Na, and cationic-anionic surfactant mixture solutions of C_nNBr-$C_{10}SO_3Na$ and C_nNBr-$C_{12}SO_3Na$, where n = 8, 10, 12, all of them in 0.1 N IS (NaBr).

The plots for the same systems on Parafilm are shown in Figures 66, 67 and 58.

Table A - 33 lists values of the slope of the plots of adhesion tension ($\gamma_{lv}Cos\theta$) versus surface tension for various surfactant solutions on Teflon, Parafilm and polyethylene. According to Eq. [I-23], the absolute value of the slope represents the relative adsorption of the surfactant at the solid/liquid and the liquid/vapor interfaces, based upon the assumption of no excess surface adsorption at the solid/vapor interface.

Table A - 33

The Slope of Plot of Adhesion Tension Versus Surface Tension on Various Low-Energy-Surface Solids

System	Teflon	Parafilm	polyethylene
C_{12}TMABr 0.1 N IS (NaBr)	-0.87	-0.96	-0.72[a]
$C_{10}SO_3Na$ 0.1 N IS (NaBr)	-0.80	-0.82	-0.65
$C_{12}SO_3Na$ 0.1 N IS (NaBr)	-0.79	-0.89	-0.77
C_{12}BMG 0.1 N IS (NaBr)	-0.95	-1.02	-0.94

a. in absence of added extra electrolyte

Although a slope of minus one has often been accepted at low-energy surfaces (35,143,144,145,146), the data in Table A - 33 show deviation from that value and dependence of the slope on the nature of the solid surface. In all the systems studied, the relative adsorption decrease in the order: Parafilm > Teflon > polyethylene. If we assume that the excess surface concentration at the solid/vapor phase for these surface is indeed zero, then this means that the adsorption of the surfactants from aqueous solution to the solid surface decreases in this same order. This is consistent with the area per molecule (A_{av}) data obtained using the Gibbs adsorption equation: A_{av} increases in the order, L/Para < L/T < L/Poly. In previous studies (147,148) it has been shown that adsorption decreases as the substrate becomes more polar. Paraffin has been shown to be extremely nonpolar and both Teflon and polyethylene exhibit some polar character (γ_s^p: paraffin = 0.0 Teflon = 1.7; polyethylene = 3.4 $mN\text{-}m^{-1}$) from wetting studies using pure liquids (125). The data shown here reflect this character.

Tables A - 34, 35 list the slopes of the plots of $\gamma_{lv}Cos\theta$ vs. γ_{lv}, the relative adsorptions to the solid/liquid and the liquid/vapor interfaces calculated based upon the Gibbs adsorption equation, A_{lv}/A_{sl}, and the critical surface tensions, γ_c obtained by extrapolating the plots of $\gamma_{lv}Cos\theta$ vs. γ_{lv} to zero contact angle for the aqueous surfactant solutions on Teflon and Parafilm, respectively.

Table A - 34

Relative Adsorptions of Individual and Mixed Surfactant in 0.1 N IS Solution and Critical Surface Tensions on Teflon

system	-Slope	A_{lv}/A_{sl}	γ_c
C_8NBr	0.93	0.84	23.1
$C_{10}NBr$	0.86	0.81	21.3
$C_{12}NBr$	0.84	0.82	20.2
$C_{12}TMABr$	0.90	0.86	20.6
C_8SO_3Na	0.83	0.78	16.6
$C_{10}SO_3Na$	0.80	0.78	19.6
$C_{12}SO_3Na$	0.79	0.78	18.2
$C_{12}BMG$	0.95	0.89	20.6
C_8NBr-$C_{10}SO_3Na$	0.93	0.87	20.5
$C_{10}NBr$-$C_{10}SO_3Na$	0.90	0.87	19.1
$C_{12}NBr$-$C_{10}SO_3Na$	0.87	0.90	18.0
C_8NBr-$C_{12}SO_3Na$	0.88	0.84	19.1
$C_{10}NBr$-$C_{12}SO_3Na$	0.88	0.86	18.6
$C_{12}NBr$-$C_{12}SO_3Na$	0.89	0.88	17.2

Table A - 35

Relative Adsorptions of Individual and Mixed Surfactant in 0.1 N IS Solution and Critical Surface Tensions on Parafilm

system	-Slope	A_{lv}/A_{sl}	γ_c
C_8NBr	0.96	0.94	24.3
$C_{10}NBr$	0.90	0.93	22.7
$C_{12}NBr$	1.00	0.96	23.8
$C_{12}TMABr$	1.02	0.94	23.7
C_8SO_3Na	0.79	0.82	18.2
$C_{10}SO_3Na$	0.82	0.83	21.1
$C_{12}SO_3Na$	0.89	0.84	21.8
$C_{12}BMG$	1.02	0.94	23.5
C_8NBr-$C_{10}SO_3Na$	0.96	0.95	22.5
$C_{10}NBr$-$C_{10}SO_3Na$	0.97	0.93	22.3
$C_{12}NBr$-$C_{10}SO_3Na$	1.03	0.99	22.5
C_8NBr-$C_{12}SO_3Na$	0.97	0.94	22.5
$C_{10}NBr$-$C_{12}SO_3Na$	1.00	0.94	22.1
$C_{12}NBr$-$C_{12}SO_3Na$	1.07	0.99	21.3

Table A - 36

The Contact Angles of Surfactant Solution at 0.1 N IS (NaBr) on Teflon and Parafilm Surface; γ_{lv} = 45 mN-m^{-1}

Surfactant	Teflon	Parafilm
C_{12}BMG	92.9°	87.6°
$C_{12}SO_3Na$	94.3°	89.0°
C_{12}NBr	90.8°	86.6°
C_{12}TMABr	91.7°	86.8°

In these studies the plot slope of $\gamma_{lv}Cos\theta$ vs. γ_{lv} does not follow the prediction of the "Good-Girifalco-Fowkers-Young" equation, Eq. [I-53], of a slope of minus one. The deviation implies that the assumption of zero surface pressure of solid, π_s = 0, is a debatable point even for low-energy-surface solids, as argued by some investigators (93,149). This suggests that the adsorption of surfactant at the solid/vapor interface is not exactly zero like usually assumed. Zografi and co-worker (149) stressed the negative contribution from a finite adsorption at the solid/vapor interface to the wetting process and van Voorst Vader (143) indicated that Γ_{sv} is about 2% of Γ_{lv} by using literature data. Murphy et al. (150) found that the adsorption at the S/V interface was significant for the butanol - a volatile chemical. For a nonvolatile surfactant the slight adsorption at the S/V may be caused by the adsorption of surfactant at the wetting meniscus. This has been used by Pletnev (151) to explain the observation that surfactant solutions having the same surface tension often produce higher contact angles at low-energy surfaces than individual liquids.

The values of the slope, which most are slightly larger than -1, means a slightly higher surfactant adsorption density at the L/V interface than at the S/L interface. This is consistent with the results obtained using the Gibbs adsorption equation, from which the area per surfactant at the L/V interface is always slightly less than at the S/L interface.

It is clear from the data in Tables A - 34 and 35 that the nature of the surfactant does have a effect on the value of the slope. On both Teflon and Parafilm the lowest slope values for anionic surfactants indicates the greatest tendency for anionic surfactant to adsorb less at the solid/liquid interface than at the liquid/vapor interface, compared to other types of surfactant. This is consistent with the contact angle values of the various surfactant solution at the same surface tension value, listed in Table A - 36, where all surfactants have the same chain length at same ionic strength. The highest contact angle is caused by the highest value of γ_{sl}, assuming constant value of γ_{sv} for all surfactants and based on Young's equation (Eq. [I-60]). The lowering of γ_{sl} is related to the surfactant adsorption at the L/S interface. The high contact angles (and correspondingly high values of γ_{sl}) for the anionic surfactant indicates relatively poor adsorption at the Teflon and Parafilm L/S interface.

The data in Table A - 36 also indicate that the anionic surfactant will give poorer wettability for Teflon and Parafilm than the other surfactants having same carbon chain length, when the value of γ_{lv} is the same.

For the same type of surfactant the slope value also shows the dependence of relative adsorption at the S/L and L/V interfaces on hydrocarbon chain length. On Teflon, the slope becomes less negative with increase in the alkyl chain length. An explanation

may be the "mutual phobicity" of the hydrocarbon chains of the adsorbed surfactant molecules and the fluorocarbon surface of the solid, which inhibits adsorption of longer chain surfactants at the liquid/Teflon interface. The reverse case on Parafilm suggests that the attractive interaction between the hydrocarbon chains of the adsorbed surfactant molecules and the hydrocarbon surface, favoring adsorption of the longer chain surfactants.

The data in Tables A -34, 35 also show that the values for the relative adsorption at the the S/L and L/V interfaces, obtained from the absolute values of the slope of the $\gamma_{lv}Cos\theta$ vs. γ_{lv} plot, are similar to the values of A_{lv}/A_{sl} calculated from the Gibbs adsorption equation. However, the former are generally slightly larger than the latter. This implies that the assumption of constant γ_{sv} (Eq. [I-17]) used in computation of A_{sl} is doubtful.

In Table A - 34 the critical surface tensions of Teflon, γ_c, obtained by extrapolating the plots of $\gamma_{lv}Cos\theta$ vs. γ_{lv} for surfactant solution up to zero contact angle ($Cos\theta = 1$), show good agreement with the value of 18 - 19 $mN\text{-}m^{-1}$, widely adopted for the Teflon surface. The larger deviation of γ_c for C_8NBr probably is due ununiform ionic strength and for C_8SO_3Na is also caused by the impurity of the solution. The cationic and anionic surfactant mixtures give γ_c values which show less variation and are closer to the value obtained by using pure liquids than that calculated from the plots of individual surfactant solutions. The average value of

18.8 mN-m^{-1}, based on six cationic-anionic surfactant mixtures, is identical with the value given by pure liquids.

The γ_c values for Parafilm in Table A - 35, are lower than the critical surface tension of paraffin, 24 mN-m^{-1}. The higher contact angle of pure water on Parafilm, 112.5°, comparing with the literature value of pure water on paraffin, 110° (116), suggests that the Parafilm has a lower surface energy than that of paraffin. An expression

$$\text{Cos}\theta = (2\gamma_c - \gamma_{lv})/\gamma_{lv}$$

was derived by Johnson (152), using the Young's and Gibbs equations, based upon the assumptions of no change in γ_{sv} and equal adsorption to the liquid/vapor and solid/liquid interfaces. The value of γ_c for Parafilm is 22.2 mN-m^{-1} by use of the contact angle of water on Parafilm in this equation. According to the "Good-Girifalco-Fowkers-Young equation" (Eq. [I-53]), the intercept of the plot of $\gamma_{lv}\text{Cos}\theta$ vs. γ_{lv} is related to the dispersion parts of the surface energies of the solid and liquid surfaces and is given by the expression $2(\gamma_s^d \cdot \gamma_{lv}^d)^{\frac{1}{2}}$. Using the intercept value of 44 mN-m^{-1} for Parafilm and the literature value of γ_{lv}^d = 21.8 mN-m^{-1} for water (143,144), the dispersion part of the surface energy of Parafilm is 22.2 mN-m^{-1}. For low-energy-surface solids the dispersion force, γ_s^d, of the solid should just equal the critical surface tension, γ_c, as obtained from the theoretical derivation and verified experimentally by Fowkers (85). Therefore, the critical surface tension value of 22.2 mN-m^{-1} for Parafilm is acceptable.

The average value of γ_c based upon the plots of the six cationic-anionic surfactant mixtures, 22.4 mN-m^{-1}, shows excellent agreement with that of 22.2 mN-m^{-1}. The slightly larger deviation of γ_c for C_8NBr and C_8SO_3Na is due to the same resons as on Teflon.

IV.C.2 Conclusions

The results of this study indicate that the relative adsorption, determined by using adhesion tension vs. surface tension plots, shows unequal adsorption of surfactant at the solid/liquid and the liquid/vapor interfaces. The values of the slope, slightly larger than minus one, suggesting less adsorption at the solid/liquid interface than at the liquid/vapor interface, show good agreement with the results obtained by use of the Gibbs adsorption equation.

The nature of solid surface affects the relative adsorption, which decrease in the order: Parafilm > Teflon > polyethylene, and it is consistent with our previous results. Anionic surfactants show lower relative adsorption values on Teflon and Parafilm surfaces. The relative adsorptions also show dependence on the hydrocarbon chain length of the adsorbed surfactant. The "mutual phobicity" between the hydrocarbon chains of the surfactant molecules and the fluorocarbon surface of Teflon causes a decrease in the relative adsorption of surfactant at the S/L and the L/V interfaces with increase in the hydrocarbon chain length of the adsorbed

surfactant. The opposite case on Parafilm is due to the attractive forces between the hydrocarbon units of the surfactant and the Parafilm surface.

From the experimental results, Parafilm has a lower surface energy than paraffin and a critical surface tension of 22.2 $mN\text{-}m^{-1}$ is a reasonable value for Parafilm. The values of the critical surface tension on both Teflon and Parafilm, obtained by extrapolating the plots of adhesion tension vs. surface tension to zero contact angle for surfactant solutions, show good agreement with that obtained using pure liquids. The results also show that the use of cationic-anionic surfactant mixture solutions is even more suitable for obtaining γ_c.

Table B 1

Adhesion Tension of C_8NBr - $C_{12}SO_3Na$ Mixtures

at Teflon/Aqueous Interface, I.S. = 0.1 N (NaBr)

$C_{C_{12}SO_3Na} = 6.636 \times 10^{-4}$ M

C (C_8NBr)	-log C (C_8NBr)	γ_{lv}	θ	$\gamma_{lv} \cdot \cos\theta$
10^4x mol/dm^3		mN/m	deg.	mN/m
6.636	3.178	30.88	76.7	7.104
4.424	3.354	32.58	80.2	5.545
2.949	3.530	34.34	83.6	3.828
1.966	3.706	35.78	86.6	2.122
1.311	3.882	37.41	88.8	0.783
0.8739	4.059	38.73	91.1	-0.744
0.5826	4.235	40.17	93.2	-2.242
0.3884	4.411	41.24	95.2	-3.738

Table B 2

Adhesion Tension of C_8NBr - $C_{12}SO_3Na$ Mixtures

at Teflon/Aqueous Interface, I.S. = 0.1 N (NaBr)

$C_{C_{12}SO_3Na} = 4.424 \times 10^{-4}$ M

C (C_8NBr)	-log C (C_8NBr)	γ_{lv}	θ	$\gamma_{lv} \cdot \cos\theta$
10^4x mol/dm^3		mN/m	deg.	mN/m
6.636	3.178	33.91	83.3	3.956
4.424	3.354	35.86	86.1	2.439
2.949	3.530	37.56	88.4	1.049
1.966	3.706	39.09	91.1	-0.750
1.311	3.882	40.56	92.9	-2.057
0.8739	4.059	42.08	94.9	-3.594
0.5826	4.235	43.38	96.4	-4.836
0.3884	4.411	44.66	98.4	-6.524

Table B 3

Adhesion Tension of C_8NBr - $C_{12}SO_3Na$ Mixtures

at Teflon/Aqueous Interface, I.S. = 0.1 N (NaBr)

$C_{C_{12}SO_3Na} = 2.949 \times 10^{-4}$ M

C (C_8NBr) 10^4x mol/dm^3	-log C (C_8NBr)	γ_{lv} mN/m	θ deg.	$\gamma_{lv} \cdot \cos\theta$ mN/m
6.636	3.178	37.19	88.9	0.714
4.424	3.354	38.84	91.6	-1.084
2.949	3.530	40.75	92.9	-2.602
1.966	3.706	42.27	95.1	-3.758
1.311	3.882	43.81	96.9	-5.263
0.8739	4.059	45.31	98.7	-6.854
0.5826	4.235	46.55	100.	-8.323
0.3884	4.411	47.79	101.0	-9.119

Table B 4

Adhesion Tension of C_8NBr - $C_{12}SO_3Na$ Mixtures

at Teflon/Aqueous Interface, I.S. = 0.1 N (NaBr)

$C_{C_{12}SO_3Na} = 1.966 \times 10^{-4}$ M

C (C_8NBr) 10^4x mol/dm^3	-log C (C_8NBr)	γ_{lv} mN/m	θ deg.	$\gamma_{lv} \cdot \cos\theta$ mN/m
6.636	3.178	40.03	93.1	-2.165
4.424	3.354	41.91	95.1	-3.726
2.949	3.530	43.67	97.1	-5.398
1.966	3.706	45.21	98.8	-6.916
1.311	3.882	46.74	100.0	-8.116
0.8739	4.059	48.23	101.5	-9.616
0.5826	4.235	49.58	103.4	-11.490
0.3884	4.411	50.72	104.4	-12.612

Table B 5

Adhesion Tension of C_8NBr - $C_{12}SO_3Na$ Mixtures

at Teflon/Aqueous Interface, I.S. = 0.1 N (NaBr)

$C_{C_{12}SO_3Na} = 1.311 \times 10^{-4}$ M

C (C_8NBr) 10^4x mol/dm^3	-log C (C_8NBr)	γ_{lv} mN/m	θ deg.	$\gamma_{lv} \cdot \cos\theta$ mN/m
6.636	3.178	42.95	96.8	-5.085
4.424	3.354	44.71	98.5	-6.609
2.949	3.530	46.52	99.9	-7.998
1.966	3.706	48.09	101.4	-9.505
1.311	3.882	49.62	102.8	-10.992
0.8739	4.059	50.99	103.8	-12.163
0.5826	4.235	52.28	104.9	-13.443
0.3884	4.411	53.57	106.3	-15.035

Table B 6

Adhesion Tension of C_8NBr - $C_{12}SO_3Na$ Mixtures

at Teflon/Aqueous Interface, I.S. = 0.1 N (NaBr)

$C_{C_{12}SO_3Na} = 8.739 \times 10^{-5}$ M

C (C_8NBr)	-log C (C_8NBr)	γ_{lv}	θ	$\gamma_{lv} \cdot \cos\theta$
10^4x mol/dm^3		mN/m	deg.	mN/m
6.636	3.178	45.73	100.1	-8.020
4.424	3.354	47.56	101.7	-9.645
2.949	3.530	49.19	102.7	-10.814
1.966	3.706	50.73	103.8	-12.101
1.311	3.882	52.31	105.5	-13.979
0.8739	4.059	53.70	106.6	-15.341
0.5826	4.235	55.02	107.9	-16.911
0.3884	4.411	56.28	108.6	-17.951

Table B 7

Adhesion Tension of C_8NBr - $C_{12}SO_3Na$ Mixtures

at Teflon/Aqueous Interface, I.S. = 0.1 N (NaBr)

$C_{C_{12}SO_3Na} = 5.826 \times 10^{-5}$ M

C (C_8NBr)	-log C (C_8NBr)	γ_{lv}	θ	$\gamma_{lv} \cdot \cos\theta$
10^4x mol/dm^3		mN/m	deg.	mN/m
6.636	3.178	48.16	102.7	-10.588
4.424	3.354	50.05	104.3	-12.362
2.949	3.530	51.89	105.7	-14.041
1.966	3.706	53.38	106.5	-15.161
1.311	3.882	54.85	107.8	-16.767
0.8739	4.059	56.24	109.0	-18.310
0.5826	4.235	57.50	109.5	-19.194
0.3884	4.411	58.85	110.7	-20.802

Table B 8

Adhesion Tension of C_8NBr - $C_{12}SO_3Na$ Mixtures

at Teflon/Aqueous Interface, I.S. = 0.1 N (NaBr)

$C_{C_{12}SO_3Na} = 3.884 \times 10^{-5}$ M

C (C_8NBr)	-log C (C_8NBr)	γ_{lv}	θ	$\gamma_{lv} \cdot \cos\theta$
10^4x mol/dm^3		mN/m	deg.	mN/m
6.636	3.178	50.82	105.2	-13.324
4.424	3.354	52.61	106.4	-14.854
2.949	3.530	54.22	107.7	-16.485
1.966	3.706	55.79	108.7	-17.887
1.311	3.882	57.17	109.9	-19.459
0.8739	4.059	58.67	110.9	-20.930
0.5826	4.235	59.99	111.8	-22.278
0.3884	4.411	61.26	112.5	-23.443

Table B 9

Adhesion Tension of C_8NBr - $C_{12}SO_3Na$ Mixtures

at Teflon/Aqueous Interface, I.S. = 0.1 N (NaBr)

$C_{C_8NBr} = 6.636 \times 10^{-4}$ M

C ($C_{12}SO_3Na$) 10^4x mol/dm^3	-log C ($C_{12}SO_3Na$)	γ_{lv} mN/m	θ deg.	$\gamma_{lv} \cdot \cos\theta$ mN/m
6.636	3.178	30.88	76.7	7.104
4.424	3.354	33.91	83.3	3.956
2.949	3.530	37.19	88.9	0.714
1.966	3.706	40.03	93.1	-2.165
1.311	3.882	42.95	96.8	-5.085
0.8739	4.059	45.73	100.1	-8.020
0.5826	4.235	48.16	102.7	-10.588
0.3884	4.411	50.82	105.2	-13.324

Table B 10

Adhesion Tension of C_8NBr - $C_{12}SO_3Na$ Mixtures

at Teflon/Aqueous Interface, I.S. = 0.1 N (NaBr)

$C_{C_8NBr} = 4.424 \times 10^{-4}$ M

C ($C_{12}SO_3Na$)	-log C ($C_{12}SO_3Na$)	γ_{lv}	θ	$\gamma_{lv} \cdot \cos\theta$
10^4x mol/dm^3		mN/m	deg.	mN/m
6.636	3.178	32.58	80.2	5.545
4.424	3.354	35.86	86.1	2.439
2.949	3.530	38.84	91.6	-1.084
1.966	3.706	41.91	95.1	-3.726
1.311	3.882	44.71	98.5	-6.609
0.8739	4.059	47.56	101.7	-9.645
0.5826	4.235	50.05	104.3	-12.362
0.3884	4.411	52.61	106.4	-14.854

Table B 11

Adhesion Tension of C_8NBr - $C_{12}SO_3Na$ Mixtures

at Teflon/Aqueous Interface, I.S. = 0.1 N (NaBr)

$C_{C_8NBr} = 2.949 \times 10^{-4}$ M

C ($C_{12}SO_3Na$) 10^4x mol/dm^3	-log C ($C_{12}SO_3Na$)	γ_{lv} mN/m	θ deg.	$\gamma_{lv} \cdot \cos\theta$ mN/m
6.636	3.178	34.34	83.6	3.828
4.424	3.354	37.56	88.4	1.049
2.949	3.530	40.75	92.9	-2.602
1.966	3.706	43.67	97.1	-5.398
1.311	3.882	46.52	99.9	-7.998
0.8739	4.059	49.19	102.7	-10.814
0.5826	4.235	51.89	105.7	-14.041
0.3884	4.411	54.22	107.7	-16.485

Table B 12

Adhesion Tension of C_8NBr - $C_{12}SO_3Na$ Mixtures

at Teflon/Aqueous Interface, I.S. = 0.1 N (NaBr)

$C_{C_8NBr} = 1.966 \times 10^{-4}$ M

C ($C_{12}SO_3Na$) 10^4x mol/dm^3	-log C ($C_{12}SO_3Na$)	γ_{lv} mN/m	θ deg.	$\gamma_{lv} \cdot \cos\theta$ mN/m
6.636	3.178	35.78	86.6	2.122
4.424	3.354	39.09	91.1	-0.750
2.949	3.530	42.27	95.1	-3.758
1.966	3.706	45.21	98.8	-6.916
1.311	3.882	48.09	101.4	-9.505
0.8739	4.059	50.73	103.8	-12.101
0.5826	4.235	53.38	106.5	-15.161
0.3884	4.411	55.79	108.7	-17.887

Table B 13

Adhesion Tension of C_8NBr - $C_{12}SO_3Na$ Mixtures

at Teflon/Aqueous Interface, I.S. = 0.1 N (NaBr)

$C_{C_8NBr} = 1.311 \times 10^{-4}$ M

C ($C_{12}SO_3Na$) 10^4x mol/dm^3	-log C ($C_{12}SO_3Na$)	γ_{lv} mN/m	θ deg.	$\gamma_{lv} \cdot \cos\theta$ mN/m
6.636	3.178	37.41	88.8	0.783
4.424	3.354	40.65	92.9	-2.057
2.949	3.530	43.81	96.9	-5.263
1.966	3.706	46.74	100.0	-8.116
1.311	3.882	49.62	102.8	-10.992
0.8739	4.059	52.31	105.5	-13.979
0.5826	4.235	54.85	107.8	-16.767
0.3884	4.411	57.17	109.9	-19.459

Table B 14

Adhesion Tension of C_8NBr - $C_{12}SO_3Na$ Mixtures

at Teflon/Aqueous Interface, I.S. = 0.1 N (NaBr)

$C_{C_8NBr} = 8.739 \times 10^{-5}$ M

C ($C_{12}SO_3Na$) 10^4x mol/dm^3	-log C ($C_{12}SO_3Na$)	γ_{lv} mN/m	θ deg.	$\gamma_{lv} \cdot \cos\theta$ mN/m
6.636	3.178	38.73	91.1	-0.744
4.424	3.354	42.08	94.9	-3.594
2.949	3.530	45.31	98.7	-6.854
1.966	3.706	48.23	101.5	-9.616
1.311	3.882	50.99	103.8	-12.163
0.8739	4.059	53.70	106.6	-15.341
0.5826	4.235	56.24	109.0	-18.310
0.3884	4.411	58.67	110.9	-20.930

Table B 15

Adhesion Tension of C_8NBr - $C_{12}SO_3Na$ Mixtures

at Teflon/Aqueous Interface, I.S. = 0.1 N (NaBr)

$C_{C_8NBr} = 5.826 \times 10^{-5}$ M

C ($C_{12}SO_3Na$) 10^4x mol/dm^3	-log C ($C_{12}SO_3Na$)	γ_{lv} mN/m	θ deg.	$\gamma_{lv} \cdot \cos\theta$ mN/m
6.636	3.178	40.17	93.2	-2.242
4.424	3.354	43.38	96.4	-4.836
2.949	3.530	46.55	100.3	-8.323
1.966	3.706	49.58	103.4	-11.490
1.311	3.882	52.28	104.9	-13.443
0.8739	4.059	55.02	107.9	-16.911
0.5826	4.235	57.50	109.5	-19.194
0.3884	4.411	59.99	111.8	-22.278

Table B 16

Adhesion Tension of C_8NBr - $C_{12}SO_3Na$ Mixtures

at Teflon/Aqueous Interface, I.S. = 0.1 N (NaBr)

$C_{C_8NBr} = 3.884 \times 10^{-5}$ M

C ($C_{12}SO_3Na$) 10^4x mol/dm^3	-log C ($C_{12}SO_3Na$)	γ_{lv} mN/m	θ deg.	$\gamma_{lv} \cdot \cos\theta$ mN/m
6.636	3.178	41.24	95.2	-3.738
4.424	3.354	44.66	98.4	-6.524
2.949	3.530	47.79	101.0	-9.119
1.966	3.706	50.72	104.4	-12.614
1.311	3.882	53.57	106.3	-15.035
0.8739	4.059	56.28	108.6	-17.951
0.5826	4.235	58.85	110.7	-20.802
0.3884	4.411	61.26	112.5	-23.443

Table B 17

Adhesion Tension of C_8NBr - $C_{12}SO_3Na$ Mixtures

at Parafilm/Aqueous Interface, I.S. = 0.1 N (NaBr)

$C_{C_{12}SO_3Na} = 6.636 \times 10^{-4}$ M

C (C_8NBr)	-log C (C_8NBr)	γ_{lv}	θ	$\gamma_{lv} \cdot \cos\theta$
10^4x mol/dm^3		mN/m	deg.	mN/m
6.636	3.178	30.88	63.6	13.730
4.424	3.354	32.58	68.9	12.099
2.949	3.530	34.34	72.4	10.383
1.966	3.706	35.78	75.5	8.959
1.311	3.882	37.41	78.7	7.330
0.8739	4.059	38.73	81.4	5.792
0.5826	4.235	40.17	84.1	4.129
0.3884	4.411	41.24	85.9	2.949

Table B 18

Adhesion Tension of C_8NBr - $C_{12}SO_3Na$ Mixtures

at Parafilm/Aqueous Interface, I.S. = 0.1 N (NaBr)

$C_{C_{12}SO_3Na} = 4.424 \times 10^{-4}$ M

C (C_8NBr)	-log C (C_8NBr)	γ_{lv}	θ	$\gamma_{lv} \cdot \cos\theta$
10^4x mol/dm^3		mN/m	deg.	mN/m
6.636	3.178	33.91	72.6	10.140
4.424	3.354	35.86	75.8	8.797
2.949	3.530	37.56	78.9	7.231
1.966	3.706	39.09	82.1	5.373
1.311	3.882	40.56	83.9	4.320
0.8739	4.059	42.08	86.5	2.569
0.5826	4.235	43.38	88.4	1.211
0.3884	4.411	44.66	90.2	-0.156

Table B 19

Adhesion Tension of C_8NBr - $C_{12}SO_3Na$ Mixtures

at Parafilm/Aqueous Interface, I.S. = 0.1 N (NaBr)

$C_{C_{12}SO_3Na} = 2.949 \times 10^{-4}$ M

C (C_8NBr) 10^4x mol/dm^3	-log C (C_8NBr)	γ_{lv} mN/m	θ deg.	$\gamma_{lv} \cdot \cos\theta$ mN/m
6.636	3.178	37.19	78.4	7.478
4.424	3.354	38.84	81.3	5.875
2.949	3.530	40.75	83.9	4.330
1.966	3.706	42.27	86.6	2.507
1.311	3.882	43.81	88.2	1.376
0.8739	4.059	45.31	90.2	-0.158
0.5826	4.235	46.55	91.7	-1.381
0.3884	4.411	47.79	93.3	-2.751

Table B 20

Adhesion Tension of C_8NBr - $C_{12}SO_3Na$ Mixtures

at Parafilm/Aqueous Interface, I.S. = 0.1 N (NaBr)

$C_{C_{12}SO_3Na} = 1.966 \times 10^{-4}$ M

C (C_8NBr)	-log C (C_8NBr)	γ_{lv}	θ	$\gamma_{lv} \cdot \cos\theta$
10^4x mol/dm^3		mN/m	deg.	mN/m
6.636	3.178	40.03	83.1	4.809
4.424	3.354	41.91	86.1	2.581
2.949	3.530	43.67	87.8	1.676
1.966	3.706	45.21	90.0	0.000
1.311	3.882	46.74	91.9	-1.550
0.8739	4.059	48.23	93.8	-3.196
0.5826	4.235	49.58	94.9	-4.235
0.3884	4.411	50.72	96.0	-5.302

Table B 21

Adhesion Tension of C_8NBr - $C_{12}SO_3Na$ Mixtures

at Parafilm/Aqueous Interface, I.S. = 0.1 N (NaBr)

$C_{C_{12}SO_3Na} = 1.311 \times 10^{-4}$ M

C (C_8NBr)	-log C (C_8NBr)	γ_{lv}	θ	$\gamma_{lv} \cdot \cos\theta$
10^4x mol/dm^3		mN/m	deg.	mN/m
6.636	3.178	42.95	87.3	2.023
4.424	3.354	44.71	90.1	-0.078
2.949	3.530	46.52	91.7	-1.380
1.966	3.706	48.09	93.3	-2.768
1.311	3.882	49.62	95.2	-4.497
0.8739	4.059	50.99	96.4	-5.684
0.5826	4.235	52.28	98.1	-7.366
0.3884	4.411	53.57	99.5	-8.842

Table B 22

Adhesion Tension of C_8NBr - $C_{12}SO_3Na$ Mixtures

at Parafilm/Aqueous Interface, I.S. = 0.1 N (NaBr)

$C_{C_{12}SO_3Na} = 8.739 \times 10^{-5}$ M

C (C_8NBr)	-log C (C_8NBr)	γ_{lv}	θ	$\gamma_{lv} \cdot \cos\theta$
10^4x mol/dm^3		mN/m	deg.	mN/m
6.636	3.178	45.73	91.2	-0.958
4.424	3.354	47.56	93.0	-2.489
2.949	3.530	49.19	94.6	-3.945
1.966	3.706	50.73	96.2	-5.479
1.311	3.882	52.31	98.2	-7.461
0.8739	4.059	53.70	99.3	-8.678
0.5826	4.235	55.02	100.5	-10.027
0.3884	4.411	56.28	101.8	-11.509

Table B 23

Adhesion Tension of C_8NBr - $C_{12}SO_3Na$ Mixtures

at Parafilm/Aqueous Interface, I.S. = 0.1 N (NaBr)

$C_{C_{12}SO_3Na} = 5.826 \times 10^{-5}$ M

C (C_8NBr)	-log C (C_8NBr)	γ_{lv}	θ	$\gamma_{lv} \cdot \cos\theta$
10^4x mol/dm^3		mN/m	deg.	mN/m
6.636	3.178	48.16	94.4	-3.695
4.424	3.354	50.05	96.1	-5.319
2.949	3.530	51.89	97.9	-7.132
1.966	3.706	53.38	99.5	-8.810
1.311	3.882	54.85	100.5	-9.996
0.8739	4.059	56.24	102.1	-11.789
0.5826	4.235	57.50	103.3	-13.228
0.3884	4.411	58.85	104.0	-14.237

Table B 24

Adhesion Tension of C_8NBr - $C_{12}SO_3Na$ Mixtures

at Parafilm/Aqueous Interface, I.S. = 0.1 N (NaBr)

$C_{C_{12}SO_3Na} = 3.884 \times 10^{-5}$ M

C (C_8NBr)	-log C (C_8NBr)	γ_{lv}	θ	$\gamma_{lv} \cdot \cos\theta$
10^4x mol/dm^3		mN/m	deg.	mN/m
6.636	3.178	50.82	97.1	-6.281
4.424	3.354	52.61	99.1	-8.321
2.949	3.530	54.22	100.0	-9.415
1.966	3.706	55.79	101.9	-11.504
1.311	3.882	57.17	103.2	-13.055
0.8739	4.059	58.67	104.1	-14.293
0.5826	4.235	59.99	105.4	-15.930
0.3884	4.411	61.26	106.2	-17.091

Table B 25

Adhesion Tension of C_8NBr - $C_{12}SO_3Na$ Mixtures

at Parafilm/Aqueous Interface, I.S. = 0.1 N (NaBr)

$C_{C_8NBr} = 6.636 \times 10^{-4}$ M

C ($C_{12}SO_3Na$) 10^4x mol/dm^3	-log C ($C_{12}SO_3Na$)	γ_{lv} mN/m	θ deg.	$\gamma_{lv} \cdot \cos\theta$ mN/m
6.636	3.178	30.88	63.6	13.730
4.424	3.354	33.91	72.6	10.140
2.949	3.530	37.19	78.4	7.478
1.966	3.706	40.03	83.1	4.809
1.311	3.882	42.95	87.3	2.023
0.8739	4.059	45.73	91.2	-0.958
0.5826	4.235	48.16	94.4	-3.695
0.3884	4.411	50.82	97.1	-6.281

Table B 26

Adhesion Tension of C_8NBr - $C_{12}SO_3Na$ Mixtures

at Parafilm/Aqueous Interface, I.S. = 0.1 N (NaBr)

$C_{C_8NBr} = 4.424 \times 10^{-4}$ M

C ($C_{12}SO_3Na$) $10^4 \times$ mol/dm^3	-log C ($C_{12}SO_3Na$)	γ_{lv} mN/m	θ deg.	$\gamma_{lv} \cdot \cos\theta$ mN/m
6.636	3.178	32.58	68.9	12.099
4.424	3.354	35.86	75.8	8.797
2.949	3.530	38.84	81.3	5.875
1.966	3.706	41.91	86.1	2.851
1.311	3.882	44.71	90.1	-0.078
0.8739	4.059	47.56	93.0	-2.489
0.5826	4.235	50.05	96.1	-5.319
0.3884	4.411	52.61	99.1	-8.321

Table B 27

Adhesion Tension of C_8NBr - $C_{12}SO_3Na$ Mixtures

at Parafilm/Aqueous Interface, I.S. = 0.1 N (NaBr)

$C_{C_8NBr} = 2.949 \times 10^{-4}$ M

C ($C_{12}SO_3Na$) $10^4 \times$ mol/dm^3	-log C ($C_{12}SO_3Na$)	γ_{lv} mN/m	θ deg.	$\gamma_{lv} \cdot \cos\theta$ mN/m
6.636	3.178	34.34	72.4	10.383
4.424	3.354	37.56	78.9	7.231
2.949	3.530	40.75	83.9	4.330
1.966	3.706	43.67	87.8	1.676
1.311	3.882	46.52	91.7	-1.380
0.8739	4.059	49.19	94.6	-3.945
0.5826	4.235	51.89	97.9	-7.132
0.3884	4.411	54.22	100.0	-9.415

Table B 28

Adhesion Tension of C_8NBr - $C_{12}SO_3Na$ Mixtures

at Parafilm/Aqueous Interface, I.S. = 0.1 N (NaBr)

$C_{C_8NBr} = 1.966 \times 10^{-4}$ M

C ($C_{12}SO_3Na$) 10^4x mol/dm^3	-log C ($C_{12}SO_3Na$)	γ_{lv} mN/m	θ deg.	$\gamma_{lv} \cdot \cos\theta$ mN/m
6.636	3.178	35.78	75.5	8.959
4.424	3.354	39.09	82.1	5.373
2.949	3.530	42.27	86.6	2.507
1.966	3.706	45.21	90.0	0.000
1.311	3.882	48.09	93.3	-2.768
0.8739	4.059	50.73	96.2	-5.479
0.5826	4.235	53.38	99.5	-8.810
0.3884	4.411	55.79	101.9	-11.504

Table B 29

Adhesion Tension of C_8NBr - $C_{12}SO_3Na$ Mixtures

at Parafilm/Aqueous Interface, I.S. = 0.1 N (NaBr)

$C_{C_8NBr} = 1.311 \times 10^{-4}$ M

C ($C_{12}SO_3Na$) 10^4x mol/dm^3	-log C ($C_{12}SO_3Na$)	γ_{lv} mN/m	θ deg.	$\gamma_{lv} \cdot \cos\theta$ mN/m
6.636	3.178	37.41	78.7	7.330
4.424	3.354	40.65	83.9	4.320
2.949	3.530	43.81	88.2	1.376
1.966	3.706	46.74	91.9	-1.550
1.311	3.882	49.62	95.2	-4.497
0.8739	4.059	52.31	98.2	-7.461
0.5826	4.235	54.85	100.5	-9.996
0.3884	4.411	57.17	103.2	-13.055

Table B 30

Adhesion Tension of C_8NBr - $C_{12}SO_3Na$ Mixtures

at Parafilm/Aqueous Interface, I.S. = 0.1 N (NaBr)

$C_{C_8NBr} = 8.739 \times 10^{-5}$ M

C ($C_{12}SO_3Na$) 10^4x mol/dm^3	-log C ($C_{12}SO_3Na$)	γ_{lv} mN/m	θ deg.	$\gamma_{lv} \cdot \cos\theta$ mN/m
6.636	3.178	38.73	81.4	5.792
4.424	3.354	42.08	86.5	2.569
2.949	3.530	45.31	90.2	-0.158
1.966	3.706	48.23	93.8	-3.196
1.311	3.882	50.99	96.4	-5.684
0.8739	4.059	53.70	99.3	-8.678
0.5826	4.235	56.24	102.1	-11.789
0.3884	4.411	58.67	104.1	-14.293

Table B 31

Adhesion Tension of C_8NBr - $C_{12}SO_3Na$ Mixtures

at Parafilm/Aqueous Interface, I.S. = 0.1 N (NaBr)

$C_{C_8NBr} = 5.826 \times 10^{-5}$ M

C ($C_{12}SO_3Na$) 10^4x mol/dm^3	-log C ($C_{12}SO_3Na$)	γ_{lv} mN/m	θ deg.	$\gamma_{lv} \cdot \cos\theta$ mN/m
6.636	3.178	40.17	84.1	4.129
4.424	3.354	43.38	88.4	1.211
2.949	3.530	46.55	91.7	-1.381
1.966	3.706	49.58	94.9	-4.235
1.311	3.882	52.28	98.1	-7.366
0.8739	4.059	55.02	100.5	-10.027
0.5826	4.235	57.50	103.3	-13.228
0.3884	4.411	59.99	105.4	-15.930

Table B 32

Adhesion Tension of C_8NBr - $C_{12}SO_3Na$ Mixtures

at Parafilm/Aqueous Interface, I.S. = 0.1 N (NaBr)

$C_{C_8NBr} = 3.884 \times 10^{-5}$ M

C ($C_{12}SO_3Na$) 10^4x mol/dm^3	-log C ($C_{12}SO_3Na$)	γ_{lv} mN/m	θ deg.	$\gamma_{lv} \cdot \cos\theta$ mN/m
6.636	3.178	41.24	85.9	2.949
4.424	3.354	44.66	90.2	-0.156
2.949	3.530	47.79	93.3	-2.751
1.966	3.706	50.72	96.0	-5.302
1.311	3.882	53.57	99.5	-8.842
0.8739	4.059	56.28	101.8	-11.509
0.5826	4.235	58.85	104.0	-14.237
0.3884	4.411	61.26	106.2	-17.091

Table B 33

Adhesion Tension of $C_{12}SO_3Na$

at Teflon/Aqueous Interface, I.S. = 0.1 N (NaBr)

α = 0.0000

C 10^3x mol/dm^3	-log C	γ_{lv} mN/m	θ deg.	$\gamma_{lv} \cdot \cos\theta$ mN/m
25.08	2.601	35.70	83.7	3.918
20.07	2.697	37.02	85.9	2.647
13.86	2.858	40.86	89.3	0.499
10.03	2.999	44.14	92.8	-2.156
6.929	3.159	47.70	95.9	-4.903
5.17	3.300	50.72	97.5	-6.620
3.64	3.460	53.92	100.4	-9.732
2.508	3.601	56.72	102.1	-11.890
1.732	3.761	59.30	104.0	-14.346
1.254	3.902	61.50	104.7	-15.606

Table B 34

Adhesion Tension of C_8NBr - $C_{12}SO_3Na$ Mixtures

at Teflon/Aqueous Interface, I.S. = 0.1 N (NaBr)

α = 0.2286

C	-log C	γ_{lv}	θ	$\gamma_{lv} \cdot \cos\theta$
10^{*}x mol/dm^3		mN/m	deg.	mN/m
8.602	3.065	35.78	86.6	2.122
5.735	3.241	40.65	92.9	-2.057
3.823	3.418	45.31	98.7	-6.854
2.549	3.594	49.58	103.4	-11.490
1.699	3.770	53.57	106.3	-15.035

Table B 35

Adhesion Tension of C_8NBr - $C_{12}SO_3Na$ Mixtures

at Teflon/Aqueous Interface, I.S. = 0.1 N (NaBr)

α = 0.5000

C	-log C	γ_{lv}	θ	$\gamma_{lv} \cdot \cos\theta$
10^4x mol/dm^3		mN/m	deg.	mN/m
13.27	2.877	30.88	76.7	7.104
8.848	3.053	35.86	86.1	2.439
5.898	3.229	40.75	92.9	-2.602
3.932	3.405	45.21	98.8	-6.916
2.622	3.581	49.62	102.8	-10.992
1.748	3.758	53.70	106.6	-15.341
1.165	3.934	57.50	109.5	-19.194
0.7768	4.110	61.26	112.5	-23.443

Table B 36

Adhesion Tension of C_8NBr - $C_{12}SO_3Na$ Mixtures

at Teflon/Aqueous Interface, I.S. = 0.1 N (NaBr)

α = 0.7714

C	-log C	γ_{lv}	θ	$\gamma_{lv} \cdot \cos\theta$
10^4x mol/dm^3		mN/m	deg.	mN/m
8.602	3.065	40.03	93.1	-2.165
5.735	3.241	44.71	98.5	-6.609
3.823	3.418	49.19	102.7	-10.814
2.549	3.594	53.38	106.5	-15.161
1.699	3.770	57.17	109.9	-19.459

Table B 37

Adhesion Tension of C_8NBr

at Teflon/Aqueous Interface, I.S. = 0.1 N (NaBr)

α = 1.000

C	-log C	γ_{lv}	θ	$\gamma_{lv} \cdot \cos\theta$
10^2x mol/dm^3		mN/m	deg.	mN/m
21.46	0.668	45.92	87.5	2.003
17.16	0.766	47.39	89.7	0.248
12.87	0.890	49.59	91.3	-1.125
9.733	1.012	51.15	93.6	-3.212
4.866	1.313	55.41	97.1	-6.849
2.433	1.614	59.22	100.2	-10.487
1.217	1.915	62.74	102.2	-13.259
0.6083	2.216	65.38	104.4	-16.259
0.3042	2.517	67.43	106.1	-18.699
0.1521	2.818	69.16	108.0	-21.372

Table B 38

Adhesion Tension of $C_{12}SO_3Na$

at Parafilm/Aqueous Interface, I.S. = 0.1 N (NaBr)

α = 0.0000

C	-log C	γ_{lv}	θ	$\gamma_{lv} \cdot \cos\theta$
10^3x mol/dm^3		mN/m	deg.	mN/m
20.07	2.697	37.02	77.1	8.265
13.86	2.858	40.86	82.7	5.192
10.03	2.999	44.14	87.4	2.002
6.929	3.159	47.70	91.7	-1.415
5.017	3.300	50.72	94.5	-3.979
3.464	3.460	53.92	97.0	-6.571
2.508	3.601	56.72	98.8	-8.677
1.732	3.761	59.30	101.1	-11.325
1.254	3.902	61.50	102.9	-13.730

Table B 39

Adhesion Tension of C_8NBr - $C_{12}SO_3Na$ Mixtures

at Parafilm/Aqueous Interface, I.S. = 0.1 N (NaBr)

α = 0.2286

C	-log C	γ_{lv}	θ	$\gamma_{lv} \cdot \cos\theta$
10^4x mol/dm^3		mN/m	deg.	mN/m
8.602	3.065	35.78	75.5	8.959
5.735	3.241	40.65	83.9	4.320
3.823	3.418	45.31	90.2	-0.158
2.549	3.594	49.58	94.9	-4.235
1.699	3.770	53.57	99.5	-8.842

Table B 40

Adhesion Tension of C_8NBr - $C_{12}SO_3Na$ Mixtures

at Parafilm/Aqueous Interface, I.S. = 0.1 N (NaBr)

α = 0.5000

C	-log C	γ_{lv}	θ	$\gamma_{lv} \cdot \cos\theta$
10^4x mol/dm^3		mN/m	deg.	mN/m
13.27	2.877	30.88	63.6	13.730
8.848	3.053	35.86	75.8	8.797
5.898	3.229	40.75	83.9	4.330
3.932	3.405	45.21	90.0	0.000
2.622	3.581	49.62	95.2	-4.497
1.748	3.758	53.70	99.3	-8.678
1.165	3.934	57.50	103.3	-13.228
0.7768	4.110	61.26	106.2	-17.091

Table B 41

Adhesion Tension of C_8NBr - $C_{12}SO_3Na$ Mixtures

at Parafilm/Aqueous Interface, I.S. = 0.1 N (NaBr)

α = 0.7714

C	-log C	γ_{lv}	θ	$\gamma_{lv} \cdot \cos\theta$
10^4x mol/dm^3		mN/m	deg.	mN/m
8.602	3.065	40.03	83.1	4.809
5.735	3.241	44.71	90.1	-0.078
3.823	3.418	49.19	94.6	-3.945
2.549	3.594	53.38	99.5	-8.810
1.699	3.770	57.17	103.2	-13.055

Table B 42

Adhesion Tension of C_8NBr

at Parafilm/Aqueous Interface, I.S. = 0.1 N (NaBr)

α = 1.000

C 10^2x mol/dm^3	-log C	γ_{lv} mN/m	θ deg.	$\gamma_{lv} \cdot \cos\theta$ mN/m
21.46	0.668	45.92	84.9	4.082
17.16	0.766	47.39	87.4	2.150
12.87	0.890	49.59	89.2	0.692
9.733	1.012	51.15	91.8	-1.607
4.866	1.313	55.41	95.0	-4.829
2.433	1.614	59.22	98.5	-8.753
1.217	1.915	62.74	101.2	-12.860
0.6083	2.216	65.38	103.2	-14.930
0.3042	2.517	67.43	104.7	-17.111
0.1521	2.818	69.16	106.2	-19.295

Table B 43

Adhesion Tension of $C_{12}NBr$ - $C_{10}SO_3Na$ Mixtures at Teflon/Aqueous Interface, I.S. = 0.1 N (NaBr)

$C_{C_{10}SO_3Na} = 2.1052 \times 10^{-4}$ M

C ($C_{12}NBr$)	-log C ($C_{12}NBr$)	γ_{lv}	θ	$\gamma_{lv} \cdot \cos\theta$
10^5x mol/dm^3		mN/m	deg.	mN/m
14.035	3.8528	31.70	81.0	4.959
9.3564	4.0289	34.30	86.0	2.393
6.2376	4.2050	37.30	90.0	0.000
4.1584	4.3811	40.03	93.8	-2.653
2.7723	4.5572	42.21	96.2	-4.559
1.8482	4.7337	45.11	98.8	-6.901
1.2321	4.9094	47.57	100.9	-8.995

Table B 44

Adhesion Tension of $C_{12}NBr$ - $C_{10}SO_3Na$ Mixtures at Teflon/Aqueous Interface, I.S. = 0.1 N (NaBr)

$C_{C_{10}SO_3Na} = 1.4035 \times 10^{-4}$ M

C ($C_{12}NBr$) 10^5x mol/dm^3	-log C ($C_{12}NBr$)	γ_{lv} mN/m	θ deg.	$\gamma_{lv} \cdot \cos\theta$ mN/m
14.035	3.8528	34.05	85.3	2.790
9.3564	4.0289	36.86	89.4	0.386
6.2376	4.2050	39.70	93.0	-2.078
4.1584	4.3811	42.37	95.7	-4.208
2.7723	4.5572	44.80	98.2	-6.390
1.8482	4.7337	47.64	100.6	-8.763
1.2321	4.9094	49.97	102.6	-10.901

Table B 45

Adhesion Tension of $C_{12}NBr$ - $C_{10}SO_3Na$ Mixtures at Teflon/Aqueous Interface, I.S. = 0.1 N (NaBr)

$C_{C_{10}SO_3Na} = 9.3564 \times 10^{-5}$ M

C ($C_{12}NBr$) 10^5x mol/dm^3	-log C ($C_{12}NBr$)	γ_{lv} mN/m	θ deg.	$\gamma_{lv} \cdot \cos\theta$ mN/m
21.052	3.6767	34.28	84.8	3.107
14.035	3.8528	36.81	88.6	0.899
9.3564	4.0289	39.31	92.6	-1.783
6.2376	4.2050	42.22	95.4	-3.973
4.1584	4.3811	45.03	97.9	-6.189
2.7723	4.5572	47.47	100.2	-8.406
1.8482	4.7337	50.08	101.9	-10.327
1.2321	4.9094	52.43	104.1	-12.773

Table B 46

Adhesion Tension of $C_{12}NBr$ - $C_{10}SO_3Na$ Mixtures

at Teflon/Aqueous Interface, I.S. = 0.1 N (NaBr)

$C_{C_{10}SO_3Na} = 6.2376 \times 10^{-5}$ M

C ($C_{12}NBr$) 10^5x mol/dm^3	-log C ($C_{12}NBr$)	γ_{lv} mN/m	θ deg.	$\gamma_{lv} \cdot \cos\theta$ mN/m
21.052	3.6767	36.60	88.5	0.958
14.035	3.8528	39.38	91.7	-1.168
9.3564	4.0289	41.83	95.0	-3.646
6.2376	4.2050	44.72	97.6	-5.915
4.1584	4.3811	47.40	100.1	-8.312
2.7723	4.5572	49.91	102.1	-10.462
1.8482	4.7337	52.49	103.8	-12.521
1.2321	4.9094	54.68	105.5	-14.613

Table B 47

Adhesion Tension of $C_{12}NBr$ - $C_{10}SO_3Na$ Mixtures

at Teflon/Aqueous Interface, I.S. = 0.1 N (NaBr)

$C_{C_{10}SO_3Na} = 4.1584 \times 10^{-5}$ M

C ($C_{12}NBr$)	-log C ($C_{12}NBr$)	γ_{lv}	θ	$\gamma_{lv} \cdot \cos\theta$
10^5x mol/dm^3		mN/m	deg.	mN/m
21.052	3.6767	39.03	91.4	-0.954
14.035	3.8528	41.85	94.2	-3.065
9.3564	4.0289	44.30	96.7	-5.169
6.2376	4.2050	47.03	100.1	-8.247
4.1584	4.3811	49.80	101.4	-9.843
2.7723	4.5572	52.25	103.7	-12.375
1.8482	4.7337	54.63	105.2	-14.323
1.2321	4.9094	57.08	106.4	-16.116

Table B 48

Adhesion Tension of $C_{12}NBr$ - $C_{10}SO_3Na$ Mixtures at Teflon/Aqueous Interface, I.S. = 0.1 N (NaBr)

$C_{C_{10}SO_3Na} = 2.7723 \times 10^{-5}$ M

C ($C_{12}NBr$)	-log C ($C_{12}NBr$)	γ_{lv}	θ	$\gamma_{lv} \cdot \cos\theta$
10^5x mol/dm^3		mN/m	deg.	mN/m
21.052	3.6767	41.67	94.4	-3.197
14.035	3.8528	44.13	96.4	-4.919
9.3564	4.0289	46.64	99.1	-7.376
6.2376	4.2050	49.41	101.6	-9.881
4.1584	4.3811	52.12	103.4	-12.079
2.7723	4.5572	54.43	105.1	-14.179
1.8482	4.7337	56.77	106.7	-16.313
1.2321	4.9094	59.20	107.8	-18.097

Table B 49

Adhesion Tension of $C_{12}NBr$ - $C_{10}SO_3Na$ Mixtures at Teflon/Aqueous Interface, I.S. = 0.1 N (NaBr)

$C_{C_{10}SO_3Na} = 1.8482 \times 10^{-5}$ M

C ($C_{12}NBr$) 10^5x mol/dm^3	-log C ($C_{12}NBr$)	γ_{lv} mN/m	θ deg.	$\gamma_{lv} \cdot \cos\theta$ mN/m
21.052	3.6767	43.90	97.0	-5.350
14.035	3.8528	46.59	99.3	-7.529
9.3564	4.0289	48.99	101.5	-9.767
6.2376	4.2050	51.60	102.9	-11.520
4.1584	4.3811	54.14	104.5	-13.556
2.7723	4.5572	56.49	106.5	-16.044
1.8482	4.7337	58.83	107.6	-17.788
1.2321	4.9094	61.02	108.7	-19.564

Table B 50

Adhesion Tension of $C_{12}NBr$ - $C_{10}SO_3Na$ Mixtures at Teflon/Aqueous Interface, I.S. = 0.1 N (NaBr)

$C_{C_{10}SO_3Na} = 1.2321 \times 10^{-5}$ M

C ($C_{12}NBr$)	-log C ($C_{12}NBr$)	γ_{lv}	θ	$\gamma_{lv} \cdot \cos\theta$
10^5x mol/dm^3		mN/m	deg.	mN/m
21.052	3.6767	46.02	98.9	-7.120
14.035	3.8528	48.64	100.5	-8.864
9.3564	4.0289	51.20	102.4	-10.994
6.2376	4.2050	53.70	104.4	-13.355
4.1584	4.3811	56.42	106.0	-15.552
2.7723	4.5572	58.42	107.3	-17.373
1.8482	4.7337	60.70	108.4	-19.160
1.2321	4.9094	62.71	109.6	-21.036

Table B 51

Adhesion Tension of $C_{12}NBr$ - $C_{10}SO_3Na$ Mixtures

at Teflon/Aqueous Interface, I.S. = 0.1 N (NaBr)

$C_{C_{10}SO_3Na} = 8.2141 \times 10^{-6}$ M

C ($C_{12}NBr$)	-log C ($C_{12}NBr$)	γ_{lv}	θ	$\gamma_{lv} \cdot \cos\theta$
10^5x mol/dm^3		mN/m	deg.	mN/m
21.052	3.6767	48.03	100.5	-8.753
14.035	3.8528	50.60	102.4	-10.866
9.3564	4.0289	53.45	104.2	-13.112
6.2376	4.2050	55.73	105.4	-14.799
4.1584	4.3811	58.13	107.1	-17.093
2.7723	4.5572	60.20	108.4	-19.002
1.8482	4.7337	62.40	109.7	-21.035
1.2321	4.9094	63.96	110.5	-22.399

Table B 52

Adhesion Tension of $C_{12}NBr$ - $C_{10}SO_3Na$ Mixtures

at Teflon/Aqueous Interface, I.S. = 0.1 N (NaBr)

$C_{C_{12}NBr} = 2.1052 \times 10^{-4}$ M

C ($C_{10}SO_3Na$)	-log C ($C_{10}SO_{Na}$)	γ_{lv}	θ	$\gamma_{lv} \cdot \cos\theta$
10^5x mol/dm^3		mN/m	deg.	mN/m
9.3564	4.0289	34.28	84.8	3.107
6.2376	4.2050	36.60	88.5	0.958
4.1584	4.3811	39.03	91.4	-0.954
2.7723	4.5572	41.67	94.4	-3.197
1.8482	4.7337	43.90	97.0	-5.350
1.2321	4.9094	46.02	98.9	-7.120
0.82141	5.0854	48.03	100.5	-8.753

Table B 53

Adhesion Tension of $C_{12}NBr$ - $C_{10}SO_3Na$ Mixtures at Teflon/Aqueous Interface, I.S. = 0.1 N (NaBr)

$C_{C_{12}NBr} = 1.4035 \times 10^{-4}$ M

C ($C_{10}SO_3Na$)	-log C ($C_{10}SO_3Na$)	γ_{lv}	θ	$\gamma_{lv} \cdot \cos\theta$
10^5x mol/dm^3		mN/m	deg.	mN/m
21.052	3.6767	31.70	81.0	4.959
14.035	3.8528	34.05	85.3	2.790
9.3564	4.0289	36.81	88.6	0.899
6.2376	4.2050	39.38	91.7	-1.168
4.1584	4.3811	41.85	94.2	-3.065
2.7723	4.5572	44.13	96.4	-4.919
1.8482	4.7337	46.59	99.3	-7.529
1.2321	4.9094	48.64	100.5	-8.864
0.82141	5.0854	50.60	102.4	-10.866

Table B 54

Adhesion Tension of $C_{12}NBr$ - $C_{10}SO_3Na$ Mixtures

at Teflon/Aqueous Interface, I.S. = 0.1 N (NaBr)

$C_{C_{12}NBr} = 9.3564 \times 10^{-5}$ M

C ($C_{10}SO_3Na$)	-log C ($C_{10}SO_3Na$)	γ_{lv}	θ	$\gamma_{lv} \cdot \cos\theta$
10^5x mol/dm^3		mN/m	deg.	mN/m
21.052	3.6767	34.30	86.0	2.393
14.035	3.8528	36.86	89.4	0.386
9.3564	4.0289	39.31	92.6	-1.783
6.2376	4.2050	41.83	95.0	-3.646
4.1584	4.3811	44.30	96.7	-5.169
2.7723	4.5572	46.64	99.1	-7.376
1.8482	4.7337	48.99	101.5	-9.767
1.2321	4.9094	51.20	102.4	-10.994
0.82141	5.0854	53.45	104.2	-13.111

Table B 55

Adhesion Tension of $C_{12}NBr$ - $C_{10}SO_3Na$ Mixtures

at Teflon/Aqueous Interface, I.S. = 0.1 N (NaBr)

$C_{C_{12}NBr} = 6.2376 \times 10^{-5}$ M

C ($C_{10}SO_3Na$)	-log C ($C_{10}SO_3Na$)	γ_{lv}	θ	$\gamma_{lv} \cdot \cos\theta$
10^5x mol/dm^3		mN/m	deg.	mN/m
21.052	3.6767	37.30	90.0	0.000
14.035	3.8528	39.70	93.0	-2.078
9.3564	4.0289	42.22	95.4	-3.973
6.2376	4.2050	44.72	97.6	-5.915
4.1584	4.3811	47.03	100.1	-8.247
2.7723	4.5572	49.41	101.6	-9.935
1.8482	4.7337	51.60	102.9	-11.520
1.2321	4.9094	53.70	104.4	-13.355
0.82141	5.0854	55.73	105.4	-14.799

Table B 56

Adhesion Tension of $C_{12}NBr$ - $C_{10}SO_3Na$ Mixtures at Teflon/Aqueous Interface, I.S. = 0.1 N (NaBr)

$C_{C_{12}NBr} = 4.1584 \times 10^{-5}$ M

C ($C_{10}SO_3Na$) 10^5x mol/dm^3	-log C ($C_{10}SO_3Na$)	γ_{lv} mN/m	θ deg.	$\gamma_{lv} \cdot \cos\theta$ mN/m
21.052	3.6767	40.03	93.8	-2.653
14.035	3.8528	42.37	95.7	-4.208
9.3564	4.0289	45.03	97.9	-6.189
6.2376	4.2050	47.40	100.1	-8.312
4.1584	4.3811	49.80	101.4	-9.843
2.7723	4.5572	52.12	103.4	-12.074
1.8482	4.7337	54.14	104.5	-13.556
1.2321	4.9094	56.42	106.0	-15.552
0.82141	5.0854	58.13	107.1	-17.093

Table B 57

Adhesion Tension of $C_{12}NBr$ - $C_{10}SO_3Na$ Mixtures

at Teflon/Aqueous Interface, I.S. = 0.1 N (NaBr)

$C_{C_{12}NBr} = 2.7723 \times 10^{-5}$ M

C ($C_{10}SO_3Na$) 10^5x mol/dm^3	-log C ($C_{10}SO_3Na$)	γ_{lv} mN/m	θ deg.	$\gamma_{lv} \cdot \cos\theta$ mN/m
21.052	3.6767	42.21	96.2	-4.559
14.035	3.8528	44.80	98.2	-6.390
9.3564	4.0289	47.47	100.2	-8.406
6.2376	4.2050	49.91	102.1	-10.462
4.1584	4.3811	52.25	103.7	-12.375
2.7723	4.5572	54.43	105.1	-14.179
1.8482	4.7337	56.49	106.5	-16.044
1.2321	4.9094	58.42	107.3	-17.373
0.82141	5.0854	60.20	108.4	-19.002

Table B 58

Adhesion Tension of $C_{12}NBr$ - $C_{10}SO_3Na$ Mixtures

at Teflon/Aqueous Interface, I.S. = 0.1 N (NaBr)

$C_{C_{12}NBr} = 1.8482 \times 10^{-5}$ M

C ($C_{10}SO_3Na$)	-log C ($C_{10}SO_3Na$)	γ_{lv}	θ	$\gamma_{lv} \cdot \cos\theta$
10^5x mol/dm^3		mN/m	deg.	mN/m
21.052	3.6767	45.11	98.8	-6.901
14.035	3.8528	47.64	100.6	-8.763
9.3564	4.0289	50.08	101.9	-10.327
6.2376	4.2050	52.49	103.8	-12.521
4.1584	4.3811	54.63	105.2	-14.323
2.7723	4.5572	56.77	106.7	-16.313
1.8482	4.7337	58.83	107.6	-17.788
1.2321	4.9094	60.70	108.4	-19.166
0.82141	5.0854	62.40	109.7	-21.035

Table B 59

Adhesion Tension of $C_{12}NBr$ - $C_{10}SO_3Na$ Mixtures at Teflon/Aqueous Interface, I.S. = 0.1 N (NaBr)

$C_{C_{12}NBr} = 1.2321 \times 10^{-5}$ M

C ($C_{10}SO_3Na$) 10^5x mol/dm^3	-log C ($C_{10}SO_3Na$)	γ_{lv} mN/m	θ deg.	$\gamma_{lv} \cdot \cos\theta$ mN/m
21.052	3.6767	47.57	100.9	-8.995
14.035	3.8528	49.97	102.6	-10.901
9.3564	4.0289	52.43	104.1	-12.773
6.2376	4.2050	54.68	105.5	-14.613
4.1584	4.3811	57.08	106.4	-16.116
2.7723	4.5572	59.20	107.8	-18.097
1.8482	4.7337	61.02	108.7	-19.564
1.2321	4.9094	62.71	109.6	-21.036
0.82141	5.0854	63.96	110.5	-22.399

Table B 60

Adhesion Tension of $C_{12}NBr$ - $C_{10}SO_3Na$ Mixtures

at Parafilm/Aqueous Interface, I.S. = 0.1 N (NaBr)

$C_{C_{10}SO_3Na} = 2.1052 \times 10^{-4}$ M

C ($C_{12}NBr$)	-log C ($C_{12}NBr$)	γ_{lv}	θ	$\gamma_{lv} \cdot \cos\theta$
10^5x mol/dm^3		mN/m	deg.	mN/m
14.035	3.8528	31.70	70.6	10.530
9.3564	4.0289	34.30	78.0	7.131
6.2376	4.2050	37.30	83.3	4.352
4.1584	4.3811	40.03	87.1	2.025
2.7723	4.5572	42.21	90.4	-0.295
1.8482	4.7337	45.11	94.4	-3.461
1.2321	4.9094	47.57	96.8	-5.632

Table B 61

Adhesion Tension of $C_{12}NBr$ - $C_{10}SO_3Na$ Mixtures

at Parafilm/Aqueous Interface, I.S. = 0.1 N (NaBr)

$C_{C_{10}SO_3Na} = 1.4035 \times 10^{-4}$ M

C ($C_{12}NBr$)	-log C ($C_{12}NBr$)	γ_{lv}	θ	$\gamma_{lv} \cdot \cos\theta$
10^5x mol/dm^3		mN/m	deg.	mN/m
14.035	3.8528	34.05	76.5	7.949
9.3564	4.0289	36.86	81.3	5.575
6.2376	4.2050	39.70	86.3	2.562
4.1584	4.3811	42.37	90.5	-0.370
2.7723	4.5572	44.80	93.6	-2.813
1.8482	4.7337	47.64	96.4	-5.310
1.2321	4.9094	49.97	98.5	-7.386

Table B 62

Adhesion Tension of $C_{12}NBr$ - $C_{10}SO_3Na$ Mixtures

at Parafilm/Aqueous Interface, I.S. = 0.1 N (NaBr)

$C_{C_{10}SO_3Na} = 9.3564 \times 10^{-5}$ M

C ($C_{12}NBr$)	-log C ($C_{12}NBr$)	γ_{lv}	θ	$\gamma_{lv} \cdot \cos\theta$
10^5x mol/dm^3		mN/m	deg.	mN/m
21.052	3.6767	34.28	75.2	8.757
14.035	3.8528	36.81	82.1	5.059
9.3564	4.0289	39.31	85.9	2.811
6.2376	4.2050	42.22	89.9	0.074
4.1584	4.3811	45.03	92.6	-2.043
2.7723	4.5572	47.47	95.6	-4.632
1.8482	4.7337	50.08	98.3	-7.229
1.2321	4.9094	52.43	100.2	-9.285

Table B 63

Adhesion Tension of $C_{12}NBr$ - $C_{10}SO_3Na$ Mixtures

at Parafilm/Aqueous Interface, I.S. = 0.1 N (NaBr)

$C_{C_{10}SO_3Na} = 6.2376 \times 10^{-5}$ M

C ($C_{12}NBr$) $10^5 \times$ mol/dm^3	-log C ($C_{12}NBr$)	γ_{lv} mN/m	θ deg.	$\gamma_{lv} \cdot \cos\theta$ mN/m
21.052	3.6767	36.60	80.5	6.041
14.035	3.8528	39.38	85.3	3.227
9.3564	4.0289	41.83	89.6	0.292
6.2376	4.2050	44.72	92.0	-1.561
4.1584	4.3811	47.40	95.4	-4.461
2.7723	4.5572	49.91	97.7	-6.689
1.8482	4.7337	52.49	100.0	-9.115
1.2321	4.9094	54.68	102.0	-11.369

Table B 64

Adhesion Tension of $C_{12}NBr$ - $C_{10}SO_3Na$ Mixtures at Parafilm/Aqueous Interface, I.S. = 0.1 N (NaBr)

$C_{C_{10}SO_3Na} = 4.1584 \times 10^{-5}$ M

C ($C_{12}NBr$)	-log C ($C_{12}NBr$)	γ_{lv}	θ	$\gamma_{lv} \cdot \cos\theta$
10^5x mol/dm^3		mN/m	deg.	mN/m
21.052	3.6767	39.03	84.7	3.605
14.035	3.8528	41.85	88.6	1.022
9.3564	4.0289	44.30	92.3	-1.778
6.2376	4.2050	47.03	94.5	-3.690
4.1584	4.3811	49.80	96.9	-5.983
2.7723	4.5572	52.25	99.5	-8.624
1.8482	4.7337	54.63	101.6	-10.985
1.2321	4.9094	57.08	103.0	-12.840

Table B 65

Adhesion Tension of $C_{12}NBr$ - $C_{10}SO_3Na$ Mixtures

at Parafilm/Aqueous Interface, I.S. = 0.1 N (NaBr)

$C_{C_{10}SO_3Na} = 2.7723 \times 10^{-5}$ M

C ($C_{12}NBr$)	-log C ($C_{12}NBr$)	γ_{lv}	θ	$\gamma_{lv} \cdot \cos\theta$
10^5x mol/dm^3		mN/m	deg.	mN/m
21.052	3.6767	41.67	88.2	1.312
14.035	3.8528	44.13	91.5	-1.155
9.3564	4.0289	46.64	94.4	-3.578
6.2376	4.2050	49.41	96.8	-5.818
4.1584	4.3811	52.12	98.7	-7.884
2.7723	4.5572	54.43	101.1	-10.479
1.8482	4.7337	56.77	102.7	-12.481
1.2321	4.9094	59.20	104.0	-14.322

Table B 66

Adhesion Tension of $C_{12}NBr$ - $C_{10}SO_3Na$ Mixtures

at Parafilm/Aqueous Interface, I.S. = 0.1 N (NaBr)

$C_{C_{10}SO_3Na} = 1.8482 \times 10^{-5}$ M

C ($C_{12}NBr$)	-log C ($C_{12}NBr$)	γ_{lv}	θ	$\gamma_{lv} \cdot \cos\theta$
10^5x mol/dm^3		mN/m	deg.	mN/m
21.052	3.6767	43.90	91.2	-0.919
14.035	3.8528	46.59	94.5	-3.655
9.3564	4.0289	48.99	97.1	-6.055
6.2376	4.2050	51.60	98.7	-7.805
4.1584	4.3811	54.14	101.2	-10.516
2.7723	4.5572	56.49	102.7	-12.419
1.8482	4.7337	58.83	104.3	-14.531
1.2321	4.9094	61.02	105.4	-16.204

Table B 67

Adhesion Tension of $C_{12}NBr$ - $C_{10}SO_3Na$ Mixtures at Parafilm/Aqueous Interface, I.S. = 0.1 N (NaBr)

$C_{C_{10}SO_3Na} = 1.2321 \times 10^{-5}$ M

C ($C_{12}NBr$)	-log C ($C_{12}NBr$)	γ_{lv}	θ	$\gamma_{lv} \cdot \cos\theta$
10^5x mol/dm^3		mN/m	deg.	mN/m
21.052	3.6767	46.02	93.9	-3.130
14.035	3.8528	48.64	96.4	-5.422
9.3564	4.0289	51.20	99.1	-8.098
6.2376	4.2050	53.70	100.8	-10.062
4.1584	4.3811	56.42	102.6	-12.308
2.7723	4.5572	58.42	104.4	-14.528
1.8482	4.7337	60.70	105.7	-16.425
1.2321	4.9094	62.71	107.0	-18.335

Table B 68

Adhesion Tension of $C_{12}NBr$ - $C_{10}SO_3Na$ Mixtures

at Parafilm/Aqueous Interface, I.S. = 0.1 N (NaBr)

$C_{C_{10}SO_3Na} = 8.2141 \times 10^{-6}$ M

C ($C_{12}NBr$)	-log C ($C_{12}NBr$)	γ_{lv}	θ	$\gamma_{lv} \cdot \cos\theta$
10^5x mol/dm^3		mN/m	deg.	mN/m
21.052	3.6767	48.03	96.4	-5.354
14.035	3.8528	50.60	98.5	-7.479
9.3564	4.0289	53.45	100.6	-9.832
6.2376	4.2050	55.73	102.0	-11.587
4.1584	4.3811	58.13	104.1	-14.161
2.7723	4.5572	60.20	105.6	-16.189
1.8482	4.7337	62.40	106.7	-17.931
1.2321	4.9094	63.96	107.9	-19.659

Table B 69

Adhesion Tension of $C_{12}NBr$ - $C_{10}SO_3Na$ Mixtures

at Parafilm/Aqueous Interface, I.S. = 0.1 N (NaBr)

$C_{C_{12}NBr} = 2.1052 \times 10^{-4}$ M

C ($C_{10}SO_3Na$)	-log C ($C_{10}SO_Na$)	γ_{lv}	θ	$\gamma_{lv} \cdot \cos\theta$
10^5x mol/dm^3		mN/m	deg.	mN/m
9.3564	4.0289	34.28	75.2	8.757
6.2376	4.2050	36.60	80.5	6.041
4.1584	4.3811	39.03	84.7	3.605
2.7723	4.5572	41.67	88.2	1.313
1.8482	4.7337	43.90	91.2	-0.919
1.2321	4.9094	46.02	93.9	-3.130
0.82141	5.0854	48.03	96.4	-5.354

Table B 70

Adhesion Tension of $C_{12}NBr$ - $C_{10}SO_3Na$ Mixtures

at Parafilm/Aqueous Interface, I.S. = 0.1 N (NaBr)

$C_{C_{12}NBr} = 1.4035 \times 10^{-4}$ M

C ($C_{10}SO_3Na$)	-log C ($C_{10}SO_3Na$)	γ_{lv}	θ	$\gamma_{lv} \cdot \cos\theta$
10^5x mol/dm^3		mN/m	deg.	mN/m
21.052	3.6767	31.70	70.6	10.530
14.035	3.8528	34.05	76.5	7.949
9.3564	4.0289	36.81	82.1	5.059
6.2376	4.2050	39.38	85.3	3.227
4.1584	4.3811	41.85	88.6	1.022
2.7723	4.5572	44.13	91.5	-1.155
1.8482	4.7337	46.59	94.5	-3.655
1.2321	4.9094	48.64	96.4	-5.422
0.82141	5.0854	50.60	98.5	-7.479

Table B 71

Adhesion Tension of $C_{12}NBr$ - $C_{10}SO_3Na$ Mixtures

at Parafilm/Aqueous Interface, I.S. = 0.1 N (NaBr)

$C_{C_{12}NBr} = 9.3564 \times 10^{-5}$ M

C ($C_{10}SO_3Na$)	-log C ($C_{10}SO_3Na$)	γ_{lv}	θ	$\gamma_{lv} \cdot \cos\theta$
10^5x mol/dm^3		mN/m	deg.	mN/m
21.052	3.6767	34.30	78.0	7.131
14.035	3.8528	36.86	81.3	5.575
9.3564	4.0289	39.31	85.9	2.811
6.2376	4.2050	41.83	89.6	0.292
4.1584	4.3811	44.30	92.3	-1.778
2.7723	4.5572	46.64	94.4	-3.578
1.8482	4.7337	48.99	97.1	-6.055
1.2321	4.9094	51.20	99.1	-8.098
0.82141	5.0854	53.45	100.6	-9.832

Table B 72

Adhesion Tension of $C_{12}NBr$ - $C_{10}SO_3Na$ Mixtures

at Parafilm/Aqueous Interface, I.S. = 0.1 N (NaBr)

$C_{C_{12}NBr} = 6.2376 \times 10^{-5}$ M

C ($C_{10}SO_3Na$)	-log C ($C_{10}SO_3Na$)	γ_{lv}	θ	$\gamma_{lv} \cdot \cos\theta$
10^5x mol/dm^3		mN/m	deg.	mN/m
21.052	3.6767	37.30	83.3	4.352
14.035	3.8528	39.70	86.3	2.562
9.3564	4.0289	42.22	89.9	0.074
6.2376	4.2050	44.72	92.0	-1.561
4.1584	4.3811	47.03	94.5	-3.690
2.7723	4.5572	49.41	96.8	-5.850
1.8482	4.7337	51.60	98.7	-7.805
1.2321	4.9094	53.70	100.8	-10.062
0.82141	5.0854	55.73	102.0	-11.587

Table B 73

Adhesion Tension of $C_{12}NBr$ - $C_{10}SO_3Na$ Mixtures

at Parafilm/Aqueous Interface, I.S. = 0.1 N (NaBr)

$C_{C_{12}NBr} = 4.1584 \times 10^{-5}$ M

C ($C_{10}SO_3Na$) 10^5x mol/dm^3	-log C ($C_{10}SO_3Na$)	γ_{lv} mN/m	θ deg.	$\gamma_{lv} \cdot \cos\theta$ mN/m
21.052	3.6767	40.03	87.1	2.025
14.035	3.8528	42.37	90.5	-0.370
9.3564	4.0289	45.03	92.6	-2.043
6.2376	4.2050	47.40	95.4	-4.461
4.1584	4.3811	49.80	96.9	-5.983
2.7723	4.5572	52.12	98.7	-7.884
1.8482	4.7337	54.14	101.2	-10.516
1.2321	4.9094	56.42	102.6	-12.308
0.82141	5.0854	58.13	104.1	-14.161

Table B 74

Adhesion Tension of $C_{12}NBr$ - $C_{10}SO_3Na$ Mixtures

at Parafilm/Aqueous Interface, I.S. = 0.1 N (NaBr)

$C_{C_{12}NBr} = 2.7723 \times 10^{-5}$ M

C ($C_{10}SO_3Na$)	-log C ($C_{10}SO_3Na$)	γ_{lv}	θ	$\gamma_{lv} \cdot \cos\theta$
10^5x mol/dm^3		mN/m	deg.	mN/m
21.052	3.6767	42.21	90.4	-0.295
14.035	3.8528	44.80	93.6	-2.813
9.3564	4.0289	47.47	95.6	-4.632
6.2376	4.2050	49.91	97.7	-6.687
4.1584	4.3811	52.25	99.5	-8.624
2.7723	4.5572	54.43	101.1	-10.479
1.8482	4.7337	56.49	102.7	-12.419
1.2321	4.9094	58.42	104.4	-14.528
0.82141	5.0854	60.20	105.6	-16.189

Table B 75

Adhesion Tension of $C_{12}NBr$ - $C_{10}SO_3Na$ Mixtures

at Parafilm/Aqueous Interface, I.S. = 0.1 N (NaBr)

$C_{C_{12}NBr} = 1.8482 \times 10^{-5}$ M

C ($C_{10}SO_3Na$) 10^5x mol/dm^3	-log C ($C_{10}SO_3Na$)	γ_{lv} mN/m	θ deg.	$\gamma_{lv} \cdot \cos\theta$ mN/m
21.052	3.6767	45.11	94.4	-3.461
14.035	3.8528	47.64	96.4	-5.310
9.3564	4.0289	50.08	98.3	-7.229
6.2376	4.2050	52.49	100.0	-9.115
4.1584	4.3811	54.63	101.6	-10.985
2.7723	4.5572	56.77	102.7	-12.481
1.8482	4.7337	58.83	104.3	-14.531
1.2321	4.9094	60.70	105.7	-16.425
0.82141	5.0854	62.40	106.7	-17.931

Table B 76

Adhesion Tension of $C_{12}NBr$ - $C_{10}SO_3Na$ Mixtures

at Parafilm/Aqueous Interface, I.S. = 0.1 N (NaBr)

$C_{C_{12}NBr} = 1.2321 \times 10^{-5}$ M

C ($C_{10}SO_3Na$) 10^5x mol/dm^3	-log C ($C_{10}SO_3Na$)	γ_{lv} mN/m	θ deg.	$\gamma_{lv} \cdot \cos\theta$ mN/m
21.052	3.6767	47.57	96.8	-5.632
14.035	3.8528	49.97	98.5	-7.386
9.3564	4.0289	52.43	100.2	-9.285
6.2376	4.2050	54.68	102.0	-11.369
4.1584	4.3811	57.08	103.0	-12.840
2.7723	4.5572	59.20	104.0	-14.322
1.8482	4.7337	61.02	105.4	-16.204
1.2321	4.9094	62.71	107.0	-18.335
0.82141	5.0854	63.96	107.9	-19.659

Table B 77

Adhesion Tension of $C_{10}SO_3Na$

at Teflon/Aqueous Interface, I.S. = 0.1 N (NaBr)

α = 0.0000

C	-log C	γ_{lv}	θ	$\gamma_{lv} \cdot \cos\theta$
10^3x mol/dm^3		mN/m	deg.	mN/m
36.93	1.433	38.66	83.9	4.108
34.30	1.465	39.27	83.9	4.173
29.17	1.535	38.94	83.7	4.273
24.00	1.620	38.66	84.0	4.041
21.28	1.672	38.76	83.8	4.186
18.46	1.734	39.68	85.6	3.044
14.59	1.836	42.26	87.6	1.770
12.00	1.921	44.14	90.0	0.000
10.64	1.973	45.50	91.5	-1.191
9.232	2.035	46.50	93.0	-2.434
7.294	2.137	49.34	95.2	-4.472
6.001	2.222	50.66	96.1	-5.383
5.320	2.274	52.42	96.3	-5.752
4.616	2.336	53.32	97.8	-7.236
3.647	2.438	55.21	99.3	-8.922
2.308	2.637	59.41	102.3	-12.656
1.500	2.824	62.13	103.8	-14.820

Table B 78

Adhesion Tension of $C_{12}NBr$ - $C_{10}SO_3Na$ Mixtures

at Teflon/Aqueous Interface, I.S. = 0.1 N (NaBr)

α = 0.2286

C	-log C	γ_{lv}	θ	$\gamma_{lv} \cdot \cos\theta$
10^4x mol/dm^3		mN/m	deg.	mN/m
2.729	3.564	37.30	90.0	0.000
1.819	3.740	42.37	95.7	-4.208
1.213	3.916	47.47	100.2	-8.406
0.8086	4.092	52.49	103.8	-12.521
0.5391	4.268	57.08	106.4	-16.116

Table B 79

Adhesion Tension of $C_{12}NBr$ - $C_{10}SO_3Na$ Mixtures

at Teflon/Aqueous Interface, I.S. = 0.1 N (NaBr)

α = 0.5000

C	-log C	γ_{lv}	θ	$\gamma_{lv} \cdot \cos\theta$
10^4x mol/dm^3		mN/m	deg.	mN/m
2.807	3.552	34.05	85.3	2.790
1.871	3.728	39.31	92.6	-1.783
1.248	3.904	44.72	97.6	-5.915
0.8317	4.080	49.80	101.4	-9.843
0.5545	4.256	54.43	105.1	-14.179
0.3696	4.432	58.83	107.6	-17.788
0.2464	4.608	62.71	109.6	-21.036

Table B 80

Adhesion Tension of $C_{12}NBr$ - $C_{10}SO_3Na$ Mixtures

at Teflon/Aqueous Interface, I.S. = 0.1 N (NaBr)

α = 0.7714

C	-log C	γ_{lv}	θ	$\gamma_{lv} \cdot \cos\theta$
10^4x mol/dm^3		mN/m	deg.	mN/m
2.729	3.564	36.60	88.5	0.958
1.819	3.740	41.85	94.2	-3.065
1.213	3.916	46.64	99.1	-7.376
0.8086	4.092	51.60	102.9	-11.520
0.5391	4.268	56.42	106.0	-15.552
0.3594	4.445	60.20	108.4	-19.002

Table B 81

Adhesion Tension of $C_{12}NBr$

at Teflon/Aqueous Interface, I.S. = 0.1 N (NaBr)

α = 1.0000

C	-log C	γ_{lv}	θ	$\gamma_{lv} \cdot \cos\theta$
10^4x mol/dm^3		mN/m	deg.	mN/m
93.56	2.029	36.87	81.0	5.768
65.50	2.184	36.87	81.6	5.386
46.78	2.330	36.87	81.6	5.386
32.75	2.485	36.95	81.1	5.717
23.39	2.631	38.20	82.3	5.118
16.37	2.786	41.11	86.8	2.295
11.70	2.932	43.78	90.1	-0.076
8.187	3.087	46.74	93.3	-2.691
5.848	3.233	49.45	95.7	-4.911
4.093	3.388	52.51	98.8	-8.033
3.275	3.485	53.84	99.8	-9.164
2.917	3.582	55.35	101.5	-11.035
2.058	3.687	56.73	102.8	-12.568
1.591	3.798	59.00	103.9	-14.173

Table B 82

Adhesion Tension of $C_{10}SO_3Na$

at Parafilm/Aqueous Interface, I.S. = 0.1 N (NaBr)

α = 0.0000

C	-log C	γ_{lv}	θ	$\gamma_{lv} \cdot \cos\theta$
10^3x mol/dm^3		mN/m	deg.	mN/m
36.93	1.433	38.66	80.6	6.314
34.30	1.465	39.27	80.4	6.549
29.17	1.535	38.94	80.3	6.561
24.00	1.620	38.66	80.4	6.447
21.28	1.672	38.76	80.6	6.331
18.46	1.734	39.68	82.1	5.454
14.59	1.836	42.26	84.9	3.757
12.00	1.921	44.14	86.8	2.464
10.64	1.973	45.50	87.5	1.985
9.232	2.035	46.50	90.2	-0.162
7.294	2.137	49.34	91.8	-1.550
6.001	2.222	50.66	94.0	-3.534
5.320	2.274	52.42	94.7	-4.295
4.616	2.336	53.32	95.2	-4.833
3.647	2.438	55.21	97.1	-7.397
3.000	2.523	56.86	98.7	-8.601
2.660	2.575	57.90	99.2	-9.257

2.308	2.637	59.41	99.5	-9.805
1.500	2.824	62.13	101.8	-12.705

Table B 83

Adhesion Tension of $C_{12}NBr$ - $C_{10}SO_3Na$ Mixtures

at Parafilm/Aqueous Interface, I.S. = 0.1 N (NaBr)

α = 0.2286

C	-log C	γ_{lv}	θ	$\gamma_{lv} \cdot \cos\theta$
10^4x mol/dm^3		mN/m	deg.	mN/m
2.729	3.564	37.30	83.3	4.352
1.819	3.740	42.37	90.5	-0.370
1.213	3.916	47.47	95.6	-4.632
0.8086	4.092	52.49	100.0	-9.115
0.5391	4.268	57.08	103.0	-12.840

Table B 84

Adhesion Tension of $C_{12}NBr$ - $C_{10}SO_3Na$ Mixtures

at Parafilm/Aqueous Interface, I.S. = 0.1 N (NaBr)

α = 0.5000

C	-log C	γ_{lv}	θ	$\gamma_{lv} \cdot \cos\theta$
10^4x mol/dm^3		mN/m	deg.	mN/m
2.807	3.552	34.05	76.5	7.945
1.871	3.728	39.31	85.9	2.811
1.248	3.904	44.72	92.0	-1.561
0.8317	4.080	49.80	96.94	-5.983
0.5545	4.256	54.43	101.1	-10.479
0.3696	4.432	58.83	104.3	-14.531
0.2464	4.608	62.71	107.0	-18.335

Table B 85

Adhesion Tension of $C_{12}NBr$ - $C_{10}SO_3Na$ Mixtures

at Parafilm/Aqueous Interface, I.S. = 0.1 N (NaBr)

α = 0.7714

C	-log C	γ_{lv}	θ	$\gamma_{lv} \cdot \cos\theta$
10^4x mol/dm^3		mN/m	deg.	mN/m
2.729	3.564	36.60	80.5	6.041
1.819	3.740	41.85	88.6	1.022
1.213	3.916	46.64	94.4	-3.578
0.8086	4.092	51.60	98.7	-7.805
0.5391	4.268	56.42	102.6	-12.308
0.3594	4.445	60.20	105.6	-16.189

Table B 86

Adhesion Tension of $C_{12}NBr$

at Parafilm/Aqueous Interface, I.S. = 0.1 N (NaBr)

α = 1.0000

C	-log C	γ_{lv}	θ	$\gamma_{lv} \cdot \cos\theta$
10^4x mol/dm^3		mN/m	deg.	mN/m
93.56	2.029	36.87	73.1	10.718
65.50	2.184	36.87	73.1	10.718
46.78	2.330	36.87	73.6	10.410
32.75	2.485	36.95	73.7	10.371
23.39	2.631	38.20	76.7	8.788
16.37	2.786	41.11	82.5	5.366
11.70	2.932	43.78	86.2	2.902
8.187	3.087	46.74	90.3	-0.245
5.848	3.233	49.45	93.0	-2.588
4.093	3.388	52.51	95.9	-5.398
3.275	3.485	53.84	97.6	-7.121
2.917	3.582	55.35	98.7	-8.372
2.058	3.687	56.73	100.3	-10.143
1.591	3.798	59.00	101.7	-12.000

Table B 87

Adhesion Tension of $C_{14}TMABr$ - C_8SO_3Na Mixtures at Teflon/Aqueous Interface, I.S. = 0.1 N (NaBr)

$C_{C_8SO_3Na} = 9.676 \times 10^{-5}$ M

C ($C_{14}TMABr$) $10^5 \times$ mol/dm^3	-log C ($C_{14}TMABr$)	γ_{lv} mN/m	θ deg.	$\gamma_{lv} \cdot \cos\theta$ mN/m
21.77	3.662	33.13	83.8	3.578
14.51	3.838	36.66	89.7	0.192
9.676	4.014	39.65	94.0	-2.766
6.451	4.190	42.84	97.5	-5.592
4.301	4.366	45.77	101.1	-8.812
2.867	4.543	48.36	104.1	-11.781
1.911	4.719	51.02	106.4	-14.405
1.274	4.895	53.36	108.7	-17.108

Table B 88

Adhesion Tension of $C_{14}TMABr$ - C_8SO_3Na Mixtures at Teflon/Aqueous Interface, I.S. = 0.1 N (NaBr)

$C_{C_8SO_3Na} = 6.451 \times 10^{-5}$ M

C ($C_{14}TMABr$) 10^5x mol/dm^3	-log C ($C_{14}TMABr$)	γ_{lv} mN/m	θ deg.	$\gamma_{lv} \cdot \cos\theta$ mN/m
21.77	3.662	34.69	85.8	2.541
14.51	3.838	38.13	91.3	-0.865
9.676	4.014	41.23	95.0	-3.593
6.451	4.190	44.32	98.9	-6.857
4.301	4.366	47.15	101.7	-9.561
2.867	4.543	50.03	104.7	-12.696
1.911	4.719	52.54	106.8	-15.186
1.274	4.895	54.93	109.2	-18.065

Table B 89

Adhesion Tension of $C_{14}TMABr$ - C_8SO_3Na Mixtures

at Teflon/Aqueous Interface, I.S. = 0.1 N (NaBr)

$C_{C_8SO_3Na} = 4.301 \times 10^{-5}$ M

C ($C_{14}TMABr$) 10^5x mol/dm^3	-log C ($C_{14}TMABr$)	γ_{lv} mN/m	θ deg.	$\gamma_{lv} \cdot \cos\theta$ mN/m
21.77	3.662	36.00	87.3	1.696
14.51	3.838	39.46	92.2	-1.515
9.676	4.014	42.60	95.8	-4.305
6.451	4.190	45.73	99.1	-7.233
4.301	4.366	48.57	102.6	-10.585
2.867	4.543	51.29	105.6	-13.793
1.911	4.719	53.94	107.5	-16.220
1.274	4.895	56.28	109.7	-18.971

Table B 90

Adhesion Tension of $C_{14}TMABr$ - C_8SO_3Na Mixtures at Teflon/Aqueous Interface, I.S. = 0.1 N (NaBr)

$C_{C_8SO_3Na} = 2.867 \times 10^{-5}$ M

C ($C_{14}TMABr$) $10^5 \times$ mol/dm^3	-log C ($C_{14}TMABr$)	γ_{lv} mN/m	θ deg.	$\gamma_{lv} \cdot \cos\theta$ mN/m
21.77	3.662	37.08	89.0	0.647
14.51	3.838	40.49	93.2	-2.260
9.676	4.014	43.65	96.3	-4.290
6.451	4.190	46.75	100.0	-8.118
4.301	4.366	49.58	103.2	-11.322
2.867	4.543	52.40	106.0	-14.443
1.911	4.719	54.95	108.3	-17.254
1.274	4.895	57.34	110.3	-19.893

Table B 91

Adhesion Tension of $C_{14}TMABr$ - C_8SO_3Na Mixtures at Teflon/Aqueous Interface, I.S. = 0.1 N (NaBr)

$C_{C_8SO_3Na} = 1.911 \times 10^{-5}$ M

C ($C_{14}TMABr$) 10^5x mol/dm^3	-log C ($C_{14}TMABr$)	γ_{lv} mN/m	θ deg.	$\gamma_{lv} \cdot \cos\theta$ mN/m
21.77	3.662	37.99	89.9	0.066
14.51	3.838	41.33	94.0	-2.883
9.676	4.014	44.54	97.6	-5.891
6.451	4.190	47.53	100.5	-8.662
4.301	4.366	50.47	103.6	-11.868
2.867	4.543	53.13	106.5	-15.090
1.911	4.719	55.98	108.6	-17.855
1.274	4.895	58.38	110.7	-20.636

Table B 92

Adhesion Tension of $C_{14}TMABr$ - C_8SO_3Na Mixtures at Teflon/Aqueous Interface, I.S. = 0.1 N (NaBr)

$C_{C_8SO_3Na} = 1.274 \times 10^{-5}$ M

C ($C_{14}TMABr$) $10^5 \times$ mol/dm^3	-log C ($C_{14}TMABr$)	γ_{lv} mN/m	θ deg.	$\gamma_{lv} \cdot \cos\theta$ mN/m
21.77	3.662	38.41	90.7	-0.469
14.51	3.838	42.02	94.9	-3.589
9.676	4.014	45.22	97.8	-6.137
6.451	4.190	48.21	101.2	-9.364
4.301	4.366	51.18	104.4	-12.728
2.867	4.543	54.01	107.2	-15.971
1.911	4.719	56.89	109.0	-18.522
1.274	4.895	59.11	111.2	-21.376

Table B 93

Adhesion Tension of $C_{14}TMABr$ - C_8SO_3Na Mixtures at Teflon/Aqueous Interface, I.S. = 0.1 N (NaBr)

$C_{C_8SO_3Na} = 8.495 \times 10^{-6}$ M

C ($C_{14}TMABr$) $10^5 \times$ mol/dm^3	-log C ($C_{14}TMABr$)	γ_{lv} mN/m	θ deg.	$\gamma_{lv} \cdot \cos\theta$ mN/m
21.77	3.662	38.90	91.5	-1.018
14.51	3.838	42.48	95.7	-4.219
9.676	4.014	45.74	98.7	-6.919
6.451	4.190	48.93	102.0	-10.146
4.301	4.366	51.59	104.9	-13.265
2.867	4.543	54.68	107.6	-16.534
1.911	4.719	57.52	109.7	-19.322
1.274	4.895	59.80	111.9	-22.305

Table B 94

Adhesion Tension of $C_{14}TMABr$ - C_8SO_3Na Mixtures at Teflon/Aqueous Interface, I.S. = 0.1 N (NaBr)

$C_{C_8SO_3Na} = 5.663 \times 10^{-6}$ M

C ($C_{14}TMABr$) $10^5 \times$ mol/dm^3	-log C ($C_{14}TMABr$)	γ_{lv} mN/m	θ deg.	$\gamma_{lv} \cdot \cos\theta$ mN/m
21.77	3.662	39.28	92.1	-1.439
14.51	3.838	42.79	96.2	-4.621
9.676	4.014	46.03	99.3	-7.439
6.451	4.190	49.28	102.4	-10.582
4.301	4.366	52.18	105.9	-14.295
2.867	4.543	55.11	108.3	-17.304
1.911	4.719	58.10	110.3	-20.157
1.274	4.895	60.57	112.2	-22.886

Table B 95

Adhesion Tension of $C_{14}TMABr$ - C_8SO_3Na Mixtures at Teflon/Aqueous Interface, I.S. = 0.1 N (NaBr)

$C_{C_{14}TMABr} = 2.177 \times 10^{-4}$ M

C (C_8SO_3Na)	-log C (C_8SO_3Na)	γ_{lv}	θ	$\gamma_{lv} \cdot \cos\theta$
10^5x mol/dm^3		mN/m	deg.	mN/m
9.676	4.014	33.13	83.8	3.578
6.451	4.190	34.69	85.8	2.541
4.301	4.366	36.00	87.3	1.696
2.867	4.543	37.08	89.0	0.647
1.911	4.719	37.99	89.9	0.066
1.274	4.895	38.41	90.7	-0.469
0.8495	5.071	38.90	91.5	-1.018
0.5663	5.247	39.28	92.1	-1.439

Table B 96

Adhesion Tension of $C_{14}TMABr$ - C_8SO_3Na Mixtures at Teflon/Aqueous Interface, I.S. = 0.1 N (NaBr)

$C_{C_{14}TMABr} = 1.451 \times 10^{-4}$ M

C (C_8SO_3Na) 10^5x mol/dm^3	-log C (C_8SO_3Na)	γ_{lv} mN/m	θ deg.	$\gamma_{lv} \cdot \cos\theta$ mN/m
9.676	4.014	36.66	89.9	0.192
6.451	4.190	38.13	91.3	-0.865
4.301	4.366	39.46	92.2	-1.515
2.867	4.543	40.49	93.2	-2.260
1.911	4.719	41.33	94.0	-2.883
1.274	4.895	42.02	94.9	-3.589
0.8495	5.071	42.48	95.7	-4.219
0.5663	5.247	42.79	96.2	-4.621

Table B 97

Adhesion Tension of $C_{14}TMABr$ - C_8SO_3Na Mixtures at Teflon/Aqueous Interface, I.S. = 0.1 N (NaBr)

$C_{C_{14}TMABr} = 9.676 \times 10^{-5}$ M

C (C_8SO_3Na) $10^5 \times$ mol/dm^3	-log C (C_8SO_3Na)	γ_{lv} mN/m	θ deg.	$\gamma_{lv} \cdot \cos\theta$ mN/m
9.676	4.014	39.65	94.0	-2.766
6.451	4.190	41.23	95.0	-3.593
4.301	4.366	42.60	95.8	-4.305
2.867	4.543	43.65	96.3	-4.790
1.911	4.719	44.54	97.6	-5.891
1.274	4.895	45.22	97.8	-6.137
0.8495	5.071	45.74	98.7	-6.919
0.5663	5.247	46.03	99.3	-7.439

Table B 98

Adhesion Tension of $C_{14}TMABr$ - C_8SO_3Na Mixtures at Teflon/Aqueous Interface, I.S. = 0.1 N (NaBr)

$C_{C_{14}TMABr} = 6.451 \times 10^{-5}$ M

C (C_8SO_3Na) $10^5 \times$ mol/dm^3	-log C (C_8SO_3Na)	γ_{lv} mN/m	θ deg.	$\gamma_{lv} \cdot \cos\theta$ mN/m
9.676	4.014	42.84	97.5	-5.592
6.451	4.190	44.32	98.9	-6.857
4.301	4.366	45.73	99.1	-7.233
2.867	4.543	46.75	100.0	-8.118
1.911	4.719	47.53	100.5	-8.662
1.274	4.895	48.21	101.2	-9.364
0.8495	5.071	48.80	102.0	-10.146
0.5663	5.247	49.28	102.4	-10.582

Table B 99

Adhesion Tension of $C_{14}TMABr$ - C_8SO_3Na Mixtures at Teflon/Aqueous Interface, I.S. = 0.1 N (NaBr)

$C_{C_{14}TMABr} = 4.301 \times 10^{-5}$ M

C (C_8SO_3Na) 10^5x mol/dm^3	-log C (C_8SO_3Na)	γ_{lv} mN/m	θ deg.	$\gamma_{lv} \cdot \cos\theta$ mN/m
9.676	4.014	45.77	101.1	-8.812
6.451	4.190	47.15	101.7	-9.561
4.301	4.366	48.57	102.6	-10.595
2.867	4.543	49.58	103.2	-11.322
1.911	4.719	50.47	103.6	-11.868
1.274	4.895	51.18	104.4	-12.728
0.8495	5.071	51.59	104.9	-13.265
0.5663	5.247	52.18	105.9	-14.295

Table B 100

Adhesion Tension of $C_{14}TMABr$ - C_8SO_3Na Mixtures at Teflon/Aqueous Interface, I.S. = 0.1 N (NaBr)

$C_{C_{14}TMABr} = 2.867 \times 10^{-5}$ M

C (C_8SO_3Na) $10^5 \times$ mol/dm^3	-log C (C_8SO_3Na)	γ_{lv} mN/m	θ deg.	$\gamma_{lv} \cdot \cos\theta$ mN/m
9.676	4.014	48.36	104.1	-11.781
6.451	4.190	50.03	104.7	-12.696
4.301	4.366	51.29	105.6	-13.793
2.867	4.543	52.40	106.0	-14.443
1.911	4.719	53.13	106.5	-15.090
1.274	4.895	54.01	107.2	-15.971
0.8495	5.071	54.68	107.6	-16.534
0.5663	5.247	55.11	108.3	-17.304

Table B 101

Adhesion Tension of $C_{14}TMABr$ - C_8SO_3Na Mixtures at Teflon/Aqueous Interface, I.S. = 0.1 N (NaBr)

$C_{C_{14}TMABr} = 1.911 \times 10^{-5}$ M

C (C_8SO_3Na) $10^5 \times$ mol/dm^3	-log C (C_8SO_3Na)	γ_{lv} mN/m	θ deg.	$\gamma_{lv} \cdot \cos\theta$ mN/m
9.676	4.014	51.02	106.4	-14.405
6.451	4.190	52.54	106.8	-15.186
4.301	4.366	53.94	107.5	-16.220
2.867	4.543	54.95	108.3	-17.254
1.911	4.719	55.98	108.6	-17.855
1.274	4.895	56.89	109.0	-18.522
0.8495	5.071	57.52	109.7	-19.322
0.5663	5.247	58.10	110.3	-20.157

Table B 102

Adhesion Tension of $C_{14}TMABr$ - C_8SO_3Na Mixtures at Teflon/Aqueous Interface, I.S. = 0.1 N (NaBr)

$C_{C_{14}TMABr} = 1.274 \times 10^{-5}$ M

C (C_8SO_3Na)	-log C (C_8SO_3Na)	γ_{lv}	θ	$\gamma_{lv} \cdot \cos\theta$
10^5x mol/dm^3		mN/m	deg.	mN/m
9.676	4.014	53.36	108.7	-17.108
6.451	4.190	54.93	109.2	-18.065
4.301	4.366	56.28	109.7	-18.971
2.867	4.543	57.34	110.3	-19.893
1.911	4.719	58.38	110.7	-20.636
1.274	4.895	59.11	111.2	-21.376
0.8495	5.071	59.80	111.9	-22.305
0.5663	5.247	60.57	112.2	-22.886

Table B 103

Adhesion Tension of $C_{14}TMABr$ - C_8SO_3Na Mixtures at Parafilm/Aqueous Interface, I.S. = 0.1 N (NaBr)

$C_{C_8SO_3Na} = 9.676 \times 10^{-5}$ M

C ($C_{14}TMABr$) $10^5 \times$ mol/dm^3	-log C ($C_{14}TMABr$)	γ_{lv} mN/m	θ deg.	$\gamma_{lv} \cdot \cos\theta$ mN/m
21.77	3.662	33.13	70.6	11.004
14.51	3.838	36.66	78.8	7.121
9.676	4.014	39.65	84.8	3.594
6.451	4.190	42.84	89.7	0.224
4.301	4.366	45.77	93.3	-2.658
2.867	4.543	48.36	96.7	-5.642
1.911	4.719	51.02	100.3	-9.122
1.274	4.895	53.36	102.6	-11.640

Table B 104

Adhesion Tension of $C_{14}TMABr$ - C_8SO_3Na Mixtures at Parafilm/Aqueous Interface, I.S. = 0.1 N (NaBr)

$C_{C_8SO_3Na} = 6.451 \times 10^{-5}$ M

C ($C_{14}TMABr$) 10^5x mol/dm^3	-log C ($C_{14}TMABr$)	γ_{lv} mN/m	θ deg.	$\gamma_{lv} \cdot \cos\theta$ mN/m
21.77	3.662	34.69	73.8	9.678
14.51	3.838	38.13	80.8	6.096
9.676	4.014	41.23	86.5	2.517
6.451	4.190	44.32	90.9	-0.696
4.301	4.366	47.15	94.6	-3.781
2.867	4.543	50.03	98.0	-6.963
1.911	4.719	52.54	101.2	-10.205
1.274	4.895	54.93	103.2	-12.543

Table B 105

Adhesion Tension of $C_{14}TMABr$ - C_8SO_3Na Mixtures at Parafilm/Aqueous Interface, I.S. = 0.1 N (NaBr)

$C_{C_8SO_3Na} = 4.301 \times 10^{-5}$ M

C ($C_{14}TMABr$) $10^5 \times$ mol/dm^3	-log C ($C_{14}TMABr$)	γ_{lv} mN/m	θ deg.	$\gamma_{lv} \cdot \cos\theta$ mN/m
21.77	3.662	36.00	75.6	8.953
14.51	3.838	39.46	82.8	4.946
9.676	4.014	42.60	87.7	1.710
6.451	4.190	45.73	91.8	-1.436
4.301	4.366	48.57	95.6	-4.740
2.867	4.543	51.29	99.0	-8.024
1.911	4.719	53.94	101.7	-10.938
1.274	4.895	56.28	103.8	-13.425

Table B 106

Adhesion Tension of $C_{14}TMABr$ - C_8SO_3Na Mixtures at Parafilm/Aqueous Interface, I.S. = 0.1 N (NaBr)

$C_{C_8SO_3Na} = 2.867 \times 10^{-5}$ M

C ($C_{14}TMABr$)	-log C ($C_{14}TMABr$)	γ_{lv}	θ	$\gamma_{lv} \cdot \cos\theta$
10^5x mol/dm^3		mN/m	deg.	mN/m
21.77	3.662	37.08	77.9	7.773
14.51	3.838	40.49	84.0	4.232
9.676	4.014	43.65	89.2	0.609
6.451	4.190	46.75	93.2	-2.610
4.301	4.366	49.58	96.5	-5.613
2.867	4.543	52.40	99.8	-8.919
1.911	4.719	54.95	102.3	-11.706
1.274	4.895	57.34	104.4	-14.230

Table B 107

Adhesion Tension of $C_{14}TMABr$ - C_8SO_3Na Mixtures at Parafilm/Aqueous Interface, I.S. = 0.1 N (NaBr)

$C_{C_8SO_3Na} = 1.911 \times 10^{-5}$ M

C ($C_{14}TMABr$) $10^5 \times$ mol/dm^3	-log C ($C_{14}TMABr$)	γ_{lv} mN/m	θ deg.	$\gamma_{lv} \cdot \cos\theta$ mN/m
21.77	3.662	37.99	79.0	7.249
14.51	3.838	41.33	85.2	3.458
9.676	4.014	44.54	90.4	-0.311
6.451	4.190	47.53	93.8	-3.150
4.301	4.366	50.47	97.2	-6.326
2.867	4.543	53.13	100.3	-9.500
1.911	4.719	55.98	102.8	-12.402
1.274	4.895	58.38	104.8	-14.913

Table B 108

Adhesion Tension of $C_{14}TMABr$ - C_8SO_3Na Mixtures at Parafilm/Aqueous Interface, I.S. = 0.1 N (NaBr)

$C_{C_8SO_3Na} = 1.274 \times 10^{-5}$ M

C ($C_{14}TMABr$) 10^5x mol/dm^3	-log C ($C_{14}TMABr$)	γ_{lv} mN/m	θ deg.	$\gamma_{lv} \cdot \cos\theta$ mN/m
21.77	3.662	38.41	80.3	6.472
14.51	3.838	42.02	86.2	2.785
9.676	4.014	45.22	91.1	-0.868
6.451	4.190	48.21	94.5	-3.783
4.301	4.366	51.18	98.1	-7.211
2.867	4.543	54.01	101.0	-10.306
1.911	4.719	56.89	103.4	-13.184
1.274	4.895	59.11	105.6	-15.896

Table B 109

Adhesion Tension of $C_{14}TMABr$ - C_8SO_3Na Mixtures at Parafilm/Aqueous Interface, I.S. = 0.1 N (NaBr)

$C_{C_8SO_3Na} = 8.495 \times 10^{-6}$ M

C ($C_{14}TMABr$) 10^5x mol/dm^3	-log C ($C_{14}TMABr$)	γ_{lv} mN/m	θ deg.	$\gamma_{lv} \cdot \cos\theta$ mN/m
21.77	3.662	38.90	81.4	5.817
14.51	3.838	42.48	87.2	2.075
9.676	4.014	45.74	91.8	-1.437
6.451	4.190	48.93	95.3	-4.508
4.301	4.366	51.59	98.5	-7.625
2.867	4.543	54.68	101.6	-10.995
1.911	4.719	57.52	104.2	-14.061
1.274	4.895	59.80	106.1	-16.583

Table B 110

Adhesion Tension of $C_{14}TMABr$ - C_8SO_3Na Mixtures at Parafilm/Aqueous Interface, I.S. = 0.1 N (NaBr)

$C_{C_8SO_3Na} = 5.663 \times 10^{-6}$ M

C ($C_{14}TMABr$) $10^5 \times$ mol/dm^3	-log C ($C_{14}TMABr$)	γ_{lv} mN/m	θ deg.	$\gamma_{lv} \cdot \cos\theta$ mN/m
21.77	3.662	39.28	82.6	5.059
14.51	3.838	42.79	88.0	1.493
9.676	4.014	46.03	92.3	-1.847
6.451	4.190	49.28	95.8	-4.980
4.301	4.366	52.18	99.2	-8.343
2.867	4.543	55.11	102.4	-11.834
1.911	4.719	58.10	104.8	-14.841
1.274	4.895	60.57	106.5	-17.203

Table B 111

Adhesion Tension of $C_{14}TMABr$ - C_8SO_3Na Mixtures at Parafilm/Aqueous Interface, I.S. = 0.1 N (NaBr)

$C_{C_{14}TMABr} = 2.177 \times 10^{-4}$ M

C (C_8SO_3Na)	-log C (C_8SO_3Na)	γ_{lv}	θ	$\gamma_{lv} \cdot \cos\theta$
10^5x mol/dm^3		mN/m	deg.	mN/m
9.676	4.014	33.13	70.6	11.004
6.451	4.190	34.69	73.8	9.678
4.301	4.366	36.00	75.6	8.953
2.867	4.543	37.08	77.9	7.773
1.911	4.719	37.99	79.0	7.249
1.274	4.895	38.41	80.3	6.472
0.8495	5.071	38.90	81.4	5.817
0.5663	5.247	39.28	82.6	5.059

Table B 112

Adhesion Tension of $C_{14}TMABr$ - C_8SO_3Na Mixtures at Parafilm/Aqueous Interface, I.S. = 0.1 N (NaBr)

$C_{C_{14}TMABr} = 1.451 \times 10^{-4}$ M

C (C_8SO_3Na) 10^5x mol/dm^3	-log C (C_8SO_3Na)	γ_{lv} mN/m	θ deg.	$\gamma_{lv} \cdot \cos\theta$ mN/m
9.676	4.014	36.66	78.8	7.121
6.451	4.190	38.13	80.8	6.096
4.301	4.366	39.46	82.8	4.946
2.867	4.543	40.49	84.0	4.232
1.911	4.719	41.33	85.2	3.458
1.274	4.895	42.02	86.2	2.785
0.8495	5.071	42.48	87.2	2.075
0.5663	5.247	42.79	88.0	1.493

Table B 113

Adhesion Tension of $C_{14}TMABr$ - C_8SO_3Na Mixtures

at Parafilm/Aqueous Interface, I.S. = 0.1 N (NaBr)

$C_{C_{14}TMABr} = 9.676 \times 10^{-5}$ M

C (C_8SO_3Na)	-log C (C_8SO_3Na)	γ_{lv}	θ	$\gamma_{lv} \cdot \cos\theta$
10^5x mol/dm^3		mN/m	deg.	mN/m
9.676	4.014	39.65	84.8	3.594
6.451	4.190	41.23	86.5	2.517
4.301	4.366	42.60	87.7	1.710
2.867	4.543	43.65	89.2	0.609
1.911	4.719	44.54	90.4	-0.311
1.274	4.895	45.22	91.1	-0.868
0.8495	5.071	45.74	91.8	-1.437
0.5663	5.247	46.03	92.3	-1.847

Table B 114

Adhesion Tension of $C_{14}TMABr$ - C_8SO_3Na Mixtures

at Parafilm/Aqueous Interface, I.S. = 0.1 N (NaBr)

$C_{C_{14}TMABr} = 6.451 \times 10^{-5}$ M

C (C_8SO_3Na) $10^5 \times$ mol/dm^3	-log C (C_8SO_3Na)	γ_{lv} mN/m	θ deg.	$\gamma_{lv} \cdot \cos\theta$ mN/m
9.676	4.014	42.84	89.7	0.224
6.451	4.190	44.32	90.9	-0.696
4.301	4.366	45.73	91.8	-1.436
2.867	4.543	46.75	93.2	-2.610
1.911	4.719	47.53	93.8	-3.150
1.274	4.895	48.21	94.5	-3.783
0.8495	5.071	48.80	95.3	-4.508
0.5663	5.247	49.28	95.8	-4.980

Table B 115

Adhesion Tension of $C_{14}TMABr$ - C_8SO_3Na Mixtures at Parafilm/Aqueous Interface, I.S. = 0.1 N (NaBr)

$C_{C_{14}TMABr} = 4.301 \times 10^{-5}$ M

C (C_8SO_3Na) 10^5x mol/dm^3	-log C (C_8SO_3Na)	γ_{lv} mN/m	θ deg.	$\gamma_{lv} \cdot \cos\theta$ mN/m
9.676	4.014	45.77	93.3	-2.635
6.451	4.190	47.15	94.6	-3.781
4.301	4.366	48.57	95.6	-4.740
2.867	4.543	49.58	96.5	-5.613
1.911	4.719	50.47	97.2	-6.326
1.274	4.895	51.18	98.1	-7.211
0.8495	5.071	51.59	98.5	-7.625
0.5663	5.247	52.18	99.2	-8.343

Table B 116

Adhesion Tension of $C_{14}TMABr$ - C_8SO_3Na Mixtures at Parafilm/Aqueous Interface, I.S. = 0.1 N (NaBr)

$C_{C_{14}TMABr} = 2.867 \times 10^{-5}$ M

C (C_8SO_3Na)	-log C (C_8SO_3Na)	γ_{lv}	θ	$\gamma_{lv} \cdot \cos\theta$
10^5x mol/dm^3		mN/m	deg.	mN/m
9.676	4.014	48.36	96.7	-5.642
6.451	4.190	50.03	98.0	-6.963
4.301	4.366	51.29	99.0	-8.024
2.867	4.543	52.40	99.8	-8.919
1.911	4.719	53.13	100.3	-9.500
1.274	4.895	54.01	101.0	-10.306
0.8495	5.071	54.68	101.6	-10.995
0.5663	5.247	55.11	102.4	-11.834

Table B 117

Adhesion Tension of $C_{14}TMABr$ - C_8SO_3Na Mixtures at Parafilm/Aqueous Interface, I.S. = 0.1 N (NaBr)

$C_{C_{14}TMABr} = 1.911 \times 10^{-5}$ M

C (C_8SO_3Na) $10^5 \times$ mol/dm^3	-log C (C_8SO_3Na)	γ_{lv} mN/m	θ deg.	$\gamma_{lv} \cdot \cos\theta$ mN/m
9.676	4.014	51.02	100.3	-9.122
6.451	4.190	52.54	101.2	-10.205
4.301	4.366	53.94	101.7	-10.938
2.867	4.543	54.95	102.3	-11.706
1.911	4.719	55.98	102.8	-12.401
1.274	4.895	56.89	103.4	-13.184
0.8495	5.071	57.52	104.2	-14.061
0.5663	5.247	58.10	104.8	-14.481

Table B 118

Adhesion Tension of $C_{14}TMABr$ - C_8SO_3Na Mixtures at Parafilm/Aqueous Interface, I.S. = 0.1 N (NaBr)

$C_{C_{14}TMABr} = 1.274 \times 10^{-5}$ M

C (C_8SO_3Na)	-log C (C_8SO_3Na)	γ_{lv}	θ	$\gamma_{lv} \cdot \cos\theta$
10^5x mol/dm^3		mN/m	deg.	mN/m
9.676	4.014	53.36	103.1	-12.094
6.451	4.190	54.93	103.2	-12.543
4.301	4.366	56.28	103.8	-13.425
2.867	4.543	57.34	104.4	-14.230
1.911	4.719	58.38	104.8	-14.913
1.274	4.895	59.11	105.6	-15.896
0.8495	5.071	59.80	106.1	-16.583
0.5663	5.247	60.57	106.5	-17.203

Table B 119

Adhesion Tension of C_8SO_3Na

at Teflon/Aqueous Interface, I.S. = 0.1 N (NaBr)

α = 0.0000

C	-log C	γ_{lv}	θ	$\gamma_{lv} \cdot \cos\theta$
10^2x mol/dm^3		mN/m	deg.	mN/m
30.28	0.519	41.37	92.0	-1.444
20.48	0.689	41.86	91.8	-1.313
18.17	0.741	42.11	91.9	-1.396
16.32	0.787	42.27	93.8	-2.801
14.15	0.849	42.78	96.0	-4.175
12.11	0.917	44.57	96.8	-5.227
10.24	0.990	45.81	98.2	-6.532
8.166	1.088	47.84	100.7	-8.882
7.570	1.121	48.38	100.9	-9.148
7.074	1.150	48.84	101.3	-9.570
6.056	1.218	50.49	102.8	-11.186
5.120	1.291	51.74	104.0	-12.517
4.080	1.389	54.05	105.4	-14.353
3.785	1.422	54.35	105.8	-14.798
3.537	1.451	55.05	106.1	-15.266
3.028	1.519	56.35	107.8	-17.226
2.560	1.592	58.02	108.2	-18.122

2.040	1.690	59.81	109.2	-19.670
1.893	1.723	60.33	110.2	-20.883

Table B 120

Adhesion Tension of $C_{14}TMABr$ - C_8SO_3Na Mixtures at Teflon/Aqueous Interface, I.S. = 0.1 N (NaBr)

α = 0.4000

C	-log C	γ_{lv}	θ	$\gamma_{lv} \cdot \cos\theta$
10^5x mol/dm^3		mN/m	deg.	mN/m
16.13	3.792	42.84	97.5	-5.592
10.75	3.969	47.15	101.7	-9.561
7.168	4.145	51.29	105.6	-13.793
4.778	4.321	54.95	108.3	-17.254
3.185	4.497	58.38	110.7	-20.636

Table B 121

Adhesion Tension of $C_{14}TMABr$ - C_8SO_3Na Mixtures at Teflon/Aqueous Interface, I.S. = 0.1 N (NaBr)

α = 0.6923

C	-log C	γ_{lv}	θ	$\gamma_{lv} \cdot \cos\theta$
10^5x mol/dm^3		mN/m	deg.	mN/m
31.45	3.502	33.13	83.8	3.578
20.96	3.679	38.13	91.3	-0.865
13.98	3.855	42.60	95.8	-4.305
9.318	4.031	46.75	100.0	-8.118
6.212	4.207	50.47	103.6	-11.868
4.141	4.383	54.01	107.2	-15.971
2.761	4.559	57.52	109.7	-19.322
1.840	4.735	60.57	112.2	-22.886

Table B 122

Adhesion Tension of $C_{14}TMABr$ - C_8SO_3Na Mixtures

at Teflon/Aqueous Interface, I.S. = 0.1 N (NaBr)

α = 0.8836

C	-log C	γ_{lv}	θ	$\gamma_{lv} \cdot \cos\theta$
10^5x mol/dm^3		mN/m	deg.	mN/m
24.64	3.608	37.08	89.0	0.647
16.42	3.785	41.33	94.0	-2.883
10.95	3.961	45.22	97.8	-6.137
7.301	4.137	48.93	102.0	-10.146
4.867	4.313	52.18	105.9	-14.295

Table B 123

Adhesion Tension of $C_{14}TMABr$

at Teflon/Aqueous Interface, I.S. = 0.1 N (NaBr)

α = 1.0000

C	-log C	γ_{lv}	θ	$\gamma_{lv} \cdot \cos\theta$
10^4x mol/dm^3		mN/m	deg.	mN/m
7.971	3.099	34.42	80.9	5.444
5.314	3.275	34.44	81.0	5.388
3.986	3.400	34.58	81.4	5.171
2.657	3.576	38.10	86.8	2.127
2.104	3.677	40.01	90.2	-0.140
1.993	3.701	40.51	90.6	-0.424
1.329	3.877	43.89	94.6	-3.520
1.102	3.958	46.11	95.3	-4.259
0.9964	4.002	46.42	97.4	-5.979
0.6643	4.178	49.71	100.2	-8.803
0.5260	4.279	51.47	101.7	-10.437
0.2754	4.560	56.39	105.8	-15.354
0.2515	4.600	57.42	106.3	-16.116
0.1315	4.881	62.29	109.0	-20.280

Table B 124

Adhesion Tension of C_8SO_3Na

at Parafilm/Aqueous Interface, I.S. = 0.1 N (NaBr)

α = 0.0000

C	-log C	γ_{lv}	θ	$\gamma_{lv} \cdot \cos\theta$
10^2x mol/dm^3		mN/m	deg.	mN/m
30.28	0.519	41.37	87.2	2.021
20.48	0.689	41.86	86.9	2.264
18.17	0.741	42.11	87.1	2.130
16.32	0.787	42.27	87.8	1.623
14.15	0.849	42.78	89.6	0.299
12.11	0.917	44.57	91.6	-1.244
10.24	0.990	45.81	93.2	-2.557
8.166	1.088	47.84	95.3	-4.419
7.570	1.121	48.38	95.8	-4.889
7.074	1.150	48.84	96.6	-5.614
6.056	1.218	50.49	97.8	-6.812
5.120	1.291	51.74	98.4	-7.558
4.080	1.389	54.05	100.1	-9.479
3.785	1.422	54.35	100.7	-10.091
3.537	1.451	55.05	101.4	-10.881
3.028	1.519	56.35	102.5	-12.196
2.560	1.592	58.02	103.3	-13.347

2.040	1.690	59.81	104.4	-14.874
1.893	1.723	60.33	105.0	-15.615

Table B 125

Adhesion Tension of $C_{14}TMABr$ - C_8SO_3Na Mixtures at Parafilm/Aqueous Interface, I.S. = 0.1 N (NaBr)

α = 0.4000

C	-log C	γ_{lv}	θ	$\gamma_{lv} \cdot \cos\theta$
10^5x mol/dm^3		mN/m	deg.	mN/m
16.13	3.792	42.84	89.7	0.224
10.75	3.969	47.15	94.6	-3.781
7.168	4.145	51.29	99.0	-8.024
4.778	4.321	54.95	102.3	-11.706
3.185	4.497	58.38	105.8	-15.890

Table B 126

Adhesion Tension of $C_{14}TMABr$ - C_8SO_3Na Mixtures

at Parafilm/Aqueous Interface, I.S. = 0.1 N (NaBr)

α = 0.6923

C	-log C	γ_{lv}	θ	$\gamma_{lv} \cdot \cos\theta$
10^5x mol/dm^3		mN/m	deg.	mN/m
31.45	3.502	33.13	70.3	11.168
20.96	3.679	38.13	80.8	6.096
13.98	3.855	42.60	87.7	1.710
9.318	4.031	46.75	93.2	-2.610
6.212	4.207	50.47	97.2	-6.326
4.141	4.383	54.01	101.0	-10.306
2.761	4.559	57.52	104.2	-14.061
1.840	4.735	60.57	107.0	-17.709

Table B 127

Adhesion Tension of $C_{14}TMABr$ - C_8SO_3Na Mixtures

at Parafilm/Aqueous Interface, I.S. = 0.1 N (NaBr)

α = 0.8836

C	-log C	γ_{lv}	θ	$\gamma_{lv} \cdot \cos\theta$
10^5x mol/dm^3		mN/m	deg.	mN/m
24.64	3.608	37.08	77.9	7.773
16.42	3.785	41.33	85.7	3.099
10.95	3.961	45.22	91.1	-0.868
7.301	4.137	48.93	95.3	-4.508
4.867	4.313	52.18	99.2	-8.343

Table B 128

Adhesion Tension of C_{14}TMABr

at Parafilm/Aqueous Interface, I.S. = 0.1 N (NaBr)

α = 1.0000

C	-log C	γ_{lv}	θ	$\gamma_{lv} \cdot \cos\theta$
10^4x mol/dm^3		mN/m	deg.	mN/m
7.971	3.099	34.42	69.9	11.829
5.314	3.275	34.44	70.1	11.723
3.986	3.400	34.58	69.7	11.997
2.657	3.576	38.10	78.4	7.661
2.104	3.677	40.01	81.9	5.637
1.993	3.701	40.51	82.3	5.428
1.329	3.877	43.89	88.2	1.319
1.102	3.958	46.11	90.3	-0.241
0.9964	4.002	46.42	91.5	-1.215
0.6643	4.178	49.71	94.9	-4.246
0.5260	4.279	51.47	97.3	-6.540
0.2754	4.560	56.39	102.0	-11.917
0.2515	4.600	57.42	102.6	-12.526
0.1315	4.881	62.29	106.8	-18.004

Table B 129

Adhesion Tension of $C_{12}SO_3Na$

in Water at Teflon/Aqueous Interface,

α = 0.0000

C	-log C	γ_{lv}	θ	$\gamma_{lv} \cdot \cos\theta$
10^3x mol/dm^3		mN/m	deg.	mN/m
20.46	1.689	38.80	82.2	5.265
10.80	1.967	39.46	82.7	5.014
8.536	2.069	42.90	87.0	2.245
7.068	2.151	45.68	89.4	0.478
4.948	2.306	50.90	95.5	-4.879
2.827	2.549	58.08	100.5	-10.582
2.120	2.674	61.30	102.9	-13.685

Table B 130

Adhesion Tension of $C_{12}BMG$ - $C_{12}SO_3Na$ Mixtures in Water at Teflon/Aqueous Interface,

α = 0.0134

C	-log C	γ_{lv}	θ	$\gamma_{lv} \cdot \cos\theta$
10^3x mol/dm^3		mN/m	deg.	mN/m
6.442	2.191	30.62	73.6	8.645
4.508	2.346	29.20	72.4	8.829
3.221	2.492	28.04	80.5	4.628
2.576	2.589	31.66	83.6	3.531
1.288	2.890	41.38	94.9	-3.535
0.9204	3.036	45.22	99.1	-7.409

Table B 131

Adhesion Tension of $C_{12}BMG$ - $C_{12}SO_3Na$ Mixtures in Water at Teflon/Aqueous Interface,

α = 0.0276

C	-log C	γ_{lv}	θ	$\gamma_{lv} \cdot \cos\theta$
10^3x mol/dm^3		mN/m	deg.	mN/m
5.875	2.231	30.66	75.0	7.935
3.524	2.453	29.06	72.5	8.739
2.244	2.649	29.28	78.8	5.687
1.762	2.754	32.50	84.7	3.002
1.175	2.930	42.49	91.0	-0.742
0.5875	3.231	50.12	97.9	-6.887

Table B 132

Adhesion Tension of $C_{12}BMG$ - $C_{12}SO_3Na$ Mixtures in Water at Teflon/Aqueous Interface,

α = 0.0884

C	-log C	γ_{lv}	θ	$\gamma_{lv} \cdot \cos\theta$
10^3x mol/dm^3		mN/m	deg.	mN/m
3.427	2.465	30.75	74.1	8.424
2.285	2.641	30.35	72.6	9.075
1.714	2.766	30.08	71.8	9.370
1.371	2.863	29.90	74.1	8.191
1.097	2.960	30.94	78.8	6.010
0.6854	3.164	36.20	85.2	3.029
0.4387	3.358	41.28	89.7	0.215
0.2194	3.659	48.28	96.7	-5.633

Table B 133

Adhesion Tension of $C_{12}BMG$ - $C_{12}SO_3Na$ Mixtures in Water at Teflon/Aqueous Interface,

α = 0.3274

C	-log C	γ_{lv}	θ	$\gamma_{lv} \cdot \cos\theta$
10^3x mol/dm^3		mN/m	deg.	mN/m
3.341	2.476	32.95	73.6	9.303
2.005	2.698	32.20	73.6	9.091
1.069	2.971	31.88	72.2	9.746
0.6682	3.175	30.72	73.7	8.622
0.4276	3.369	34.52	79.6	6.232
0.2138	3.670	41.38	88.1	1.374
0.1710	3.767	43.35	90.9	-0.681
0.08552	4.068	49.00	96.8	-5.802

Table B 134

Adhesion Tension of $C_{12}BMG$ - $C_{12}SO_3Na$ Mixtures in Water at Teflon/Aqueous Interface,

α = 0.6864

C	-log C	γ_{lv}	θ	$\gamma_{lv} \cdot \cos\theta$
10^4x mol/dm^3		mN/m	deg.	mN/m
18.44	2.734	33.04	73.3	9.494
12.91	2.889	32.62	73.1	9.483
9.220	3.035	32.20	72.7	9.575
5.163	3.287	31.35	72.9	9.218
3.614	3.442	33.12	74.5	8.851
2.582	3.588	36.53	80.4	6.092
1.807	3.743	39.92	83.4	4.588
1.033	3.986	44.70	89.7	0.234
0.6609	4.180	48.32	92.9	-3.885

Table B 135

Adhesion Tension of $C_{12}BMG$ - $C_{12}SO_3Na$ Mixtures in Water at Teflon/Aqueous Interface,

α = 0.9448

C 10^4x mol/dm^3	-log C	γ_{lv} mN/m	θ deg.	$\gamma_{lv} \cdot \cos\theta$ mN/m
15.38	2.813	33.20	68.9	11.952
10.77	2.968	33.20	69.2	11.790
4.306	3.366	33.20	69.3	11.735
3.017	3.520	35.58	74.8	9.329
2.307	3.637	37.68	77.8	7.963
1.722	3.764	40.00	81.6	5.843
0.6870	4.162	46.73	91.1	-0.897
0.3445	4.463	51.28	96.4	-5.716

Table B 136

Adhesion Tension of $C_{12}BMG$

in Water at Teflon/Aqueous Interface,

α = 1.000

C	-log C	γ_{lv}	θ	$\gamma_{lv} \cdot \cos\theta$
10^4x mol/dm^3		mN/m	deg.	mN/m
8.910	3.050	32.80	70.0	11.218
8.479	3.072	32.80	70.1	11.164
4.455	3.351	34.15	69.6	11.904
3.564	3.448	35.68	74.0	9.833
1.859	3.731	40.32	81.6	5.891
1.069	3.971	44.28	88.2	1.391
0.7128	4.147	47.18	91.9	-1.564
0.3564	4.448	52.40	96.9	-6.295

Table B 137

Adhesion Tension of $C_{12}SO_3Na$

in Water at Parafilm/Aqueous Interface,

α = 0.0000

C	-log C	γ_{lv}	θ	$\gamma_{lv} \cdot \cos\theta$
10^3x mol/dm^3		mN/m	deg.	mN/m
20.46	1.689	38.80	67.9	14.598
10.80	1.967	39.46	69.7	13.690
8.536	2.069	42.90	76.8	9.796
7.068	2.151	45.68	80.5	7.539
6.844	2.165	46.15	81.2	7.060
3.915	2.407	54.04	90.6	-0.566
2.349	2.629	60.20	97.5	-7.858
2.120	2.674	61.30	99.4	-10.012

Table B 138

Adhesion Tension of $C_{12}BMG$ - $C_{12}SO_3Na$ Mixtures in Water at Teflon/Aqueous Interface,

α = 0.0134

C	-log C	γ_{lv}	θ	$\gamma_{lv} \cdot \cos\theta$
10^3x mol/dm^3	-	mN/m	deg.	mN/m
6.532	2.185	30.70	51.8	18.985
4.180	2.379	29.62	51.6	18.398
3.344	2.476	28.40	56.8	15.551
2.675	2.573	31.10	63.7	13.780
1.672	2.777	38.00	75.4	9.579
1.254	2.902	41.74	82.6	5.376
0.6684	3.175	48.70	94.0	-3.397

Table B 139

Adhesion Tension of $C_{12}BMG$ - $C_{12}SO_3Na$ Mixtures in Water at Parafilm/Aqueous Interface,

α = 0.0276

C	-log C	γ_{lv}	θ	$\gamma_{lv} \cdot \cos\theta$
10^3x mol/dm^3		mN/m	deg.	mN/m
7.557	2.122	31.25	52.8	18.894
3.023	2.520	28.60	51.7	17.726
2.418	2.617	28.30	55.8	15.907
1.511	2.821	34.50	70.6	11.460
1.209	2.918	37.36	75.6	9.291
0.9672	3.014	40.40	79.3	7.501
0.4836	3.316	47.80	92.1	-1.752
0.1934	3.714	56.75	101.6	-11.411

Table B 140

Adhesion Tension of $C_{12}BMG$ - $C_{12}SO_3Na$ Mixtures in Water at Parafilm/Aqueous Interface,

α = 0.0884

C	-log C	γ_{lv}	θ	$\gamma_{lv} \cdot \cos\theta$
10^3x mol/dm^3		mN/m	deg.	mN/m
3.427	2.465	30.75	54.4	18.900
2.285	2.641	30.35	53.0	18.259
1.714	2.766	30.08	49.0	19.734
1.371	2.863	29.90	50.3	19.099
1.097	2.960	30.94	56.5	17.082
0.6854	3.164	36.20	69.3	12.796
0.4387	3.358	41.28	79.4	7.594
0.2194	3.659	48.28	90.4	-0.337
0.1097	3.960	54.54	97.0	-6.647

Table B 141

Adhesion Tension of $C_{12}BMG$ - $C_{12}SO_3Na$ Mixtures in Water at Parafilm/Aqueous Interface,

α = 0.3274

C	-log C	γ_{lv}	θ	$\gamma_{lv} \cdot \cos\theta$
10^3x mol/dm^3		mN/m	deg.	mN/m
3.341	2.476	32.95	58.9	17.020
2.005	2.698	32.20	58.2	16.968
1.609	2.793	31.93	58.7	16.588
0.6682	3.175	30.72	56.5	16.961
0.4276	3.369	34.56	63.6	15.367
0.2138	3.670	41.36	78.4	8.317
0.1710	3.767	43.35	82.3	5.808
0.08552	4.068	49.02	89.9	0.086

Table B 142

Adhesion Tension of $C_{12}BMG$ - $C_{12}SO_3Na$ Mixtures in Water at Parafilm/Aqueous Interface,

α = 0.6864

C	-log C	γ_{lv}	θ	$\gamma_{lv} \cdot \cos\theta$
10^4x mol/dm^3		mN/m	deg.	mN/m
18.44	2.734	33.03	59.1	16.962
12.91	2.889	32.60	58.5	17.033
9.220	3.035	32.20	58.2	16.968
5.163	3.287	31.35	58.1	16.567
3.614	3.442	33.12	58.3	17.404
2.582	3.588	36.53	66.8	14.395
1.807	3.743	39.95	74.4	10.743
1.033	3.986	44.70	84.1	4.595
0.8261	4.083	46.54	86.4	2.922
0.6609	4.180	48.32	88.5	1.265
0.3304	4.481	53.31	93.2	-2.976

Table B 143

Adhesion Tension of $C_{12}BMG$ - $C_{12}SO_3Na$ Mixtures in Water at Parafilm/Aqueous Interface,

α = 0.9448

C	-log C	γ_{lv}	θ	$\gamma_{lv} \cdot \cos\theta$
10^4x mol/dm^3		mN/m	deg.	mN/m
7.690	3.114	33.20	57.0	18.136
4.306	3.366	33.20	56.7	18.228
3.017	3.520	35.58	59.3	18.165
2.307	3.637	37.68	67.2	14.602
1.722	3.764	40.00	71.2	12.891
0.8612	4.065	45.18	82.0	6.288
0.6890	4.162	46.76	84.5	4.482
0.3445	4.463	51.36	91.1	-0.986

Table B 144

Adhesion Tension of $C_{12}BMG$

in Water at Parafilm/Aqueous Interface,

α = 1.000

C	-log C	γ_{lv}	θ	$\gamma_{lv} \cdot \cos\theta$
10^4x mol/dm^3		mN/m	deg.	mN/m
8.190	3.087	32.80	52.6	19.922
4.704	3.328	33.20	52.0	20.440
4.455	3.351	34.15	53.0	20.552
3.564	3.448	35.68	57.8	19.013
1.859	3.731	40.50	71.7	12.717
1.069	3.971	44.28	76.6	10.262
0.6479	4.188	47.84	85.8	3.504
0.2113	4.675	55.30	94.3	-4.146

Table B 145

Adhesion Tension of $C_{12}SO_3Na$

in Water at Polyethylene/Aqueous Interface,

$\alpha' = 0.0000$

C	-log C	γ_{lv}	θ	$\gamma_{lv} \cdot \cos\theta$
10^3x mol/dm^3		mN/m	deg.	mN/m
20.46	1.689	38.80	54.5	22.531
10.80	1.967	39.46	54.8	22.746
8.536	2.069	42.90	61.5	20.470
7.068	2.151	45.68	68.1	17.038
4.948	2.306	50.83	73.5	14.436
3.915	2.407	54.04	78.3	10.959
2.827	2.549	58.06	80.7	9.383
2.120	2.674	61.30	84.8	5.556

Table B 146

Adhesion Tension of $C_{12}BMG$ - $C_{12}SO_3Na$ Mixtures in Water at Polyethylene/Aqueous Interface,

α = 0.0884

C	-log C	γ_{lv}	θ	$\gamma_{lv} \cdot \cos\theta$
10^3x mol/dm^3		mN/m	deg.	mN/m
1.714	2.766	30.08	43.3	21.891
1.371	2.863	29.90	42.3	22.115
1.097	2.960	30.94	49.5	20.094
0.6854	3.164	36.20	60.9	17.605
0.4387	3.358	41.28	69.6	14.389
0.2194	3.659	48.28	77.3	10.614
0.1316	3.881	52.98	82.7	6.732

Table B 147

Adhesion Tension of $C_{12}BMG$ - $C_{12}SO_3Na$ Mixtures in Water at Polyethylene/Aqueous Interface,

α = 0.3274

C	-log C	γ_{lv}	θ	$\gamma_{lv} \cdot \cos\theta$
10^3x mol/dm^3		mN/m	deg.	mN/m
3.341	2.476	32.95	44.0	23.702
2.005	2.698	32.20	43.4	23.396
1.069	2.971	31.38	43.0	22.950
0.6682	3.175	30.72	43.2	22.394
0.4276	3.369	34.56	53.7	20.460
0.2138	3.670	41.36	66.8	16.293
0.1710	3.767	43.35	69.6	15.111
0.08552	4.068	49.02	77.9	10.276

Table B 148

Adhesion Tension of $C_{12}BMG$ - $C_{12}SO_3Na$ Mixtures in Water at Polyethylene/Aqueous Interface,

α = 0.6864

C	-log C	γ_{lv}	θ	$\gamma_{lv} \cdot \cos\theta$
10^4x mol/dm^3		mN/m	deg.	mN/m
12.91	2.889	32.60	40.9	24.641
9.220	3.035	32.20	40.6	24.449
5.163	3.287	31.35	39.1	24.469
2.582	3.588	36.53	54.8	21.057
1.807	3.743	39.95	61.6	19.001
1.033	3.986	44.70	69.8	15.435
0.8261	4.083	46.54	71.6	14.690
0.6609	4.180	48.32	75.7	11.932
0.3304	4.481	53.31	80.0	9.257

Table B 149

Adhesion Tension of $C_{12}BMG$ - $C_{12}SO_3Na$ Mixtures in Water at Polyethylene/Aqueous Interface,

α = 0.9448

C	-log C	γ_{lv}	θ	$\gamma_{lv} \cdot \cos\theta$
10^4x mol/dm^3		mN/m	deg.	mN/m
15.38	2.813	33.20	41.4	24.904
10.77	2.968	33.20	41.9	24.711
3.017	3.520	35.58	49.0	23.343
2.307	3.637	37.68	55.1	21.558
1.722	3.764	40.00	60.5	19.697
0.8612	4.065	45.18	70.2	15.304
0.6890	4.162	46.76	72.4	14.139
0.3445	4.463	51.36	77.8	10.854

Table B 150

Adhesion tension of $C_{12}BMG$

in Water at Polyethylene/Aqueous Interface,

$\alpha = 1.000$

C	-log C	γ_{lv}	θ	$\gamma_{lv} \cdot \cos\theta$
10^4x mol/dm^3		mN/m	deg.	mN/m
8.479	3.072	32.80	34.9	26.901
5.087	3.294	32.80	35.5	26.703
4.455	3.351	34.15	37.2	27.201
3.564	3.448	35.68	44.9	25.273
1.859	3.731	40.50	59.1	20.798
1.069	3.971	44.28	67.5	16.945
0.7128	4.147	47.18	71.5	14.970
0.3564	4.448	51.90	78.1	10.702

Table B 151

Adhesion Tension of $C_{12}BMG$ - $C_{12}SO_3Na$ Mixtires

at Teflon/Aqueous Interface, I.S. = 0.1 N (NaBr)

α = 0.02035

C	-log C	γ_{lv}	θ	$\gamma_{lv} \cdot \cos\theta$
10^4x mol/dm^3		mN/m	deg.	mN/m
10.22	2.991	29.96	73.2	8.659
5.110	3.292	35.23	85.0	3.070
2.555	3.593	42.52	94.7	-3.484
1.277	3.894	49.18	102.0	-10.225
0.6387	4.195	55.35	105.3	-14.605
0.3193	4.496	60.50	106.0	-16.676

Table B 152

Adhesion Tension of $C_{12}BMG$ - $C_{12}SO_3Na$ Mixtires

at Teflon/Aqueous Interface, I.S. = 0.1 N (NaBr)

α = 0.08488

C	-log C	γ_{lv}	θ	$\gamma_{lv} \cdot \cos\theta$
10^4x mol/dm^3		mN/m	deg.	mN/m
9.956	3.002	29.21	63.4	13.079
4.978	3.303	30.87	73.5	8.768
2.489	3.604	37.83	87.0	1.980
1.245	3.905	44.48	96.2	-4.804
0.6222	4.206	50.94	100.6	-9.370
0.3111	4.507	56.73	104.3	-14.012

Table B 153

Adhesion Tension of $C_{12}BMG$ - $C_{12}SO_3Na$ Mixtires

at Teflon/Aqueous Interface, I.S. = 0.1 N (NaBr)

α = 0.3550

C	-log C	γ_{lv}	θ	$\gamma_{lv} \cdot \cos\theta$
10^4x mol/dm^3		mN/m	deg.	mN/m
7.777	3.109	29.22	66.1	11.838
3.794	3.421	29.16	65.6	12.046
1.897	3.722	34.31	80.6	5.604
0.9484	4.023	41.17	91.3	-0.934
0.4742	4.324	47.26	97.5	-6.169
0.2371	4.625	52.84	102.3	-11.256

Table B 154

Adhesion Tension of $C_{12}BMG$ - $C_{12}SO_3Na$ Mixtires

at Teflon/Aqueous Interface, I.S. = 0.1 N (NaBr)

α = 0.6926

C	-log C	γ_{lv}	θ	$\gamma_{lv} \cdot \cos\theta$
10^5x mol/dm^3		mN/m	deg.	mN/m
32.64	3.486	29.96	68.2	11.126
16.32	3.787	34.51	80.8	5.517
8.160	4.088	40.82	90.6	-0.427
4.080	4.389	46.77	96.4	-5.213
2.040	4.690	52.48	100.4	-9.474
1.020	4.991	57.36	104.4	-14.265

Table B 155

Adhesion Tension of $C_{12}BMG$ - $C_{12}SO_3Na$ Mixtires

at Teflon/Aqueous Interface, I.S. = 0.1 N (NaBr)

α = 0.9186

C	-log C	γ_{lv}	θ	$\gamma_{lv} \cdot \cos\theta$
10^5x mol/dm^3		mN/m	deg.	mN/m
61.63	3.210	30.73	69.6	10.712
30.81	3.511	30.58	70.0	10.459
15.41	3.812	36.56	82.9	4.519
7.704	4.113	42.50	91.7	-1.261
3.852	4.414	48.00	97.1	-5.933
1.926	4.715	52.93	101.7	-10.734

Table B 156

Adhesion Tension of $C_{12}BMG$

at Teflon/Aqueous Interface, I.S. = 0.1 N (NaBr)

α = 1.000

C	-log C	γ_{lv}	θ	$\gamma_{lv} \cdot \cos\theta$
10^5x mol/dm^3		mN/m	deg.	mN/m
60.28	3.220	32.40	73.1	9.419
30.14	3.521	34.60	76.6	8.018
18.04	3.744	38.32	85.7	2.873
9.645	4.016	42.84	91.5	-1.121
4.823	4.317	47.70	96.4	-5.317
2.411	4.618	52.46	100.8	-9.830
1.206	4.919	57.04	104.1	-13.896

Table B 157

Adhesion Tension of $C_{12}BMG$ - $C_{12}SO_3Na$ Mixtires

at Parafilm/Aqueous Interface, I.S. = 0.1 N (NaBr)

α = 0.02035

C	-log C	γ_{lv}	θ	$\gamma_{lv} \cdot \cos\theta$
10^4x mol/dm^3		mN/m	deg.	mN/m
10.22	2.991	29.96	64.4	12.945
5.110	3.292	35.23	78.0	7.325
2.555	3.593	42.52	89.9	0.074
1.277	3.894	49.18	97.1	-6.079
0.6387	4.195	55.35	102.7	-12.168
0.3193	4.496	60.50	105.5	-16.168

Table B 158

Adhesion Tension of $C_{12}BMG$ - $C_{12}SO_3Na$ Mixtires

at Parafilm/Aqueous Interface, I.S. = 0.1 N (NaBr)

α = 0.08488

C	-log C	γ_{lv}	θ	$\gamma_{lv} \cdot \cos\theta$
10^4x mol/dm^3		mN/m	deg.	mN/m
9.956	3.002	29.21	53.8	17.252
4.978	3.303	30.87	62.6	14.206
2.489	3.604	37.83	79.1	7.153
1.245	3.905	44.48	90.0	0.000
0.6222	4.206	50.94	97.2	-6.384
0.3111	4.507	56.73	103.2	-12.954

Table B 159

Adhesion Tension of $C_{12}BMG$ - $C_{12}SO_3Na$ Mixtires

at Parafilm/Aqueous Interface, I.S. = 0.1 N (NaBr)

α = 0.3550

C	-log C	γ_{lv}	θ	$\gamma_{lv} \cdot \cos\theta$
10^4x mol/dm^3		mN/m	deg.	mN/m
7.777	3.109	29.22	53.2	17.503
3.794	3.421	29.16	52.8	17.630
1.897	3.722	34.31	72.2	10.488
0.9484	4.023	41.17	84.7	3.803
0.4742	4.324	47.26	92.3	-1.897
0.2371	4.625	52.84	97.4	-6.804

Table B 160

Adhesion Tension of $C_{12}BMG$ - $C_{12}SO_3Na$ Mixtires

at Parafilm/aqueous Interface, I.S. = 0.1 N (NaBr)

α = 0.6926

C	-log C	γ_{lv}	θ	$\gamma_{lv} \cdot \cos\theta$
10^5x mol/dm^3		mN/m	deg.	mN/m
32.64	3.486	29.96	53.1	17.989
16.32	3.787	34.51	70.3	11.633
8.160	4.088	40.82	84.0	4.267
4.080	4.389	46.77	91.5	-1.224
2.040	4.690	52.48	96.7	-6.123
1.020	4.991	57.36	100.4	-10.355

Table B 161

Adhesion Tension of $C_{12}BMG$ - $C_{12}SO_3Na$ Mixtires

at Parafilm/Aqueous Interface, I.S. = 0.1 N (NaBr)

α = 0.9186

C	-log C	γ_{lv}	θ	$\gamma_{lv} \cdot \cos\theta$
10^5x mol/dm^3		mN/m	deg.	mN/m
61.63	3.210	30.73	54.8	17.714
30.81	3.511	30.58	54.9	17.584
15.41	3.812	36.56	74.5	9.770
7.704	4.113	42.50	85.6	3.261
3.852	4.414	48.00	93.0	-2.512
1.926	4.715	52.93	97.4	-6.817

Table B 162

Adhesion Tension of $C_{12}BMG$

at Parafilm/Aqueous Interface, I.S. = 0.1 N (NaBr)

α = 1.000

C	-log C	γ_{lv}	θ	$\gamma_{lv} \cdot \cos\theta$
10^5x mol/dm^3		mN/m	deg.	mN/m
60.28	3.220	32.40	61.9	15.261
30.14	3.521	34.60	69.4	12.174
18.04	3.744	38.32	78.2	7.836
9.645	4.016	42.84	85.7	3.212
4.823	4.317	47.70	92.4	-1.997
2.411	4.618	52.46	97.0	-6.393
1.206	4.919	57.04	100.2	-10.101

Table 163

Adhesion Tension of $C_{12}SO_3Na$

at Polyethylene/Aqueous Interface, I.S. = 0.1 N (NaBr)

α = 0.0000

C	-log C	γ_{lv}	θ	$\gamma_{lv} \cdot \cos\theta$
10^4x mol/dm^3		mN/m	deg.	mN/m
20.07	2.697	37.02	54.1	21.708
13.86	2.858	40.86	57.7	21.834
10.03	2.999	44.14	64.5	19.003
6.929	3.159	47.70	70.4	16.001
5.017	3.300	50.72	74.4	13.640
3.464	3.460	53.92	78.1	11.119
2.508	3.601	56.72	81.5	8.384
1.732	3.761	59.30	84.1	6.096
1.254	3.902	61.50	86.2	4.076

Table B 164

Adhesion Tension of $C_{12}BMG$ - $C_{12}SO_3Na$ Mixtires

at Polyethylene/Aqueous Interface, I.S. = 0.1 N (NaBr)

α = 0.02035

C	-log C	γ_{lv}	θ	$\gamma_{lv} \cdot \cos\theta$
10^4x mol/dm^3		mN/m	deg.	mN/m
10.22	2.991	29.96	37.5	23.769
5.110	3.292	35.23	54.7	20.358
2.555	3.593	42.52	70.3	14.333
1.277	3.894	49.18	80.2	8.371
0.6387	4.195	55.35	86.5	3.379
0.3193	4.496	60.50	90.2	-0.211

Table B 165

Adhesion Tension of $C_{12}BMG$ - $C_{12}SO_3Na$ Mixtires

at Polyethylene/Aqueous Interface, I.S. = 0.1 N (NaBr)

α = 0.08488

C	-log C	γ_{lv}	θ	$\gamma_{lv} \cdot \cos\theta$
10^4x mol/dm^3		mN/m	deg.	mN/m
9.956	3.002	29.21	35.5	23.780
4.978	3.303	30.87	40.1	23.613
2.489	3.604	37.83	61.2	18.225
1.245	3.905	44.48	73.2	12.856
0.6222	4.206	50.94	79.9	8.933
0.3111	4.507	56.73	86.1	3.859

Table B 166

Adhesion Tension of $C_{12}BMG$ - $C_{12}SO_3Na$ Mixtires

at Polyethylene/Aqueous Interface, I.S. = 0.1 N (NaBr)

α = 0.3550

C	-log C	γ_{lv}	θ	$\gamma_{lv} \cdot \cos\theta$
10^4x mol/dm^3		mN/m	deg.	mN/m
7.777	3.109	29.22	26.0	26.263
3.794	3.421	29.16	26.5	26.096
1.897	3.722	34.31	52.0	21.123
0.9484	4.023	41.17	67.4	15.821
0.4742	4.324	47.26	76.4	11.113
0.2371	4.625	52.84	82.1	7.263

Table B 167

Adhesion Tension of $C_{12}BMG$ - $C_{12}SO_3Na$ Mixtires

at Polyethylene/aqueous Interface, I.S. = 0.1 N (NaBr)

α = 0.6926

C	-log C	γ_{lv}	θ	$\gamma_{lv} \cdot \cos\theta$
10^5x mol/dm^3		mN/m	deg.	mN/m
32.64	3.486	29.96	27.1	26.671
16.32	3.787	34.51	50.0	22.183
8.160	4.088	40.82	65.4	16.993
4.080	4.389	46.77	73.9	12.970
2.040	4.690	52.48	80.2	8.933
1.020	4.991	57.36	84.6	5.398

Table B 168

Adhesion Tension of $C_{12}BMG$ - $C_{12}SO_3Na$ Mixtires

at Polyethylene/Aqueous Interface, I.S. = 0.1 N (NaBr)

α = 0.9186

C	-log C	γ_{lv}	θ	$\gamma_{lv} \cdot \cos\theta$
10^5x mol/dm^3		mN/m	deg.	mN/m
61.63	3.210	30.73	26.7	27.453
30.81	3.511	30.58	26.0	27.485
15.41	3.812	36.56	54.4	21.282
7.704	4.113	42.50	67.9	15.990
3.852	4.414	48.00	75.5	12.018
1.926	4.715	52.93	81.4	7.915

Table B 169

Adhesion Tension of $C_{12}BMG$

at Polyethylene/Aqueous Interface, I.S. = 0.1 N (NaBr)

α = 1.000

C	-log C	γ_{lv}	θ	$\gamma_{lv} \cdot \cos\theta$
10^5x mol/dm^3		mN/m	deg.	mN/m
60.28	3.220	32.40	30.1	28.031
30.14	3.521	34.60	41.8	25.793
18.04	3.744	38.32	55.5	21.705
9.645	4.016	42.84	66.8	16.876
4.823	4.317	47.70	74.8	12.506
2.411	4.618	52.46	81.2	8.026
1.206	4.919	57.04	84.5	5.467

Table B 170

Adhesion Tension of $C_{12}TMABr$ - $C_{10}SO_3Na$ Mixtures at Teflon/Aqueous Interface, I.S. = 0.1 N (NaBr)

α = 0.500

C	-log C	γ_{lv}	θ	$\gamma_{lv} \cdot \cos\theta$
10^5x mol/dm^3		mN/m	deg.	mN/m
26.11	3.583	36.50	91.4	-0.892
17.03	3.769	42.01	97.1	-5.192
13.06	3.884	45.58	100.4	-8.228
8.514	4.070	50.67	104.2	-12.430
6.528	4.185	54.24	105.8	-14.768
4.257	4.371	59.30	108.4	-18.718
3.264	4.486	62.32	109.4	-20.700
2.129	4.672	66.16	110.8	-23.490

Table B 171

Adhesion Tension of C_{12}TMABr

at Teflon/Aqueous Interface, I.S. = 0.1 N (NaBr)

α = 1.00

C	-log C	γ_{lv}	θ	$\gamma_{lv} \cdot \cos\theta$
10^3x mol/dm^3		mN/m	deg.	mN/m
9.451	2.025	36.58	80.4	6.100
4.726	2.326	36.57	80.5	6.036
2.859	2.544	40.01	85.6	3.070
1.418	2.848	45.84	92.1	-1.680
0.8270	3.082	50.20	96.6	-5.770
0.4726	3.326	54.71	100.3	-9.782

Table B 172

Adhesion Tension of $C_{12}TMABr$ - $C_{10}SO_3Na$ Mixtures at Parafilm/Aqueous Interface, I.S. = 0.1 N (NaBr)

α = 0.500

C 10^5x mol/dm^3	-log C	γ_{lv} mN/m	θ deg.	$\gamma_{lv} \cdot \cos\theta$ mN/m
26.11	3.583	36.50	81.8	5.206
17.03	3.769	42.01	89.9	0.073
13.06	3.884	45.58	93.8	-3.021
8.514	4.070	50.67	98.9	-7.839
6.528	4.185	54.24	101.2	-10.535
4.257	4.371	59.30	104.7	-15.048
3.264	4.486	62.32	106.6	-17.804
2.129	4.672	66.16	109.2	-21.758

Table B 173

Adhesion Tension of $C_{12}TMABr$

at Parafilm/Aqueous Interface, I.S. = 0.1 N (NaBr)

α = 1.00

C	-log C	γ_{lv}	θ	$\gamma_{lv} \cdot \cos\theta$
10^3x mol/dm^3		mN/m	deg.	mN/m
9.451	2.025	36.58	72.9	10.756
4.726	2.326	36.57	73.0	10.692
2.859	2.544	40.01	79.8	7.085
1.418	2.848	45.84	87.8	1.760
0.8270	3.082	50.20	92.9	-2.540
0.4726	3.326	54.71	97.0	-6.667

Table B 174

Adhesion Tension of $C_{10}SO_3Na$ in Water

at Teflon/Aqueous Interface,

α = 0.00

C	-log C	γ_{lv}	θ	$\gamma_{lv} \cdot \cos\theta$
10^2x mol/dm^3		mN/m	deg.	mN/m
3.902	1.409	42.70	87.7	1.714
2.939	1.532	47.64	91.3	-1.081
1.987	1.702	53.80	96.1	-5.717
1.781	1.749	55.32	97.3	-7.089
1.264	1.898	59.52	100.2	-10.540
0.9993	2.000	62.00	102.1	-12.996

Table B 175

Adhesion Tension of $C_{12}TMABr$ - $C_{10}SO_3Na$ Mixtures in Water at Teflon/Aqueous Interface,

α = 0.500

C	-log C	γ_{lv}	θ	$\gamma_{lv} \cdot \cos\theta$
10^5x mol/dm^3		mN/m	deg.	mN/m
8.409	4.075	40.00	99.9	-6.877
7.834	4.106	41.20	102.9	-9.198
6.817	4.166	43.50	105.5	-11.625
5.886	4.230	45.92	105.9	-12.580
5.459	4.264	47.17	106.9	-13.712
3.784	4.422	52.70	108.2	-16.460
2.523	4.598	58.30	108.8	-18.788
1.682	4.774	63.00	109.5	-21.030

Table B 176

Adhesion Tension of $C_{12}TMABr$

in Water at Teflon/Aqueous Interface,

α = 1.00

C	-log C	γ_{lv}	θ	$\gamma_{lv} \cdot \cos\theta$
10^3x mol/dm^3		mN/m	deg.	mN/m
96.04	1.018	39.00	81.5	5.765
17.72	1.752	39.00	81.3	5.899
15.85	1.800	39.00	81.4	5.832
14.08	1.851	39.52	81.2	6.046
11.16	1.952	43.62	87.0	2.283
7.973	2.098	48.94	91.1	-0.940
5.493	2.260	54.00	96.0	-5.645
3.030	2.519	60.35	100.3	-10.791
1.065	2.973	67.76	107.9	-20.826

Table B 177

Adhesion Tension of $C_{10}SO_3Na$

in Water at Polyethylene/Aqueous Interface,

$\alpha = 0.00$

C	-log C	γ_{lv}	θ	$\gamma_{lv} \cdot \cos\theta$
10^2x mol/dm^3		mN/m	deg.	mN/m
3.902	1.409	42.70	61.4	20.440
2.939	1.532	47.64	67.6	18.154
1.987	1.702	53.80	74.0	14.829
1.781	1.749	55.32	76.2	13.196
1.264	1.898	59.52	79.9	10.438
0.9993	2.000	62.00	81.7	8.950
0.7810	2.107	64.22	84.4	6.267

Table B 178

Adhesion Tension of $C_{12}TMABr$ -- $C_{10}SO_3Na$ Mixtures in Water at Polyethylene/Aqueous Interface,

α = 0.500

C	-log C	γ_{lv}	θ	$\gamma_{lv} \cdot \cos\theta$
10^5x mol/dm^3		mN/m	deg.	mN/m
8.409	4.075	40.00	76.1	9.609
6.817	4.166	43.50	79.5	7.927
5.886	4.230	45.92	80.6	7.500
3.784	4.422	52.70	85.8	3.860
2.523	4.598	58.30	89.4	0.611
1.682	4.774	63.00	92.1	-2.309

Table B 179

Adhesion Tension of $C_{12}TMABr$

in Water at Polyethylene/Aqueous Interface,

α = 1.00

C	-log C	γ_{lv}	θ	$\gamma_{lv} \cdot \cos\theta$
10^3x mol/dm^3		mN/m	deg.	mN/m
17.72	1.752	39.00	60.8	19.027
11.16	1.952	43.62	64.9	18.504
0.7973	2.098	48.94	71.3	15.691
0.5493	2.260	54.00	76.5	12.606
0.3030	2.519	60.35	83.1	7.250
0.1065	2.973	67.76	91.4	-1.656

Table B 180

Adhesion Tension of $C_{12}TMABr$ - $C_{12}SO_4Na$ Mixtures in Water at Teflon/Aqueous Interface,

α = 0.500

C	-log C	γ_{lv}	θ	$\gamma_{lv} \cdot \cos\theta$
10^6x mol/dm^3		mN/m	deg.	mN/m
50.11	4.300	29.96	88.7	0.680
26.06	4.584	34.24	100.5	-6.240
15.03	4.823	43.20	105.6	-11.617
8.018	5.096	52.24	108.3	-16.403
4.009	5.397	61.12	109.5	-20.402
2.005	5.698	69.40	109.89	-23.508

Table B 181

Adhesion Tension of $C_{12}TMABr$ - $C_{12}SO_4Na$ Mixtures in Water at Teflon/Aqueous Interface,

α = 0.667

C	-log C	γ_{lv}	θ	$\gamma_{lv} \cdot \cos\theta$
10^6x mol/dm^3		mN/m	deg.	mN/m
63.15	4.200	29.96	89.8	0.105
31.58	4.501	31.60	103.1	-7.162
17.68	4.753	40.56	108.6	-12.937
9.473	5.024	50.25	110.6	-17.680
5.025	5.297	58.41	111.0	-20.932
2.526	5.598	67.04	111.3	-24.352

Table B 182

Adhesion Tension of $C_{12}SO_4Na$

in Water at Teflon/Aqueous Interface,

α = 1.00

C	-log C	γ_{lv}	θ	$\gamma_{lv} \cdot \cos\theta$
10^3x mol/dm^3		mN/m	deg.	mN/m
21.83	1.661	40.00	83.4	4.597
10.91	1.962	40.00	83.5	4.528
7.894	2.103	40.60	84.8	3.680
4.500	2.347	50.60	93.1	-2.736
2.526	2.598	59.40	97.8	-8.062
1.184	2.927	67.42	103.3	-15.510

Table B 183

Adhesion Tension of $C_{12}TMABr$ - $C_{12}SO_4Na$ Mixtures in Water at Polyetylene/Aqueous Interface,

α = 0.500

C	-log C	γ_{lv}	θ	$\gamma_{lv} \cdot \cos\theta$
10^6x mol/dm^3		mN/m	deg.	mN/m
50.11	4.300	29.96	65.5	12.424
26.06	4.584	34.24	79.2	6.416
15.03	4.823	43.20	85.0	3.765
8.018	5.096	52.24	89.3	0.638
4.009	5.397	61.12	87.8	2.346
2.005	5.698	69.40	86.7	3.995

Table B 184

Adhesion Tension of $C_{12}TMABr$ - $C_{12}SO_4Na$ Mixtures in Water at Polyethylene/Aqueous Interface,

α = 0.667

C	-log C	γ_{lv}	θ	$\gamma_{lv} \cdot \cos\theta$
10^6x mol/dm^3		mN/m	deg.	mN/m
63.15	4.200	29.96	70.8	9.853
31.58	4.501	31.60	80.3	5.324
17.68	4.753	40.56	88.1	1.345
9.473	5.024	50.25	92.3	-2.017
5.025	5.297	58.41	90.8	-0.816
2.526	5.598	67.04	89.3	0.819

Table B 185

Adhesion Tension of $C_{12}SO_4Na$

in Water at Polyethylene/Aqueous Interface,

α = 1.00

C	-log C	γ_{lv}	θ	$\gamma_{lv} \cdot \cos\theta$
10^3x mol/dm^3		mN/m	deg.	mN/m
78.94	1.103	40.00	62.6	18.408
21.83	1.661	40.00	63.4	17.910
10.91	1.962	40.00	62.5	18.470
7.894	2.103	40.60	64.2	17.670
4.500	2.347	50.60	76.0	12.241
2.526	2.598	59.40	83.3	6.930
1.184	2.927	67.40	90.0	0.000

Table B 186

Adhesion Tension of $C_{10}NBr$ Mixtures

at Teflon/Aqueous Interface, I.S. = 0.1 N (NaBr)

α = 1.000

C	-log C	γ_{lv}	θ	$\gamma_{lv} \cdot \cos\theta$
10^3x mol/dm^3		mN/m	deg.	mN/m
34.80	1.459	40.36	83.5	4.569
24.94	1.605	40.37	83.6	4.500
21.02	1.677	41.76	85.2	3.494
17.40	1.760	43.83	86.9	2.370
10.51	1.978	46.79	90.7	-0.572
8.699	2.061	48.67	91.8	-1.529
5.256	2.279	52.25	95.3	-4.826
4.350	2.362	53.78	97.1	-6.647
2.628	2.580	56.90	98.1	-8.017
2.175	2.663	58.18	99.8	-9.903
1.314	2.881	61.10	102.1	-12.808
1.087	2.964	62.16	103.0	-13.983
0.6570	3.182	64.70	104.5	-16.200
0.5437	3.265	65.63	105.2	-17.207

Table B 187

Adhesion Tension of C_8NBr -- $C_{10}SO_3Na$ Mixtures

at Teflon/Aqueous Interface, I.S. = 0.1 N (NaBr)

α = 0.500

C	-log C	γ_{lv}	θ	$\gamma_{lv} \cdot \cos\theta$
10^3x mol/dm^3		mN/m	deg.	mN/m
2.129	2.672	42.57	90.3	-0.223
1.420	2.848	46.94	95.1	-4.173
1.065	2.973	50.24	97.8	-6.818
0.7102	3.149	54.17	101.3	-10.614
0.5323	3.274	56.82	103.6	-13.361
0.3551	3.450	60.49	106.2	-16.876

Table B 188

Adhesion Tension of $C_{10}NBr$ -- $C_{10}SO_3Na$ Mixtures

at Teflon/Aqueous Interface, I.S. = 0.1 N (NaBr)

α = 0.500

C	-log C	γ_{lv}	θ	$\gamma_{lv} \cdot \cos\theta$
10^4x mol/dm^3		mN/m	deg.	mN/m
14.96	2.825	29.95	70.5	9.998
13.03	2.885	31.90	75.9	7.771
12.47	2.904	32.47	77.5	7.028
9.423	3.026	35.90	83.4	4.126
8.982	3.047	37.00	85.0	3.225
6.515	3.186	41.02	90.0	0.000
6.233	3.205	41.59	91.5	-1.089
4.712	3.327	44.95	95.4	-4.230
4.491	3.348	45.63	96.6	-5.245
3.258	3.487	49.14	100.0	-8.533
3.117	3.506	49.72	100.5	-9.061
2.356	3.628	52.45	102.9	-11.709
2.245	3.649	53.00	103.3	-12.193
1.629	3.788	56.72	104.9	-14.585
1.178	3.929	59.86	105.9	-16.399
1.123	3.950	60.41	106.1	-16.753

Table B 189

Adhesion Tension of $C_{10}NBr$ - $C_{12}SO_3Na$ Mixtures

at Teflon/Aqueous Interface, I.S. = 0.1 N (NaBr)

α = 0.500

C	-log C	γ_{lv}	θ	$\gamma_{lv} \cdot \cos\theta$
10^4x mol/dm^3		mN/m	deg.	mN/m
7.194	3.143	24.93	58.3	13.100
4.996	3.301	25.81	62.0	12.171
3.597	3.444	30.24	74.3	8.183
2.498	3.602	35.20	83.2	4.168
1.799	3.745	39.54	89.8	0.138
1.249	3.903	44.00	94.5	-3.452
0.8993	4.046	47.52	97.9	-6.531
0.6245	4.205	51.67	101.8	-10.566
0.4497	4.347	55.17	104.0	-13.347
0.3123	4.506	59.12	106.9	-17.186

Table B 190

Adhesion Tension of $C_{12}NBr$ -- $C_{12}SO_3Na$ Mixtures

at Teflon/Aqueous Interface, I.S. = 0.1 N (NaBr)

α = 0.500

C	-log C	γ_{lv}	θ	$\gamma_{lv} \cdot \cos\theta$
10^5x mol/dm^3		mN/m	deg.	mN/m
4.584	4.339	41.83	97.3	-5.315
4.211	4.376	42.02	97.3	-5.339
3.444	4.463	43.20	98.6	-6.460
3.159	4.501	44.37	99.3	-7.170
2.290	4.640	48.59	102.9	-10.848
2.106	4.677	49.59	103.8	-11.829
1.722	4.764	51.83	106.0	-14.286
1.579	4.802	53.10	106.6	-15.170
1.146	4.941	57.51	108.5	-18.248
1.053	4.978	58.32	109.2	-19.180
0.8609	5.065	60.07	110.7	-21.233
0.7897	5.103	61.09	111.1	-21.992

Table B 191

Adhesion Tension of $C_{10}NBr$

at Parafilm/Aqueous Interface, I.S. = 0.1 N (NaBr)

α = 1.000

C	-log C	γ_{lv}	θ	$\gamma_{lv} \cdot \cos\theta$
10^3x mol/dm^3		mN/m	deg.	mN/m
34.80	1.459	40.36	80.5	6.661
29.83	1.525	40.36	80.7	6.522
24.94	1.605	40.37	80.9	6.385
21.02	1.677	41.76	82.6	5.379
17.40	1.760	43.83	84.8	3.972
10.51	1.978	46.79	88.5	1.225
8.699	2.061	48.67	90.3	-0.255
5.256	2.279	52.25	93.2	-2.917
4.350	2.362	53.78	95.3	-4.968
2.628	2.580	56.90	97.3	-7.230
2.175	2.663	58.18	98.8	-8.901
1.314	2.881	61.10	101.1	-11.763
1.087	2.964	62.16	101.4	-12.286
0.6570	3.182	64.70	104.0	-15.652
0.5437	3.265	65.63	104.8	-16.765

Table B 192

Adhesion Tension of C_8NBr -- $C_{10}SO_3Na$ Mixtures

at Parafilm/Aqueous Interface, I.S. = 0.1 N (NaBr)

α = 0.500

C	-log C	γ_{lv}	θ	$\gamma_{lv} \cdot \cos\theta$
10^3x mol/dm^3		mN/m	deg.	mN/m
2.129	2.672	42.57	85.5	3.340
1.420	2.848	46.94	90.7	-0.574
1.065	2.973	50.24	94.6	-4.029
0.7102	3.149	54.17	98.8	-8.287
0.5323	3.274	56.82	101.5	-11.328
0.3551	3.450	60.49	104.4	-15.043

Table B 193

Adhesion Tension of $C_{10}NBr$ - $C_{10}SO_3Na$ Mixtures

at Parafilm/Aqueous Interface, I.S. = 0.1 N (NaBr)

α = 0.500

C	-log C	γ_{lv}	θ	$\gamma_{lv} \cdot \cos\theta$
10^4x mol/dm^3		mN/m	deg.	mN/m
14.96	2.825	29.95	60.8	14.611
13.03	2.885	31.90	66.2	12.873
12.47	2.904	32.47	68.3	12.006
9.423	3.026	35.90	75.2	9.171
8.982	3.047	37.00	77.7	7.882
6.515	3.186	41.02	84.0	4.288
6.233	3.205	41.59	84.8	3.769
4.712	3.327	44.95	89.5	0.392
4.491	3.348	45.63	90.3	-0.239
3.258	3.487	49.14	94.9	-4.197
3.117	3.506	49.72	95.1	-4.420
2.356	3.628	52.45	97.7	-7.028
2.245	3.649	53.00	98.2	-7.559
1.629	3.788	56.72	100.9	-10.725
1.178	3.929	59.86	103.6	-14.076
1.123	3.950	60.41	104.3	-14.921

Table B 194

Adhesion Tension of $C_{10}NBr$ -- $C_{12}SO_3Na$ Mixtures

at Parafilm/Aqueous Interface, I.S. = 0.1 N (NaBr)

α = 0.500

C	-log C	γ_{lv}	θ	$\gamma_{lv} \cdot \cos\theta$
10^4x mol/dm^3		mN/m	deg.	mN/m
7.194	3.143	24.93	39.4	19.264
4.996	3.301	25.81	44.4	18.441
3.597	3.444	30.24	62.6	13.916
2.498	3.602	35.20	74.9	9.170
1.799	3.745	39.54	83.3	4.613
1.249	3.903	44.00	88.9	0.845
0.8993	4.046	47.52	93.4	-2.818
0.6245	4.205	51.67	98.0	-7.191
0.4497	4.347	55.17	101.7	-11.188
0.3123	4.506	59.12	104.5	-14.803

Table B 195

Adhesion Tension of $C_{12}NBr$ - $C_{12}SO_3Na$ Mixtures

at Parafilm/Aqueous Interface, I.S. = 0.1 N (NaBr)

α = 0.500

C	-log C	γ_{lv}	θ	$\gamma_{lv} \cdot \cos\theta$
10^5x mol/dm^3		mN/m	deg.	mN/m
4.584	4.339	41.83	90.6	-0.438
4.211	4.376	42.02	90.7	-0.513
3.444	4.463	43.20	93.0	-2.261
3.159	4.501	44.37	95.1	-3.944
2.290	4.640	48.59	99.7	-8.187
2.106	4.677	49.59	100.8	-9.292
1.722	4.764	51.83	102.7	-11.395
1.579	4.802	53.10	104.1	-12.936
1.146	4.941	57.51	107.4	-17.198
1.053	4.978	58.32	108.0	-18.022
0.8609	5.065	60.07	109.5	-20.052
0.7897	5.103	61.09	110.3	-21.194

Table B 196

Adhesion Tension of $C_{12}(EO)_8$ - $C_{12}SO_4Na$ Mixtures in Water at Teflon/Aqueous Interface, $\alpha = 4.87 \times 10^{-3}$

C	-log C	γ_{lv}	θ	$\gamma_{lv} \cdot \cos\theta$
10^3x mol/dm^3		mN/m	deg.	mN/m
2.371	2.625	39.46	86.7	2.270
1.280	2.893	44.74	95.1	-3.977
0.6639	3.178	50.40	101.8	-10.307
0.3557	3.449	55.90	107.2	-16.530

Table B 197

Adhesion Tension of $C_{12}(EO)_8$

in Water at Teflon/Aqueous Interface,

α = 1.00

C	-log C	γ_{lv}	θ	$\gamma_{lv} \cdot \cos\theta$
10^5x mol/dm^3		mN/m	deg.	mN/m
6.486	4.188	37.78	81.6	5.519
3.243	4.489	42.12	88.2	1.323
1.622	4.790	46.42	93.9	-3.157
0.7783	5.109	50.78	98.3	-7.330
0.6486	5.188	51.80	99.3	-8.371

Table B 198

Adhesion Tension of $C_{12}SO_4Na$

at Teflon/Aqueous Interface, I.S. = 0.1 N (NaCl)

α = 0.00

C	-log C	γ_{lv}	θ	$\gamma_{lv} \cdot \cos\theta$
10^4x mol/dm^3		mN/m	deg.	mN/m
12.40	2.907	45.00	88.5	1.178
8.064	3.094	48.76	93.4	-2.892
4.962	3.304	52.97	98.1	-7.464
3.101	3.508	57.00	101.6	-11.461

Table B 199

Adhesion Tension of $C_{12}(EO)_8$ - $C_{12}SO_4Na$ Mixtures at Teflon/Aqueous Interface, I.S. = 0.1 N (NaCl)

$\alpha = 5.35 \times 10^{-2}$

C	-log C	γ_{lv}	θ	$\gamma_{lv} \cdot \cos\theta$
10^5x mol/dm^3		mN/m	deg.	mN/m
34.07	3.468	34.74	81.9	4.895
17.04	3.769	40.22	91.1	-0.772
8.518	4.070	45.62	97.3	-5.797
4.088	4.388	51.38	103.0	-11.558

Table B 200

Adhesion Tension of $C_{12}(EO)_8$

at Teflon/Aqueous Interface, I.S. = 0.1 N (NaCl)

α = 1.00

C	-log C	γ_{lv}	θ	$\gamma_{lv} \cdot \cos\theta$
10^5x mol/dm^3		mN/m	deg.	mN/m
5.837	4.234	37.52	82.1	5.157
2.919	4.535	41.83	88.7	0.949
1.492	4.826	45.97	94.2	-3.367
0.7783	5.109	50.02	98.5	-7.393
0.3892	5.410	54.22	102.3	-11.551

Table B 201

Adhesion Tension of $C_{12}SO_4Na$

at Teflon/Aqueous Interface, I.S. = 0.5 N (NaCl)

α = 0.00

C	-log C	γ_{lv}	θ	$\gamma_{lv} \cdot \cos\theta$
10^4x mol/dm^3		mN/m	deg.	mN/m
2.854	3.545	35.08	88.5	0.918
1.998	3.699	39.22	94.8	-3.282
1.199	3.921	45.30	100.8	-8.488
0.7420	4.130	50.86	105.5	-13.592

Table B 202

Adhesion Tension of $C_{12}(EO)_8$ -- $C_{12}SO_4Na$ Mixtures at Teflon/Aqueous Interface, I.S. = 0.5 N (NaCl)

$\alpha = 9.02 \times 10^{-2}$

C	-log C	γ_{lv}	θ	$\gamma_{lv} \cdot \cos\theta$
10^5x mol/dm^3		mN/m	deg.	mN/m
6.408	4.193	38.48	90.1	-0.067
4.485	4.348	41.62	95.4	-3.917
2.691	4.570	46.18	102.1	-9.680
1.666	4.778	50.45	107.2	-14.918

Table B 203

Adhesion Tension of $C_{12}(EO)_8$

at Teflon/Aqueous Interface, I.S. = 0.5 N (NaCl)

α = 1.00

C	-log C	γ_{lv}	θ	$\gamma_{lv} \cdot \cos\theta$
10^5x mol/dm^3		mN/m	deg.	mN/m
2.919	4.535	38.62	87.7	1.550
1.459	4.836	43.30	94.2	-3.171
0.7460	5.127	47.72	100.6	-8.778
0.3892	5.410	52.24	103.3	-12.018

Table B 204

Adhesion Tension of $C_{12}(EO)_8$ - $C_{12}SO_3Na$ Mixtures in Water at Teflon/Aqueous Interface, $\alpha = 4.15 \times 10^{-3}$

C	-log C	γ_{lv}	θ	$\gamma_{lv} \cdot \cos\theta$
10^3x mol/dm^3		mN/m	deg.	mN/m
3.563	2.448	40.65	85.9	2.906
2.494	2.603	43.50	90.6	-0.456
1.354	2.868	48.28	96.9	-5.800
0.7839	3.106	52.55	102.4	-11.284

Table B 205

Adhesion Tension of $C_{12}SO_3Na$

at Teflon/Aqueous Interface, I.S. = 0.1 N (NaCl)

α = 0.00

C	-log C	γ_{lv}	θ	$\gamma_{lv} \cdot \cos\theta$
10^4x mol/dm^3		mN/m	deg.	mN/m
22.90	2.640	36.22	84.7	3.346
13.74	2.862	41.18	91.5	-1.078
7.328	3.135	47.20	97.0	-5.752
3.893	3.410	53.53	101.7	-10.855

Table B 206

Adhesion Tension of $C_{12}(EO)_8$ - $C_{12}SO_3Na$ Mixtures

at Teflon/Aqueous Interface, I.S. = 0.1 N (NaCl)

$\alpha = 3.23 \times 10^{-2}$

C	-log C	γ_{lv}	θ	$\gamma_{lv} \cdot \cos\theta$
10^4x mol/dm^3		mN/m	deg.	mN/m
6.427	3.192	35.90	80.2	6.111
3.214	3.493	41.18	89.1	0.647
1.607	3.794	46.82	96.2	-5.057
0.7713	4.113	52.80	102.0	-10.978

Table B 207

Adhesion Tension of $C_{12}SO_3Na$

at Teflon/Aqueous Interface, I.S. = 0.5 N (NaCl)

α = 0.00

C	-log C	γ_{lv}	θ	$\gamma_{lv} \cdot \cos\theta$
10^4x mol/dm^3		mN/m	deg.	mN/m
3.958	3.403	38.32	92.7	-1.805
2.771	3.557	41.56	96.9	-4.993
1.583	3.801	47.08	102.0	-9.788
0.8708	4.060	52.90	105.9	-14.492

Table B 208

Adhesion Tension of $C_{12}(EO)_8$ - $C_{12}SO_3Na$ Mixtures

at Teflon/Aqueous Interface, I.S. = 0.5 N (NaCl)

$\alpha = 5.26 \times 10^{-2}$

C	-log C	γ_{lv}	θ	$\gamma_{lv} \cdot \cos\theta$
10^5x mol/dm^3		mN/m	deg.	mN/m
16.65	3.779	37.10	88.4	1.036
11.66	3.933	40.18	93.7	-2.593
6.993	4.155	44.64	99.0	-6.983
3.996	4.398	49.52	104.4	-12.320

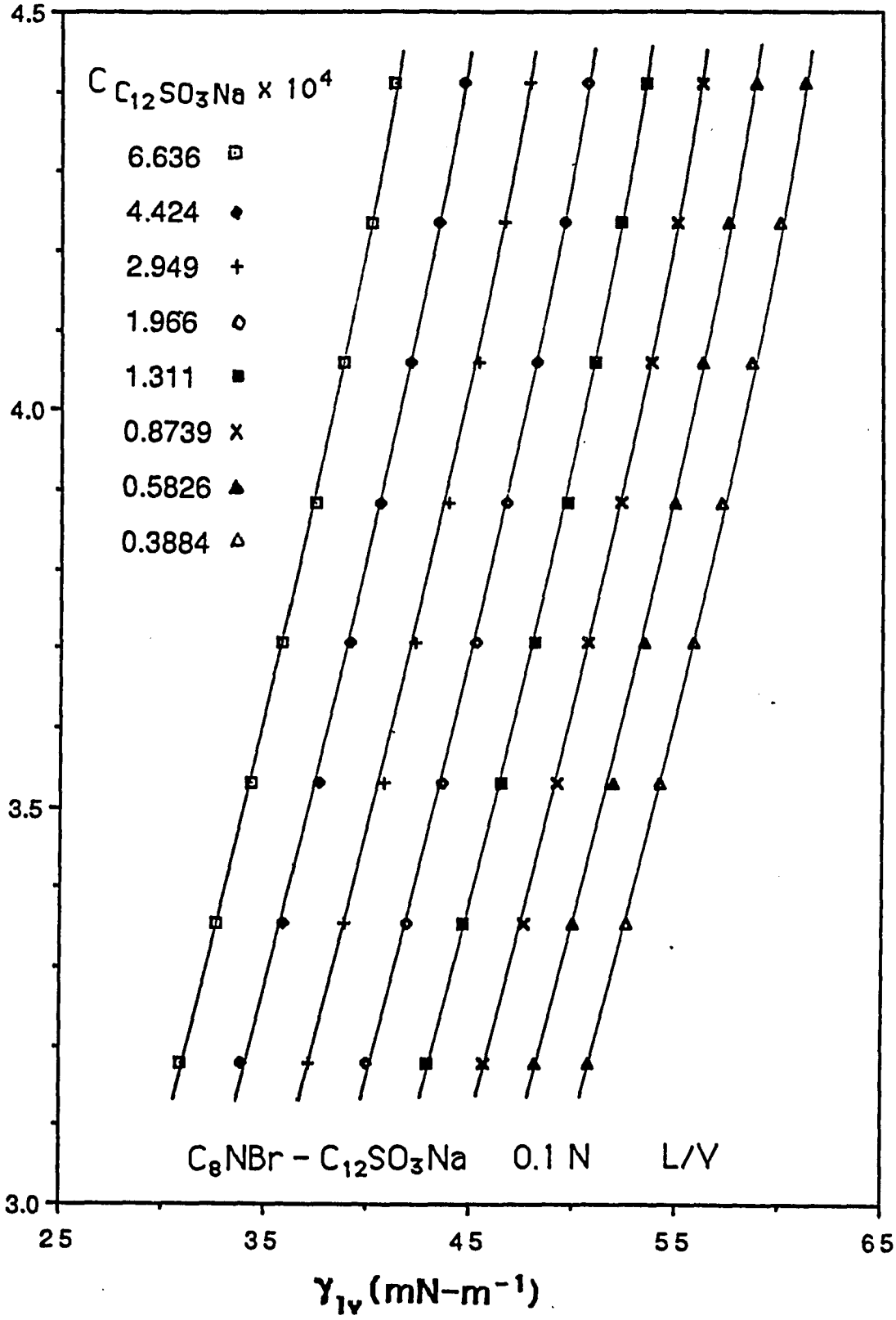
4.5
4.0
3.5
3.0
25
35
45
55
65
C C12SO3Na x 10^4
6.636
4.424
2.949
1.966
1.311
0.8739
0.5826
0.3884
C8NBr - C12SO3Na 0.1 N L/V
γlv (mN-m-1)

Figure 1

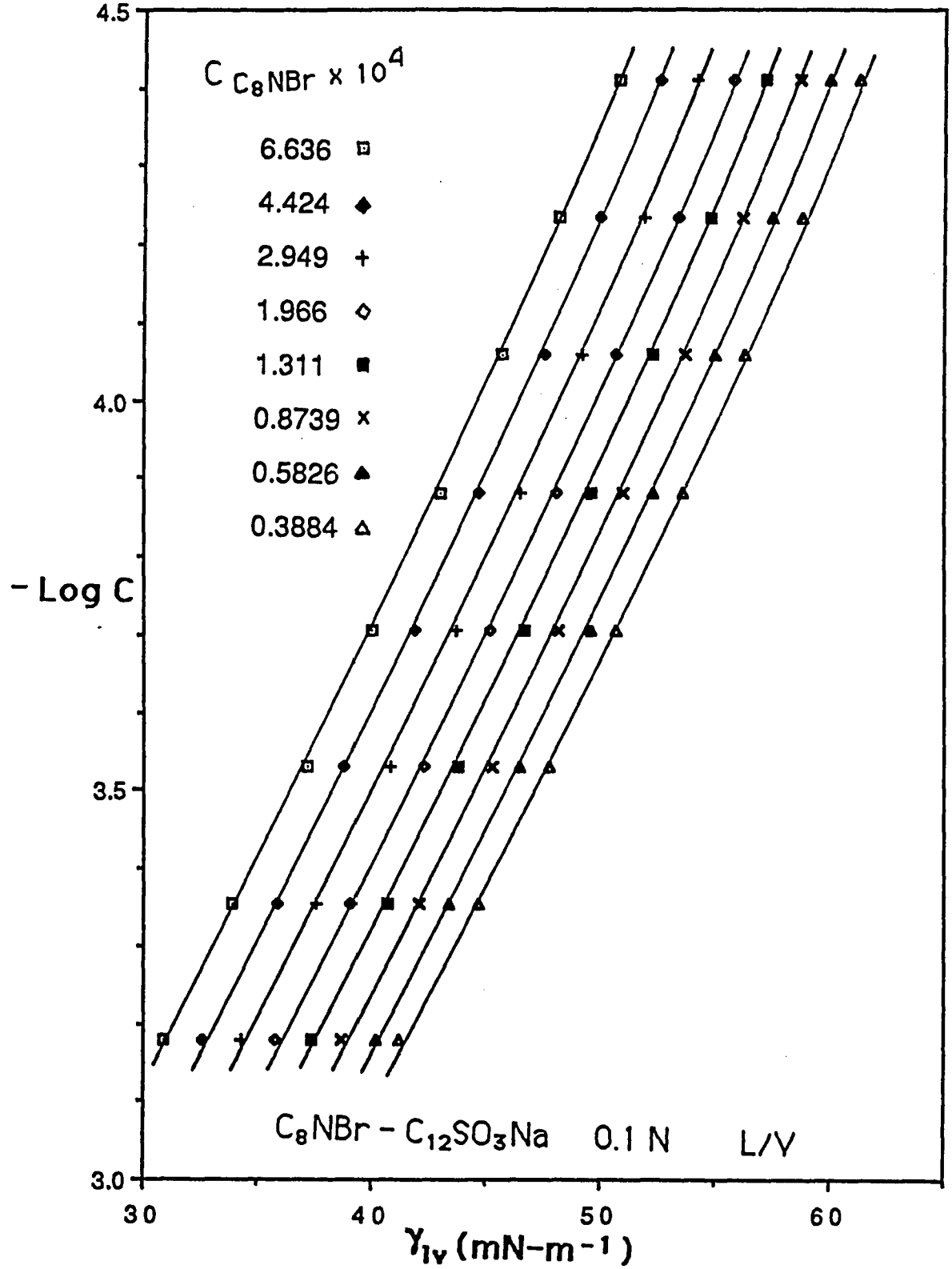
4.5
4.0
3.5
3.0
- Log C
C C8NBr x 10^4
6.636
4.424
2.949
1.966
1.311
0.8739
0.5826
0.3884
C8NBr - C12SO3Na 0.1 N L/V
30
40
50
60
γlv (mN-m-1)

Figure 2

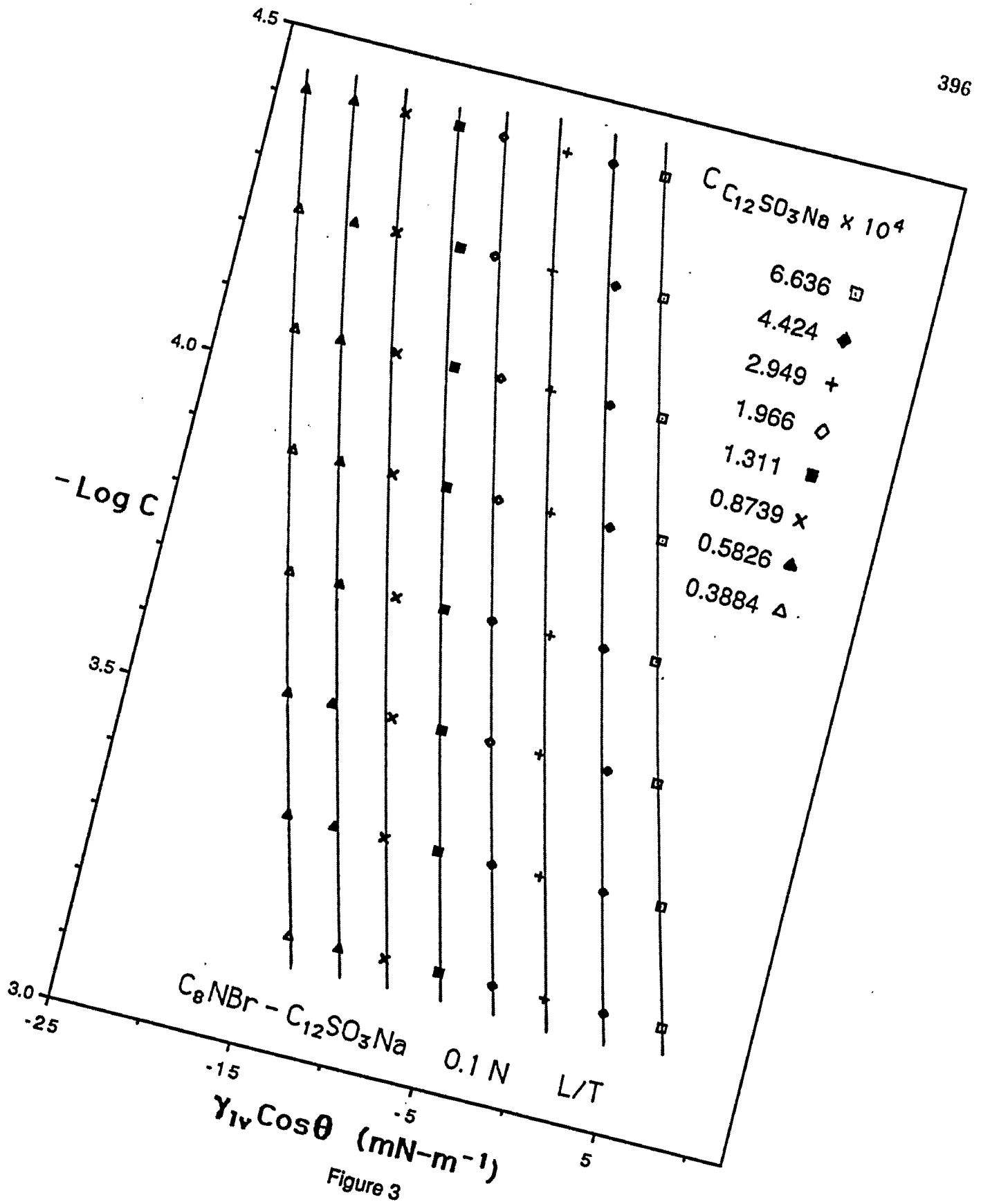
4.5
4.0
3.5
3.0
-Log C
-25
-15
-5
5
γ_{lv} Cosθ (mN-m^{-1})
$C_8NBr - C_{12}SO_3Na$ 0.1 N L/T
$C_{C_{12}SO_3Na}$ X 10^4
6.636
4.424
2.949
1.966
1.311
0.8739
0.5826
0.3884

Figure 3

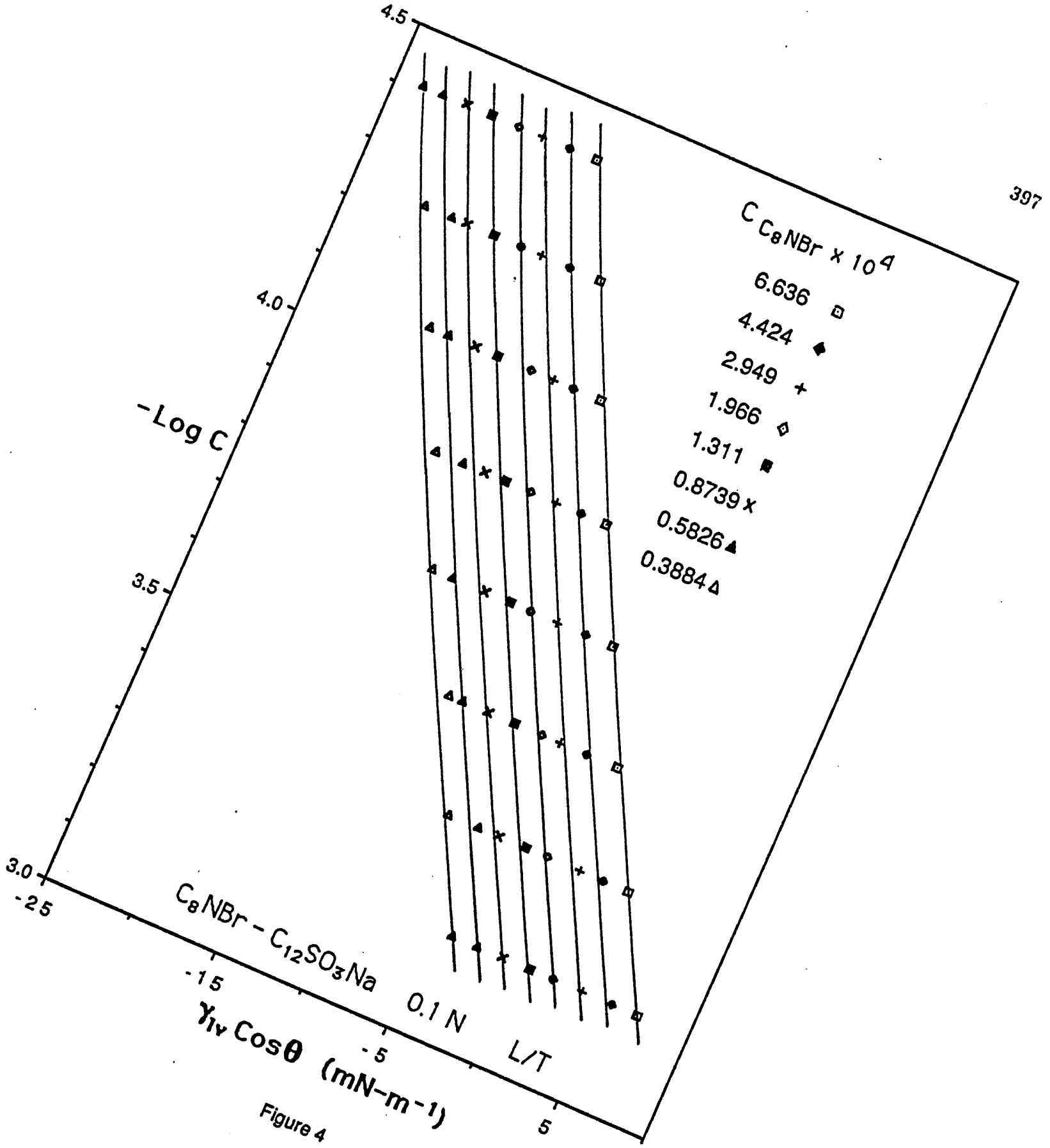
4.5
4.0
3.5
3.0
-Log C
-25
-15
-5
5
γ_{lv} Cosθ (mN-m^{-1})
$C_8NBr - C_{12}SO_3Na$ 0.1 N L/T
C_{C_8NBr} x 10^4
6.636
4.424
2.949
1.966
1.311
0.8739
0.5826
0.3884

Figure 4

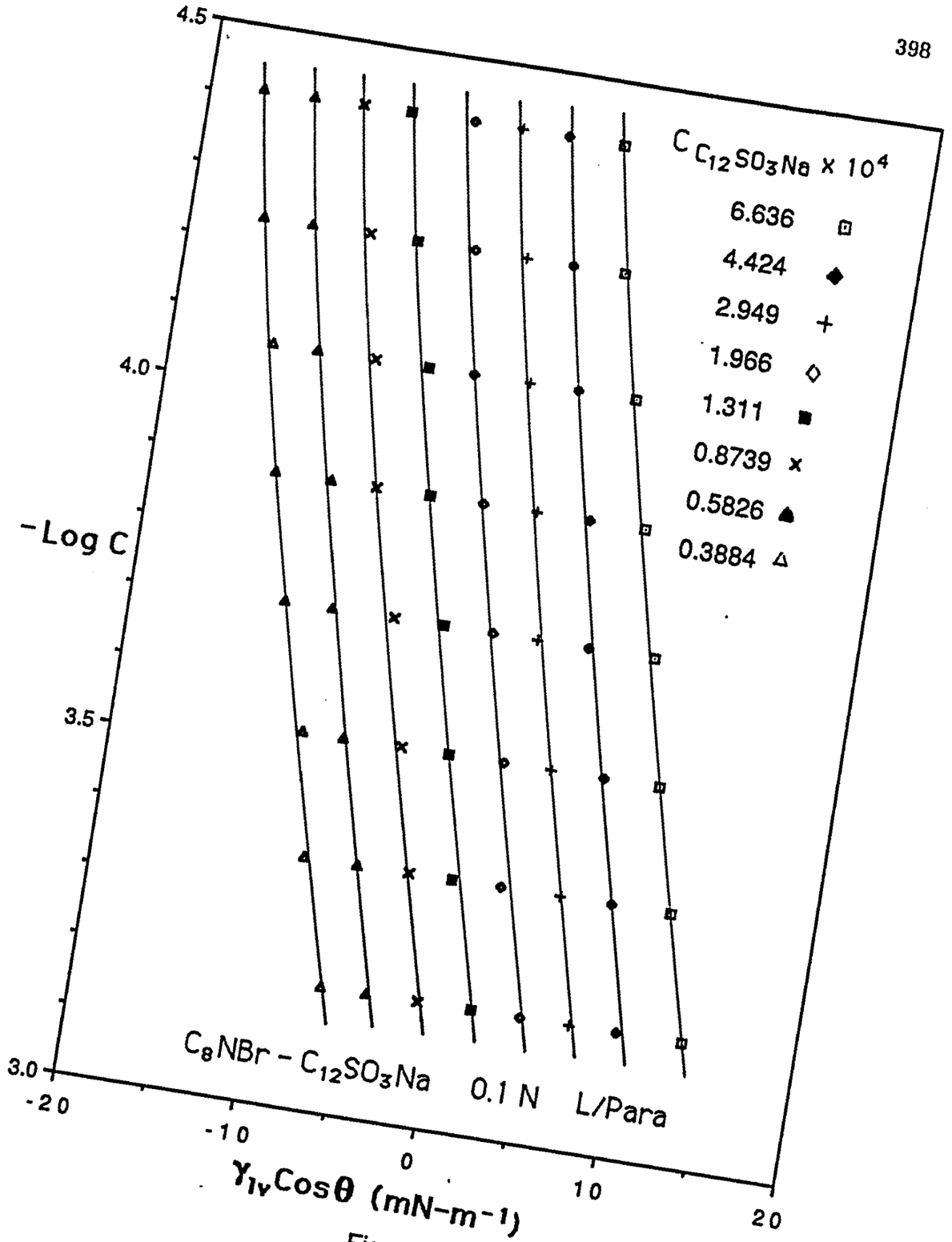
4.5
4.0
3.5
3.0
-Log C
$C_{C_{12}SO_3Na} \times 10^4$
6.636
4.424
2.949
1.966
1.311
0.8739
0.5826
0.3884
$C_8NBr - C_{12}SO_3Na$ 0.1 N L/Para
-20
-10
0
10
20
$\gamma_{lv}Cos\theta$ (mN-m^{-1})

Figure 5

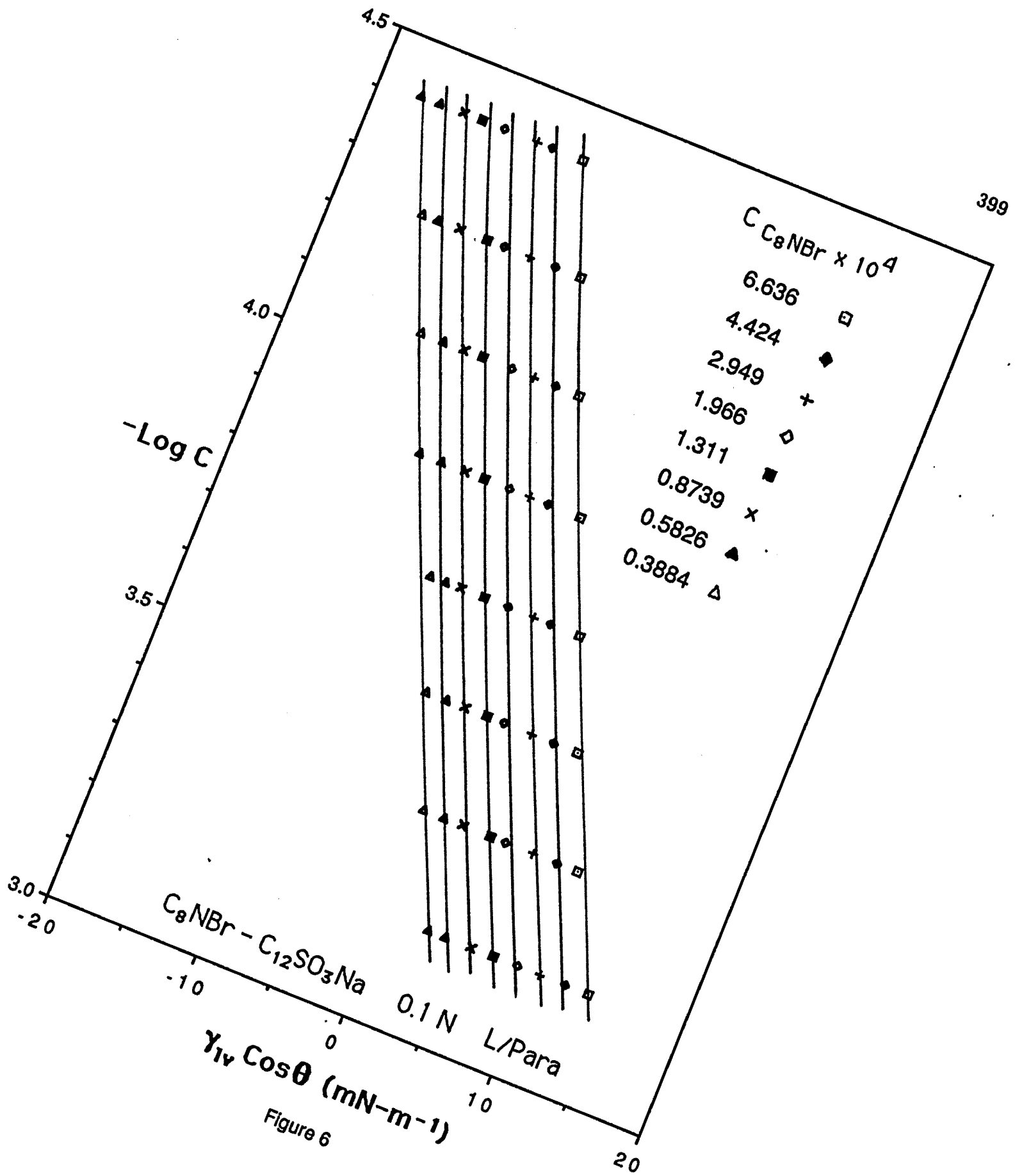
4.5
4.0
3.5
3.0
-Log C
399
C C8NBr x 10^4
6.636
4.424
2.949
1.966
1.311
0.8739
0.5826
0.3884
-20
-10
0
10
20
C8NBr - C12SO3Na 0.1 N L/Para
γlv Cosθ (mN-m-1)

Figure 6

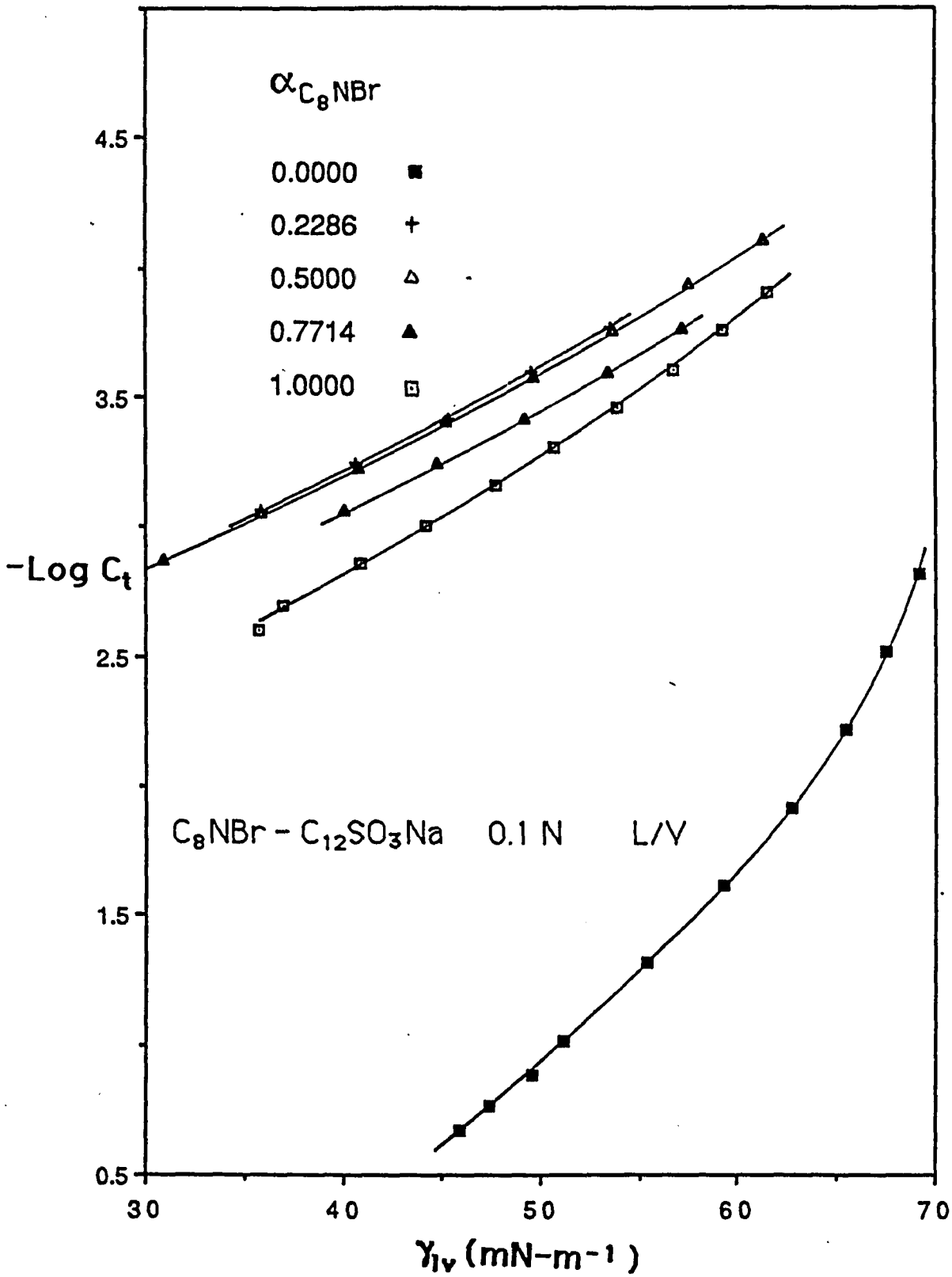
α_{C_8NBr}
0.0000
0.2286
0.5000
0.7714
1.0000
4.5
3.5
2.5
1.5
0.5
-Log C_t
$C_8NBr - C_{12}SO_3Na$ 0.1 N L/V
30
40
50
60
70
γ_{lv} (mN-m^{-1})

Figure 7

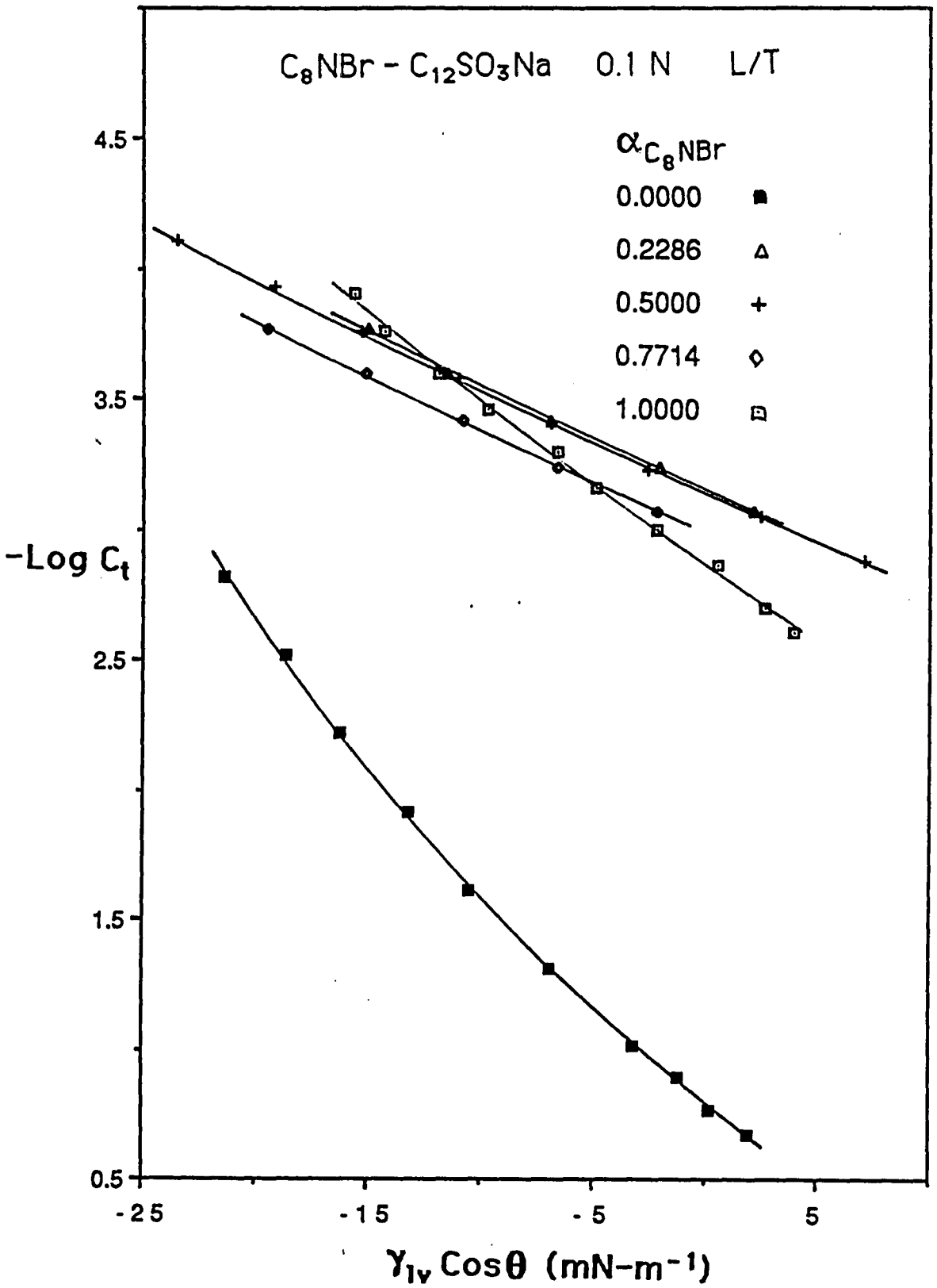
$C_8NBr - C_{12}SO_3Na$ 0.1 N L/T
α_{C_8NBr}
0.0000
0.2286
0.5000
0.7714
1.0000
-Log C_t
4.5
3.5
2.5
1.5
0.5
-25
-15
-5
5
$\gamma_{lv} \cos\theta$ (mN-m^{-1})

Figure 8

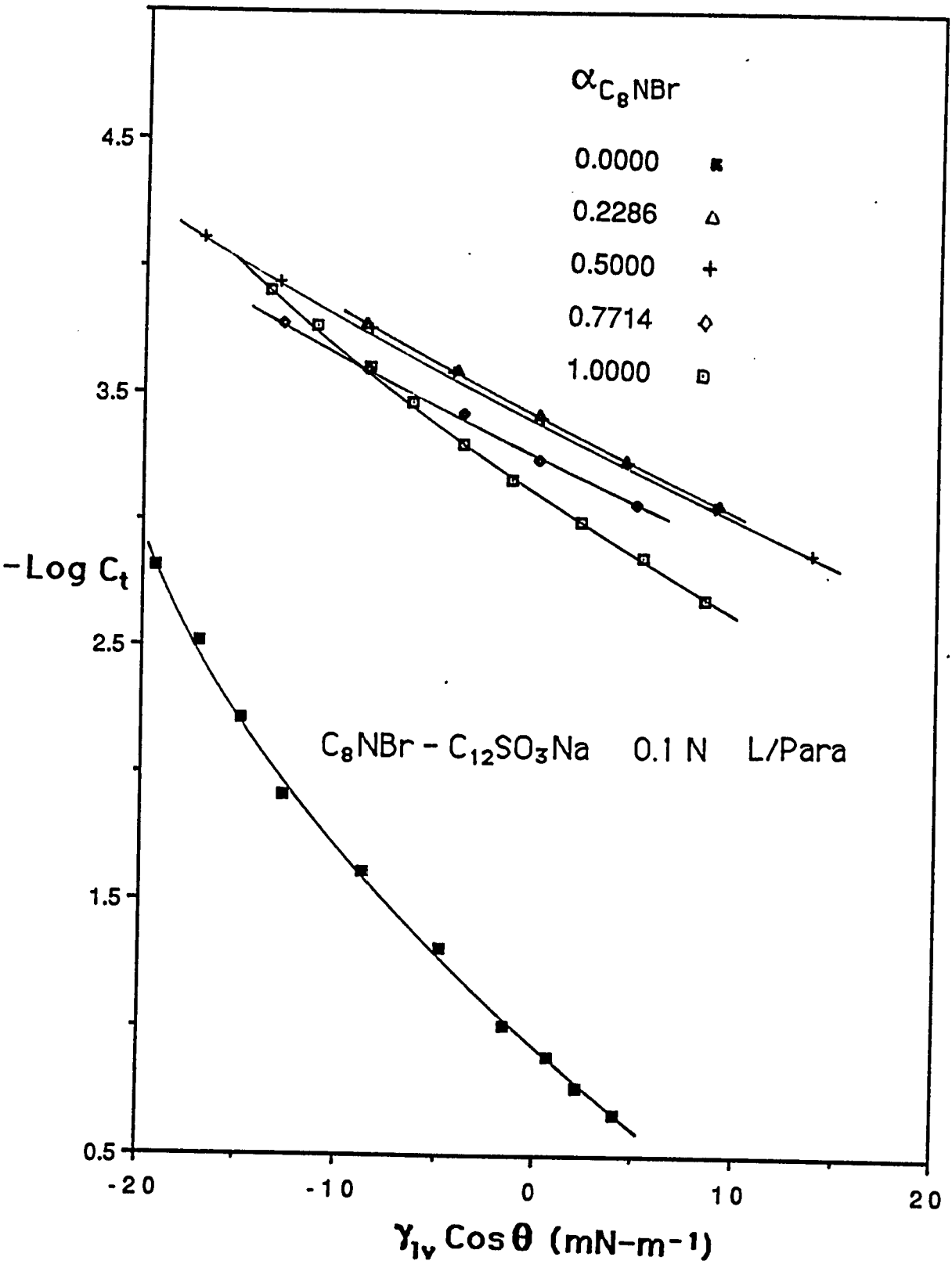
α_{C_8NBr}
0.0000
0.2286
0.5000
0.7714
1.0000
4.5
3.5
2.5
1.5
0.5
-Log C_t
$C_8NBr - C_{12}SO_3Na$ 0.1 N L/Para
-20
-10
0
10
20
γ_{lv} Cos θ (mN-m^{-1})

Figure 9

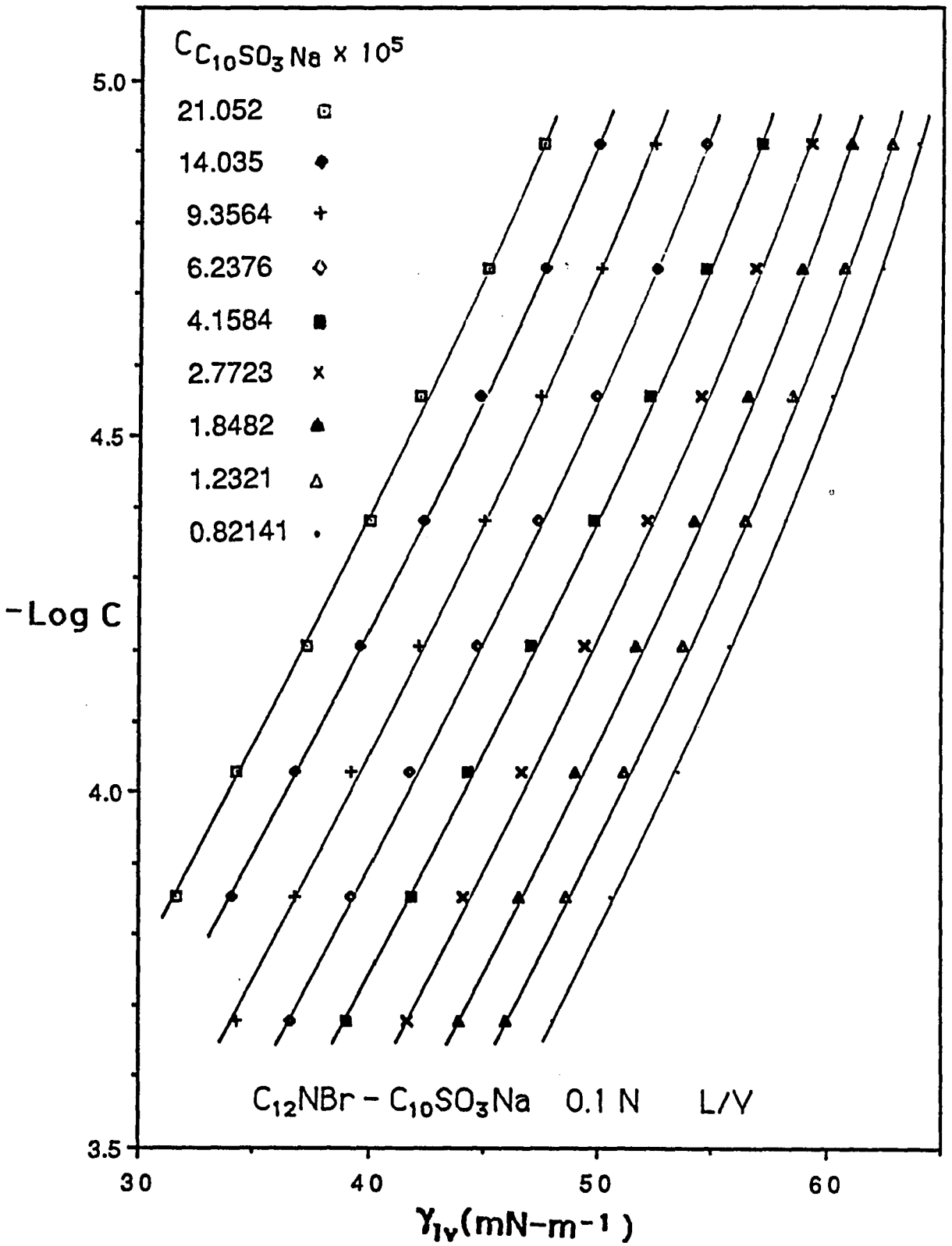
$C_{C_{10}SO_3Na} \times 10^5$
21.052
14.035
9.3564
6.2376
4.1584
2.7723
1.8482
1.2321
0.82141
5.0
4.5
4.0
3.5
-Log C
30
40
50
60
$\gamma_{lv}(mN-m^{-1})$
$C_{12}NBr - C_{10}SO_3Na$ 0.1 N L/V

Figure 10

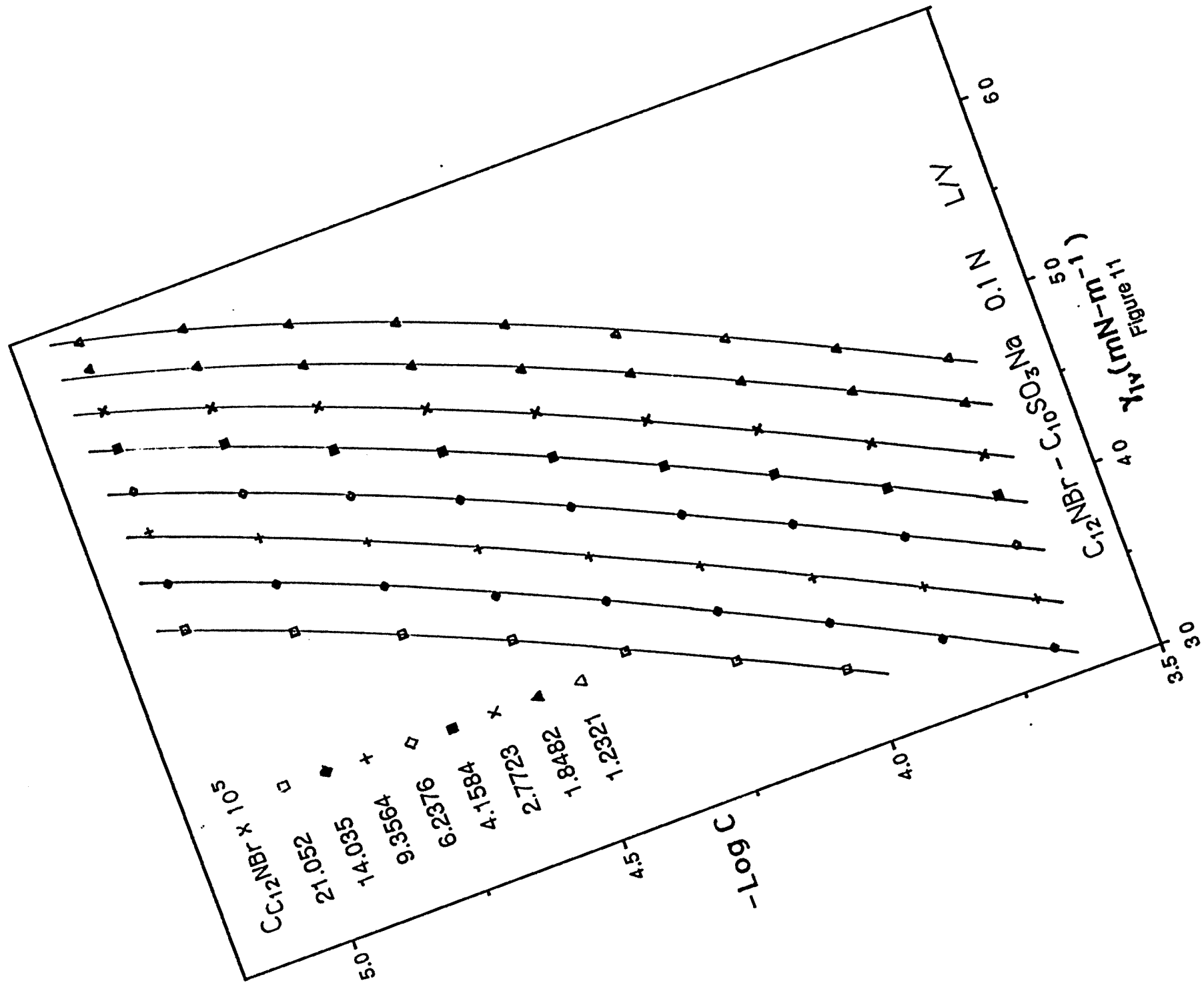
$C_{12}NBr - C_{10}SO_3Na$ 0.1 N
γ_{LV} (mN-m^{-1})
60
50
40
35
30
-Log C
5.0
4.5
4.0
$C_{C_{12}NBr} \times 10^5$
21.052
14.035
9.3564
6.2376
4.1584
2.7723
1.8482
1.2321

Figure 11

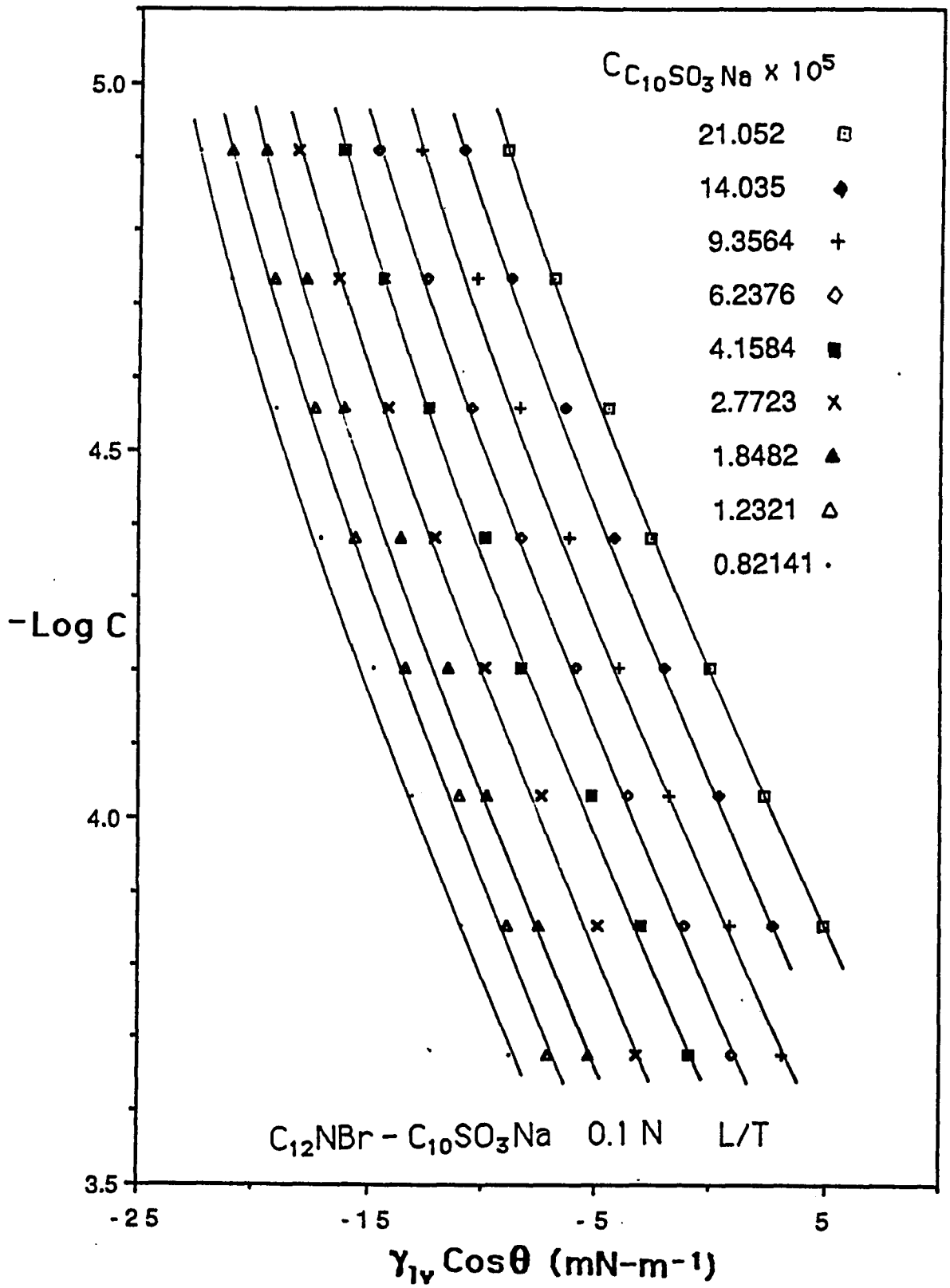
$C_{C_{10}SO_3Na} \times 10^5$
21.052
14.035
9.3564
6.2376
4.1584
2.7723
1.8482
1.2321
0.82141
5.0
4.5
4.0
3.5
-Log C
$C_{12}NBr - C_{10}SO_3Na$ 0.1 N L/T
-25
-15
-5
5
$\gamma_{lv} \cos\theta$ (mN-m^{-1})

Figure 12

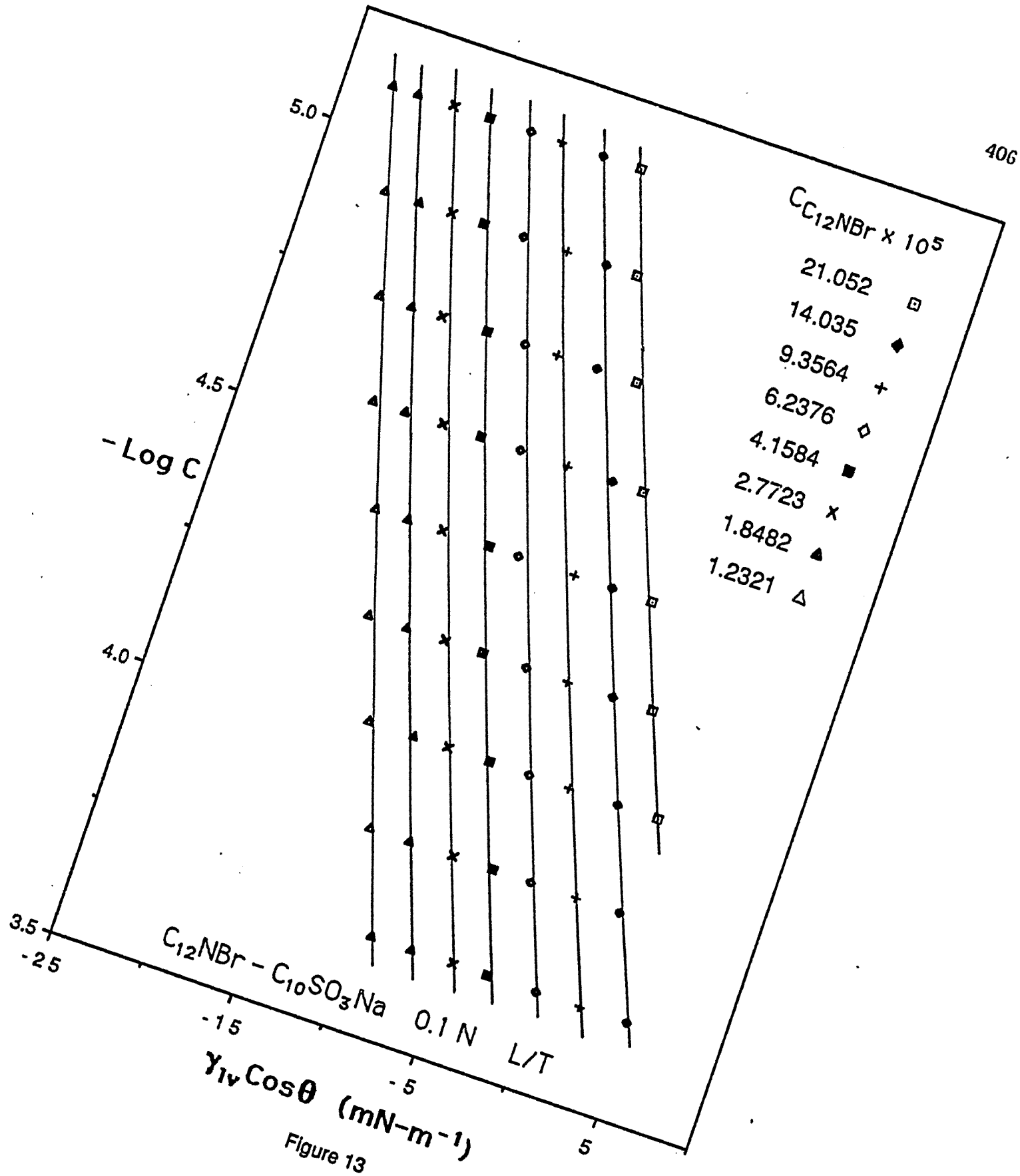
5.0
4.5
4.0
3.5
- Log C
-25
-15
-5
5
γ_{lv} Cosθ (mN-m^{-1})
$C_{12}NBr - C_{10}SO_3Na$ 0.1 N L/T
$C_{C_{12}NBr}$ x 10^5
21.052
14.035
9.3564
6.2376
4.1584
2.7723
1.8482
1.2321

Figure 13

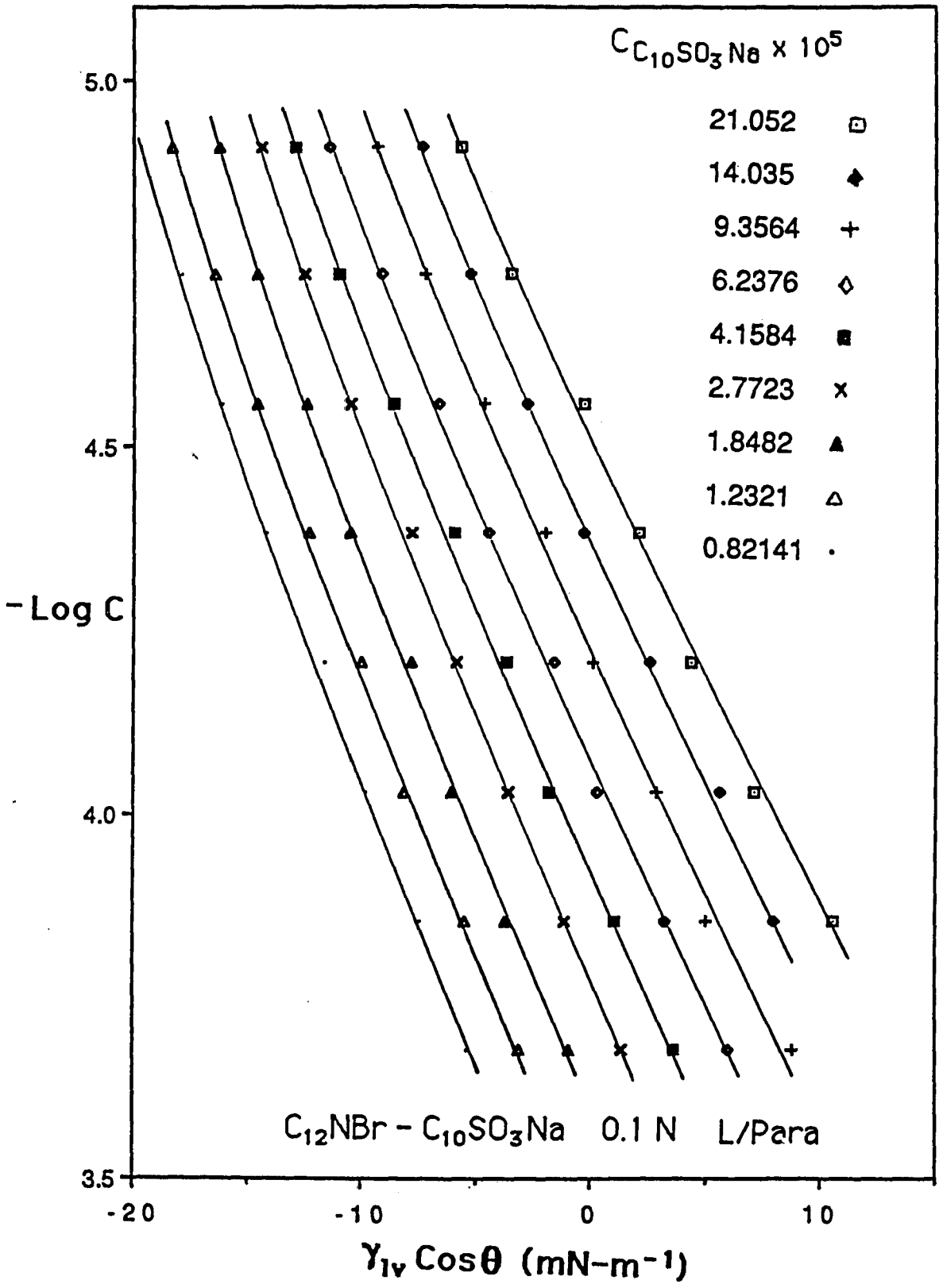
$C_{C_{10}SO_3Na} \times 10^5$
21.052
14.035
9.3564
6.2376
4.1584
2.7723
1.8482
1.2321
0.82141
5.0
4.5
4.0
3.5
-Log C
-20
-10
0
10
$\gamma_{lv} \cos\theta$ (mN-m^{-1})
$C_{12}NBr - C_{10}SO_3Na$ 0.1 N L/Para

Figure 14

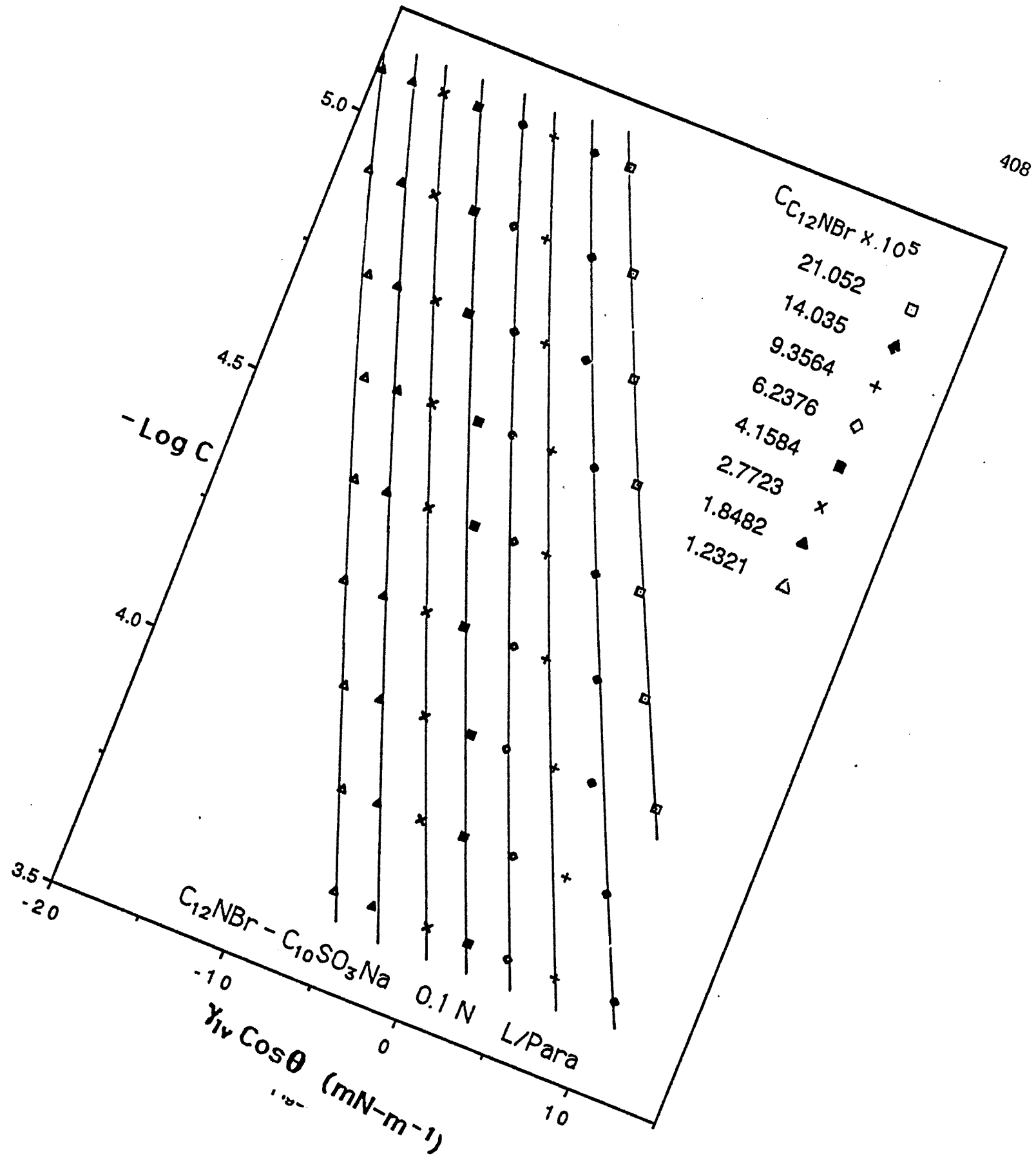
$C_{C_{12}NBr} \times 10^5$
21.052
14.035
9.3564
6.2376
4.1584
2.7723
1.8482
1.2321
5.0
4.5
4.0
3.5
- Log C
-20
-10
0
10
$C_{12}NBr - C_{10}SO_3Na$ 0.1 N L/Para
$\gamma_{lv} \cos\theta$ (mN-m^{-1})

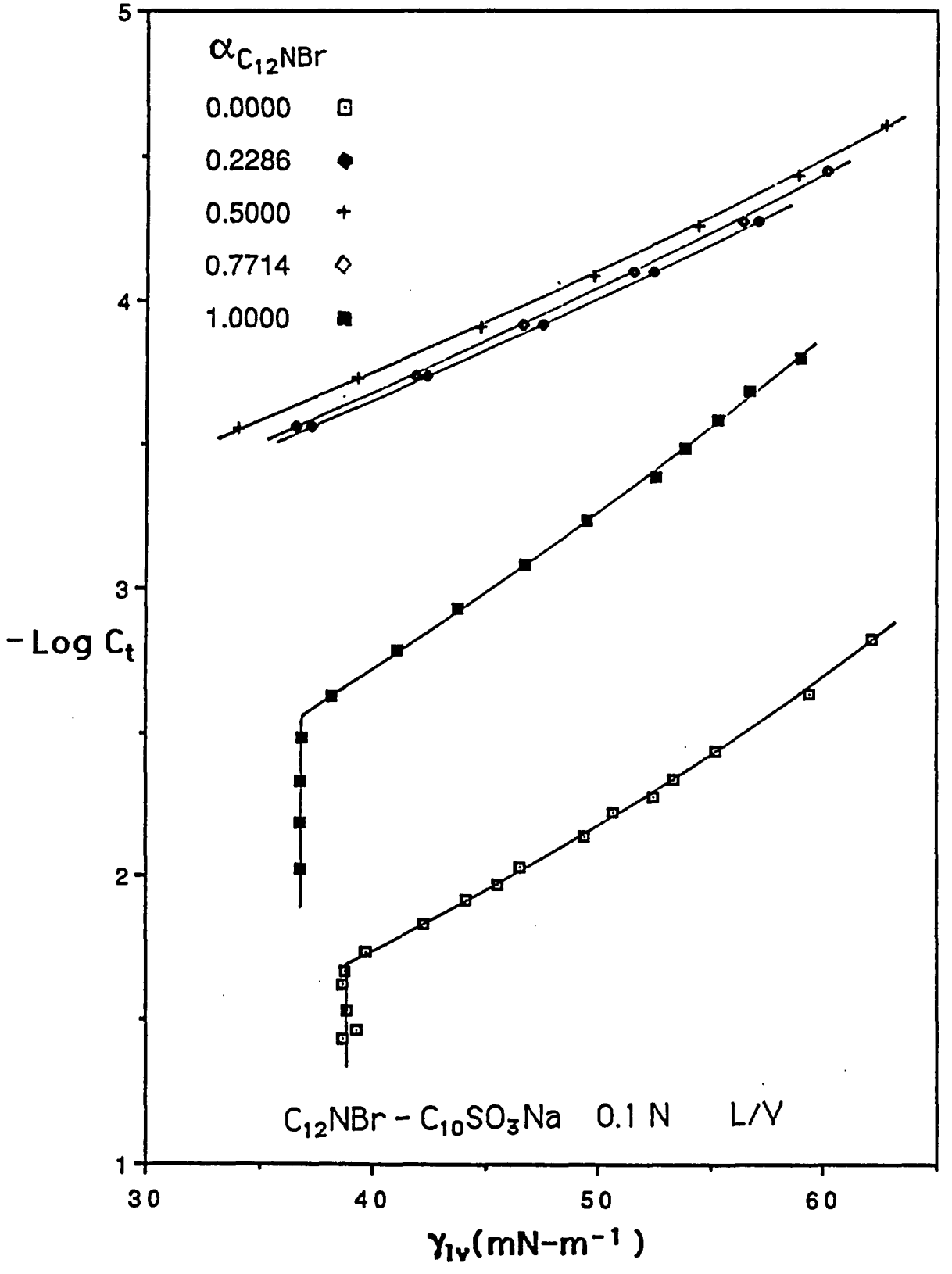
$\alpha_{C_{12}NBr}$
0.0000
0.2286
0.5000
0.7714
1.0000
$C_{12}NBr - C_{10}SO_3Na$ 0.1 N L/V
- Log C_t
γ_{lv}(mN-m^{-1})
5
4
3
2
1
30
40
50
60

Figure 16

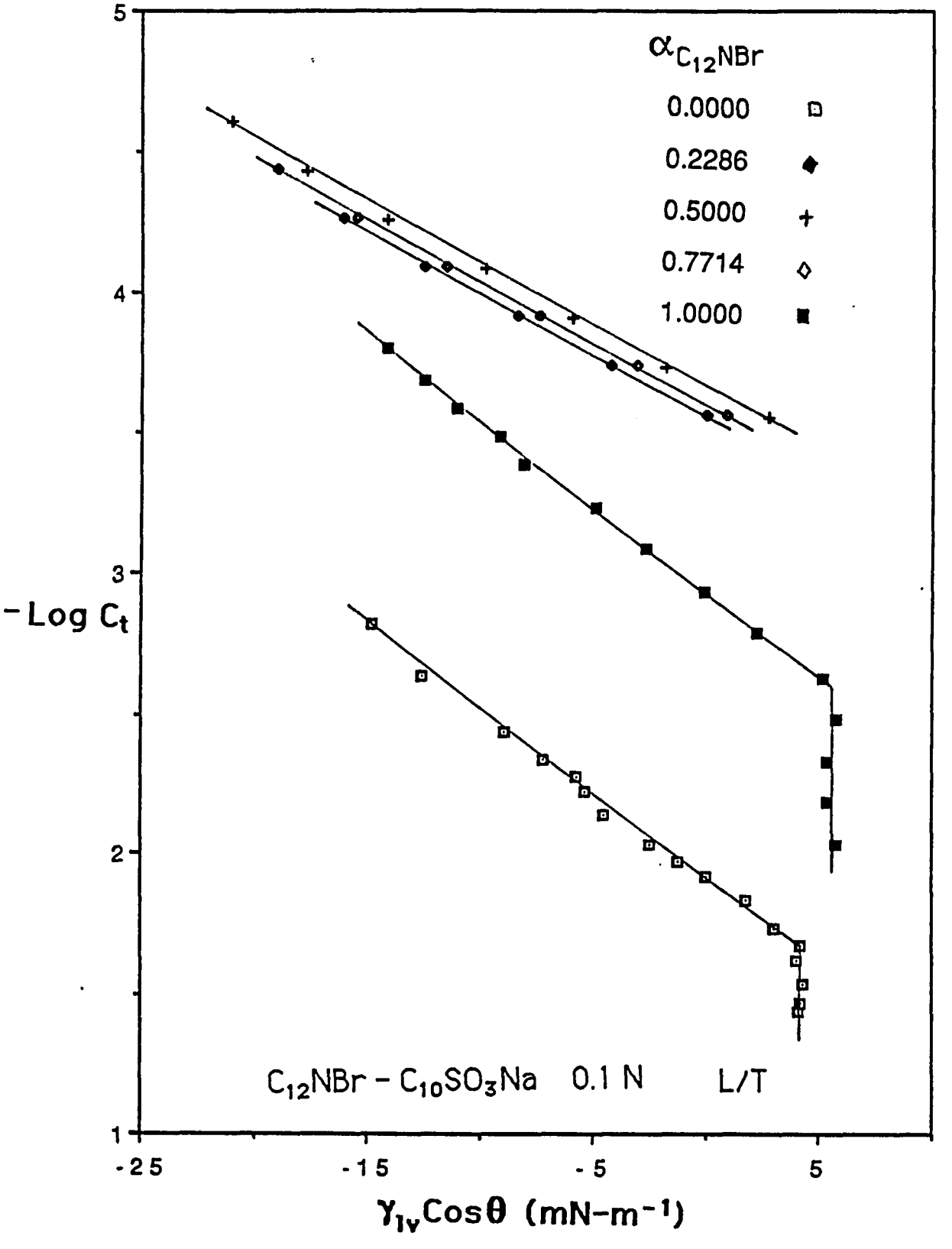
$\alpha_{C_{12}NBr}$
0.0000
0.2286
0.5000
0.7714
1.0000
5
4
3
2
1
- Log C_t
$C_{12}NBr - C_{10}SO_3Na$ 0.1 N L/T
-25
-15
-5
5
$\gamma_{lv}Cos\theta$ (mN-m^{-1})

Figure 17

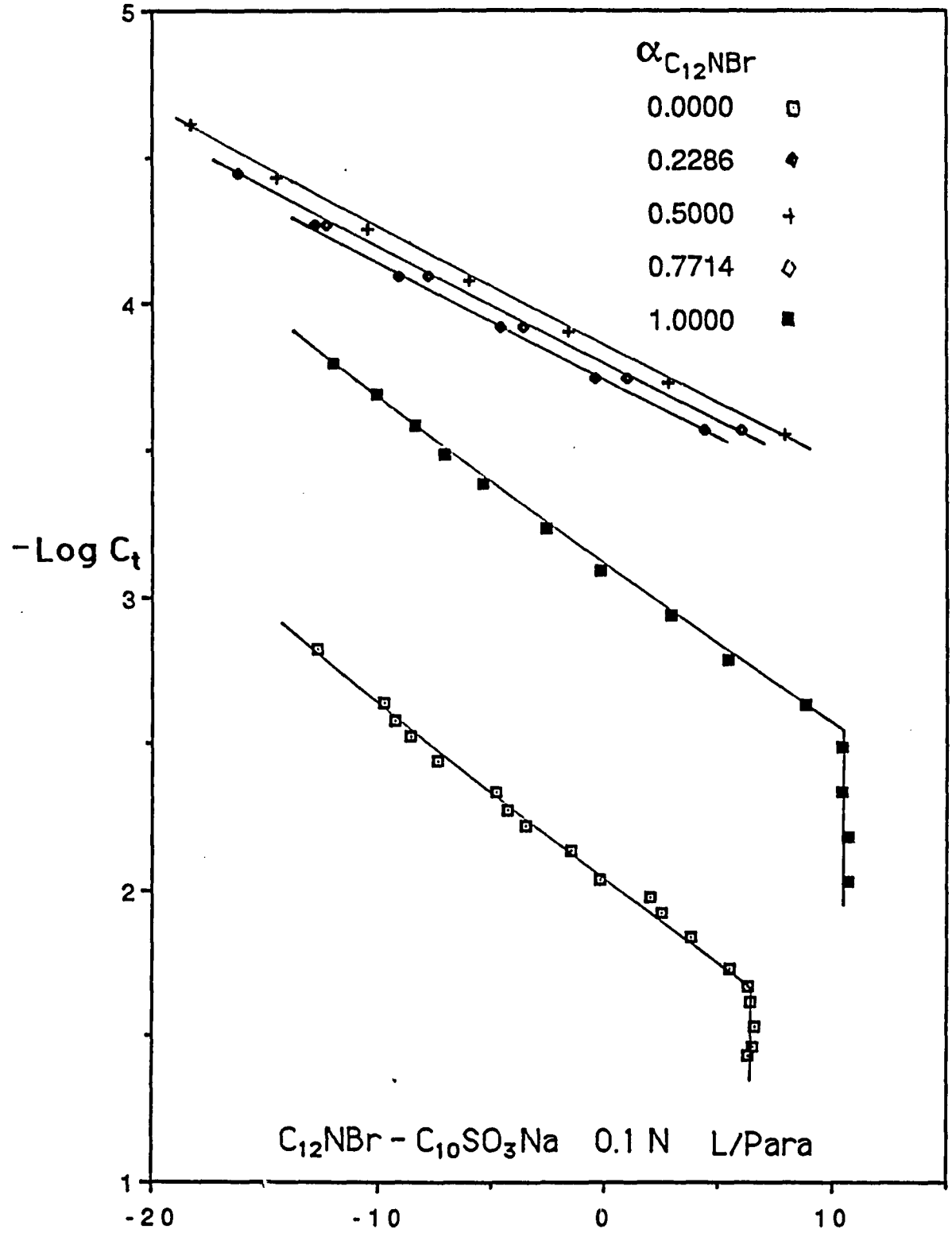
$\alpha_{C_{12}NBr}$
0.0000
0.2286
0.5000
0.7714
1.0000
-Log C_t
5
4
3
2
1
-20
-10
0
10
$C_{12}NBr - C_{10}SO_3Na$ 0.1 N L/Para

Figure 18

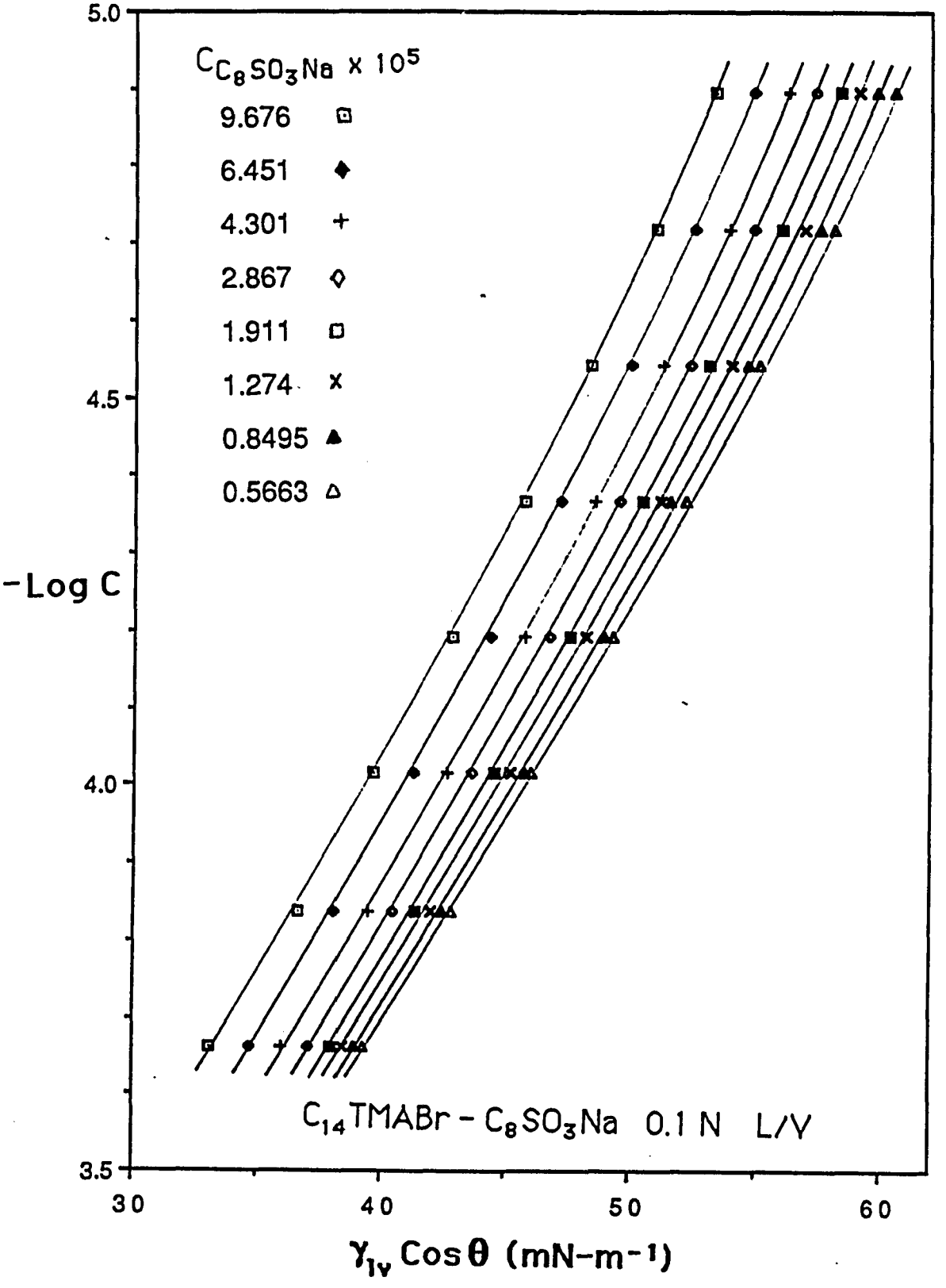
5.0
4.5
4.0
3.5
-Log C
$C_{C_8SO_3Na}$ x 10^5
9.676
6.451
4.301
2.867
1.911
1.274
0.8495
0.5663
$C_{14}TMABr - C_8SO_3Na$ 0.1 N L/V
30
40
50
60
γ_{lv} Cos θ (mN-m^{-1})

Figure 19

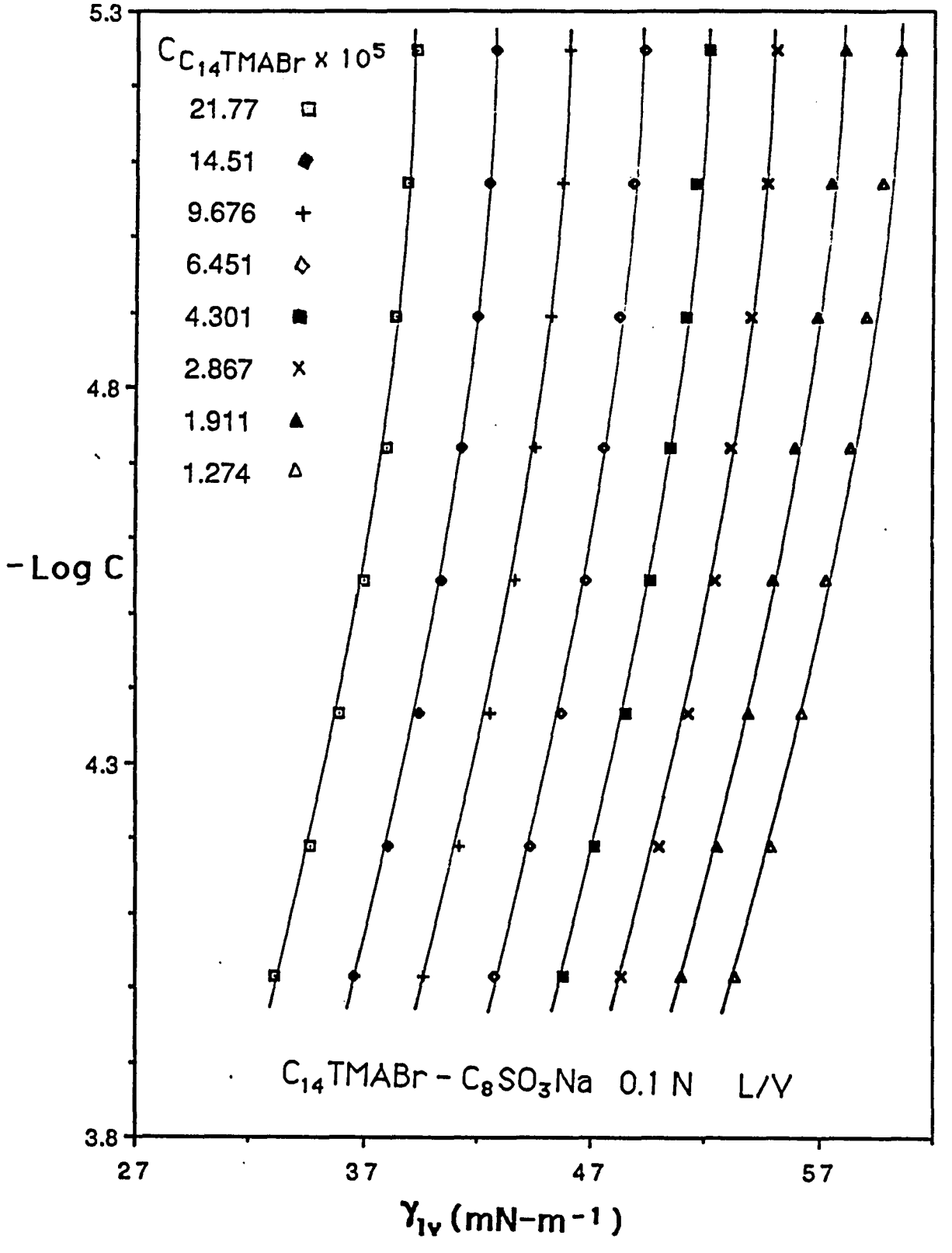
5.3
4.8
4.3
3.8
$C_{C_{14}TMABr} \times 10^5$
21.77
14.51
9.676
6.451
4.301
2.867
1.911
1.274
-Log C
$C_{14}TMABr - C_8SO_3Na$ 0.1 N L/V
27
37
47
57
γ_{lv} (mN-m^{-1})

Figure 20

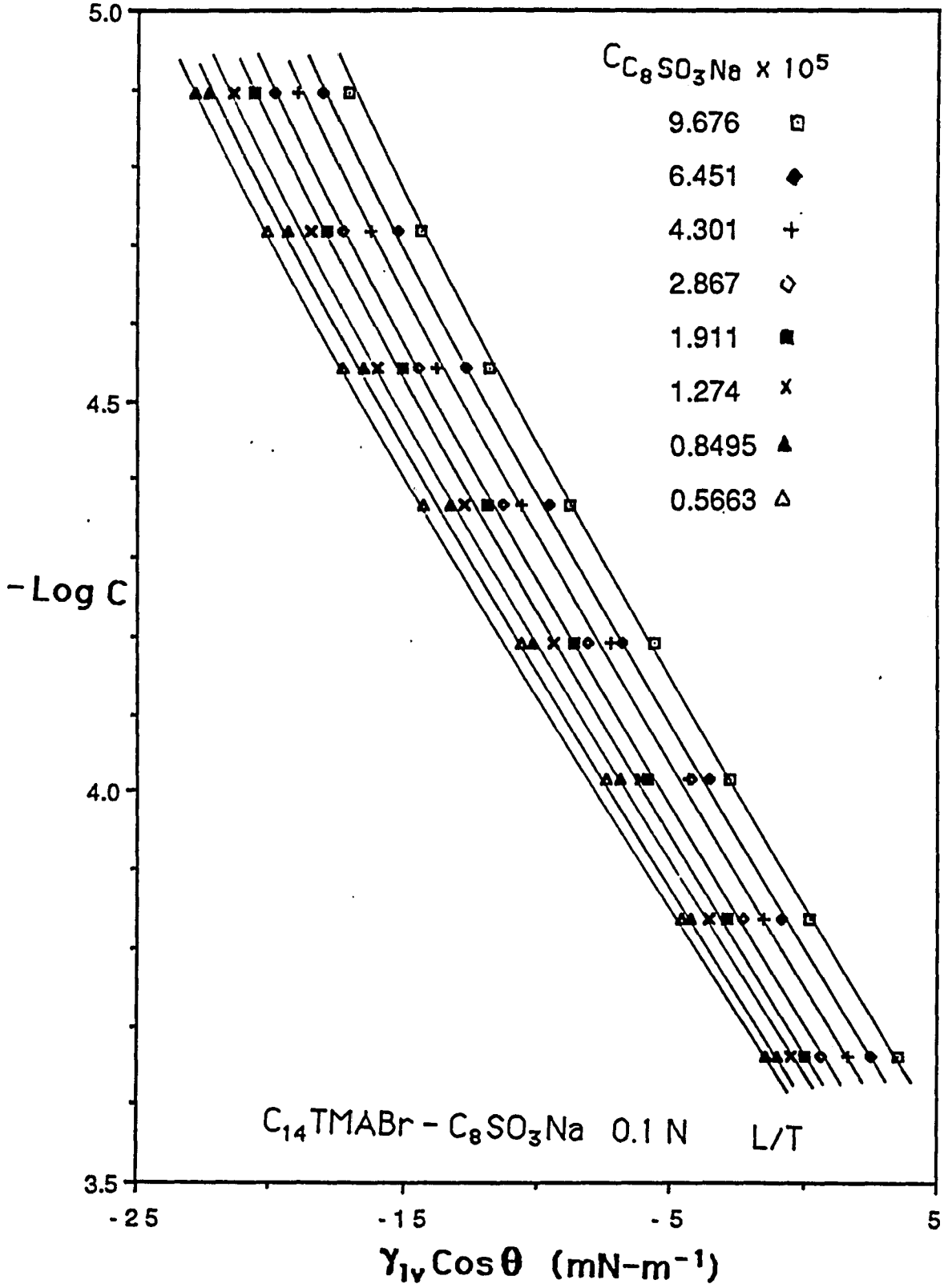
5.0
4.5
4.0
3.5
-Log C
$C_{C_8SO_3Na}$ x 10^5
9.676
6.451
4.301
2.867
1.911
1.274
0.8495
0.5663
$C_{14}TMABr - C_8SO_3Na$ 0.1 N L/T
-25
-15
-5
5
$\gamma_{lv}\cos\theta$ (mN-m^{-1})

Figure 21

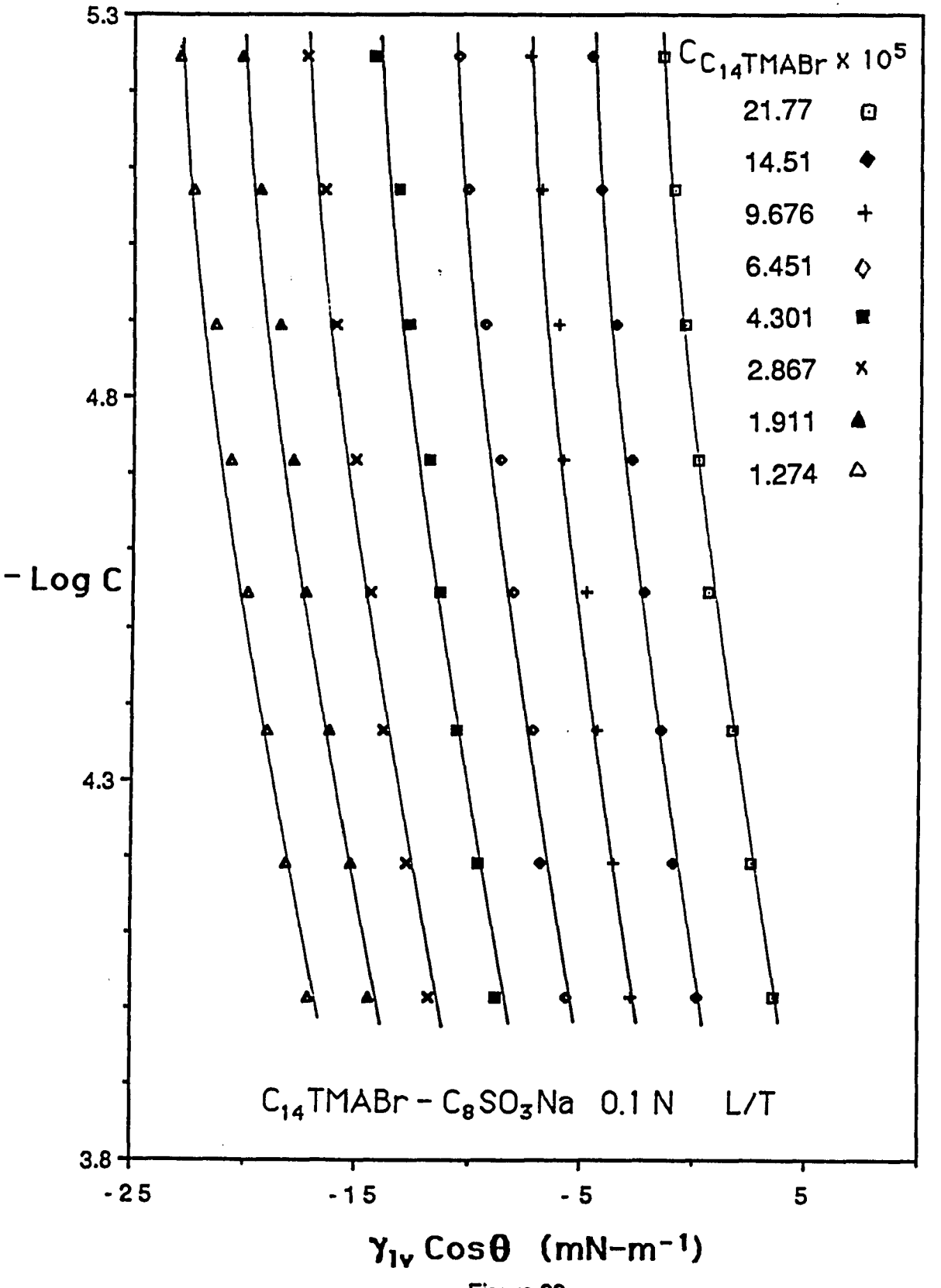
5.3
4.8
4.3
3.8
- Log C
-25
-15
-5
5
γ_{lv} Cosθ (mN-m^{-1})
$C_{C_{14}TMABr}$ x 10^5
21.77
14.51
9.676
6.451
4.301
2.867
1.911
1.274
$C_{14}TMABr - C_8SO_3Na$ 0.1 N L/T

Figure 22

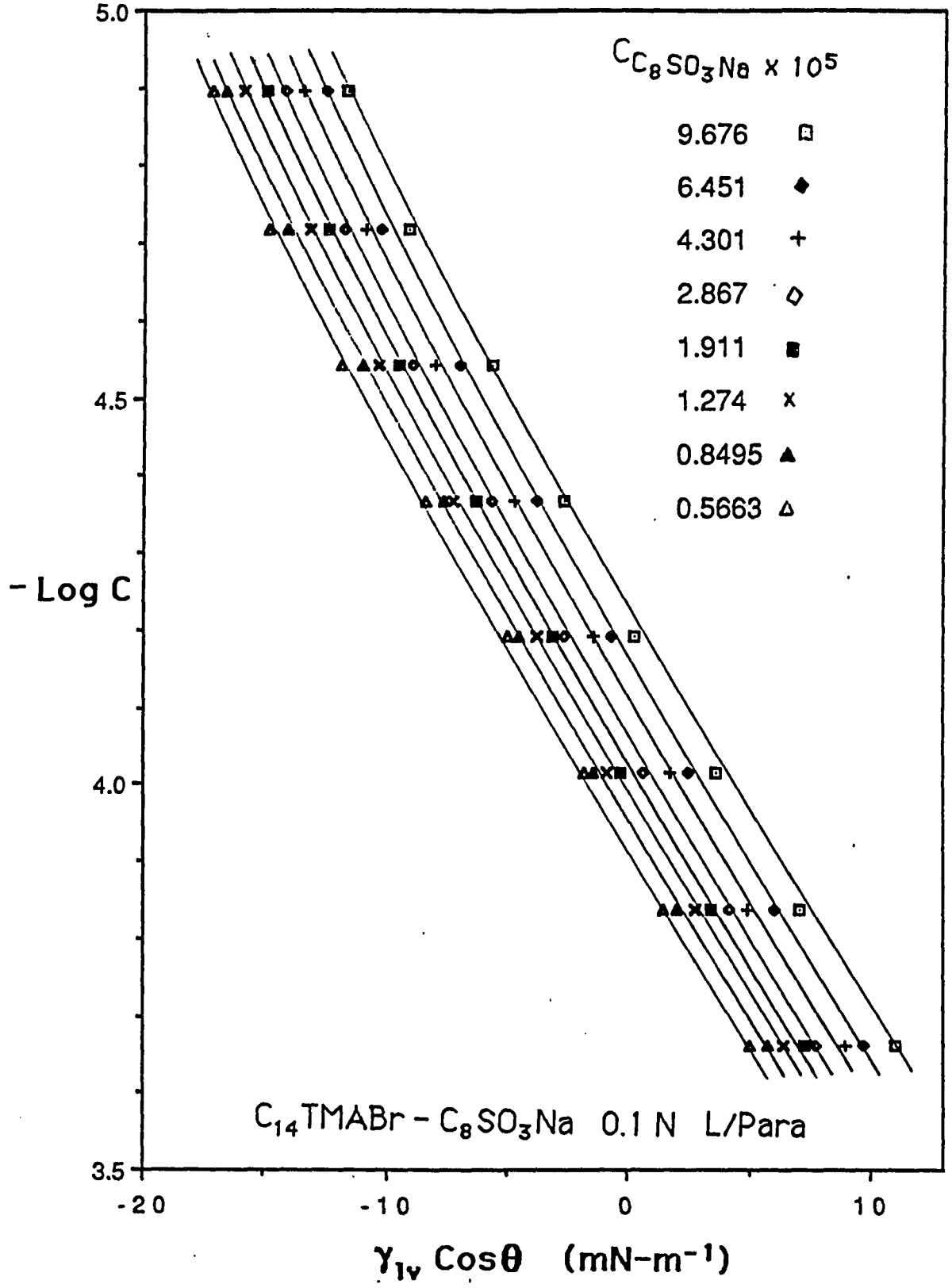
5.0
4.5
4.0
3.5
- Log C
-20
-10
0
10
γ_{lv} Cosθ (mN-m^{-1})
$C_{C_8SO_3Na}$ x 10^5
9.676
6.451
4.301
2.867
1.911
1.274
0.8495
0.5663
C_{14}TMABr - C_8SO_3Na 0.1 N L/Para

Figure 23

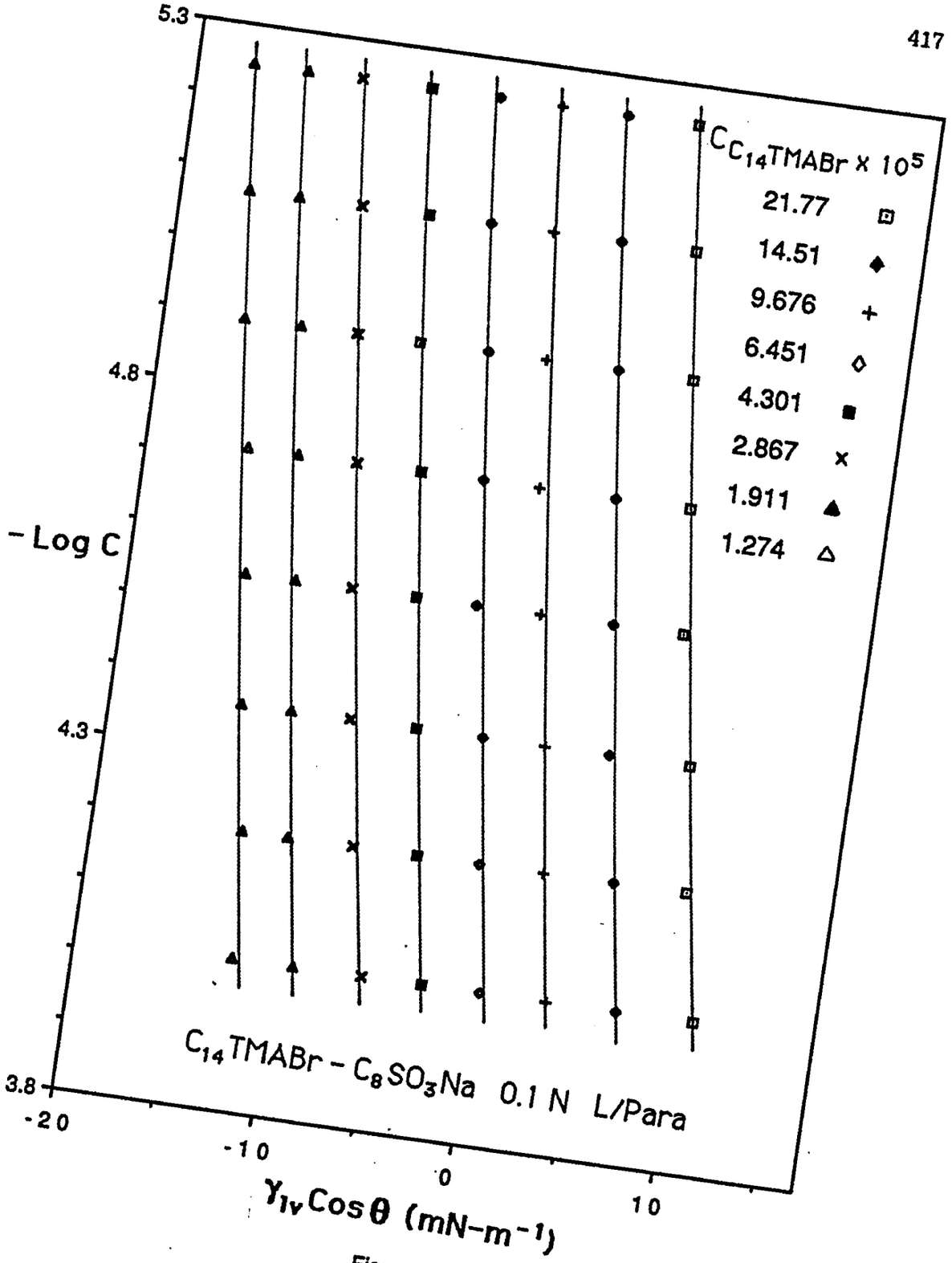
5.3
4.8
4.3
3.8
- Log C
-20
-10
0
10
γ_{lv} Cos θ (mN-m^{-1})
$C_{14}TMABr - C_8SO_3Na$ 0.1 N L/Para
$C_{C_{14}TMABr} \times 10^5$
21.77
14.51
9.676
6.451
4.301
2.867
1.911
1.274

Figure 24

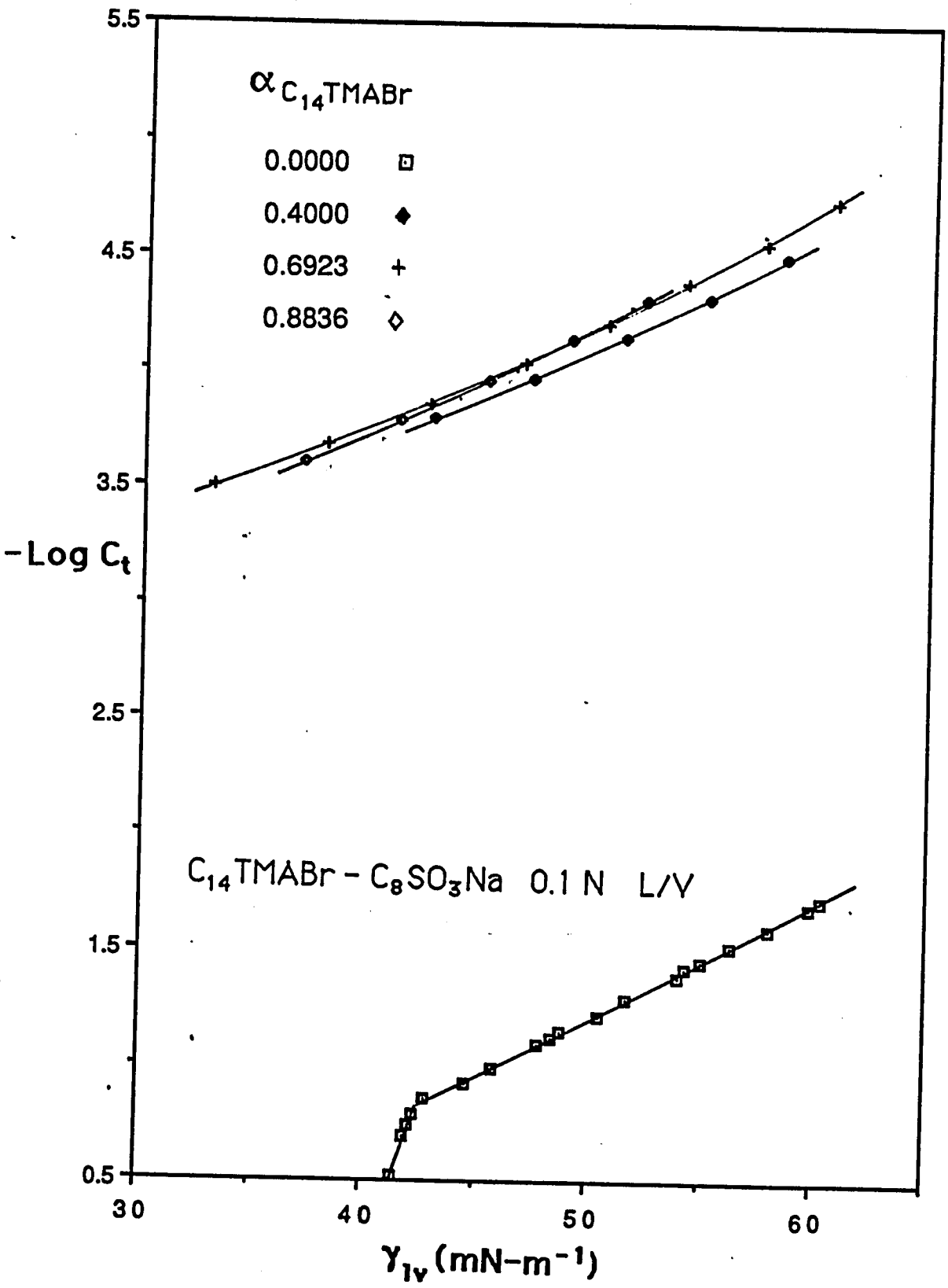
α C14TMABr
0.0000
0.4000
0.6923
0.8836
C14TMABr - C8SO3Na 0.1 N L/V
-Log Ct
γlv (mN-m-1)
5.5
4.5
3.5
2.5
1.5
0.5
30
40
50
60

Figure 25

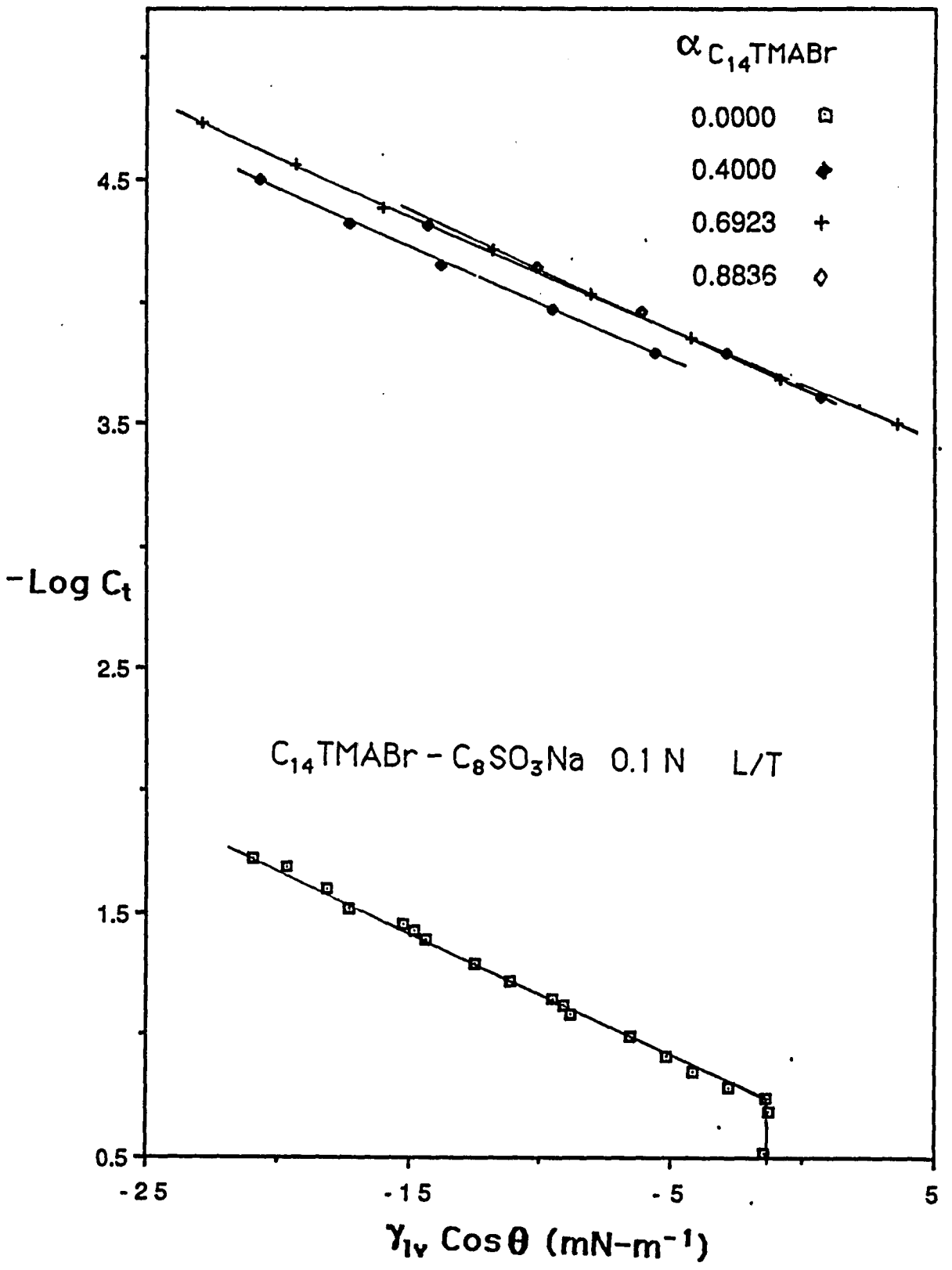
α C14TMABr
0.0000
0.4000
0.6923
0.8836
4.5
3.5
2.5
1.5
0.5
-Log Ct
C14TMABr - C8SO3Na 0.1 N L/T
-25
-15
-5
5
γlv Cos θ (mN-m-1)

Figure 26

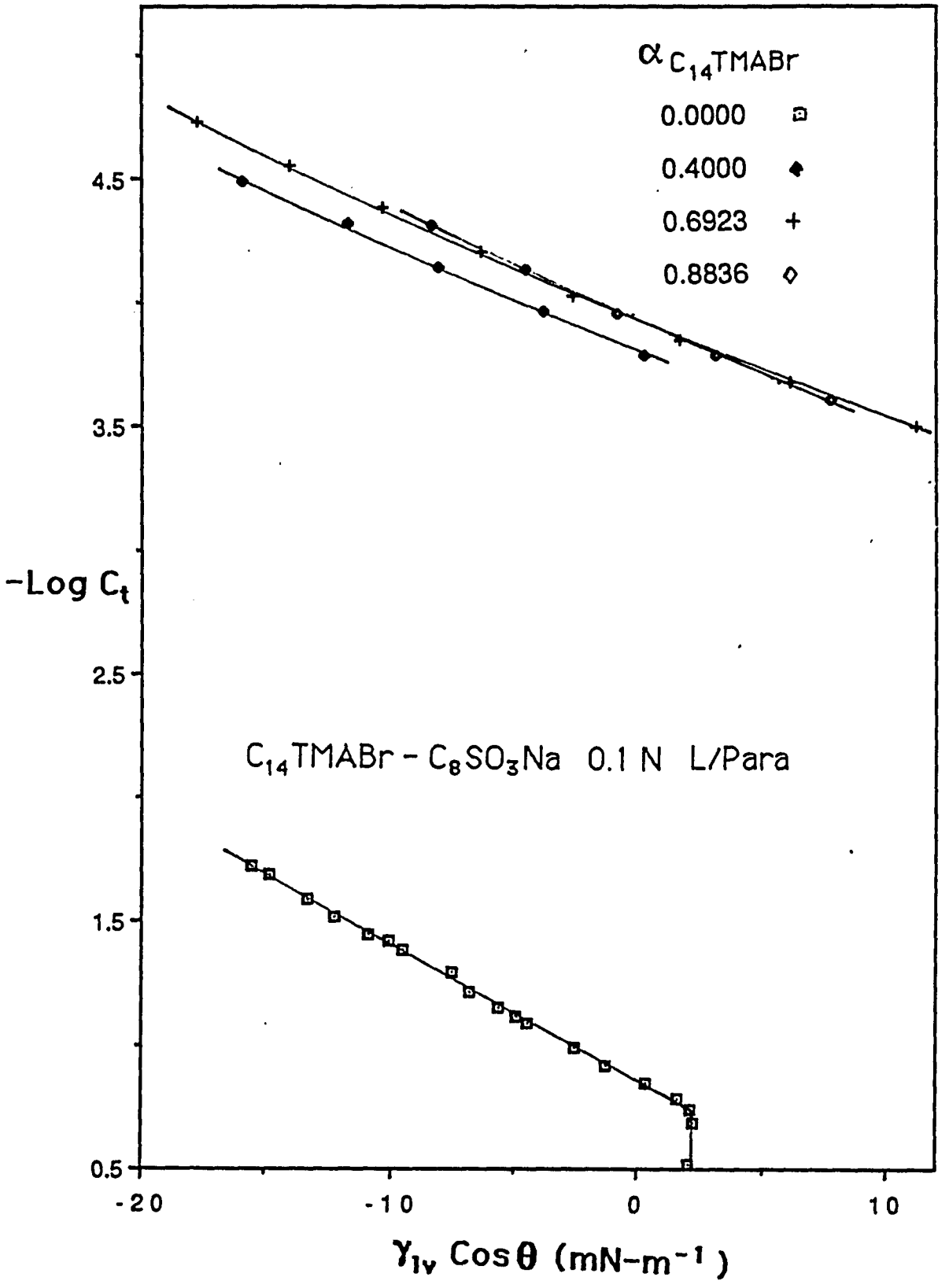
α C14TMABr
0.0000
0.4000
0.6923
0.8836
4.5
3.5
2.5
1.5
0.5
-Log Ct
C14TMABr - C8SO3Na 0.1 N L/Para
-20
-10
0
10
γlv Cos θ (mN-m-1)

Figure 27

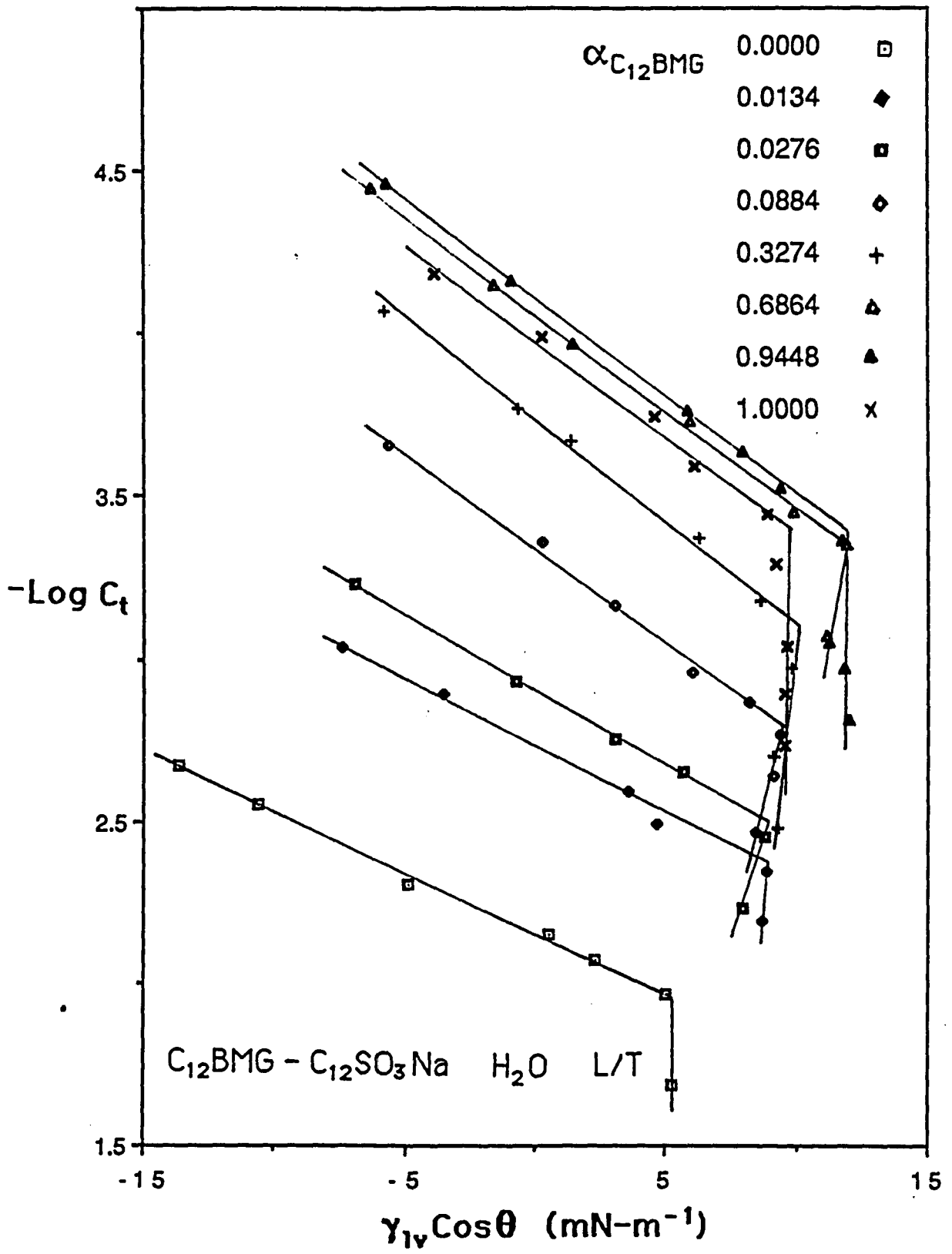
$\alpha_{C_{12}BMG}$
0.0000
0.0134
0.0276
0.0884
0.3274
0.6864
0.9448
1.0000
4.5
3.5
2.5
1.5
-Log C_t
-15
-5
5
15
$\gamma_{lv}Cos\theta$ (mN-m^{-1})
$C_{12}BMG - C_{12}SO_3Na$ H_2O L/T

Figure 28

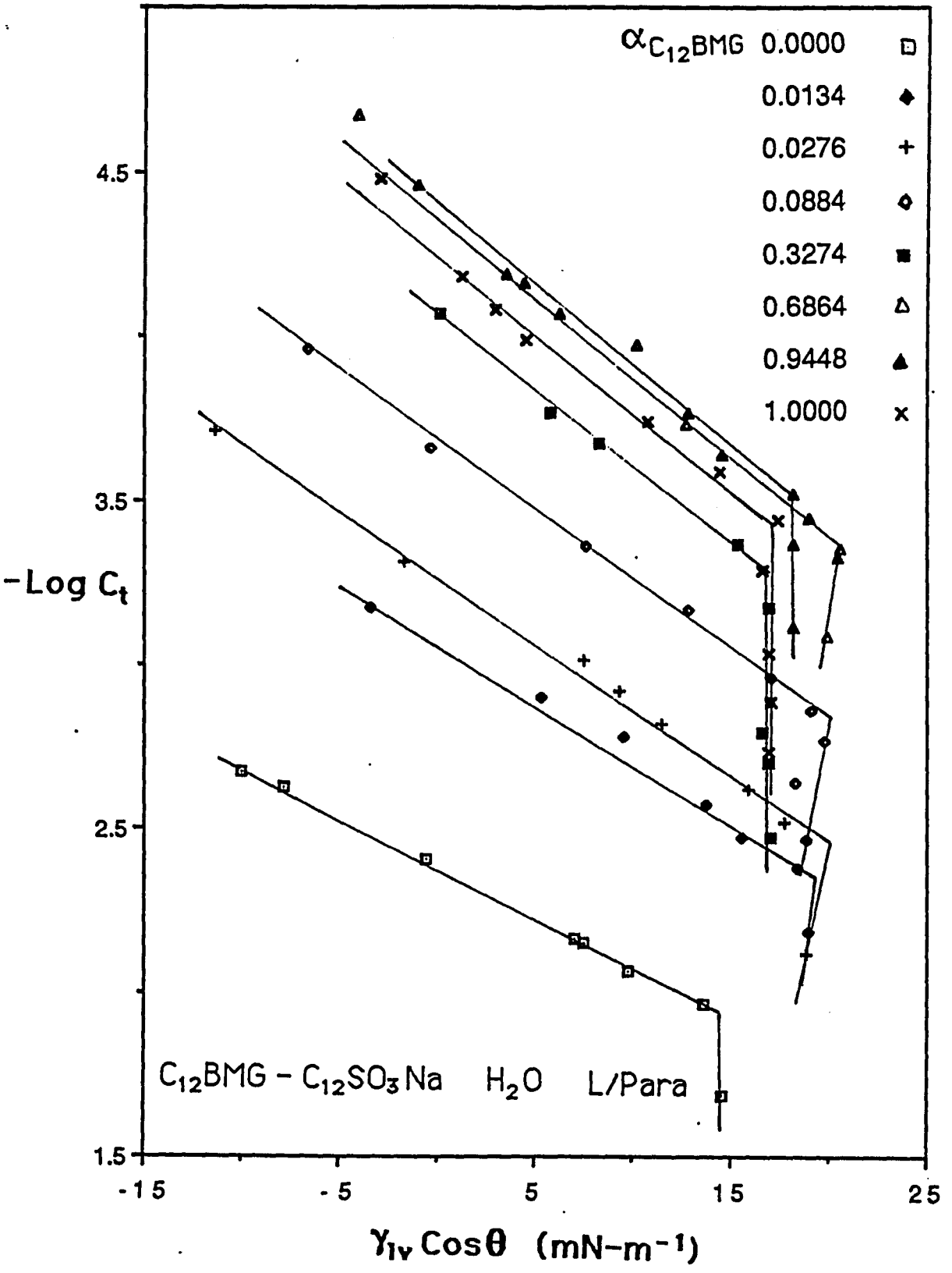
$\alpha_{C_{12}BMG}$ 0.0000
0.0134
0.0276
0.0884
0.3274
0.6864
0.9448
1.0000
4.5
3.5
2.5
1.5
-Log C_t
$C_{12}BMG - C_{12}SO_3Na$ H_2O L/Para
-15
-5
5
15
25
$\gamma_{lv} \cos\theta$ (mN-m^{-1})

Figure 29

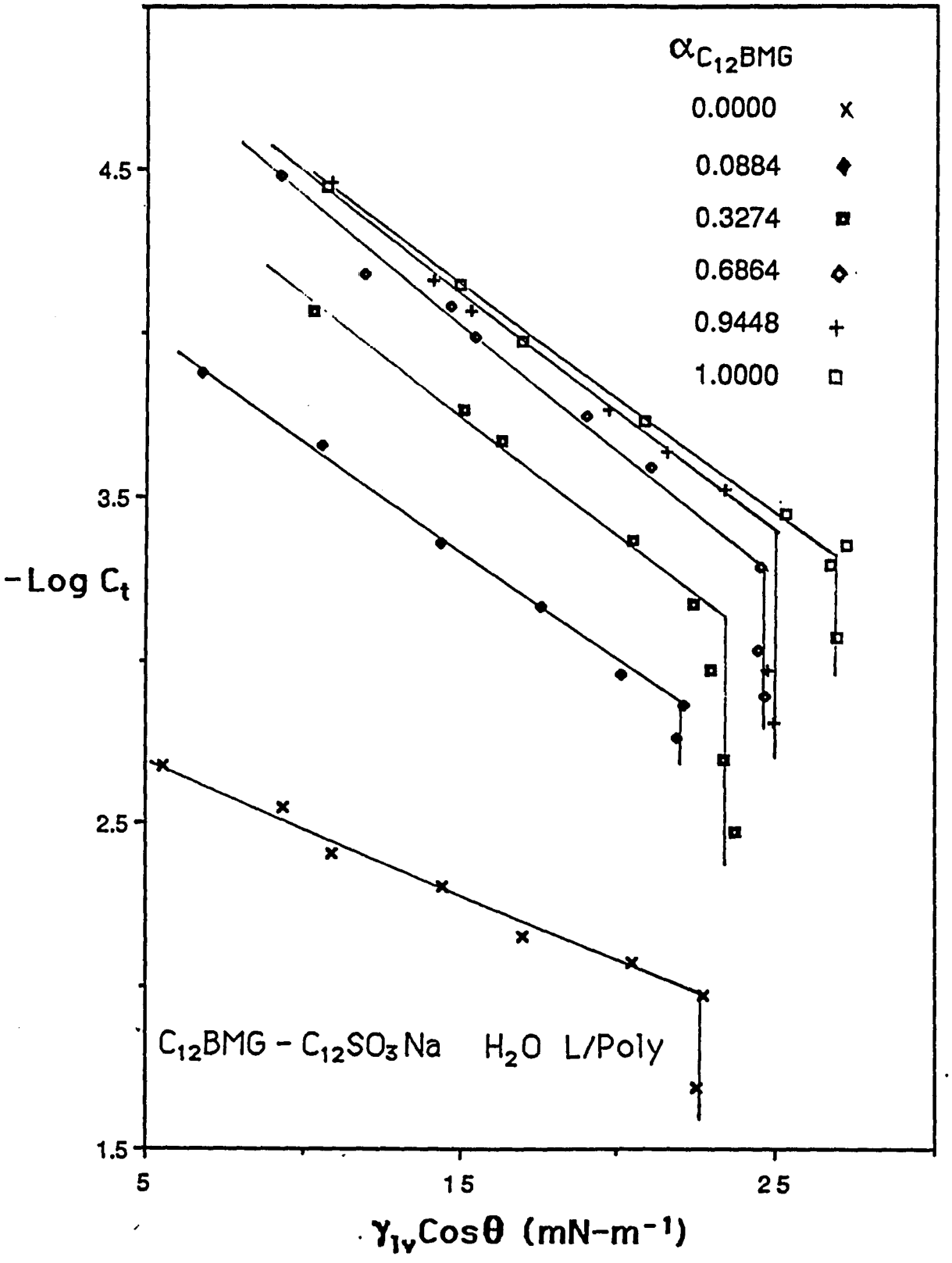
$\alpha_{C_{12}BMG}$
0.0000
0.0884
0.3274
0.6864
0.9448
1.0000
4.5
3.5
2.5
1.5
-Log C_t
$C_{12}BMG - C_{12}SO_3Na$ H_2O L/Poly
5
15
25
$\gamma_{lv}Cos\theta$ (mN-m^{-1})

Figure 30

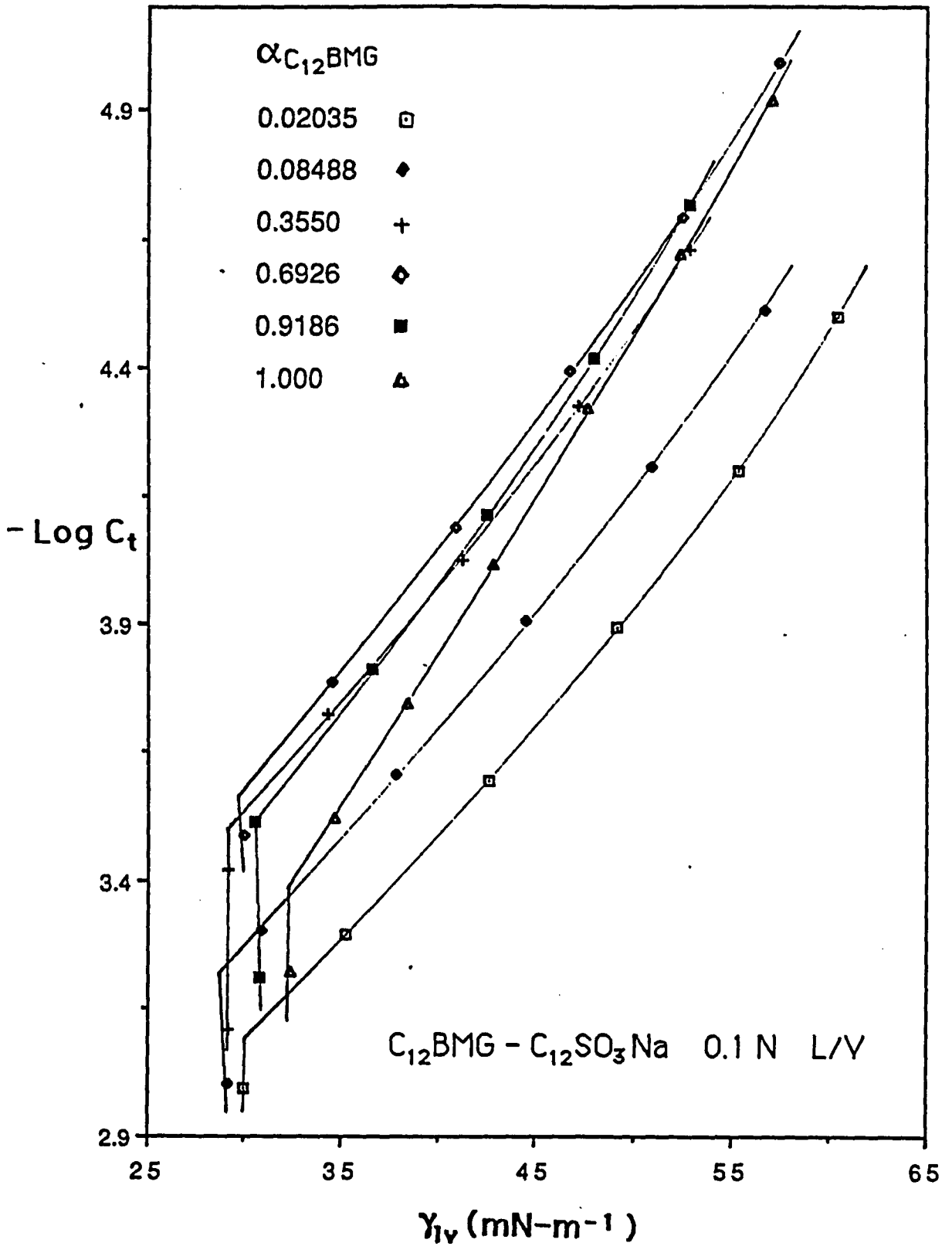
$\alpha_{C_{12}BMG}$
0.02035
0.08488
0.3550
0.6926
0.9186
1.000
4.9
4.4
3.9
3.4
2.9
- Log C_t
25
35
45
55
65
γ_{lv} (mN-m^{-1})
$C_{12}BMG - C_{12}SO_3Na$ 0.1 N L/V

Figure 31

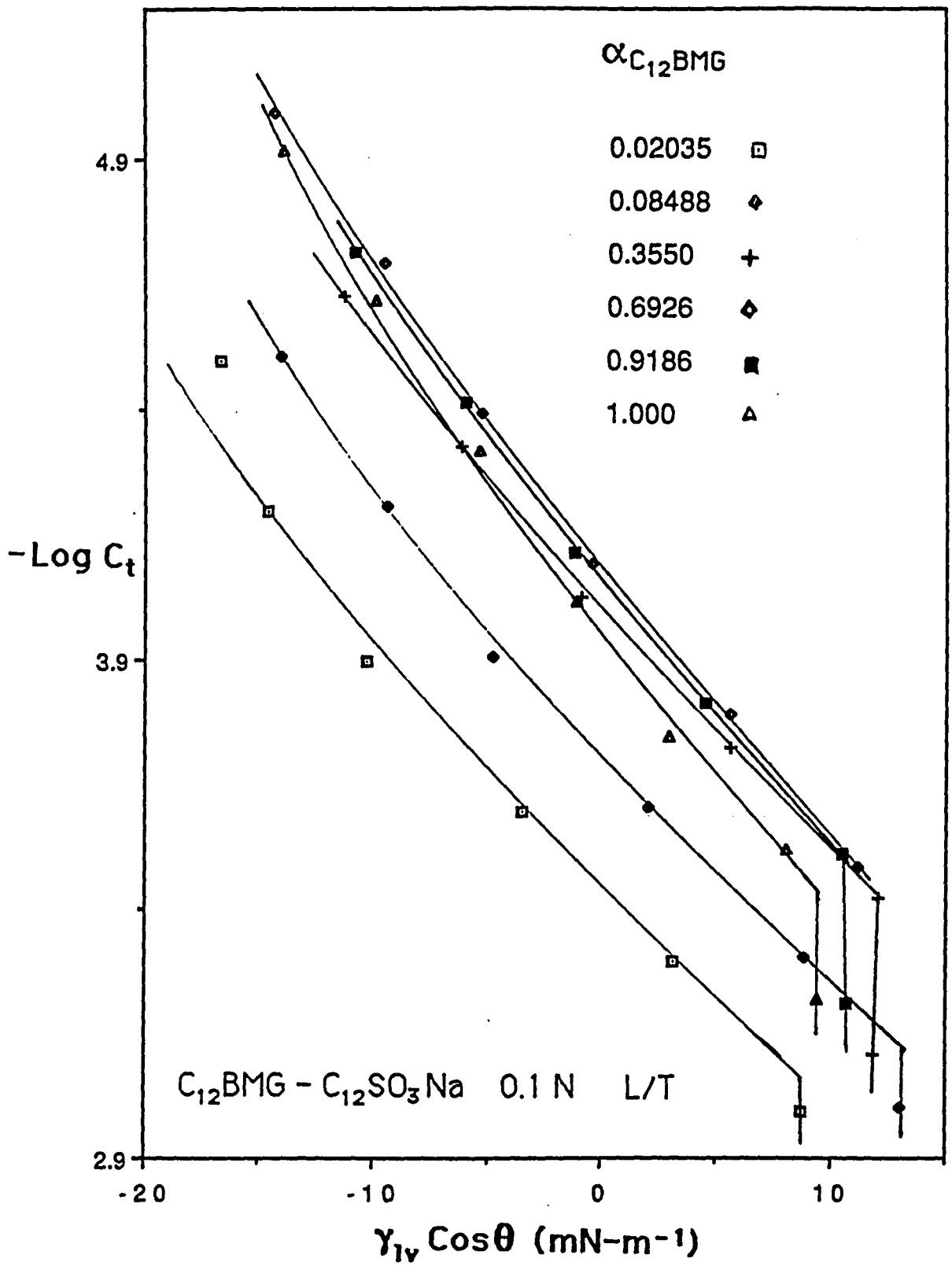
$\alpha_{C_{12}BMG}$
0.02035
0.08488
0.3550
0.6926
0.9186
1.000
4.9
3.9
2.9
-Log C_t
$C_{12}BMG - C_{12}SO_3Na$ 0.1 N L/T
-20
-10
0
10
γ_{lv} Cosθ (mN-m^{-1})

Figure 32

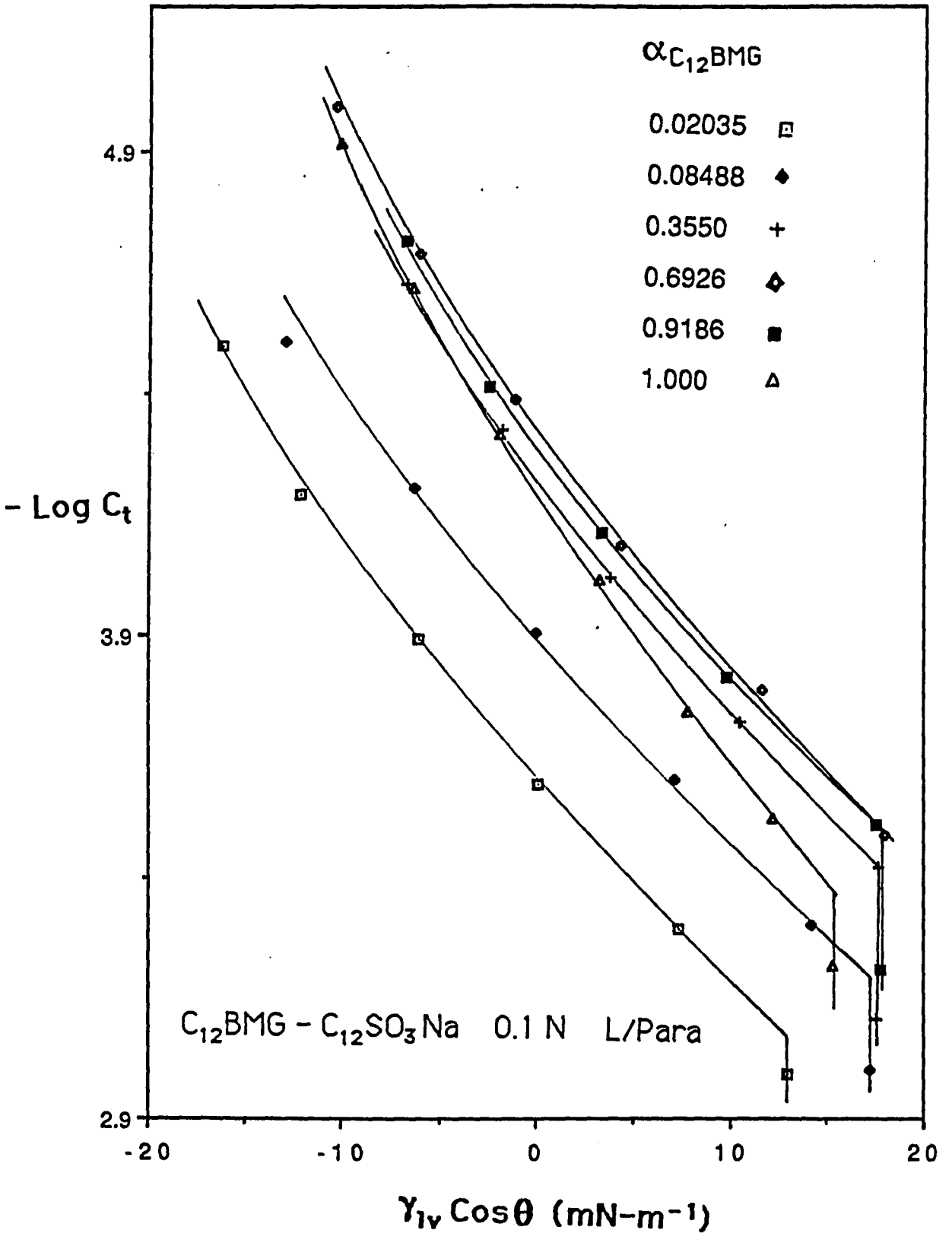
$\alpha_{C_{12}BMG}$
0.02035
0.08488
0.3550
0.6926
0.9186
1.000
4.9
3.9
2.9
- Log C_t
$C_{12}BMG - C_{12}SO_3Na$ 0.1 N L/Para
-20
-10
0
10
20
$\gamma_{lv} \cos\theta$ (mN-m^{-1})

Figure 33

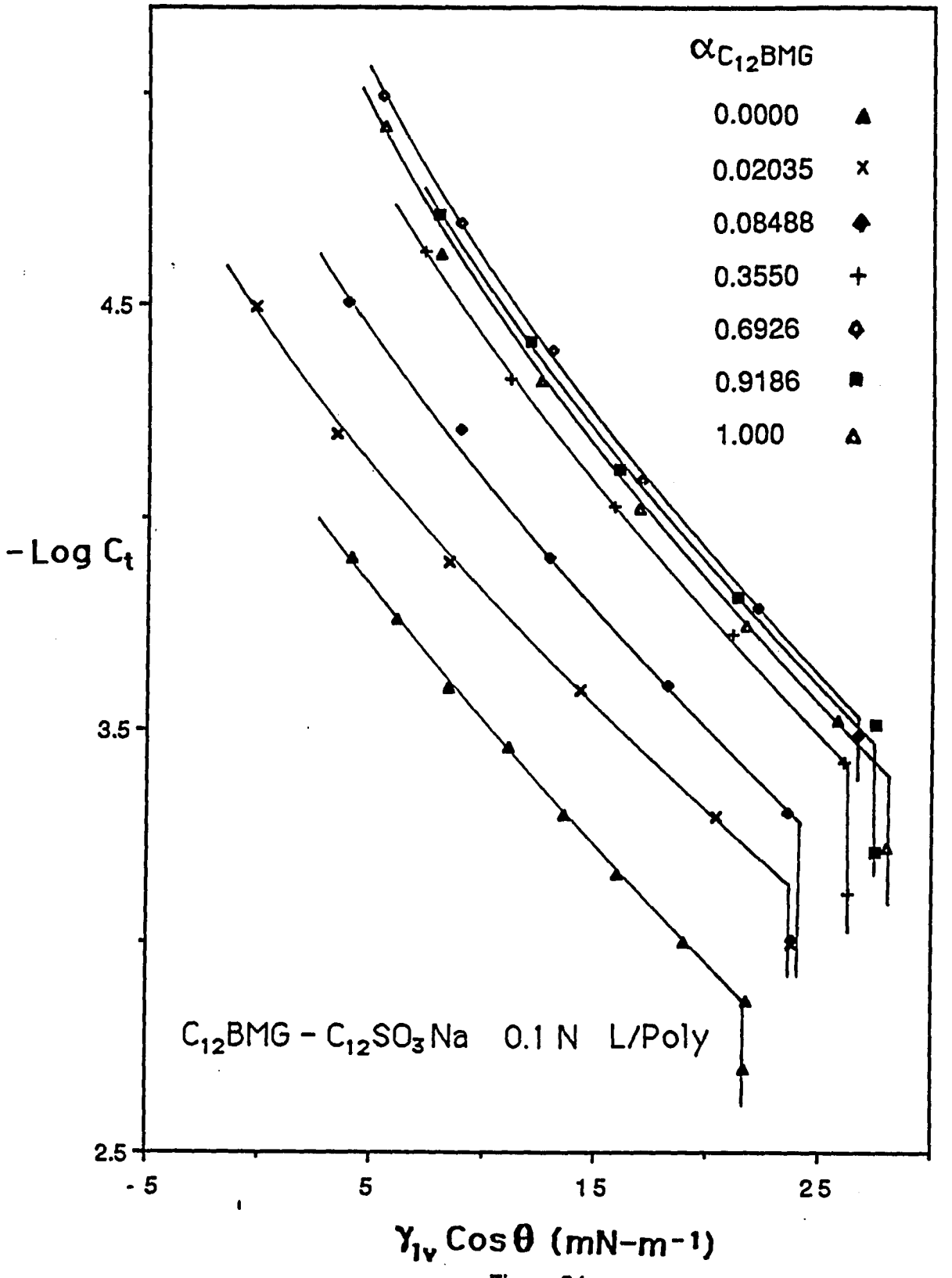
$\alpha_{C_{12}BMG}$
0.0000
0.02035
0.08488
0.3550
0.6926
0.9186
1.000
-Log C_t
4.5
3.5
2.5
$C_{12}BMG - C_{12}SO_3Na$ 0.1 N L/Poly
-5
5
15
25
$\gamma_{lv} \cos\theta$ (mN-m^{-1})

Figure 34

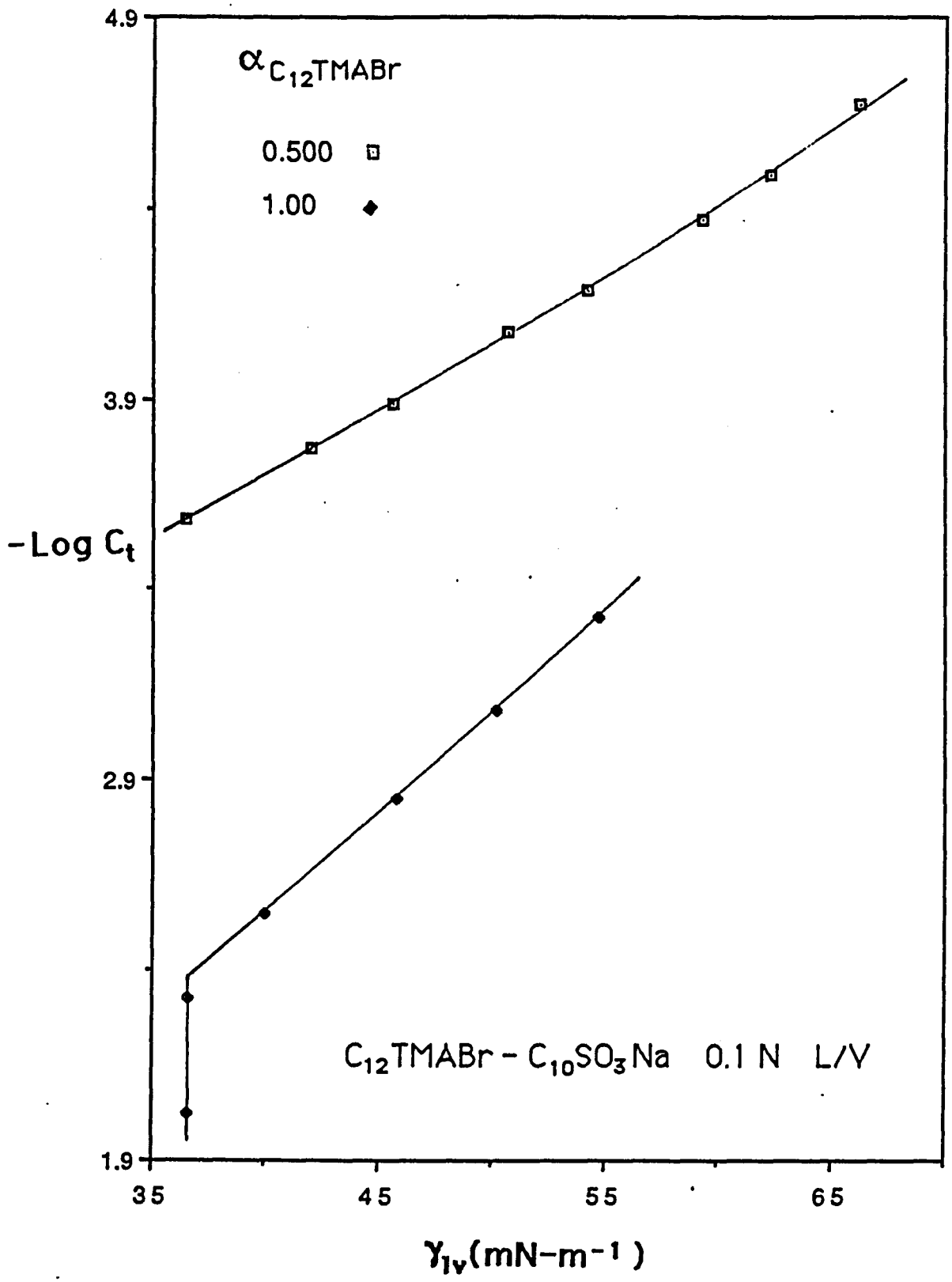
4.9
3.9
2.9
1.9
-Log C_t
$\alpha_{C_{12}TMABr}$
0.500
1.00
$C_{12}TMABr - C_{10}SO_3Na$ 0.1 N L/V
35
45
55
65
$\gamma_{lv}(mN-m^{-1})$

Figure 35

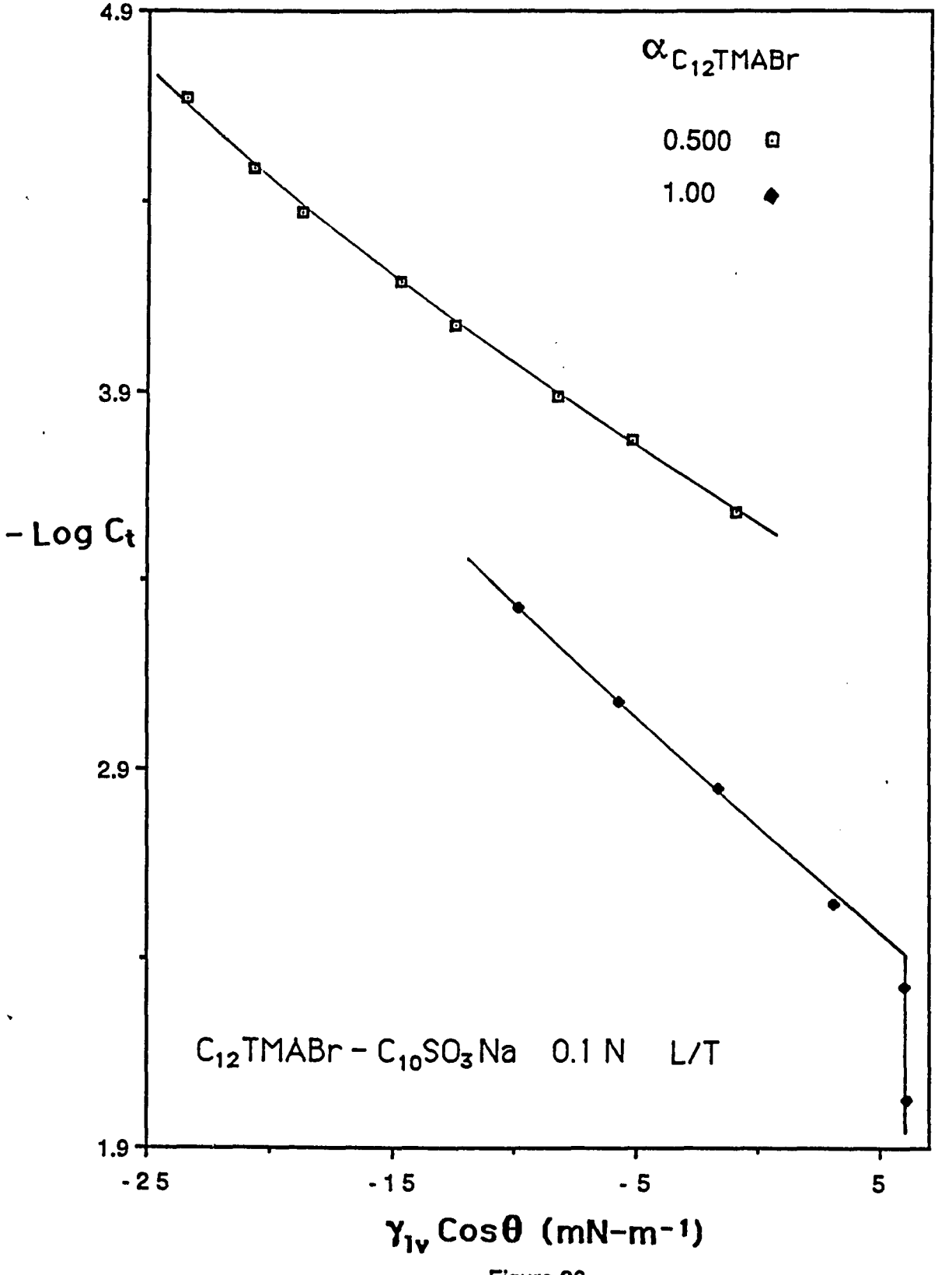
4.9
3.9
2.9
1.9
- Log C_t
$\alpha_{C_{12}TMABr}$
0.500
1.00
$C_{12}TMABr - C_{10}SO_3Na$ 0.1 N L/T
-25
-15
-5
5
$\gamma_{lv} \cos\theta$ (mN-m^{-1})

Figure 36

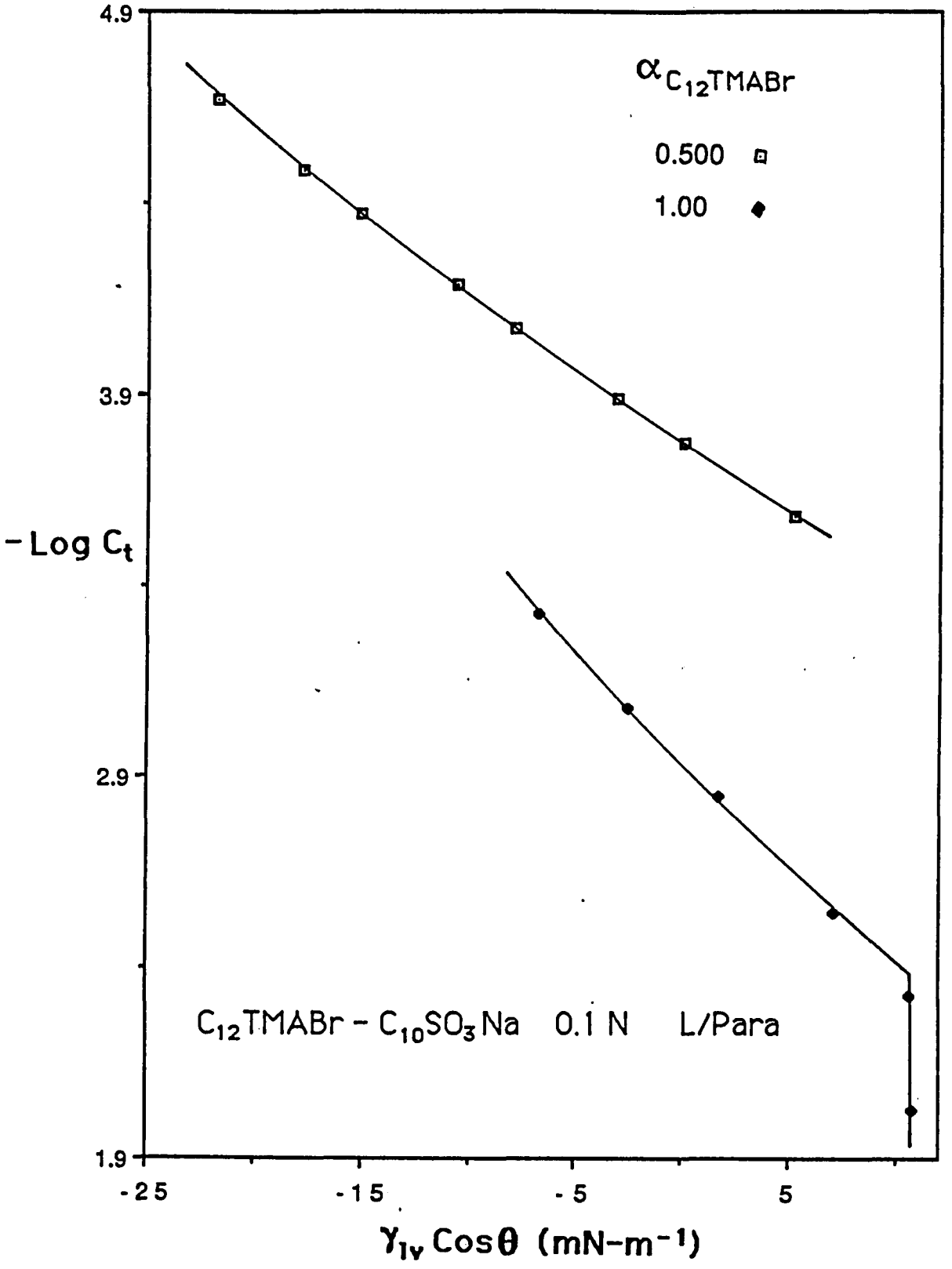
4.9
3.9
2.9
1.9
- Log C_t
$\alpha_{C_{12}TMABr}$
0.500
1.00
$C_{12}TMABr - C_{10}SO_3Na$ 0.1 N L/Para
-25
-15
-5
5
$\gamma_{lv} \cos\theta$ (mN-m^{-1})

Figure 37

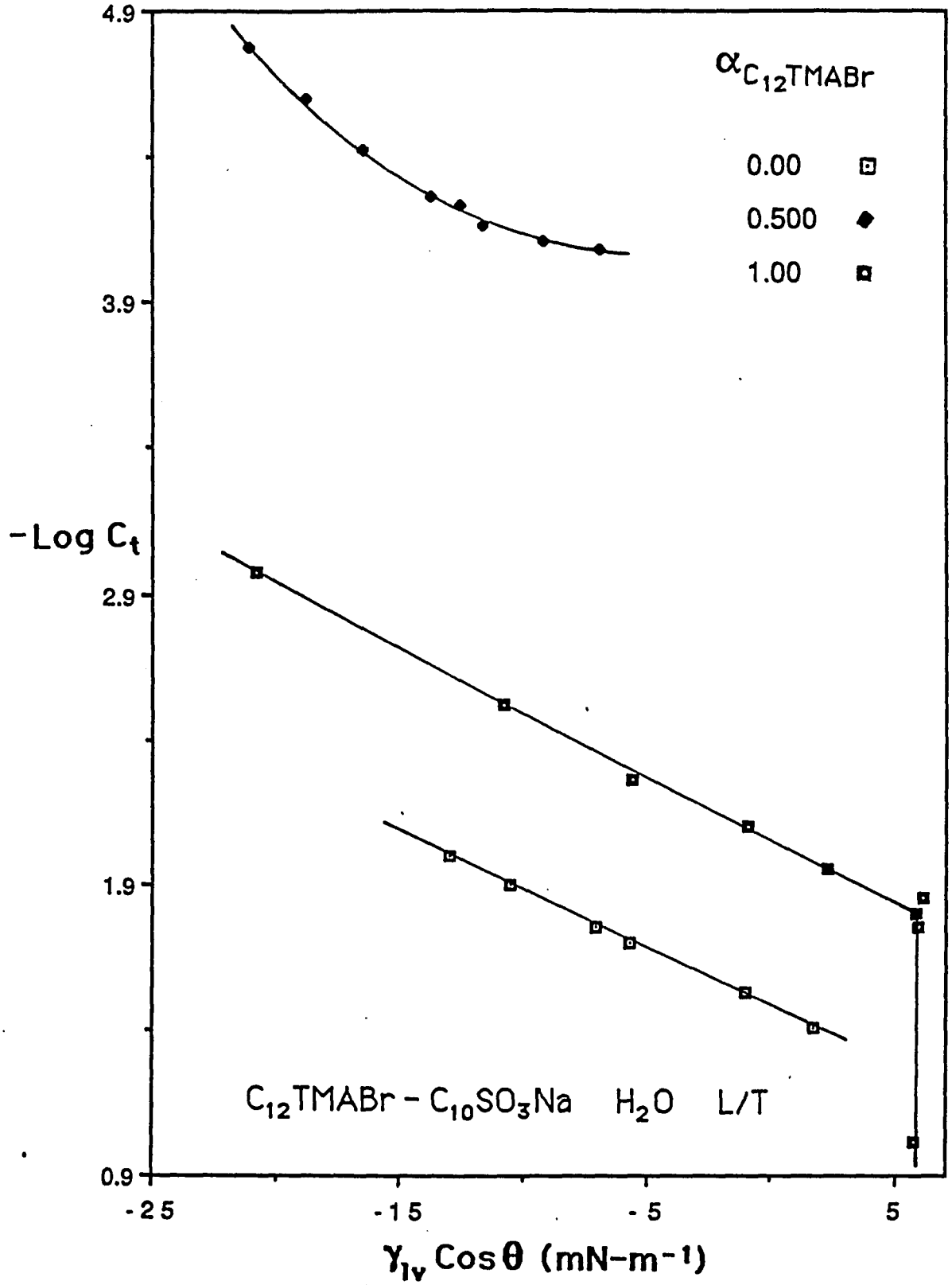
4.9
3.9
2.9
1.9
0.9
-Log C_t
$\alpha_{C_{12}TMABr}$
0.00
0.500
1.00
$C_{12}TMABr - C_{10}SO_3Na$ H_2O L/T
-25
-15
-5
5
$\gamma_{lv} \cos\theta$ (mN-m^{-1})

Figure 38

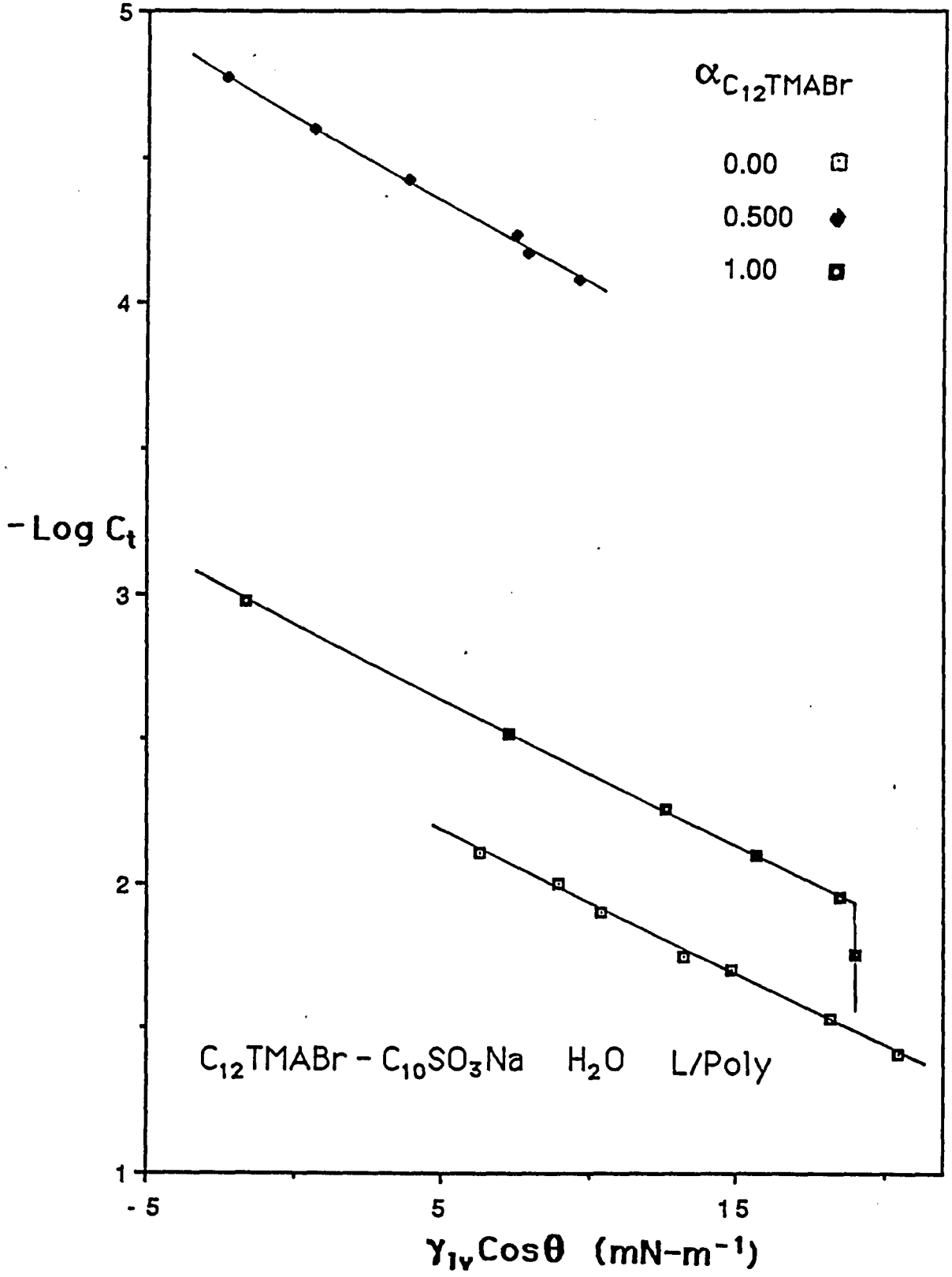
5
4
3
2
1
- Log C_t
$\alpha_{C_{12}TMABr}$
0.00
0.500
1.00
$C_{12}TMABr - C_{10}SO_3Na$ H_2O L/Poly
- 5
5
15
$\gamma_{lv}Cos\theta$ (mN-m^{-1})

Figure 39

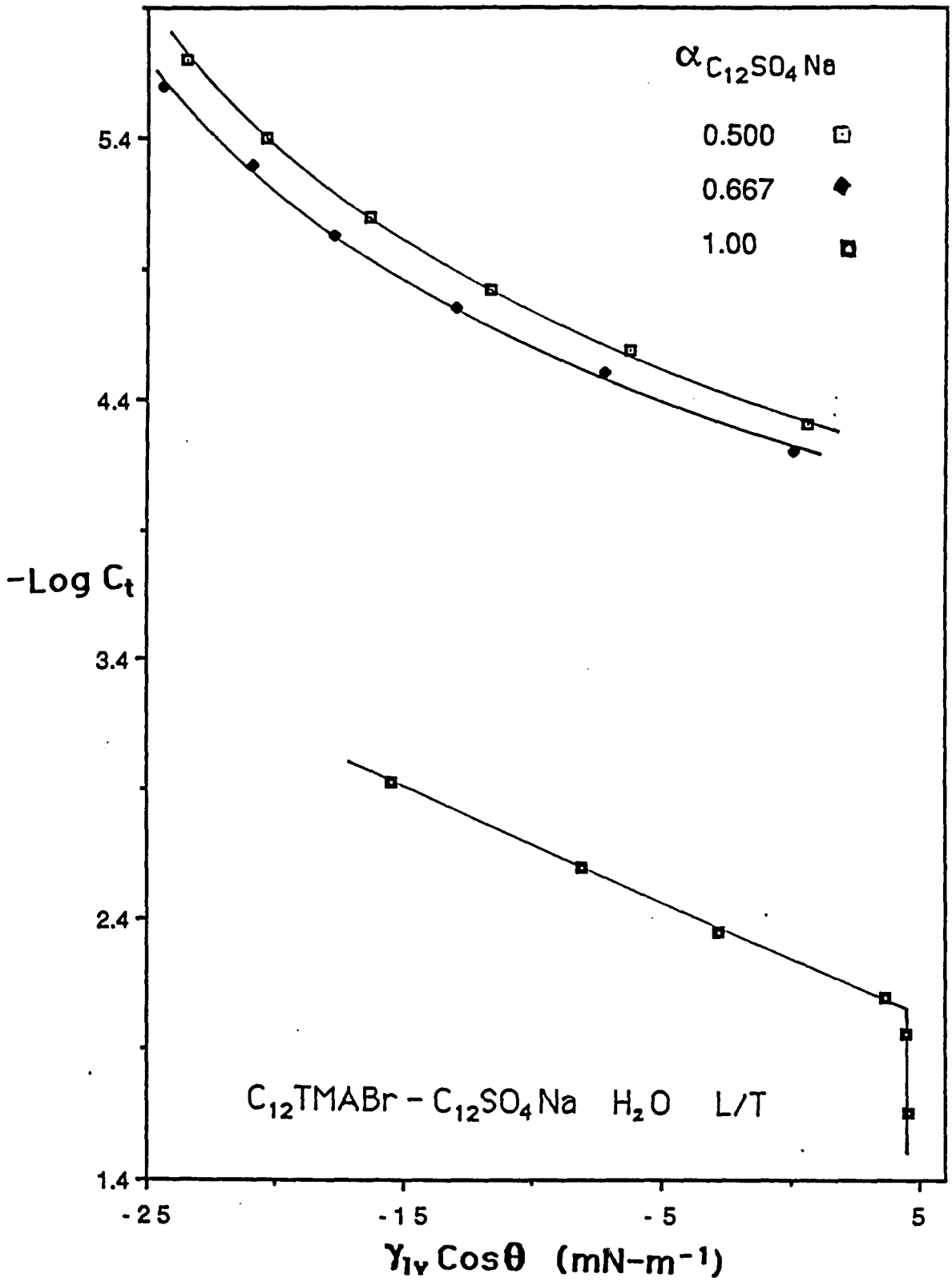
$\alpha_{C_{12}SO_4Na}$
0.500
0.667
1.00
5.4
4.4
3.4
2.4
1.4
-Log C_t
$C_{12}TMABr - C_{12}SO_4Na$ H_2O L/T
-25
-15
-5
5
γ_{lv} Cosθ (mN-m^{-1})

Figure 40

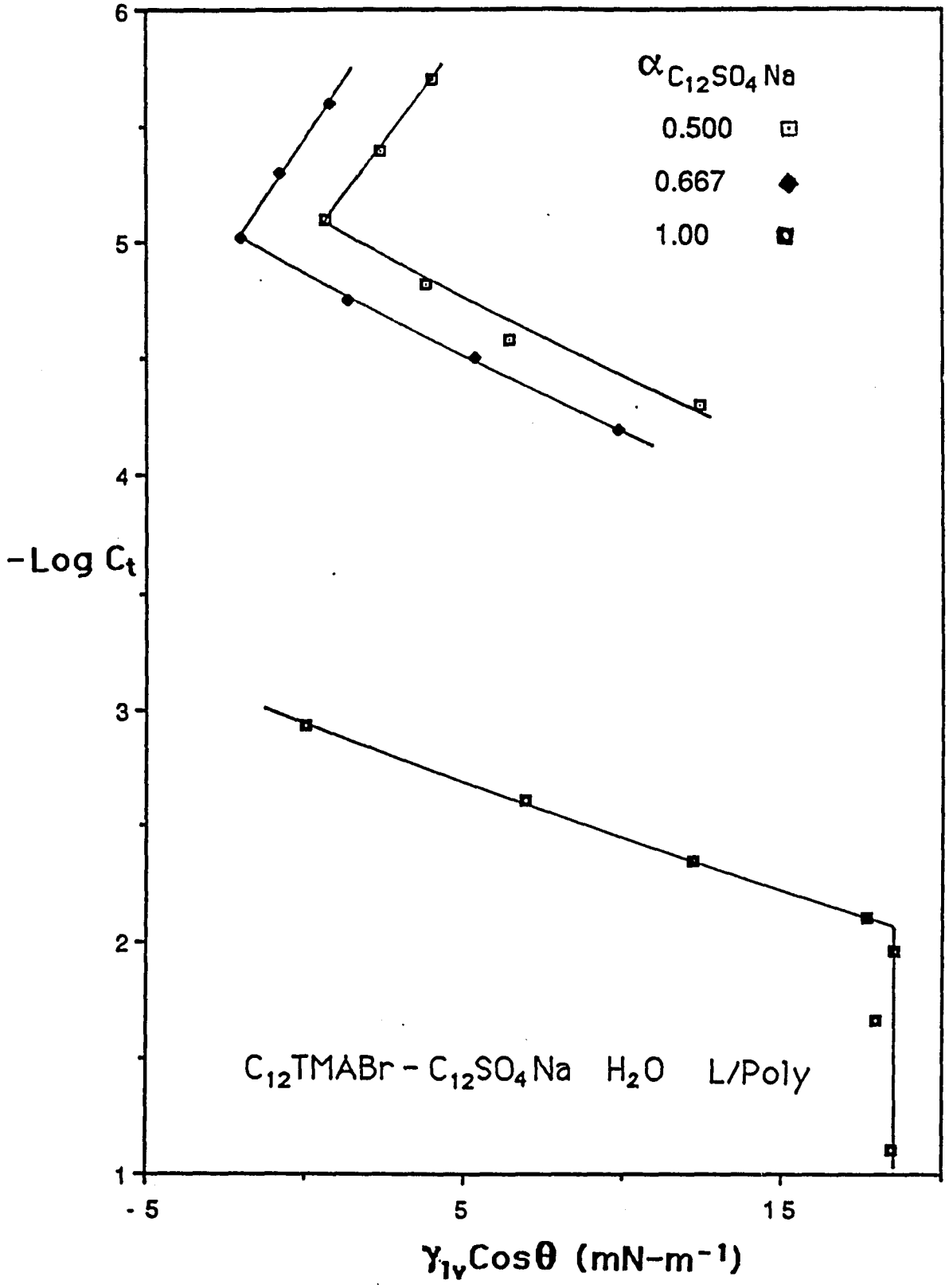
6
5
4
3
2
1
-Log C_t
$\alpha_{C_{12}SO_4Na}$
0.500
0.667
1.00
$C_{12}TMABr - C_{12}SO_4Na$ H_2O L/Poly
- 5
5
15
$\gamma_{lv}Cos\theta$ (mN-m^{-1})

Figure 41

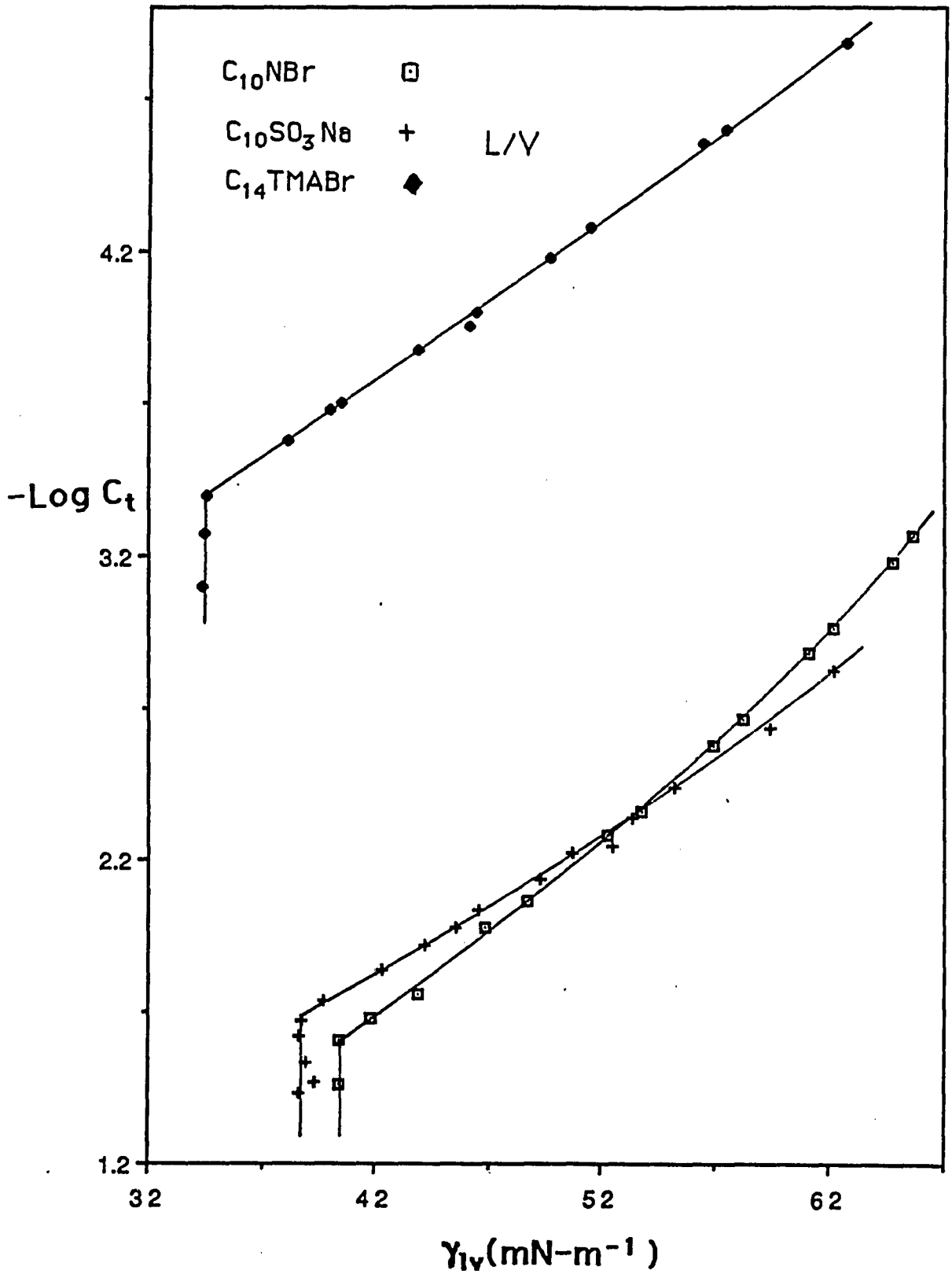
$C_{10}NBr$
$C_{10}SO_3Na$
$C_{14}TMABr$
L/V
-Log C_t
4.2
3.2
2.2
1.2
32
42
52
62
$\gamma_{lv}(mN-m^{-1})$

Figure 42

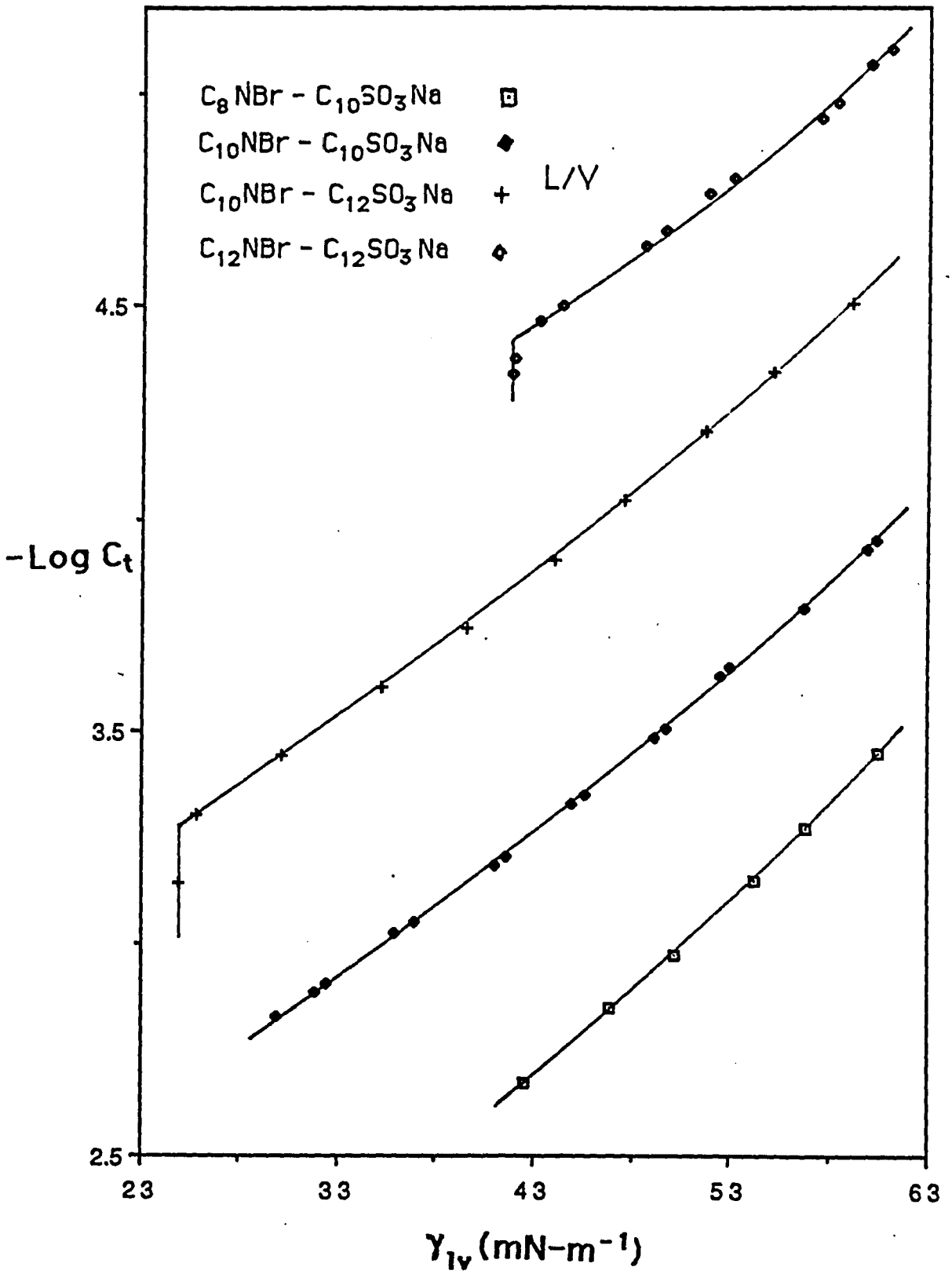
$C_8NBr - C_{10}SO_3Na$
$C_{10}NBr - C_{10}SO_3Na$
$C_{10}NBr - C_{12}SO_3Na$
$C_{12}NBr - C_{12}SO_3Na$
L/V
-Log C_t
4.5
3.5
2.5
23
33
43
53
63
γ_{lv} (mN-m^{-1})

Figure 43

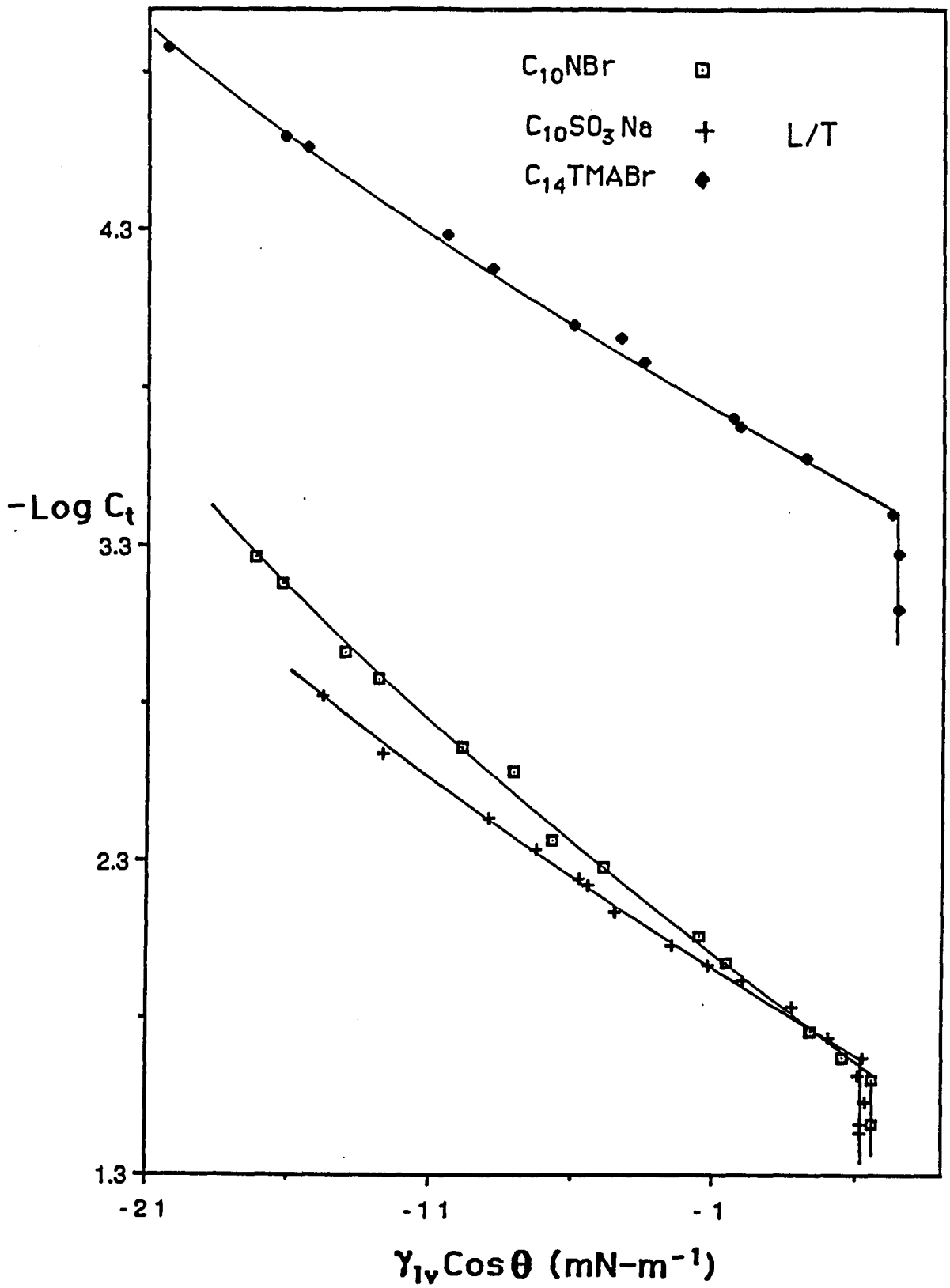
$C_{10}NBr$
$C_{10}SO_3Na$
$C_{14}TMABr$
L/T
4.3
3.3
2.3
1.3
-Log C_t
-2 1
-1 1
-1
$\gamma_{lv}Cos\theta$ (mN-m^{-1})

Figure 44

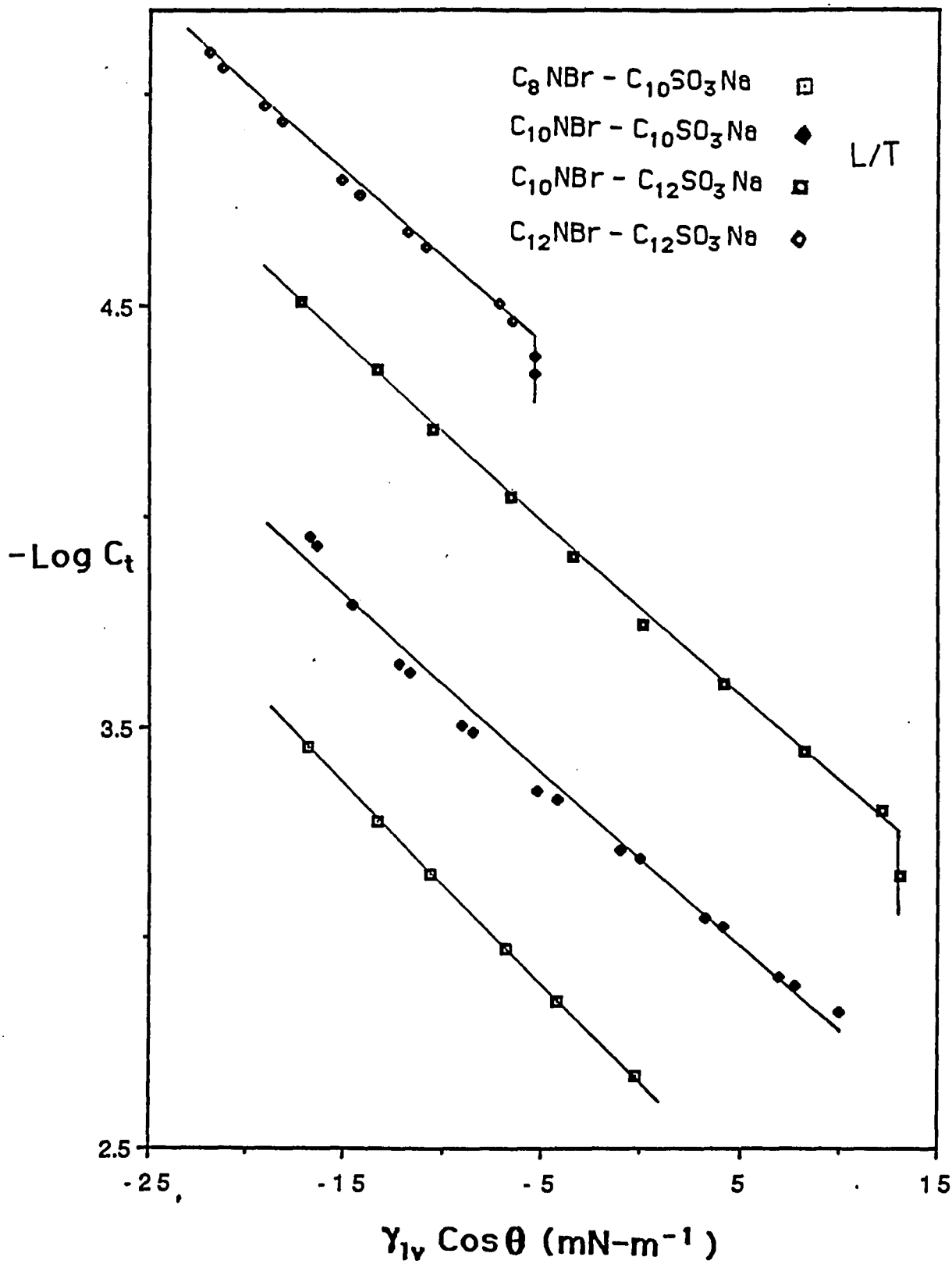
$C_8NBr - C_{10}SO_3Na$
$C_{10}NBr - C_{10}SO_3Na$
$C_{10}NBr - C_{12}SO_3Na$
$C_{12}NBr - C_{12}SO_3Na$
L/T
4.5
3.5
2.5
-Log C_t
-25
-15
-5
5
15
γ_{lv} Cos θ (mN-m^{-1})

Figure 45

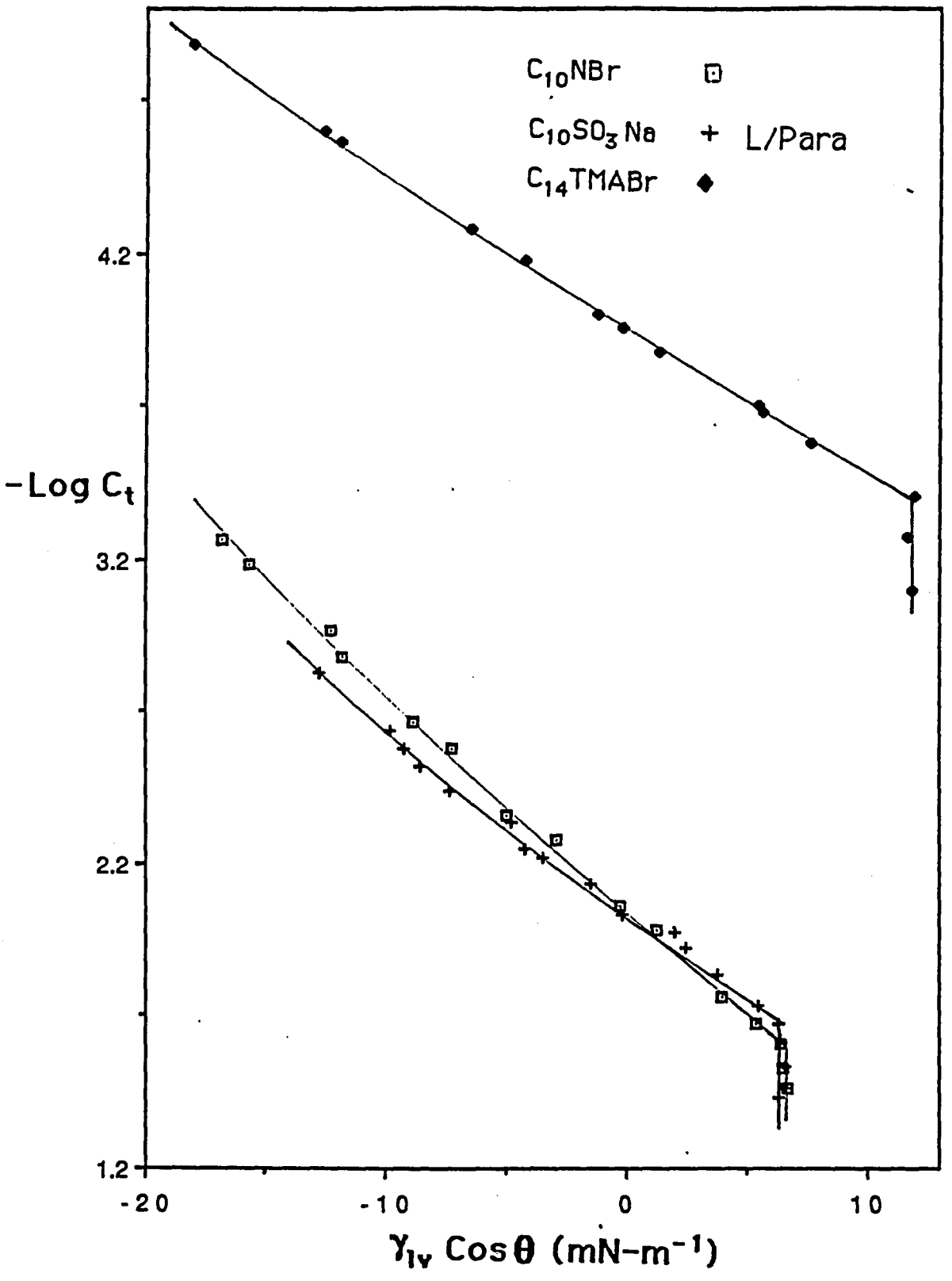
$C_{10}NBr$
$C_{10}SO_3Na$ + L/Para
$C_{14}TMABr$
4.2
3.2
2.2
1.2
-Log C_t
-20
-10
0
10
γ_{lv} Cos θ (mN-m^{-1})

Figure 46

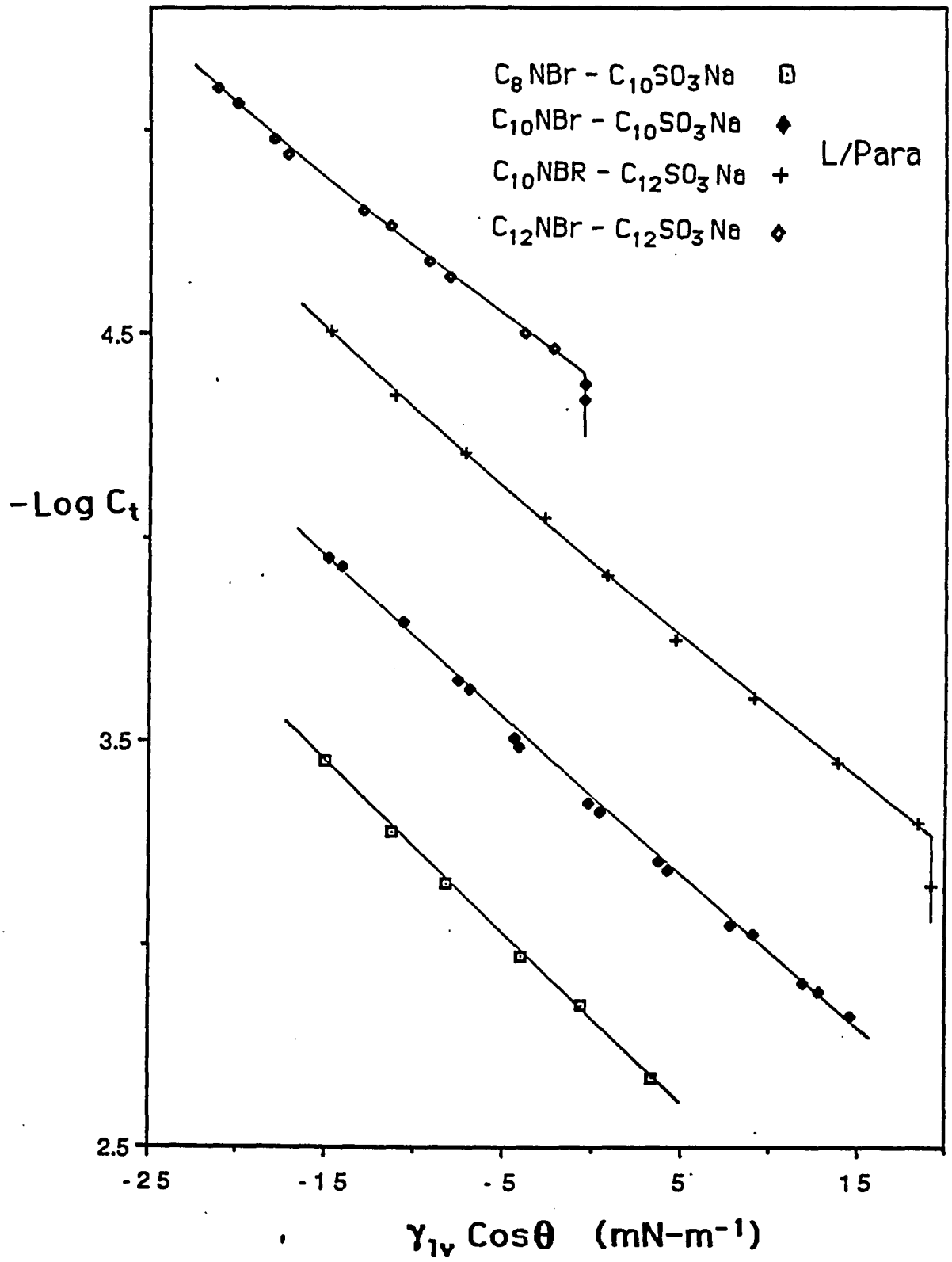
C8 NBr - C10SO3Na
C10NBr - C10SO3Na
C10NBR - C12SO3Na
C12NBr - C12SO3Na
L/Para
4.5
3.5
2.5
-Log Ct
-25
-15
-5
5
15
γ1v Cosθ (mN-m-1)

Figure 47

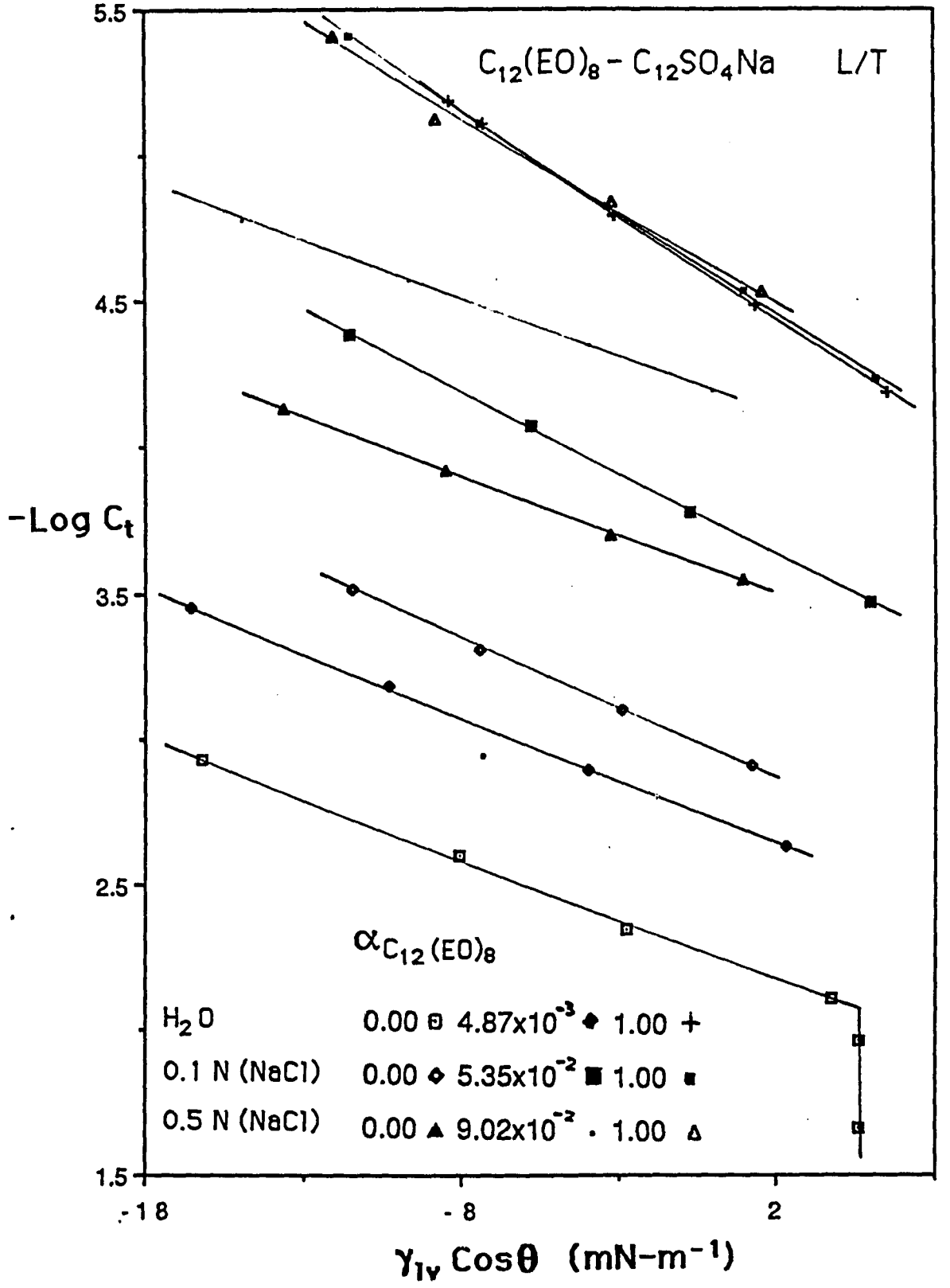
$C_{12}(EO)_8 - C_{12}SO_4Na$ L/T
-Log C_t
5.5
4.5
3.5
2.5
1.5
-18
-8
2
γ_{lv} Cosθ (mN-m^{-1})
$\alpha_{C_{12}(EO)_8}$
H_2O 0.00 ⊡ $4.87x10^{-3}$ ◆ 1.00 +
0.1 N (NaCl) 0.00 ◆ $5.35x10^{-2}$ ■ 1.00 ■
0.5 N (NaCl) 0.00 ▲ $9.02x10^{-2}$ • 1.00 Δ

Figure 48

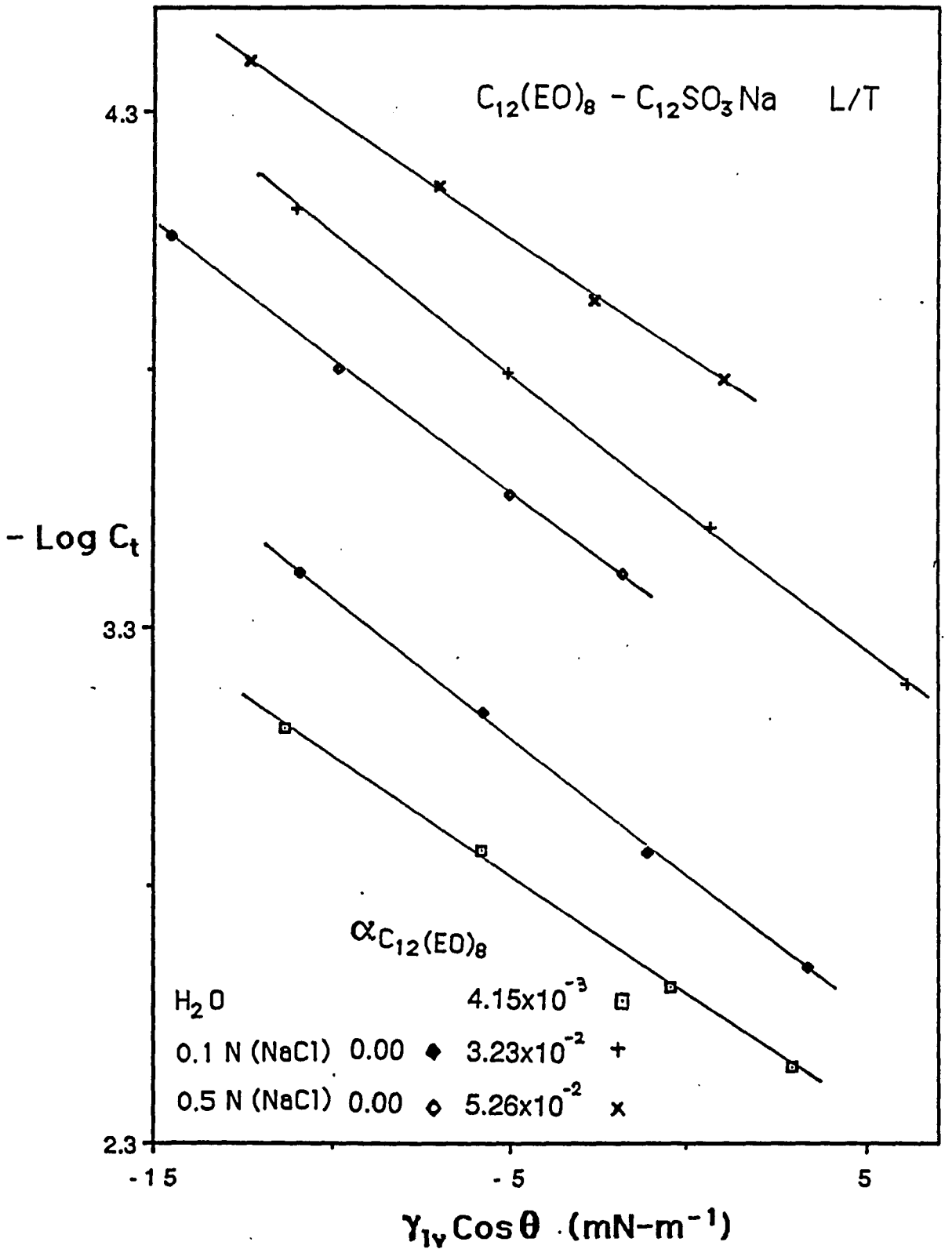
$C_{12}(EO)_8 - C_{12}SO_3Na$ L/T
4.3
3.3
2.3
- Log C_t
-15
-5
5
γ_{1v} Cos θ (mN-m^{-1})
$\alpha_{C_{12}(EO)_8}$
H_2O $4.15x10^{-3}$
0.1 N (NaCl) 0.00 $3.23x10^{-2}$
0.5 N (NaCl) 0.00 $5.26x10^{-2}$

Figure 49

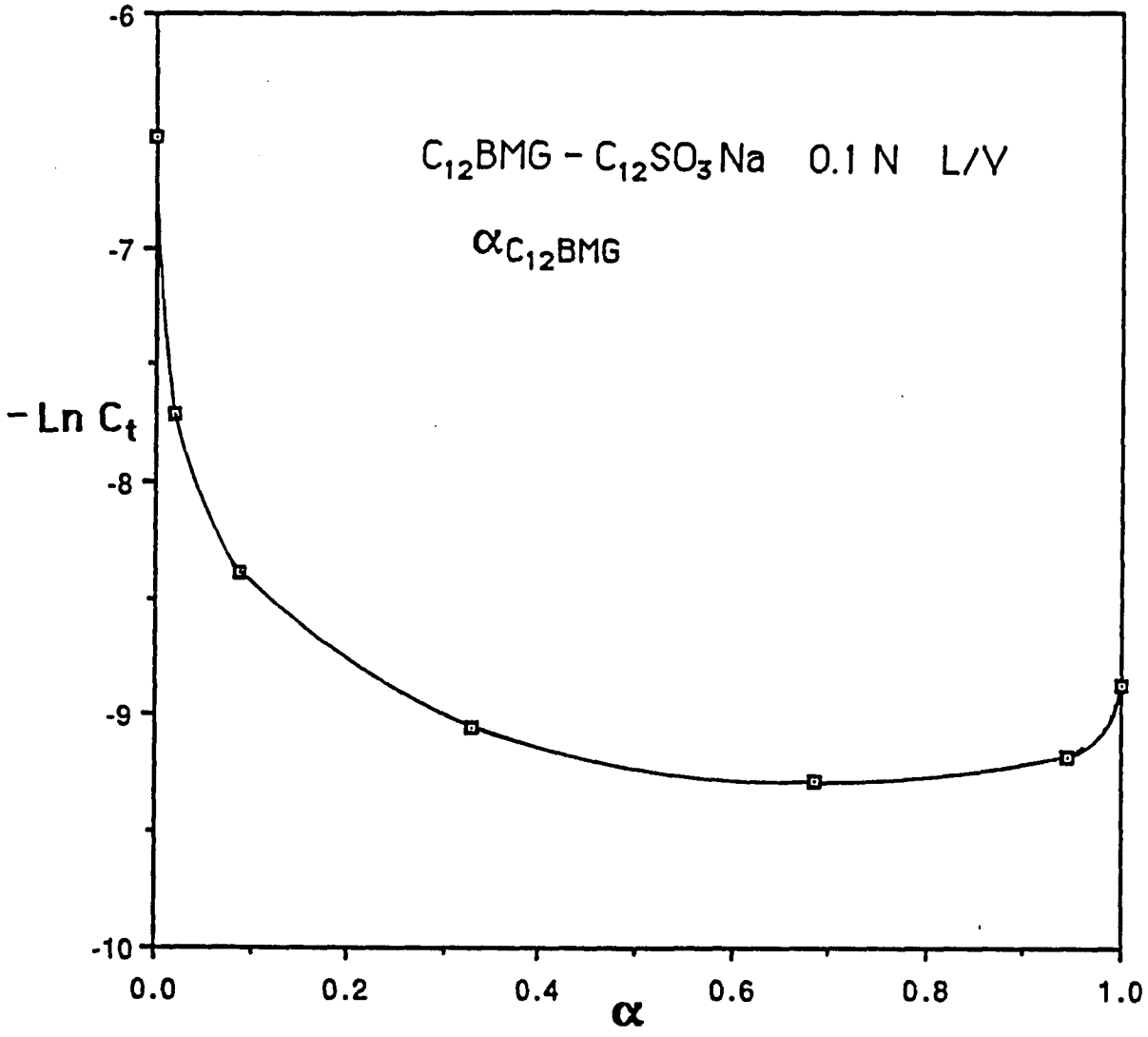
$C_{12}BMG - C_{12}SO_3Na$ 0.1 N L/V
$\alpha_{C_{12}BMG}$
-Ln C_t
-6
-7
-8
-9
-10
0.0
0.2
0.4
0.6
0.8
1.0
α

Figure 50

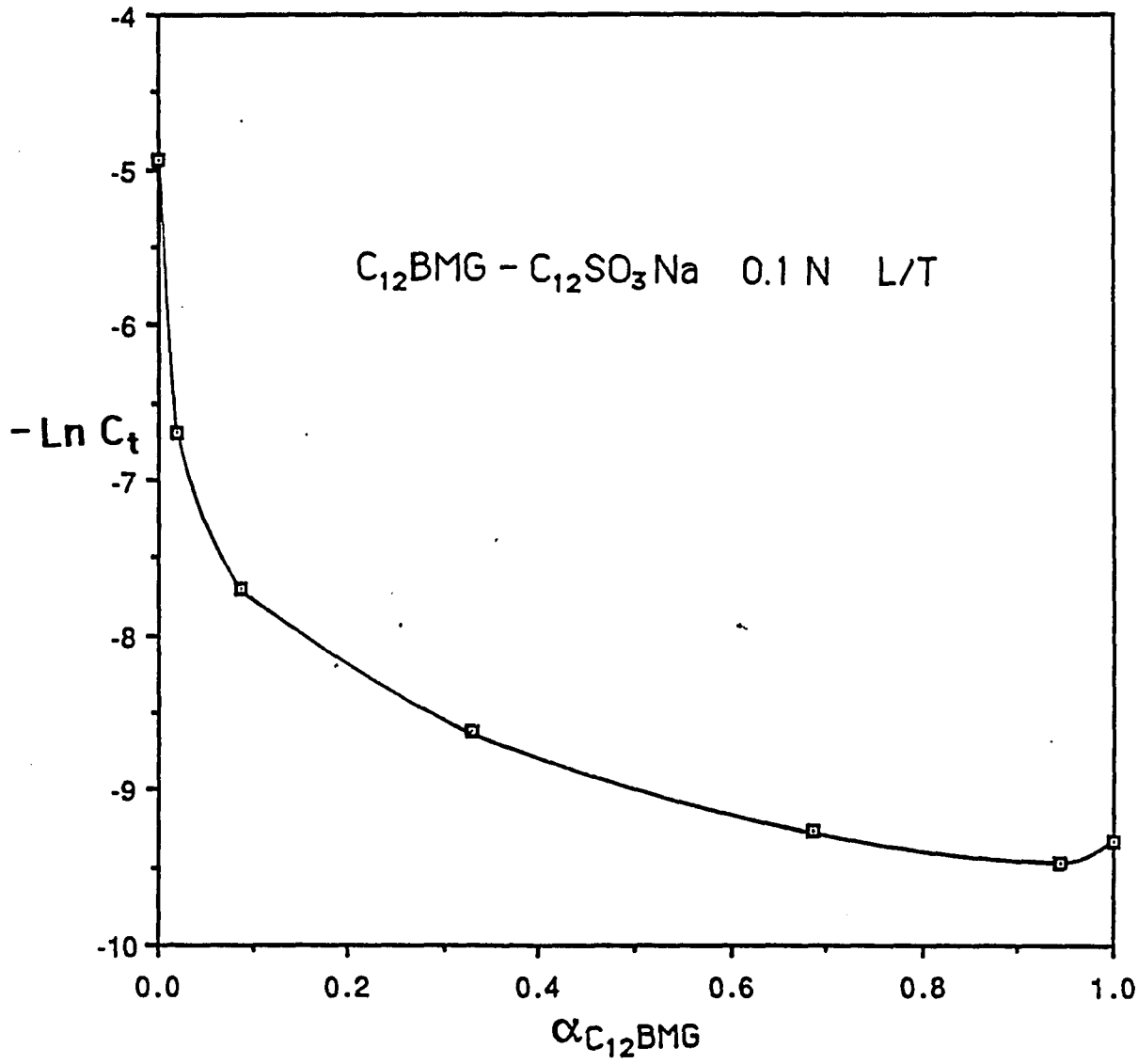
$C_{12}BMG - C_{12}SO_3Na$ 0.1 N L/T
$-Ln\ C_t$
-4
-5
-6
-7
-8
-9
-10
0.0
0.2
0.4
0.6
0.8
1.0
$\alpha_{C_{12}BMG}$

Figure 51

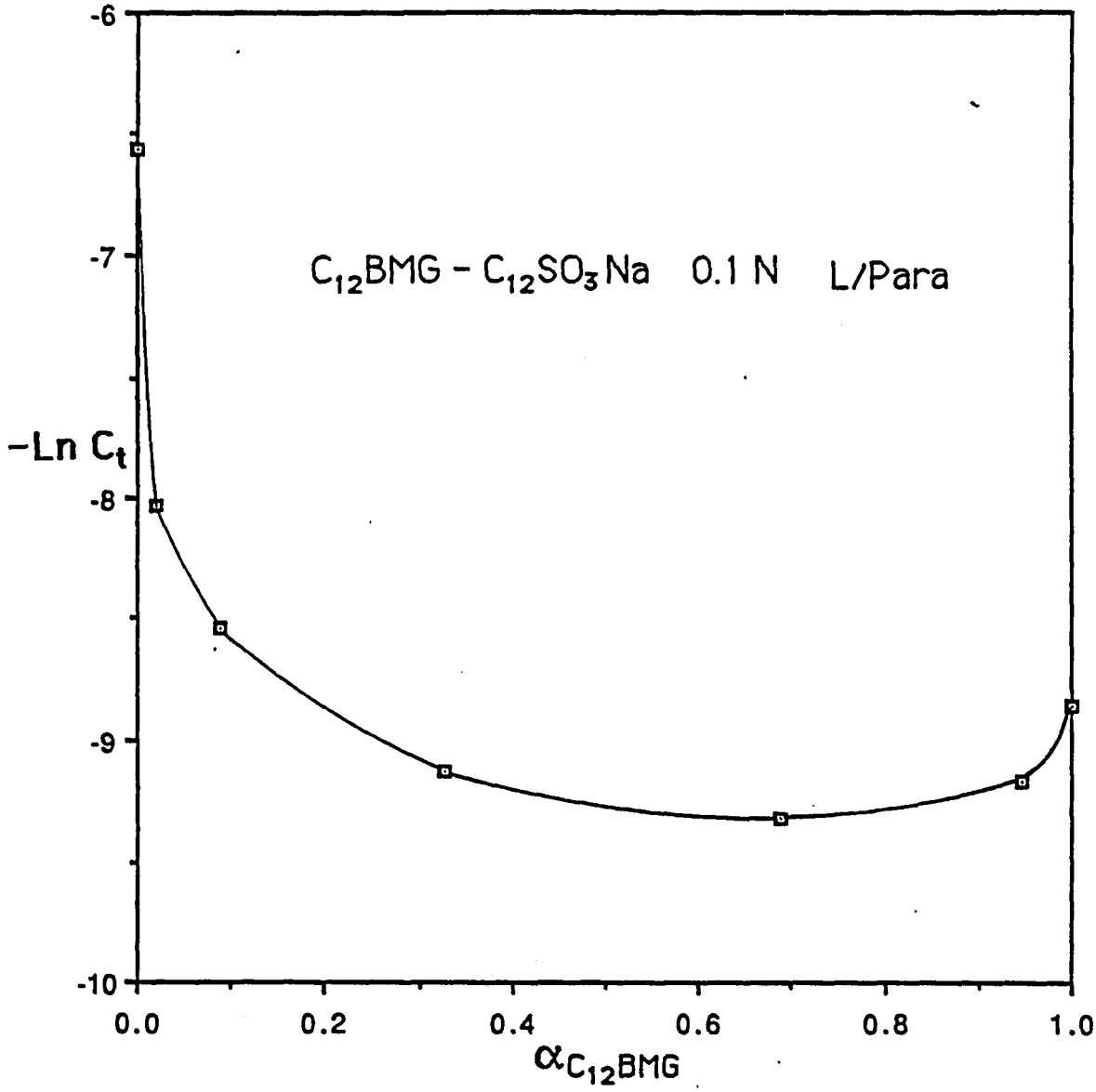
-6
-7
-8
-9
-10
$C_{12}BMG - C_{12}SO_3Na$ 0.1 N L/Para
-Ln C_t
0.0
0.2
0.4
0.6
0.8
1.0
$\alpha_{C_{12}BMG}$

Figure 52

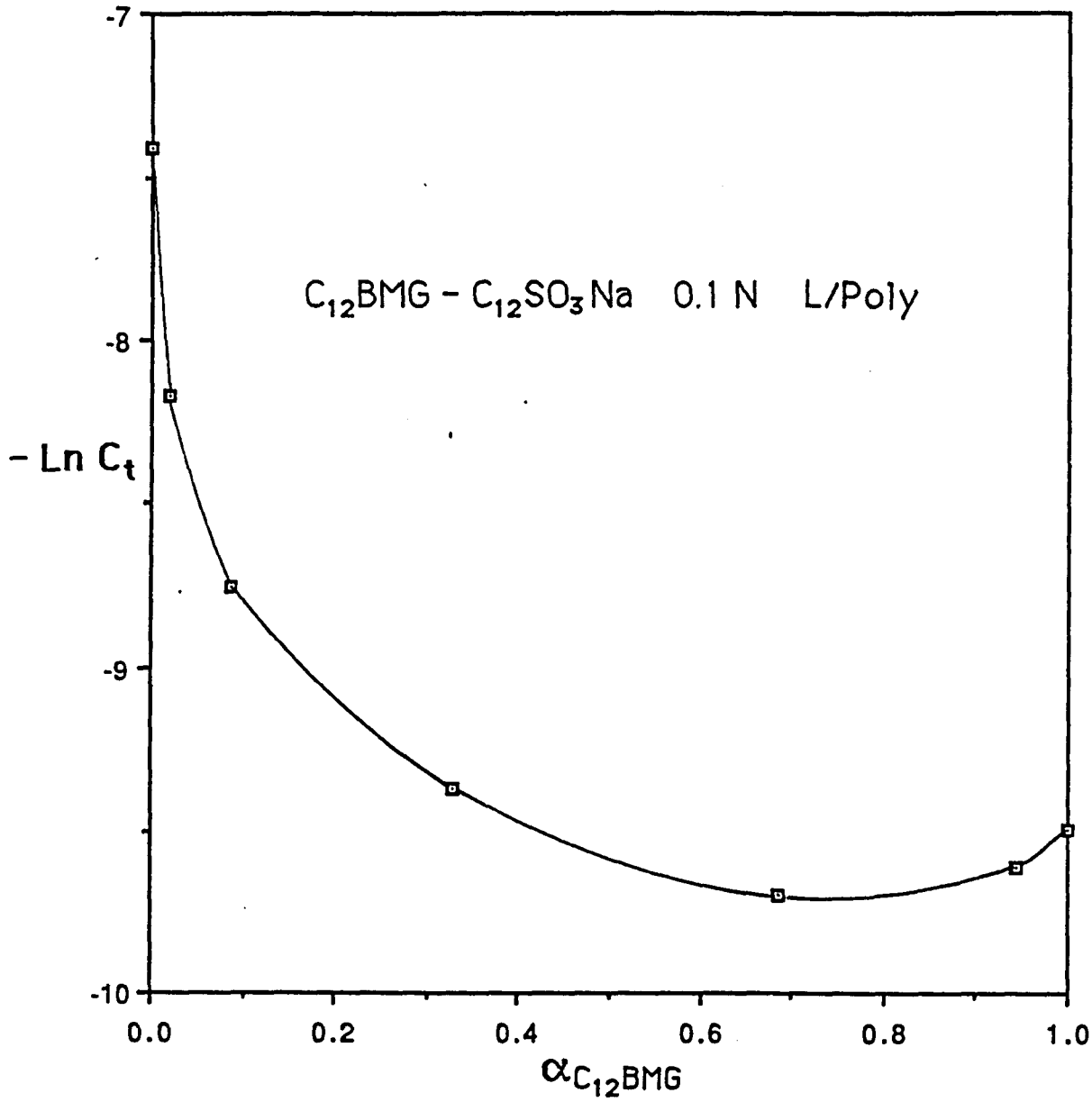
-7
-8
-9
-10
$C_{12}BMG - C_{12}SO_3Na$ 0.1 N L/Poly
- Ln C_t
0.0
0.2
0.4
0.6
0.8
1.0
$\alpha_{C_{12}BMG}$

Figure 53

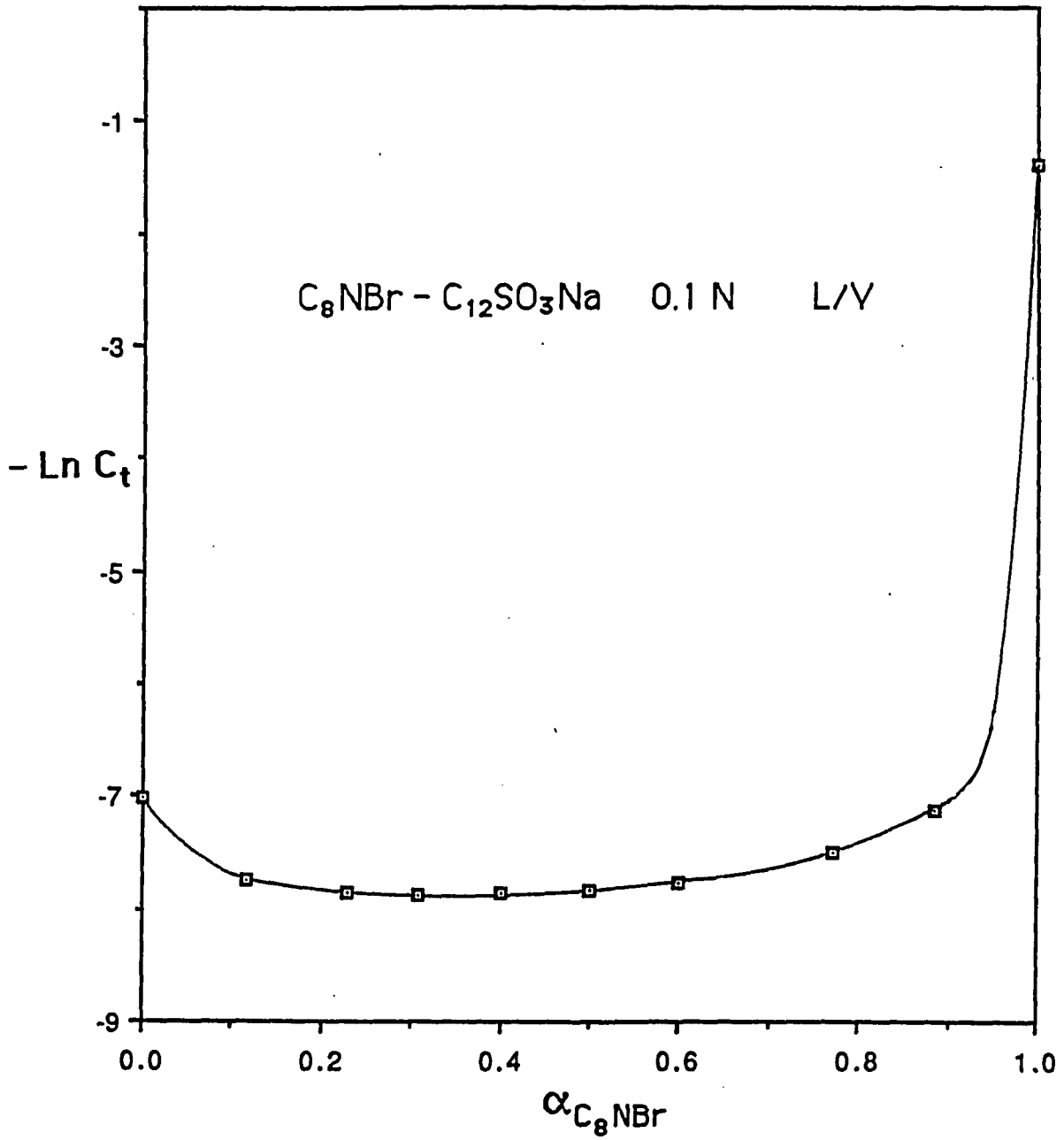

Figure 54

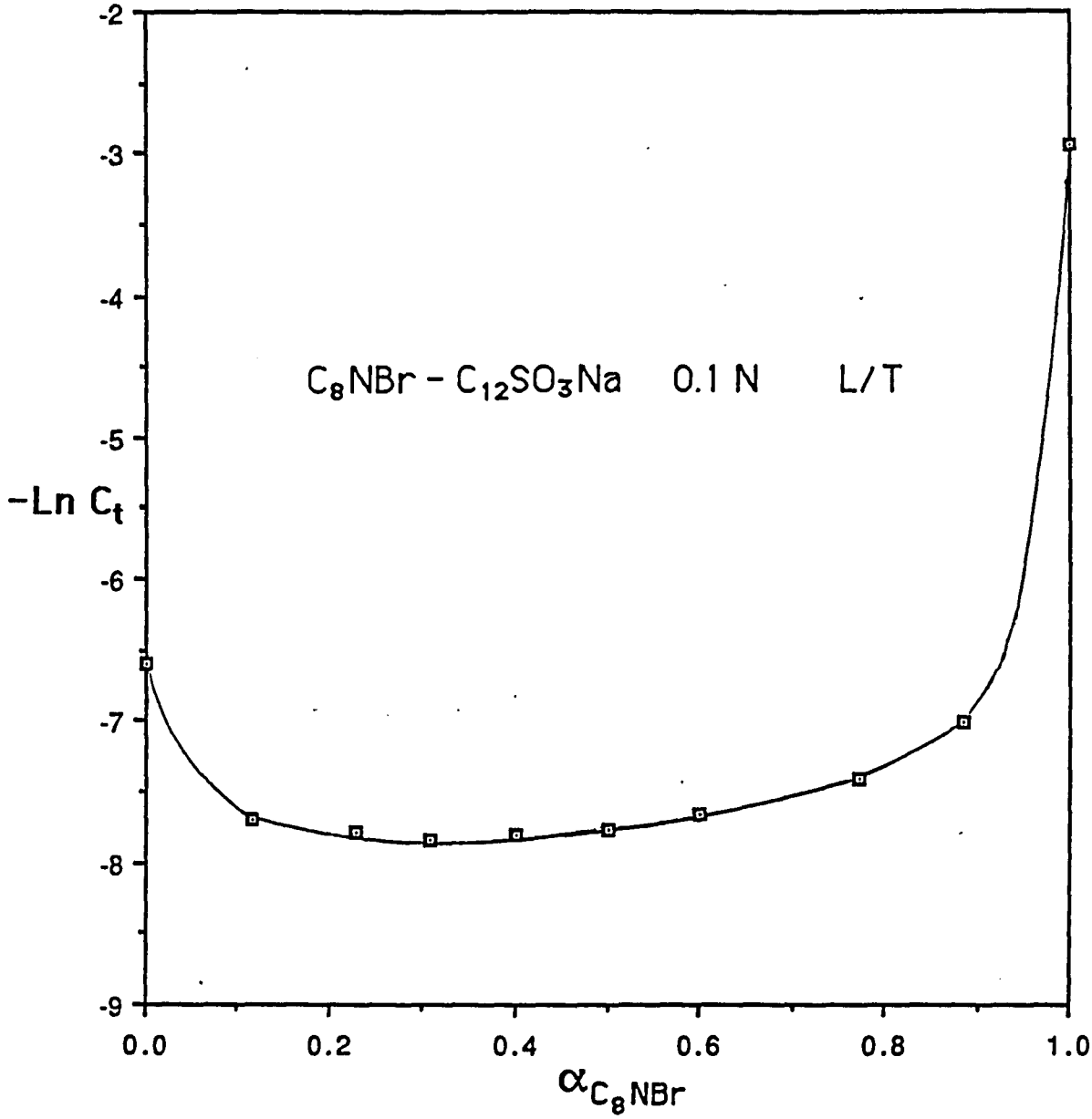
-2
-3
-4
-5
-6
-7
-8
-9
$C_8NBr - C_{12}SO_3Na$ 0.1 N L/T
$-Ln\ C_t$
0.0
0.2
0.4
0.6
0.8
1.0
α_{C_8NBr}

Figure 55

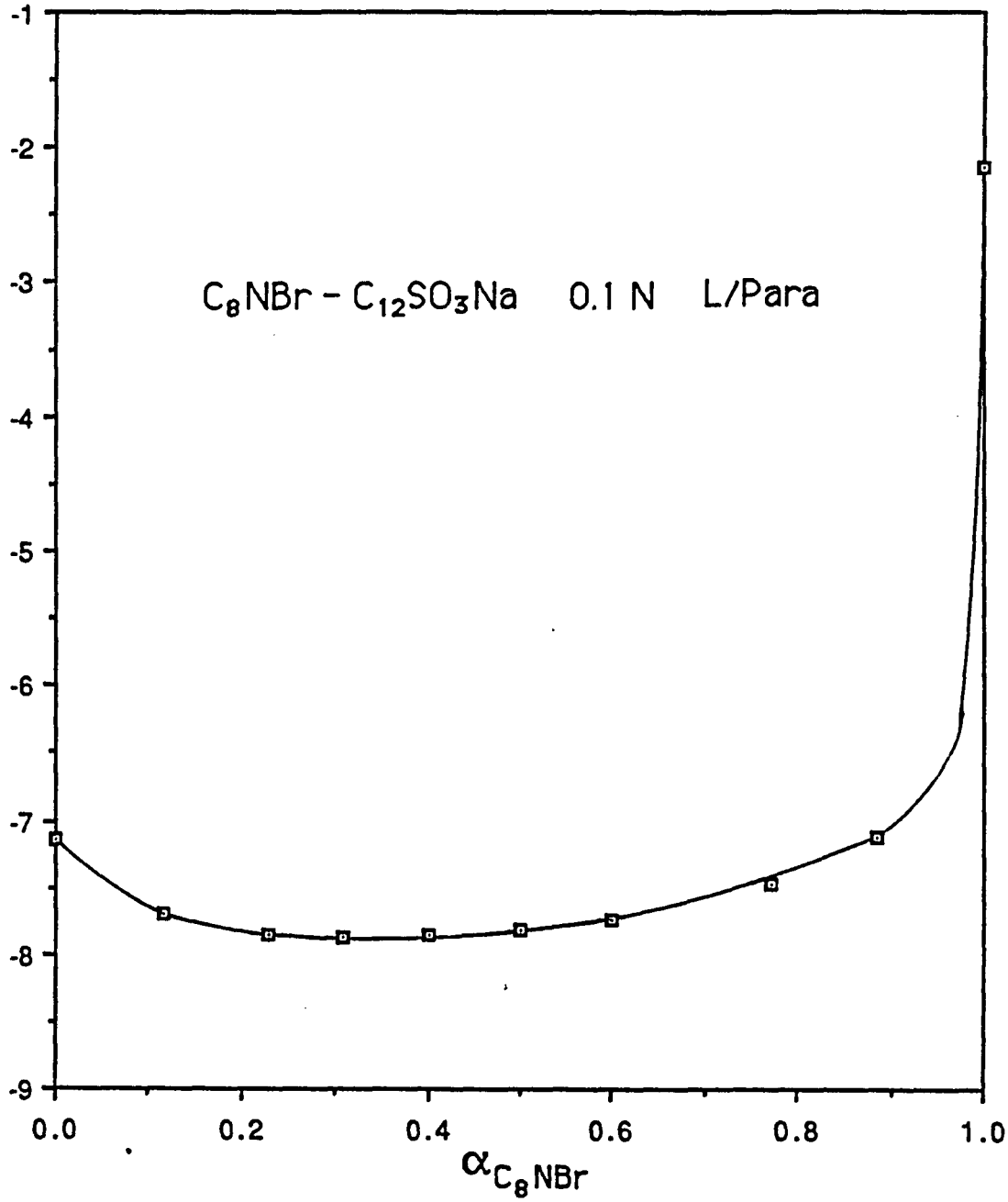
-1
-2
-3
-4
-5
-6
-7
-8
-9
$C_8NBr - C_{12}SO_3Na$ 0.1 N L/Para
0.0
0.2
0.4
0.6
0.8
1.0
α_{C_8NBr}

Figure 56

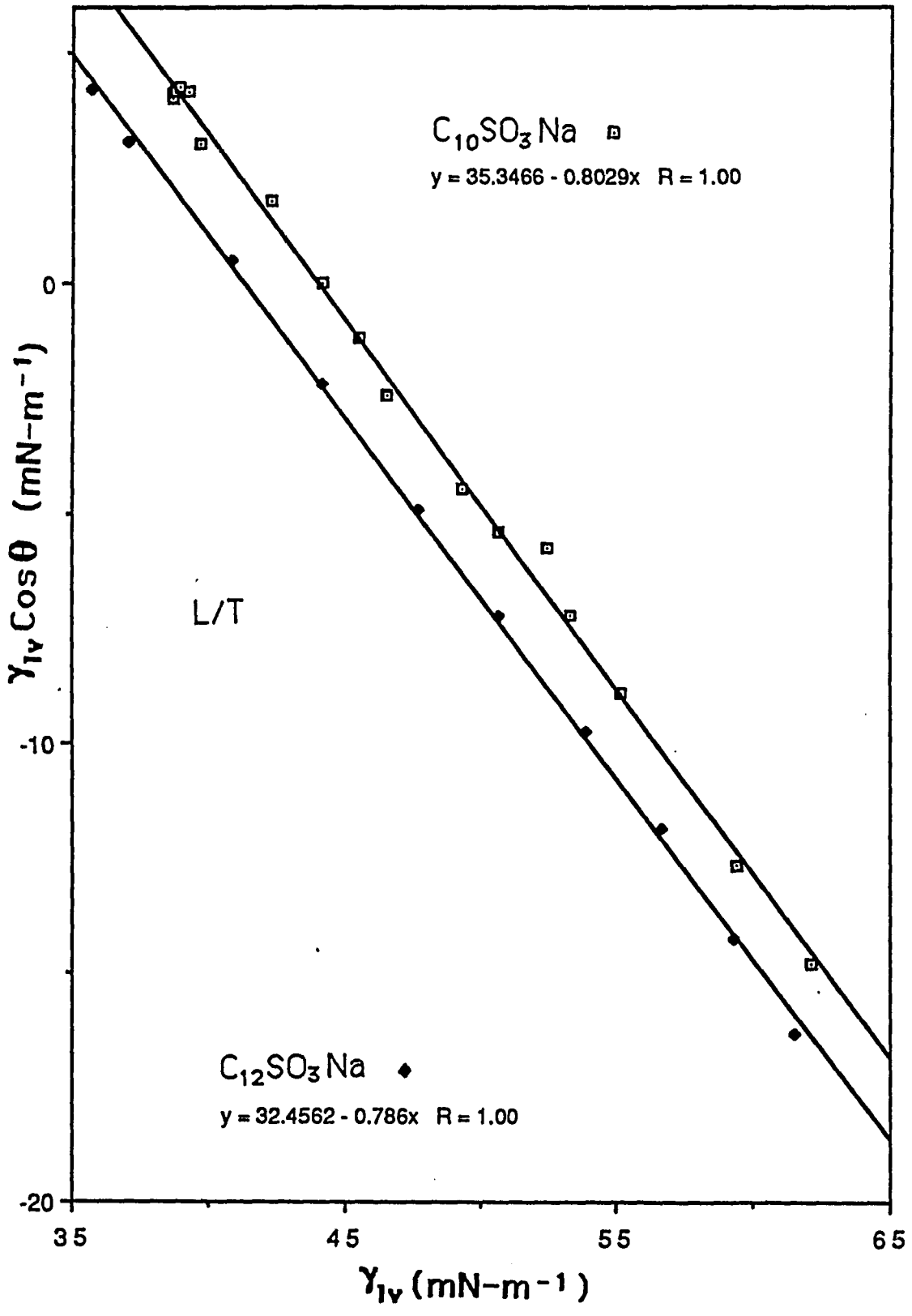
$C_{10}SO_3Na$
y = 35.3466 - 0.8029x R = 1.00
L/T
$C_{12}SO_3Na$
y = 32.4562 - 0.786x R = 1.00
0
-10
-20
35
45
55
65
$\gamma_{lv}\cos\theta$ (mN-m^{-1})
γ_{lv} (mN-m^{-1})

Figure 57

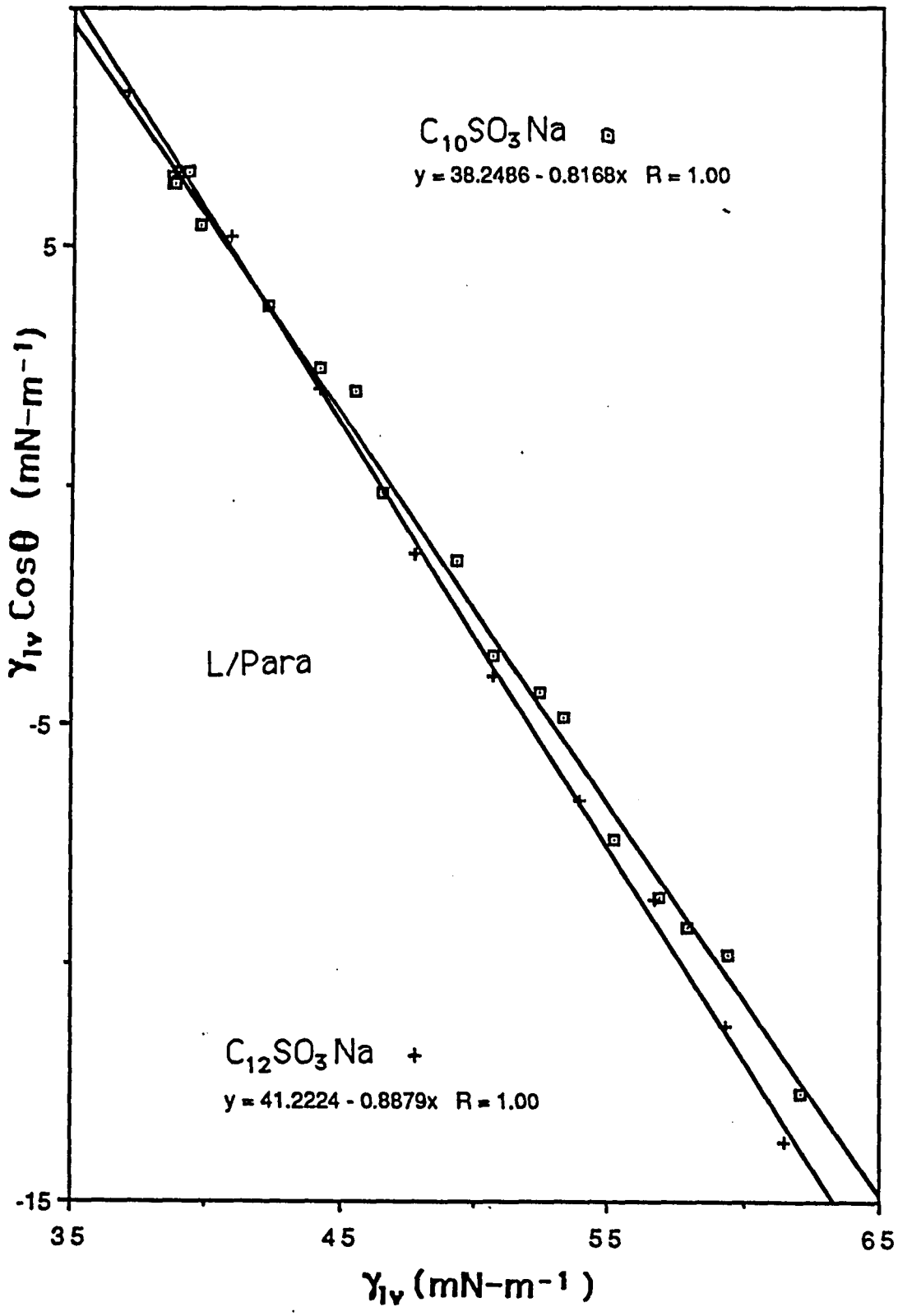
$C_{10}SO_3Na$
y = 38.2486 - 0.8168x R = 1.00
$C_{12}SO_3Na$ +
y = 41.2224 - 0.8879x R = 1.00
L/Para
5
-5
-15
35
45
55
65
γ_{lv} Cosθ (mN-m^{-1})
γ_{lv} (mN-m^{-1})

Figure 58

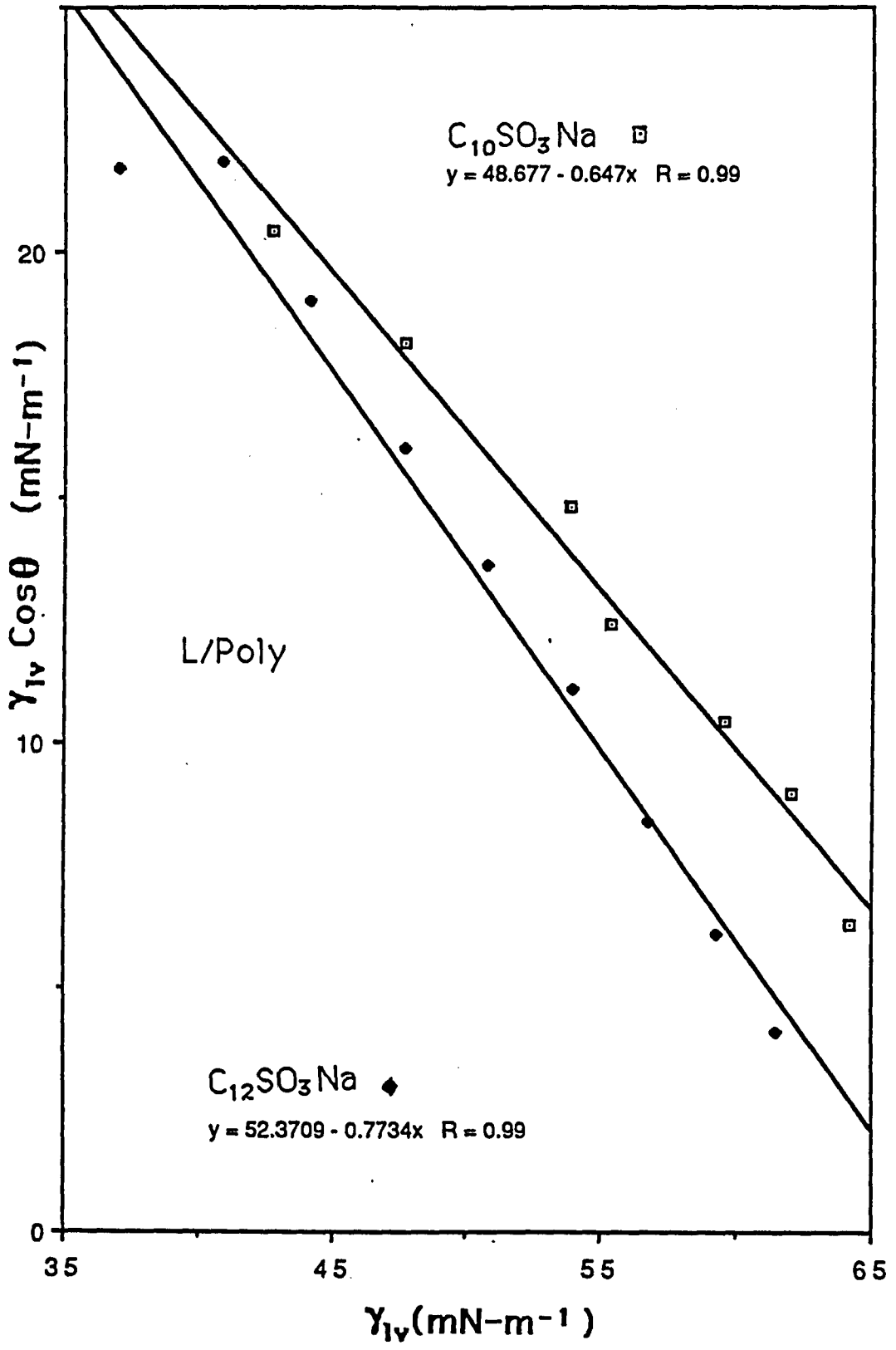
$C_{10}SO_3Na$
y = 48.677 - 0.647x R = 0.99
L/Poly
$C_{12}SO_3Na$
y = 52.3709 - 0.7734x R = 0.99
γ_{lv} Cosθ (mN-m^{-1})
γ_{lv}(mN-m^{-1})
0
10
20
35
45
55
65

Figure 59

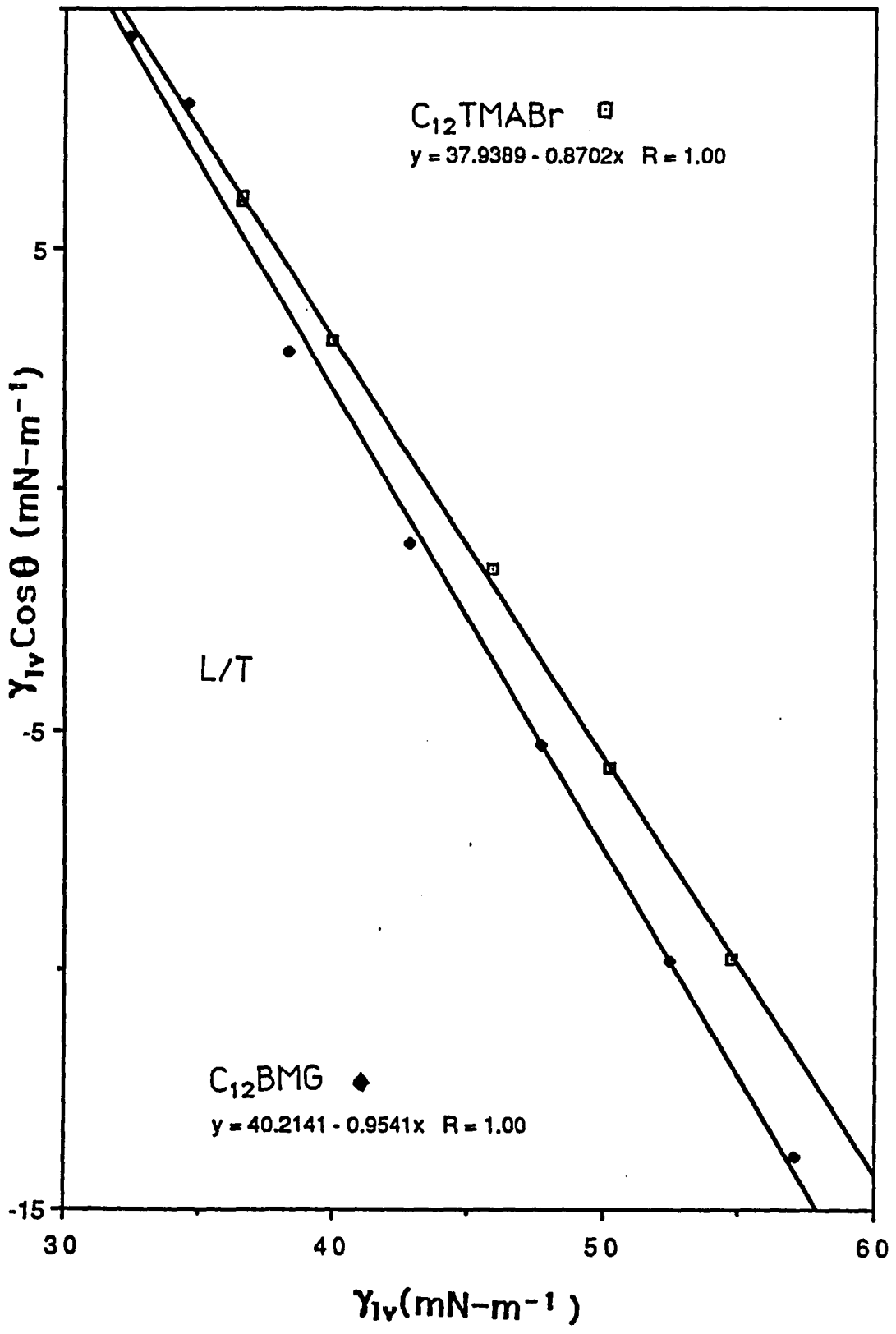
C_{12}TMABr
y = 37.9389 - 0.8702x R = 1.00
L/T
C_{12}BMG
y = 40.2141 - 0.9541x R = 1.00
5
-5
-15
30
40
50
60
$\gamma_{lv}\cos\theta$ (mN-m^{-1})
γ_{lv}(mN-m^{-1})

Figure 60

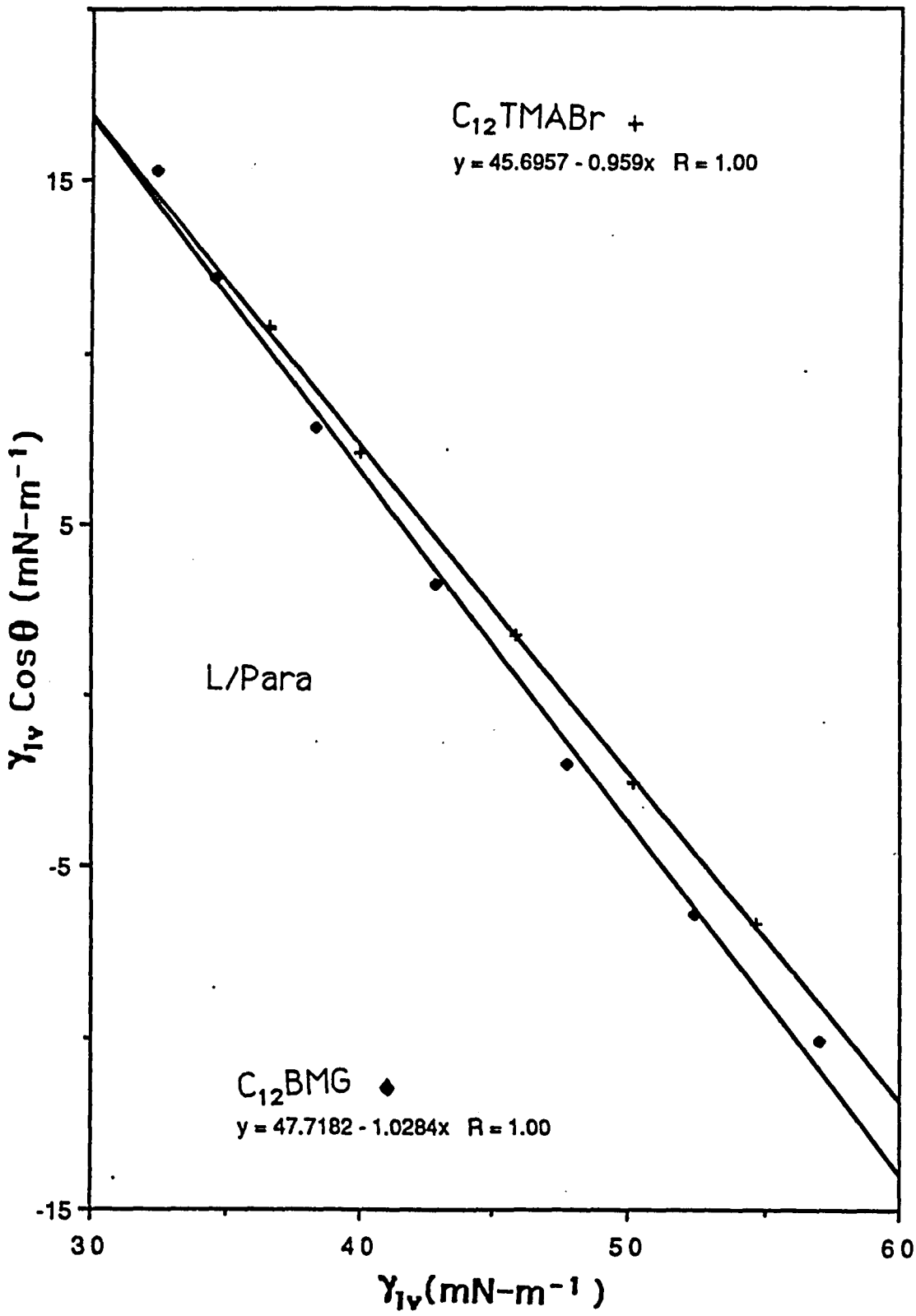
C_{12}TMABr +
y = 45.6957 - 0.959x R = 1.00
L/Para
C_{12}BMG ◆
y = 47.7182 - 1.0284x R = 1.00
15
5
-5
-15
30
40
50
60
γ_{lv} Cosθ (mN-m^{-1})
γ_{lv}(mN-m^{-1})

Figure 61

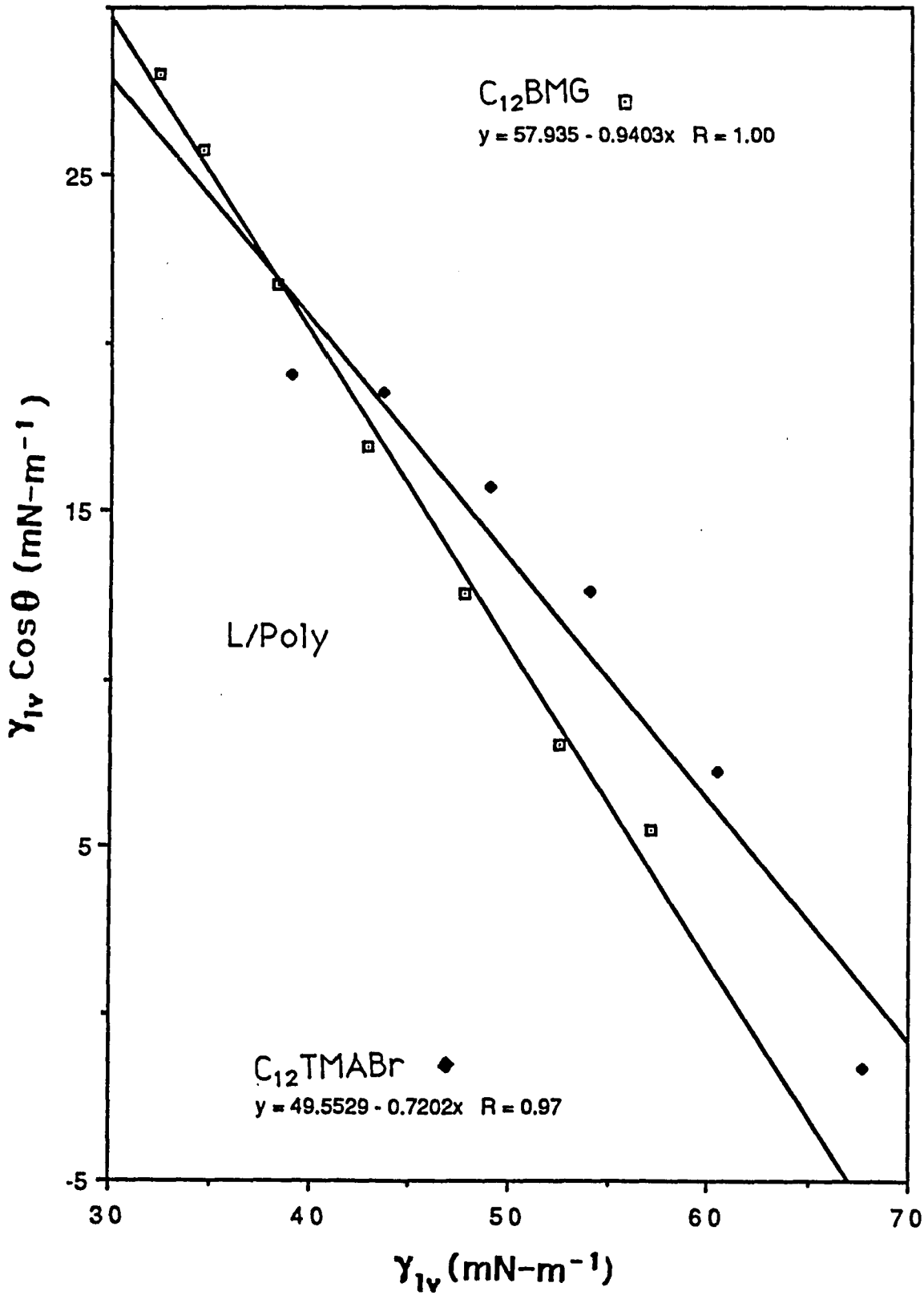
C12BMG
y = 57.935 - 0.9403x R = 1.00
L/Poly
C12TMABr
y = 49.5529 - 0.7202x R = 0.97
25
15
5
-5
30
40
50
60
70
γ1v Cosθ (mN-m-1)
γ1v (mN-m-1)

Figure 62

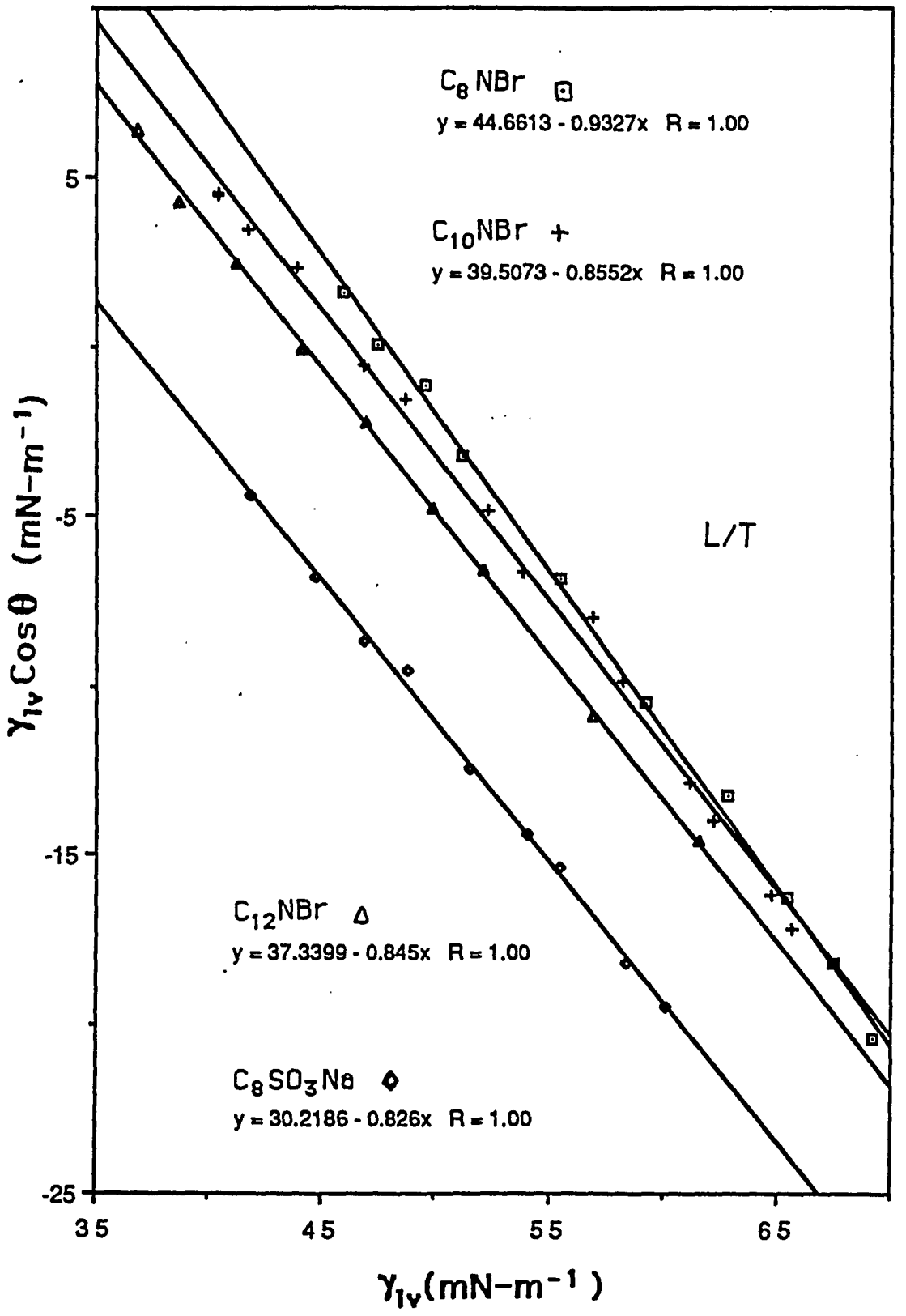
C_8NBr ⊡
y = 44.6613 - 0.9327x R = 1.00
$C_{10}NBr$ +
y = 39.5073 - 0.8552x R = 1.00
L/T
$C_{12}NBr$ Δ
y = 37.3399 - 0.845x R = 1.00
C_8SO_3Na ◆
y = 30.2186 - 0.826x R = 1.00
5
-5
-15
-25
35
45
55
65
$\gamma_{lv}Cos\theta$ (mN-m^{-1})
γ_{lv}(mN-m^{-1})

Figure 63

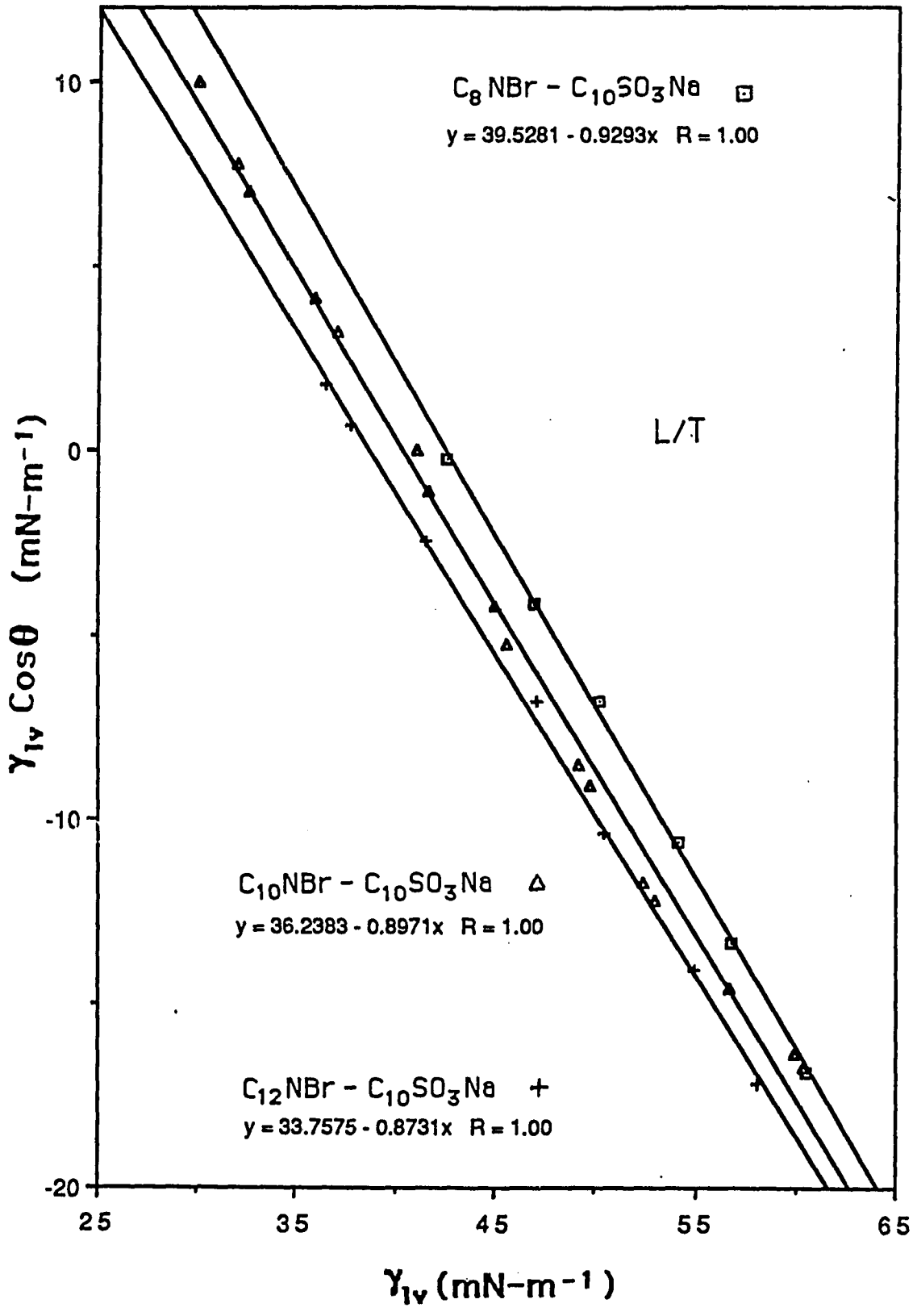
$C_8NBr - C_{10}SO_3Na$
y = 39.5281 - 0.9293x R = 1.00
L/T
$C_{10}NBr - C_{10}SO_3Na$
y = 36.2383 - 0.8971x R = 1.00
$C_{12}NBr - C_{10}SO_3Na$
y = 33.7575 - 0.8731x R = 1.00
10
0
-10
-20
25
35
45
55
65
γ_{lv} Cosθ (mN-m^{-1})
γ_{lv} (mN-m^{-1})

Figure 64

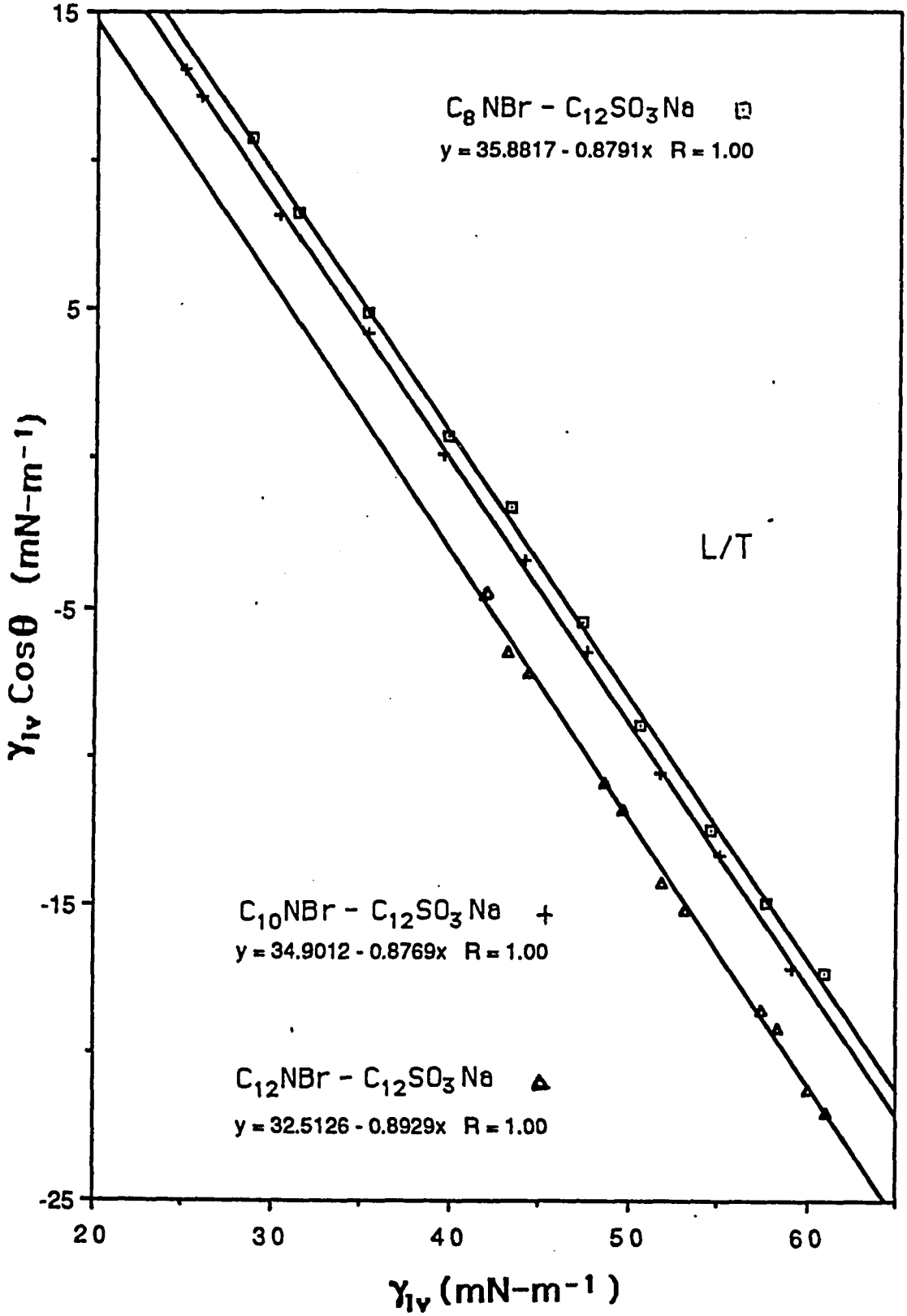
15
5
-5
-15
-25
20
30
40
50
60
γ_{lv} Cosθ (mN-m^{-1})
γ_{lv} (mN-m^{-1})
$C_8NBr - C_{12}SO_3Na$
y = 35.8817 - 0.8791x R = 1.00
L/T
$C_{10}NBr - C_{12}SO_3Na$
y = 34.9012 - 0.8769x R = 1.00
$C_{12}NBr - C_{12}SO_3Na$
y = 32.5126 - 0.8929x R = 1.00

Figure 65

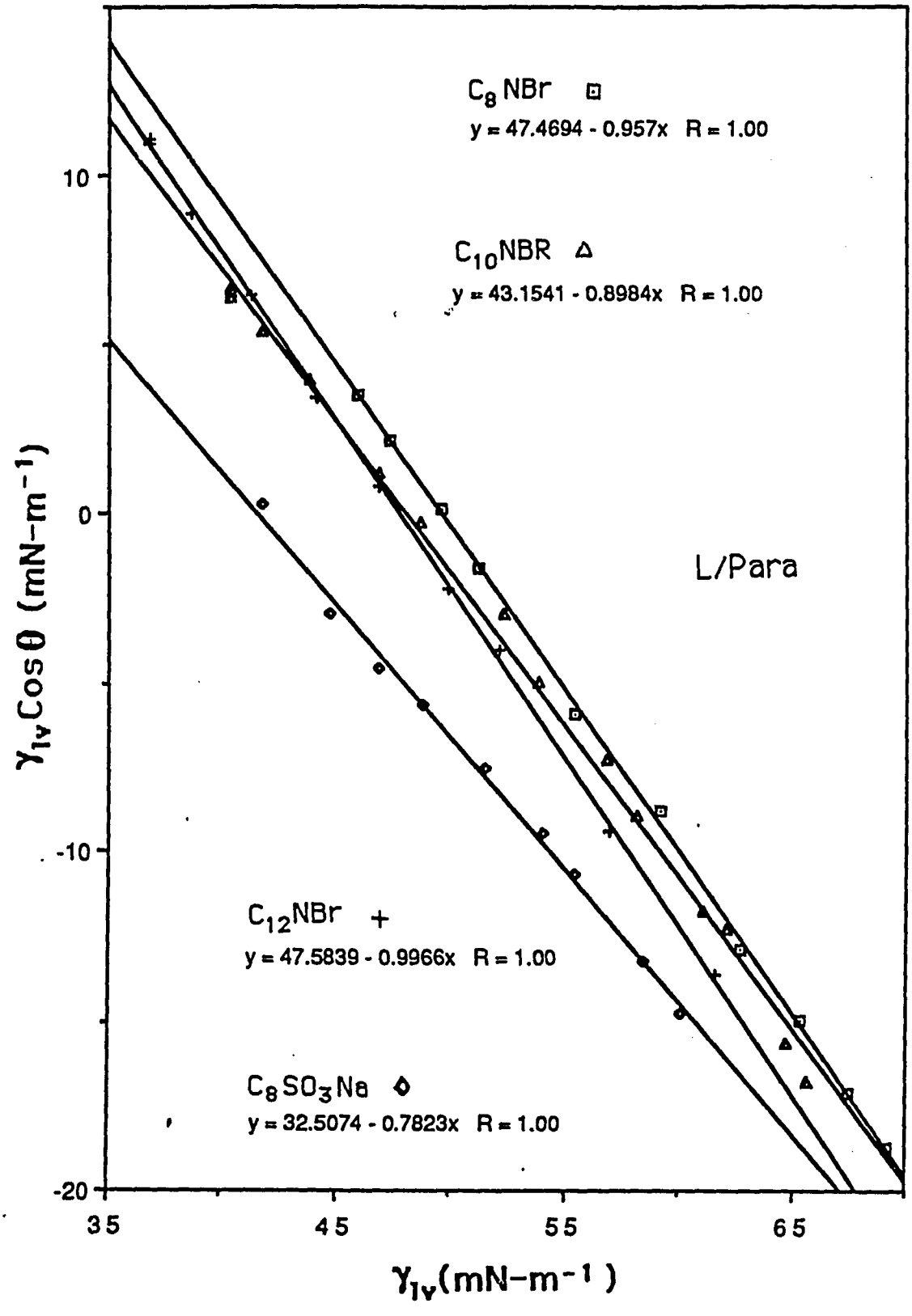
C_8NBr ⊡
y = 47.4694 - 0.957x R = 1.00
C_{10}NBR △
y = 43.1541 - 0.8984x R = 1.00
L/Para
C_{12}NBr +
y = 47.5839 - 0.9966x R = 1.00
C_8SO_3Na ◇
y = 32.5074 - 0.7823x R = 1.00
10
0
-10
-20
35
45
55
65
γ_{lv}Cosθ (mN-m^{-1})
γ_{lv}(mN-m^{-1})

Figure 66

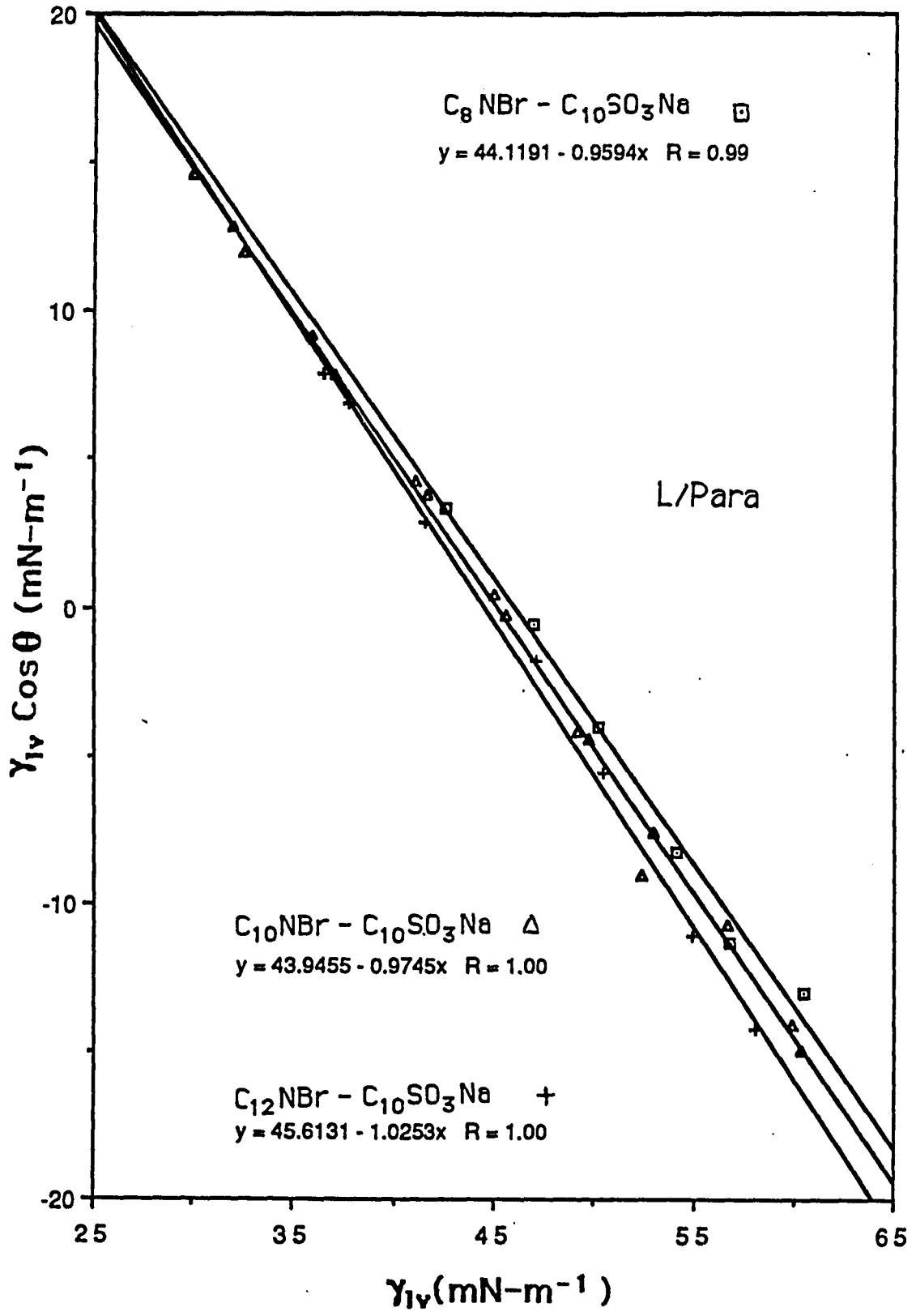
20
10
0
-10
-20
25
35
45
55
65
γ_{lv} Cosθ (mN-m^{-1})
γ_{lv}(mN-m^{-1})
$C_8NBr - C_{10}SO_3Na$
y = 44.1191 - 0.9594x R = 0.99
L/Para
$C_{10}NBr - C_{10}SO_3Na$ Δ
y = 43.9455 - 0.9745x R = 1.00
$C_{12}NBr - C_{10}SO_3Na$ +
y = 45.6131 - 1.0253x R = 1.00

Figure 67

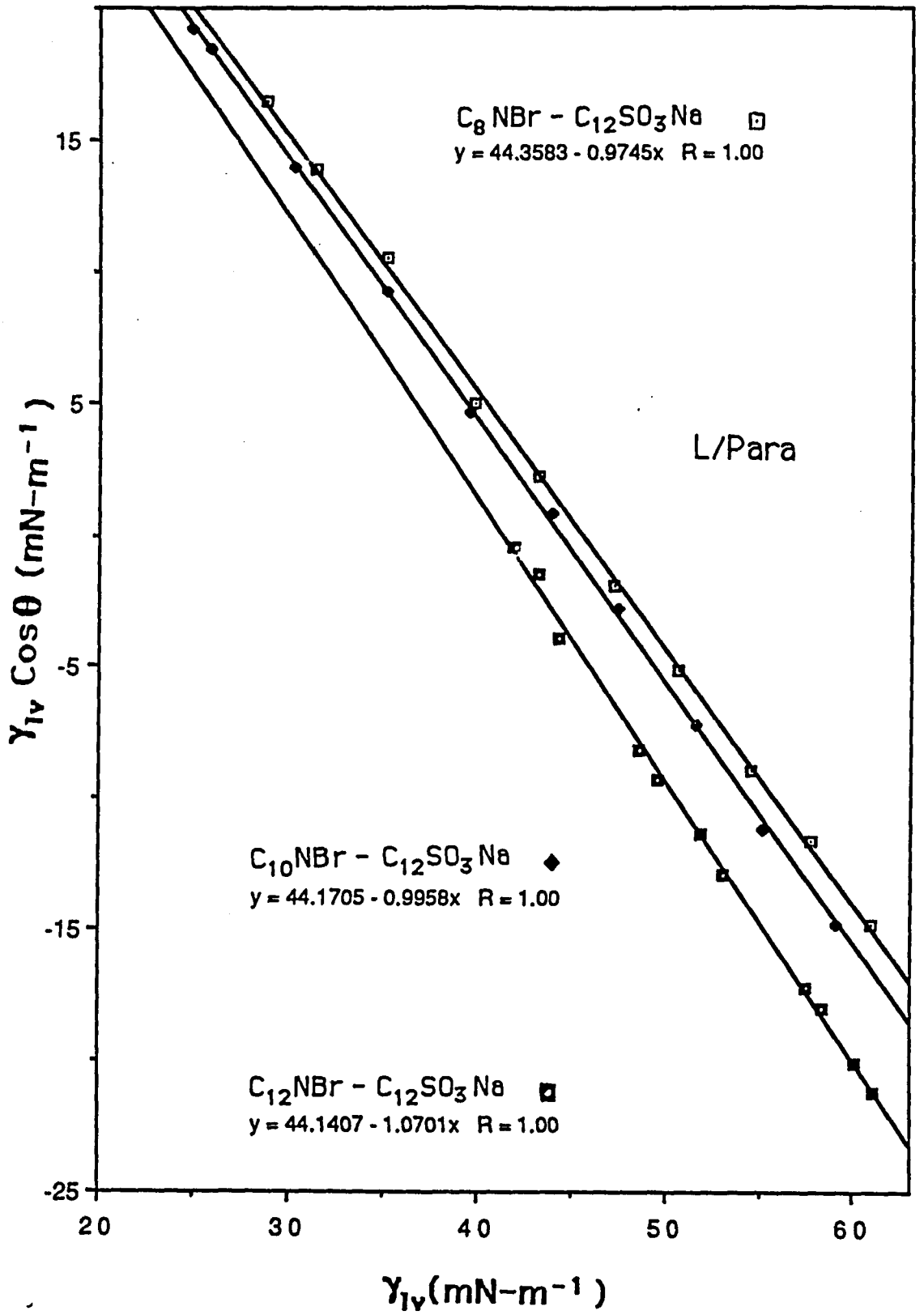
$C_8NBr - C_{12}SO_3Na$
y = 44.3583 - 0.9745x R = 1.00
L/Para
$C_{10}NBr - C_{12}SO_3Na$
y = 44.1705 - 0.9958x R = 1.00
$C_{12}NBr - C_{12}SO_3Na$
y = 44.1407 - 1.0701x R = 1.00
15
5
-5
-15
-25
20
30
40
50
60
$\gamma_{lv}\ Cos\theta\ (mN-m^{-1})$
$\gamma_{lv}(mN-m^{-1})$

Figure 68

Bibliography

1. Adam, N. K., The Physics and Chemistry of Surfaces, Ooxford University Press, London and New York, 1967
2. Payens, T. A. P., Proc. 2nd Int. Cong. Surf. Activ., 1957, 1, 61 (London)
3. Van Voorst Vader, F., Trans. Faraday Soc., 1961, 57, 2263
4. Webb, D. A.; Danielli, J. F., Nature, 1940, 146, 197
5. Sasaki, J.; Tajima, K.; Sasaki, T., Bull. Chem. Soc. Jap., 1972, 45, 348
6. Lange, H.; Schwuger, M. J., Kolloid - Z. Z. Polym., 1971, 243, 120
7. Schwuger, M. J., Kolloid - Z. Z. Polym., 1971, 243, 129
8. Hua, H. Y.; Chao, K. H., Acta Chimica Sinica, 1964, 30, 441
9. Sanoda, K., Colloidal Surfactants, Academic Press, New York, 1963; Charpter 1
10. Lange, H., Kolloid - Z. Z. Polym., 1953, 13, 96
11. Shinoda, K., J. Phys. Chem., 1954, 58, 541
12. Shedlovsky, L.; Jakob, C. W.; Epstein, M. B., J. Phys. Chem., 1963, 67, 2075
13. Iwadare, Y., Bull. Chem. Soc. Jpn., 1970, 43, 3364
14. Moro, Y.; Motomura, K.; Matuura, R., J. Colloid Interface Sci., 1974, 46, 111
15. Clint, J. H., J. C. S. Faraday I, 1975, 71, 1327

16. Ingram, B. T.; Luckhurst, A. H. W., Sueface Active Agents, The Society of Chemical Faraday, London, 1979; P 89

17. Rubingh, D. N., in Solution Chemistry of Surfactants, Mitlal, L., Ed., Plenum Press, New York, 1979; Vol.1; P 337

18. Ingram, B. T., Colloid Polym. Soi., 1980, 25, 191

19. Scamehorn, J. F.; Schechter, R. S.; Wade, W. H., J. Disp. Sci. Tech., 1982, 3, 26

20. Holland, P. M.; Rubingh, D. N., J. Phys. Chem., 1983, 87, 1984

21. Kamrath, R. F.; Franses, E. T., Ind. Eng. Chem. Fandam., 1983, 22, 230

22. Hall, D. G.; Huddlleston, R. W., Colloids Surfaces, 1985, 13, 209

23. Osborne-Lee, I. W.; Schechter, R. S.; Wade, W. H.; Barakat, Y., J. Colloid Interface Sci., 1985, 108, 60

24. Rosen, M. J., in Phenomena in Mixed Surfactant Systems Scamehorn, J. F., Ed., American Chemical Society, Washington, DC, 1986; ACS Symposium Series Vol.311; P 144

25. Rosen, M. J.; Hua, X. Y., J. Colloid Interface Sci., 1982, 86, 164

26. Rosen, M. J.; Hua, X. Y., J. Colloid Interface Sci., 1982, 90, 212

27. Rosen, M. J.; Zhao, F., J. Colloid Interface Sci., 1983, 95, 443

28. Zhu, B, Y.,; Rosen. M. J., J. Colloid Interface Sci., 1984, 99, 435

29. Rosen, M. J.; Murphy, D., J. Colloid Interface Sci., 1986, 101, 224

30. Rosen, M. J.; Gu, B., Colloids and Surfaces, 1987, 23, 119

31. Everett, D. H., Pure Appl. Chem., 1972, 31, 579

32. Gibbs, J. W., The Collect Work of J. W. Gibbs Longmans, Green, New York, 1930; Vol.I; P 219

33. Defay, R.; Prigogine, I.; Bellemans, A.; Everett, D. H., Surface Tension and Adsorption, Translated by Everett, D. H., John Wiley & Sons, New York, 1966; Charpter V; P 62

34. Young, T., in Miscellaneous Works Peacock, G., Ed., Murrary, London, 1855; Vol.1; P 418

35. Lucassen-Reynders, E. H., J. Phys. Chem., 1963, 67, 969

36. Bargeman, D., J. Colloid Interface Sci., 1972, 40(3), 344

37. Zisman, W. A., Ind. Eng. Chem., 1963, 55, 19

38. Johnson, R. E.; Dettre, R. H., J. Colloid Sci., 1966, 21, 610

39. Lucassen-Reynders, E. H., Progr. Sueface Membrane Sci., 1976, 10, 253

40. Lucassen-Reynders, E. H., J. Colloid Interface Sci., 1972, 41, 156

41. Lucassen-Reynders, E. H., J. Colloid Interface Sci., 1973, 42, 554 563; 573

42. Lucassen-Reynders, E. H. Anionic Surfactants, Marcel Dekker, New York and Basel, 1981; Surfactant Science Series Vol.11; P 1

43. Go'ralczyk, D.; Waligo'ra, B., J. Colloid Interface Sci., 1981, 82(1), 1

44. Rodakiewicz-Nowak, J., J. Colloid Interface Sci., 1982, 84(2), 532

45. Rodakiewicz-Nowak, J., J. Colloid Interface Sci., 1982, 85, 586

46. Go'ralczyk, D.; Waligo'ra, B., J. Colloid Interface Sci., 1982, 88(2), 590

47. Rodakiewicz-Nowak, J., J. Colloid Interface Sci., 1983, 91(2), 368

48. Rodakiewicz-Nowak, J., Colloids and Surfaces, 1983, 6, 143

49. Go'ralczyk, D., Colloids and Surfaces, 1984, 11(3/4), 287

50. Gillap, W. R.; Weiner, N. D.; Gibaldi, M., J. Phys. Chem., 1968, 72, 2218

51. Skange, A.; Spitzer, J. J., J. Phys. Chem., 1983, 87(13), 2398

52. Mukerjee, P.; Handa, T., J. Phys. Chem., 1981, 85(15), 2298

53. Lucassen-Reynders, E. H.; Lucassen, J.; Giles, D.; J. Colloid Interface Sci., 1981, 81, 150

54. Rosen, M. J.; Aronsen, S., Colloids and Surfaces, 1981, 3(3), 201

55. Crowther, J. G., Famous American Men of Science, W. W. Norton & Company, Inc., New York, 1937

56. Pockels, F. A., Nature, 1891, 43, 437

57. Rayleigh, L., Phil. Mag., 1899, 48, 337

58. Langmuir, I., J. Amer. Chem. Soc., 1916, 38, 2221

59. Langmuir, I., J. Amer. Chem. Soc., 1917, 39, 1848

60. Adamson, A. W., Physical Chemistry of Surfaces, 4th Ed. John Wiley & Sons, New York, 1982; P 125

61. Davies, J. T.; Ridel, E. K., Interfacial Phenomena, 2nd Ed., Academic Press, New York and London, 1963; Charpter 5

62. Gaines, G. L., Insoluble Monolayers at Liquid-Gas Interfaces, John Wiley & Sons, New York, London and Syndey, 1966; Charpter 4

63. Defay, R.; Prigogine, I.; Bellemans, A.; Everett, D. H., Surface Tension and Adsorption, Translated by Everett, D. H., John Wiley & Sons, New York, 1966; Charpter XII

64. Lucassen-Reynder, E. H., in Anionic Surfactants, Lucassen-Reynder, E. H. Ed., Marcel Dekker, New York and Basel, 1981; Surfactant Science Series Vol. 11; P 1

65. Adam, N. K., The Physics and Chemistry of Suefaces, Oxford University Press, London and New York, 1941

66. Davies, J. T.; Rideal, E. K., Interfacial Phenomena, Academic Press, New York, 1961

67. Butler, J. A. V., Proc. Roy. Soc., Ser. A, 1932, 134, 348

68. Tolman, R. C., J. Chem. Phys., 1948, 16, 758

69. Van Voorst Vader, F., Trans. Faraday Soc., 1960, 56, 1067

70. Kling, W.; Lange, H., Proc. 2nd Int. Cong. Surf. Activ., 1957, 1, 248 (London)

71. Fowkes, F. M., J. Phys. Chem., 1962, 66, 385

72. Brooks, J. H.; Pethica, B. A., Proc. 4th Int. Cong. Surf. Activ. Subst., 1964, 2, 191 (Brussels)

73. Lange, H., in Nonionic Surfactants, Schick, M. J. Ed., Marcel Dekker, New York, 1966

74. Lucassen-Reynders, E. H., Progr. Surf. Membrane Sci., 1976, 3, 253

75. Lucassen-Reynders, E. H., J. Phys. Chem., 1966, 70(6), 1777

76. Goddard, E. D.; Kao, O.; Kung, H. C., J. Colloid Interface Sci., 1968, 27,, 616

77. Gaines, G. L., Jr., J. Chem. Phys., 1978, 69, 924; 2627

78. Defay, R.; Prigogine, I.; Bellemans, A.; Everett, D. H., Surface Tension and Adsorption, Translated by Everett, D. H., John Wiley & Sons, inc., New York, 1966; Charpter VII

79. Defay, R.; Prigogine, I.; Bellemans, A.; Everett, D. H., Surface Tension and Adsorption, Translated by Everett, D. H., John Wiley & Sons, inc., New York, 1966; Charpter IV, P 46; 48

80. Adamson, A. W., Physical Chemistry of Surfaces, 4th Ed., John Wiley & Sons, Inc., New York, 1982; P 261

81. Brunauer, S., in Solid/Gas Interface, Schulman, J. H. Ed., Academic Press Inc., New York, 1957; P 17

82. Jura, G.; Garland, C. W., J. Amer. Chem. Soc., 1952, 74, 6033

83. Bangham, D. H.; Razouk, R. I., Trans. Faraday Soc., 1937, 33, 1459

84. Good, R. J.; Girifalco, L. A., J. Phys. Chem., 1960, 64, 561

85. Fowkes, F. M., in Advan. Chem. Series 43, Gould, R. F. Ed., American Chemical Society, 1964; P 99

86. Dann, J. R., J. Colloid Interface Sci., 1970, 32, 302

87. Zisman, W. A., in Advan. Chem. Series 43, Gould, R. F. Ed., American Chemical Society, 1964; P 1

88. Fox, H. W.; Zisman, W. A., J. Colloid Sci., 1950, 5, 514

89. Shafrim, E. G.; Zisman, W. A., J. Phys. Chem., 1967, 71, 1309

90. Shafrim, E. G.; Zisman, W. A., J. Phys. Chem., 1960, 64, 519

91. Good, R. J., in Surface and Colloid Science, Good, R. J. and Stramberg, R. R. Ed., Plenum Press, New York and London, 1979; Vol.11; P 1

92. Somorjai, G. A., in Chemistay in Two Dimensions Surfaces, Cornell University Press, Ithaca and London, 1981; P 26

93. Wenzel, R. N., Ind. Eng. Chem., 1936, 28, 988

94. Freundlich, H., Colloid and Capillary, 1926; P 157

95. Bigelow, W. C.; Pickett, D. L.; Zisman, W. A., Colloid and Surfaces, 1946, 1, 513

96. Newman, A. W.; Good, R. J., in Colloid and Surface Science, Good, R. J. and Stromberg, R. R., Ed., Plenum, New York, 1979; Vol. 11; P 31

97. Good, R. J.; Koo, M. N., J. Colloid Interface Sci., 1979, 71(2), 283

98. Adamson, A. W., Physical Chemistry of Surfaces, 4th Ed., John Wiley & Sons, Inc., New York, 1982; P 347

99. Fowkes, F. W.; Harkins, W. D., J. Am. Chem. Soc., 1940, 62, 3377

100. Mark, G. L., J. Phys. Chem., 1936, 40, 159

101. Leja, J.; Poling, G. W., in Proceeding of the International Mineral Processing Congress, London, 1960, Institute of Mining and Metallurgy, London, 1960

102. Pethica, B. A., Rep. Prog. Appl. Chem., 1961, 46, 14

103. Phillips, M. C.; Riddiford, A. C., Nature, 1965, 205, 1005

104. Holland, P. M., in Phenomena in Mixed Surfactant Systems, Scamehorn, J.F., Ed., ACS Symposium 311, American Chemical Society, Washington, DC. 1986; P 102

105. Kronberg, B.; Lindstrom, M.; Stenius, P., in Phenomena in Mixed Surfactant Systems, Scamehorn, J.F., Ed., ACS Symposium 311, American Chemical Society, Washington, DC, 1986; P 225

106. Fried, V.; Blukins, U.; Hameka, H. F., Physical Chemistry, Macmillam, Co., New York, 1977; P 224; 252

107. Hutchinson, E., J. Colloid Sci., 1948, 3, 413

108 Fowkes, F. W., J. Phys. Chem., 1962, 66, 385

109. Joos, P., Bull. Soc. Chim. Belg., 1967, 76, 591

110. Dahanayake, M., Ph. D. Thesis, The City University of New York, 1985

111. Li, Z.; Rosen, M. J., Anal. Chem., 1981, 53(9), 1516

112. Rosen, M. J.; Goldsmith, H. A., Systematic Analysis of Surface-Active Agents, 2nd Ed., Wiley-Interscience, New York, 1972; P 427

113. Dahanayake, M.; Rosen, M. J., in Structure/Performace Relationships in Surfactants, Rosen, M. J., Ed., ACS Symposium Series 253, Amer. Chem. Soc., Washington, DC, 1984

114. Rosen, M. J., J. Colloid and Interface Sci., 1981, 79(2), 587

115. Reid, V. M.; Alston, T.; Heinerth, E., Tenside, 1967, 4, 292

116. Dann, J. R., J. Colloid Interface Sci., 1970, 32, 302

117. Zettlemoyer, A. C., J. Colloid Interface Sci., 1968, 28, 343

118. Pyter, R. A.; Zografi, G.; Mukerjee, P., J. Colloid Interface Sci., 1982, 89, 144

119. Wilhelmy, L., Ann. Phys., 1863, 119, 177

120. Rosen, M. J.; Hua, X. Y., J. Am. Oil Chem. Soc., 1982, 59, 580

121. Corkill, J. M.; Goodman, J. F.; Ogden, C. P.; Tate, J. R., Proc. Royal Soc., 1963, A273, 84

122. Chang, D. L.; Rosano, H. L., in Phenomena in Mixed Surfactant Systems, Scamehorn, J. F., Ed., American Chemical Society, Washington, DC, 1986; ACS Symposium Series Vol.311; P 116

123. Johnson, B. A.; Kreuter, J.; Zografi, G., Colloids Surfaces, 1986, 17, 325

124. Aveyard, R.; Haydon, D. A., An Introduction to the Principles of Surface Chemistry, Cambridge University Press, Cambridge, 1973; P 76

125. El-Shimi, A.; Goddard. E. D., J. Colloid Interface Sci., 1974, 48, 242

126. Mukerjee, P., JAOCS, 1982, 59, 573

127. Mukerjee, P.; Mysels, K. J., in Colloidal Dispersion and Micellar Behavior, ACS Symp., 1975; P 239

128. Honda, T.; Mukerjee, P., J. Phys. Chem., 1981, 85, 3916

129. Zhao, G. X.; Zhu, B. Y.; Zhou, Y. P.; Shi, L., Acta Chem. Sinica, 1984, 42, 416

130. Zhu, B. Y.; Zhao, G. X.; Cu, J. G., in Phenomena in Mixed Surfactant Systems, Scamehorn, J. F., Ed., American Chemical Society, Washington, DC, 1986; ACS Symposium Series Vol.311; P 172

131. Zhao, G. X.; Zhu, B. Y.; in Phenomena in Mixed Surfactant Systems, Scamehorn, J. F., Ed., American Chemical Society, Washington, DC, 1986; ACS Symposium Series Vol.311; P 184

132. Honda, T.; Mukerjee, P., J. Phys. Chem., 1981, 85, 2298

133. Shibata, O.; Kaneshina, S.; Nakamura, M., J. Colloid Interface Sci., 1980, 77, 182

134. Shah, D. O.; Shiao, S. Y., in Monolayer, Goddard, E. D., Ed., Advanced In Chemistry Series 144, American Chemical Society, Washington D. C., 1975; P 153

135. Okahara, M.; Kuo, P. L.; Yamamura, S.; Ikeda, I., J. Chem. Soc., Chem. Commun., 1980, 586

136. Rosen, M. J.; Utarapichart, C., Unpublished data.

137. Rosen, M. J.; Friedman, D.; Gross. M., J. Phys. Chem., 1964, 68, 3219

138. Rosen, M. J.; Zhu, B. Y., J. Colloid Interface Sci., 1984, 90(2), 427

139. Rosen, M. J., J. Amer. Oil Chem. Soc., 1974, 51, 461

140. Boucher, E. S.; Grinchuk, T. M.; Zettlemoyer, A. C., J. Am. Oil Chem. Soc., 1968, 49, 45

141. Mukejee, P., Adv. Colloid Interface Sci., 1967, 1, 244

142. Rosen, M. J.; Zhu, Z.; Gu, B.; Murphy, D., Langmuir, in press

143. Bargeman, D.; van Voorst Vader, F., J. Colloid Interface Sci., 1973, 42, 467

144. Fowkes, F. M., in Advan. Chem. Series, No. 43, Gould, R. F., Ed., American Chemical Society, 1964; P 99

145. van Voorst Vader, F., Chem. Ing. Tech., 1977, 49, 488

146. Paddy, J. F., in Wetting, S.C.I. Monograph No. 25, Soc. Chem. Ind., London, 1967; P 234

147. Bartell, F. E.; Davis, J. K., J. Phys. Chem., 1941, 45, 1321

148. Piirma, I.; Chem, S. J. Colloid Interface Sci., 1980, 74, 90

149. Johnson, B. A.; Kreuter, J.; Zografi, G., Colloids and Surfaces, 1986, 17, 325

150. Murphy, M. J.; Roberts, M. W.; Ross, J. R. H., J. Chem. Soc. Faraday Trans. I, 1972, 1190

151. Pletnev, M. Y.; Tereshchenko, N. B., Zh. Fiz. Khim., 1985, 59(1), 140

152. Johnson, R. E.; Dettre, R. H., in Surface and Colloid Sciences, Matizevic, E., Ed., Wiley-Interscience, New York, 1969; Vol. 2; P 85